

5-9-2014

# Recombinant Human Lactoferrin Injectable Hydrogel as an Osteogenic Biomaterial

Ashley Amini

*University of Connecticut*, [ashaliamini@yahoo.com](mailto:ashaliamini@yahoo.com)

Follow this and additional works at: <https://opencommons.uconn.edu/dissertations>

---

## Recommended Citation

Amini, Ashley, "Recombinant Human Lactoferrin Injectable Hydrogel as an Osteogenic Biomaterial" (2014). *Doctoral Dissertations*. 428.

<https://opencommons.uconn.edu/dissertations/428>

## **Recombinant Human Lactoferrin Injectable Hydrogel as an Osteogenic Biomaterial**

Ashley Ali Amini, PhD

University of Connecticut, [2014]

The bidirectional signaling of lactoferrin (LF) that suppresses osteoclastogenesis and enhances osteoblast proliferation and survival supports the notion that LF is a strong candidate for bone tissue engineering. The proposed studies were aimed to increase our understanding of the effect of recombinant human LF (rhLF) in modulating skeletal cells and further establish rhLF crosslinked gel as an excellent candidate for a skeletal regenerative biomaterial.

*In situ* formation of injectable biomaterials has several advantages as cell delivery vehicles. In this study, the biological properties rhLF were utilized as the building block, to develop the engineered cell delivery system. These studies reported the development of a novel injectable cell delivery vehicle that can significantly improve cell survival and osteogenic functions by serving as a biomaterial ligand to induce receptor mediated cell signaling of encapsulated cells. Furthermore, the bioactive rhLF gel matrix was shown to promote cell survival, proliferation and differentiation. The positive effects of rhLF gel on cellular processes supports the notion that rhLF gel is a strong candidate for bone tissue engineering.

# **Recombinant Human Lactoferrin Injectable Hydrogel as an Osteogenic Biomaterial**

Ashley Ali Amini

B.A., Stony Brook University, [2007]

D.M.D., University of Connecticut, [2014]

A Dissertation

Submitted in Partial Fulfillment of the

Requirements for the Degree of Doctor of Philosophy

at the

University of Connecticut

[2014]

Copyright by  
Ashley Ali Amini

[2014]



APPROVAL PAGE

Doctor of Philosophy Dissertation

**Recombinant Human Lactoferrin Injectable Hydrogel as an Osteogenic Biomaterial**

Presented by

Ashley Ali Amini, B.A.

Major Advisor

---

Lakshmi S. Nair

Associate Advisor

---

Cato T. Laurencin

Associate Advisor

---

Yusuf M. Khan

Associate Advisor

---

Mina Mina

Associate Advisor

---

Barbara E. Kream

University of Connecticut  
[2014]

## ACKNOWLEDGEMENTS

I would like to thank many people who have helped me through the completion of this dissertation. The first is my advisor, Dr. Lakshmi Nair, for her professional inspiration, support, encouragement and enthusiasm throughout my research. Dr. Nair's patience and kindness has been invaluable to me. In combination with the mentorship of my advisor, I am also thankful for my dynamic committee members, Dr. Cato Laurencin, Dr. Yusuf Khan, Dr. Mina Mina, Dr. Barbara Kream and Dr. Sunil Wadhwa for their support and invaluable feedback. As a receipt of NIH T32 and F30 grant, I would like to recognize NIH for their support during my combined DMD/PhD training.

I would like to thank many past and current colleagues of the Institute for Regenerative Engineering, including Ms. Ami Amini, Ms. Eva Kan, Ms. Paiyz Mikael, Mr. Eric James, Mr. Shaun McLaughlin, Mr. Clarke Nelson, Dr. Bret Ulery and Dr. Meng Deng, for their help and assistance during my research. I would like to thank Ms. Eva Kan for teaching me cell culture and cell biology techniques as well as her assistance in in confocal microscopy and RT-PCR analysis. I would like to thank Dr. Bret Ulery and Mr. Eric James for their assistance with SEM. I would also like to thank Dr. Doug Adams for his assistance in x-ray analysis.

I would like to thank my friends and colleagues that I have made at Uconn Health, whose friendship encouraged me during these years. Thank you all for making my stay memorable and enjoyable.

I dedicate my thesis to the pillars of my life: my family and husband, who have been a constant source of strength. This dissertation would not be possible without the unlimited support from my twin sister, Ami, who has been next to me throughout my

entire life. My brothers, Alexander and Andrew, for being my motivation and making me smile. I am indebted to my wonderful parents, for their unconditional love, support, and always being proud of me. My dear father for teaching me to never give up and my beautiful mother for teaching me to always do my best. I also dedicate this thesis to my amazing husband, Nevit, for his love, patience and encouragement. I love you all.

## ***Table of Contents***

<b>1 Synopsis .....</b>	<b>26</b>
<b>2 Literature review .....</b>	<b>30</b>
<b>2.1 Injectable hydrogels for skeletal repair .....</b>	<b>30</b>
2.1.1 Hydrogels as skeletal ECM mimetic scaffolds .....	31
2.1.2 <i>In situ</i> gelling hydrogel systems .....	34
2.1.2.1 Physically crosslinked hydrogels .....	35
2.1.2.2 Covalently crosslinked hydrogels .....	40
2.1.2.2.1 Enzymatically crosslinked hydrogels.....	44
2.1.3 Application of hydrogels.....	49
2.1.3.1 Enhancing mechanical properties and mineralization of hydrogels.....	50
2.1.3.2 Enhancing biological properties by growth factor loading.....	51
2.1.3.3 Enhancing biological properties by drug delivery.....	55
2.1.3.4 Enhancing biological properties by gene delivery.....	56
2.1.3.5 Enhancing biological properties by cell encapsulation .....	57
2.1.4 Conclusions .....	62
<b>2.2 Lactoferrin as a biologically active molecule for bone regeneration.....</b>	<b>63</b>
2.2.1 Molecular structure and composition .....	64
2.2.2 Role of lactoferrin in ferrokinetics .....	67
2.2.3 Positive skeletal regulator .....	69
2.2.4 Lactoferrin as an immunomodulatory protein.....	75
2.2.5 Lactoferrins's link to osteoimmunology.....	80
2.2.5.1 Lactoferrin and periodontitis-induced bone loss.....	84
2.2.5.2 Lactoferrin and osteoporotic bone loss.....	86
2.2.6 Angiogenesis modulator .....	88

2.2.7	Candidate for bone regeneration applications .....	91
2.2.8	Conclusions .....	93
<b>3</b>	<b>Preliminary studies.....</b>	<b>94</b>
<b>3.1</b>	<b>Enzymatically—crosslinked bovine lactoferrin hydrogel as an osteogenic cell delivery vehicle .....</b>	<b>94</b>
3.1.1	Introduction .....	94
3.1.2	Methods .....	100
3.1.2.1	Synthesis of bLF-tyramine conjugates (modified bLF).....	100
3.1.2.2	Quantification of tyramine modification of bLF.....	101
3.1.2.3	Gelation time .....	101
3.1.2.4	Morphology.....	101
3.1.2.5	Protein expression analysis of encapsulated cells.....	101
3.1.2.5.1	Western Blot Analysis.....	101
3.1.2.5.2	Immunofluorescence.....	102
3.1.3	Results .....	102
3.1.3.1	Development of injectable gels from tyrosinated bLF .....	102
3.1.3.2	Bioactivity of bLF gels .....	104
3.1.4	Discussion .....	107
3.1.5	Conclusions .....	112
<b>4</b>	<b>Evaluation of the bioactivity of recombinant human lactoferrins.....</b>	<b>112</b>
<b>4.1</b>	<b>Evaluation of the bioactivity of recombinant human lactoferrins (apo-, pis- and holo-) towards murine MC3T3 preosteoblast cells .....</b>	<b>112</b>
4.1.1	Introduction .....	112
4.1.2	Methods .....	115
4.1.2.1	Cell proliferation.....	115

4.1.2.2	Protein expression analysis.....	116
4.1.2.2.1	Western blot analysis.....	116
4.1.2.2.2	Immunocytochemistry .....	116
4.1.2.3	Microarray gene expression analysis.....	117
4.1.2.4	Statistical data analysis .....	117
4.1.3	Results .....	117
4.1.4	Discussion .....	129
4.1.5	Conclusions .....	136
<b>4.2</b>	<b>Bioactivity of holo-rhLF towards MC3T3 murine preosteoblast cells and</b>	
	<b>NH0st primary cells: a comparative study .....</b>	<b>136</b>
4.2.1	Introduction .....	136
4.2.2	Methods .....	138
4.2.2.1	Proliferation assays.....	138
4.2.2.1.1	Thymidine incorporation .....	138
4.2.2.1.2	MTS assay.....	138
4.2.2.2	Differentiation assays.....	139
4.2.2.2.1	Alkaline phosphatase assay.....	139
4.2.2.2.2	Mineralization assay.....	139
4.2.2.3	Protein expression.....	139
4.2.3	Results .....	140
4.2.4	Discussion .....	143
4.2.5	Conclusions .....	147
<b>4.3</b>	<b>Evaluation of the mechanism behind the anti-apoptotic and osteogenic</b>	
	<b>activity of rhLF towards MC3T3 cells.....</b>	<b>148</b>
4.3.1	Introduction .....	148
4.3.2	Methods .....	152

4.3.2.1	Cell viability/ survival assays .....	152
4.3.2.1.1	Serum starvation and cell viability assay .....	152
4.3.2.1.2	Protein expression (Immunocytochemistry) .....	152
4.3.2.1.3	Wnt signalling pathway .....	153
4.3.2.1.4	Inhibitor studies for signalling pathway probing .....	153
4.3.2.1.4.1	Protein expression (Western blot analysis) .....	153
4.3.2.1.4.2	Bioluminescent caspase-3 assay .....	153
4.3.2.1.5	Osteogenesis assays .....	154
4.3.2.1.5.1	Protein expression .....	154
4.3.2.1.5.1.1	Total $\beta$ catenin expression .....	154
4.3.2.1.5.1.1.1	Canonical Wnt signaling pathway activation .....	154
4.3.2.1.5.1.1.2	Time course of $\beta$ catenin expression .....	154
4.3.2.1.5.1.2	Nuclear/cytoplasmic $\beta$ catenin expression .....	155
4.3.2.1.5.1.2.1	Western blot .....	155
4.3.2.1.5.1.2.2	Immunocytochemistry .....	155
4.3.2.1.5.2	RNA expression .....	155
4.3.2.1.5.3	Inhibitor studies for signaling pathway probing .....	156
4.3.3	Results .....	156
4.3.3.1	Anti-apoptotic effect of holo-rhLF toward MC3T3 cells .....	156
4.3.3.2	Osteogenic effect of holo-rhLF towards MC3T3 cells .....	161
4.3.3.2.1	rhLF increases osteogenesis via $\beta$ catenin signaling pathway .....	161
4.3.4	Discussion .....	165
4.3.5	Conclusions .....	172

## **5 Preparation and characterization of injectable holo-rhLF and gelatin gels**

**173**

<b>5.1 Development and characterization of bioactive holo-rhLF injectable gel via enzymatic crosslinking.....</b>	<b>173</b>
---	------------

5.1.1	Introduction .....	173
5.1.2	Methods .....	175
5.1.2.1	Synthesis of holo-rhLF tyramine conjugates (modified holo-rhLF) .....	175
5.1.2.2	Preparation of holo-rhLF gels.....	175
5.1.2.3	Quantification of tyramine modification.....	175
5.1.2.4	Gelation time .....	175
5.1.2.5	Soluble holo-rhLF protein release from holo-rhLF gel .....	176
5.1.2.6	Percentage water uptake .....	176
5.1.2.7	Morphology.....	176
5.1.2.8	Rheological analysis .....	176
5.1.2.9	Biomaterial degradation in vivo .....	177
5.1.3	Results .....	177
5.1.4	Discussion .....	186
5.1.5	Conclusions .....	191
<b>5.2</b>	<b>Enzymatically crosslinked injectable gelatin gel as an osteoblast delivery</b>	
	<b>vehicle .....</b>	<b>192</b>
5.2.1	Introduction .....	192
5.2.2	Methods .....	195
5.2.2.1	Preparation of gelatin gel .....	195
5.2.2.1.1	Synthesis of gelatin tyramine conjugates (modified gelatin) .....	195
5.2.2.1.2	Preparation of gelatin gels.....	195
5.2.2.2	Morphology.....	195
5.2.2.3	Rheological analysis of gelatin gels .....	195
5.2.2.4	Cell encapsulation in gelatin gel .....	196
5.2.2.4.1	Cell viability and spreading .....	196
5.2.2.5	Bioactivity of gelatin and modified gelatin .....	197
5.2.2.5.1.1	Western blot analysis .....	197



5.2.2.5.1.2	Alkaline phosphatase activity .....	197
5.2.2.5.1.3	Mineralization assay .....	197
5.2.2.6	Bioactivity of gelatin gels.....	198
5.2.2.7	Statistical data analysis .....	198
5.2.3	Results .....	198
5.2.3.1.1	Synthesis of gelatin-tyramine conjugates .....	198
5.2.3.1.2	Preparation of gelatin gels.....	199
5.2.3.1.3	Morphology .....	199
5.2.3.1.4	Rheological Analysis.....	201
5.2.3.2	Cell-Gelatin Interactions .....	202
5.2.3.2.1	Cell viability and spreading.....	202
5.2.3.2.2	Bioactivity of gelatin and modified gelatin.....	204
5.2.3.2.3	Bioactivity of injectable gelatin gels .....	207
5.2.4	Discussion .....	209
5.2.5	Conclusions .....	213
<b>5.3</b>	<b>Evaluation of the bioactivity of holo-rhLF gel as a novel cell delivery vehicle</b>	
	<b>214</b>	
5.3.1	Introduction .....	214
5.3.2	Methods .....	218
5.3.2.1	Determination of optimal cell seeding density for cell encapsulation in hydrogel .....	218
5.3.2.2	Mitogenic Activity .....	218
5.3.2.2.1	EdU incorporation .....	218
5.3.2.2.2	Protein expression (2D Immunocytochemistry) .....	219
5.3.2.2.3	Protein expression (3D Immunocytochemistry) .....	219
5.3.2.2.4	Long term culture of encapsulated cells in the gels.....	219
5.3.2.3	Anti-apoptotic effect of rhLF gels.....	219
5.3.2.3.1	Serum starvation-induced apoptosis .....	219

5.3.2.3.2	Protein expression .....	220
5.3.2.3.3	Holo-rhLF/ gelatin composite gels.....	220
5.3.2.4	Cell differentiation .....	221
5.3.2.4.1	Protein Expression.....	221
5.3.3	Results .....	222
5.3.3.1	Effect of holo-rhLF and holo-rhLF gel encapsulation on MC3T3 cell proliferation.....	223
5.3.3.2	Anti-apoptotic effect of holo-rhLF gel .....	227
5.3.3.3	Effect of holo-rhLF gel encapsulation on MC3T3 cell osteogenesis .....	232
5.3.4	Discussion .....	233
5.3.5	Conclusions .....	237
<b>6</b>	<b>Future studies .....</b>	<b>239</b>
6.1	Molecular mechanism underlying LF.....	239
6.2	LF composite gels.....	239
6.3	Holo-rhLF gel bone regeneration study in vivo .....	240
<b>7</b>	<b>Appendix of Protocols .....</b>	<b>241</b>
7.1	Cell culture .....	241
7.1.1	Materials .....	241
7.1.2	Methods .....	242
7.1.2.1	MC3T3 cell culture.....	242
7.1.2.2	Human osteoblast cell culture .....	242
7.2	Protein analysis.....	243
7.2.1	Materials .....	243
7.2.2	Methods .....	244
7.2.2.1	Extraction .....	244
7.2.2.2	Bicinchoninic Acid (BCA) total protein assay .....	244
7.2.2.3	Western blot analysis .....	245

7.2.2.4	Nuclear/ cytoplasmic protein extraction.....	246
7.2.2.5	Immunocytochemistry.....	247
<b>7.3</b>	<b>Gene expression analysis .....</b>	<b>248</b>
7.3.1	Materials.....	248
7.3.2	Methods .....	248
7.3.2.1	RNA extraction and purification.....	248
7.3.2.2	Real time PCR analysis.....	249
7.3.2.3	Microarray analysis.....	249
7.3.2.4	Mouse Wnt signaling pathway array .....	250
<b>7.4</b>	<b>Cell Imaging .....</b>	<b>250</b>
7.4.1	Materials.....	250
7.4.2	Methods .....	250
7.4.2.1	Cell morphology.....	250
7.4.2.1.1	Actin staining via Alexa Fluor 488 phalloidin .....	250
7.4.2.1.2	Nuclear staining via propidium iodide .....	251
<b>7.5</b>	<b>Cell survival and viability .....</b>	<b>251</b>
7.5.1	Materials.....	251
7.5.2	Methods .....	251
7.5.2.1	Live/Dead Viability assay .....	251
7.5.2.2	Colorimetric CaspACE assay.....	252
<b>7.6</b>	<b>Proliferation assays .....</b>	<b>253</b>
7.6.1	Materials.....	253
7.6.2	Methods .....	253
7.6.2.1	MTS assay .....	253
7.6.2.2	Thymidine incorporation .....	254
7.6.2.3	EdU incorporation .....	254

7.6.2.3.1	Preparation of stock solutions .....	254
7.6.2.3.2	EdU labeling .....	254
7.6.2.3.3	EdU detection .....	255
7.6.2.3.4	Counter DNA stain .....	256
<b>7.7</b>	<b>Cell differentiation assays .....</b>	<b>256</b>
7.7.1	Materials .....	256
7.7.2	Methods .....	256
7.7.2.1	Alkaline phosphatase assay .....	256
7.7.2.2	Alizarin red (Calcium staining) .....	257
<b>7.8</b>	<b>Signalling pathway probing .....</b>	<b>257</b>
7.8.1	Materials .....	257
7.8.2	Methods .....	258
7.8.2.1	Pharmalogical pathway inhibitors .....	258
7.8.2.2	Wnt signalling array .....	258
<b>7.9</b>	<b>Biomaterial studies .....</b>	<b>258</b>
7.9.1	Materials .....	258
7.9.2	Methods .....	259
7.9.2.1	Formation of protein crosslinked hydrogels .....	259
7.9.2.1.1	Synthesis of protein-tyramine conjugates .....	259
7.9.2.1.1.1	Quantification of tyramine modification .....	260
7.9.2.1.2	Preparation of protein crosslinked gels .....	261
7.9.2.1.2.1	Gelatin gel .....	261
7.9.2.1.2.1.1	Gelatin Gel (dissolved in H <sub>2</sub> O) .....	261
7.9.2.1.2.1.2	Gelatin Gel (dissolved in 1:1 PBS:H <sub>2</sub> O ratio) .....	262
7.9.2.1.2.2	LF gels .....	262
7.9.2.2	Characterization of hydrogels .....	263
7.9.2.2.1	Gelation time .....	263

7.9.2.2.2	Rheological testing.....	263
7.9.2.2.3	Gel morphology .....	263
7.9.2.2.4	Percentage of water uptake.....	264
7.9.2.2.5	Degradation of holo-rhLF biogels <i>in vivo</i> .....	264
7.9.2.3	Soluble holo-rhLF protein release from holo-rhLF gel .....	265
7.9.2.4	Cell encapsulation in hydrogel .....	265
<b>8</b>	<b>References.....</b>	<b>266</b>

### ***i. List of Abbreviations***

LF	Lactoferrin
bLF	Bovine Lactoferrin
hLF	Human Lactoferrin
rhLF	Recombinant Human Lactoferrin
Holo-	Fully iron saturated (>90%) LF
Pis-	Partially iron saturated (~50%) LF
Apo-	Iron depleted (<10%) LF
Erk	Extracellular Signal Regulated Kinase
MAPK	Mitogen Activated Protein Kinase
VEGF	Vascular Endothelial Growth Factor
FGF	Fibroblast Growth Factor
BMP	Bone Morphogenic Protein
PDGF	Platelet Derived Growth Factor
IGF	Insulin-like Growth Factor
TGF	Transforming Growth Factor
TCF	T Cell-Specific Transcription Factor
LEF	Lymphoid-Enhancer Binding Factor
NFκB	Nuclear Factor κ β
IL	Interleukin
NHOst	Normal Human Osteoblast
MSC	Mesenchymal Stromal Cell
MC3T3	MC3T3-E1 Murine Preosteoblast Cell
HUVEC	Human Umbilical Vein Endothelial Cells
LRP	Low Density Lipoprotein Receptor-Related Protein
PI3K	Phosphoinositide 3-Kinase
PKA	Protein Kinase A
cAMP	Cyclic Adenosine Monophosphate
CREB	cAMP Response Element-Binding
Dsh	Disheveled
Gsk3β	Glycogen Synthase Kinase 3 β
H89	PKA inhibitor
LY294002	PI3K inhibitor
DKK1	Dickkopf-related protein 1
RAP	Receptor Associated Protein

## **ii. List of Tables**

Table 1. Various hydrogel materials, crosslinking initiators and mechanism. ....	35
Table 2. Enzyme-catalyzed crosslinkable hydrogels and potential applications. ....	46
Table 3. Genes up-regulated by rhLF of different iron concentrations. ....	123
Table 4. Genes down-regulated by rhLF of different iron concentrations ....	125
Table 5. Genes differentially regulated by rhLF of different iron concentrations.....	129
Table 6. Primary and secondary antibodies used for western blot and immunocytochemistry studies. ....	244
Table 7. Diluted albumin (BSA) standards. ....	245
Table 8. Reagent volumes for different packed cell volumes. ....	246
Table 9. Caspase assay control sample preparation. ....	253
Table 10. Click-iT reaction cocktails. ....	255

### **iii. List of Figures**

Figure 1. Crystal structure of (A) bLF of (B) hLF.....	28
Figure 2. Enzymatically crosslinked recombinant protein by transglutaminase (TG) enzymatic crosslinking.....	45
Figure 3. Schematic mechanism of the enzyme-mediated crosslinking systems. ....	48
Figure 4. Examples of hydrogels as growth factor, gene and cell delivery systems. ....	50
Figure 5. The wide range of beneficial functional properties decribed for LF.....	63
Figure 6. Through bidirectional signalling, LF enhances osteoblast activity and suppresses osteoclastogenesis. ....	74
Figure 7. Anabolic effect on mouse hemi-calvaria in response to bLF after 10 days treatment. ....	75
Figure 8. Comparison of periodontitis versus healthy/LF treated tissue. ....	85
Figure 9. Schematic representation of the role of estrogen deprivation and bLF on bone loss and bone resorption markers through APC and T cell modulation. ....	87
Figure 10. (A) Promoting effect of bLF—embedded collagen membrane on ALP activitiy and osteocalcin production in MG63 cells.....	96
Figure 11. (A) Structure of Human LF. (B) Tyrosine amino acid groups contained in human LF. (C) Carboxylic acid containing amino acid groups (aspartate and glutamate) in human LF. (D) Theoretically available crosslinking amino acid sites after tyramine modification of human LF. ....	99
Figure 12. Amino acid sequence of human lactoferrin.....	99



Figure 13. Schematic showing the modification of LF's acidic groups with tyramine to yield greater enzymatic crosslinking sites. Addition of HRP and H <sub>2</sub> O <sub>2</sub> yields a LF crosslinked gel. ....	100
Figure 14. Effect of modification time on (A) bLF phenolic content and (B) gelation time. ....	103
Figure 15. Morphology of 10 mg/ml bLF gel.....	104
Figure 16. Increased stabilization of $\beta$ catenin and phosphorylation of Akt in MC3T3 after 24 hour treatment of 100 $\mu$ g/ml bLF solution and encapsulation in 10 mg/ml bLF gel.....	106
Figure 17. Effect of 100 $\mu$ g/ml bLF solution on MC3T3 protein expression after 24 hours treatment. ....	106
Figure 18. Increased IGF2 and VEGF $\alpha$ expression in 10 mg/ml bLF gel encapsulated MC3T3 cells after 2 days of culture. ....	107
Figure 19. Effect of rhLF concentration and iron saturation on MC3T3 cell proliferation after 24 hour treatment measured by thymidine incorporation.....	118
Figure 20. Effect of rhLF iron concentration on Akt phosphorylation in MC3T3 cells.....	119
Figure 21. Effect of rhLF iron concentration on LRP1 expression in MC3T3 cells. ....	119
Figure 22. Effect of rhLF iron concentration on Dishevelled 2, Gsk3 $\beta$ phosphorylation and $\beta$ catenin activation in MC3T3 cells. ....	120
Figure 23. Immunocytochemistry analysis of (A) active $\beta$ catenin, (B) IL6 and (C) VEGF $\alpha$ of 100 $\mu$ g/ml of apo- or holo-rhLF treated + or untreated (control).....	121
Figure 24. Global expression profiles in MC3T3 murine preosteoblasts treated with varying iron saturations of rhLF. ....	123

Figure 25. Effect of holo-rhLF treatment on MC3T3 and NHOst cell proliferation. ....	140
Figure 26. Alkaline phosphatase activity in MC3T3 and NHOst cells treated with holo-rhLF.....	142
Figure 27. Mineral deposition by MC3T3 and NHOst cells treated with holo-rhLF. ...	142
Figure 28. Holo-rhLF increases (a) phosphorylation of Akt and (b) activation of $\beta$ catenin in NHOst cells after 24 hours of treatment.....	143
Figure 29. Representative bioluminescence imaging of a mice transplanted with human mesenchymal stem cells in a critical-size segmental femoral defect and <i>in vivo</i> kinetic cell survival quantification.....	149
Figure 30. Schematic showing the summary of known mechanisms of action of LF in osteoblasts. ....	151
Figure 31. Viability of serum starved MC3T3 cells after holo-rhLF treatment. ....	157
Figure 32. Increased phosphorylation of Akt in MC3T3 cells after holo-rhLF treatment. ....	157
Figure 33. Regulation of Wnt signaling pathway in MC3T3 cells by holo-rhLF.....	159
Figure 34. 30 $\mu$ M H89 and 10 $\mu$ M of LY294002 inhibited holo-rhLF-induced phosphorylation of Akt in MC3T3 cells after 24 hours. ....	160
Figure 35. Caspase-3 activity after 24 hours of holo-rhLF treatment with signaling pathway inhibitors, H89 and LY294002.....	160
Figure 36. Increased $\beta$ catenin signaling cascade by holo-rhLF treatment.....	162
Figure 37. Active $\beta$ catenin expression induced in MC3T3 cells by 100 $\mu$ g/ml holo-rhLF. ....	162

Figure 38. Increased accumulation/activation of $\beta$ catenin in nucleus and cytoplasm of rhLF treated MC3T3 cells after 24 hours treatment. ....	163
Figure 39. Increased $\beta$ catenin in MC3T3 cells treated with 100 $\mu$ g/ml holo-rhLF. ....	163
Figure 40. mRNA expression of LRP receptors after holo-rhLF treatment. ....	164
Figure 41. Inhibitor studies (30 $\mu$ M H89 and 100 ng/ml DKK1) to understand the osteogenic pathways and $\beta$ catenin activation. ....	165
Figure 42. Schematic of signaling pathways induced by holo-rhLF in MC3T3 cells. ..	172
Figure 43. Inverse effect of tyramine modification time (over 24 hours) on phenolic content and gelation time of rhLF.....	178
Figure 44. Gelation time of rhLF gel upon addition of dilute $H_2O_2$ as determined by the vial inversion technique. ....	179
Figure 45. Effect of gel precursors (modified rhLF, HRP, $H_2O_2$ ) concentration on gelation time.....	179
Figure 46. Soluble holo-rhLF release from crosslinked 10 mg/ml holo-rhLF gel as a function of time.....	180
Figure 47. Morphology of 10 mg/ml holo-rhLF gel.....	181
Figure 48. Morphology of holo-rhLF gel at various gel precursor concentrations .....	182
Figure 49. A) Effect of holo-rhLF polymer concentration on hydrogel mechanical strength as a function of storage moduli, $G'$ . B) Effect of temperature (25°C vs. 37°C) on storage moduli, $G'$ , of 50 mg/ml holo-rhLF gel. ....	182
Figure 50. Effect of holo-rhLF concentration on holo-rhLF gel water uptake over 8 days. ....	183
Figure 51. Effect of HRP concentration on holo-rhLF gel water uptake over 8 days. ..	184

Figure 52. Effect of H <sub>2</sub> O <sub>2</sub> concentration on holo-rhLF gel water uptake over 8 days. .	184
Figure 53. <i>In vivo</i> degradation of 10 mg/ml holo-rhLF gel in rat subcutaneous tissue after 4 and 12 weeks.....	185
Figure 54. Cellular spreading in 10, 25 and 50 mg/ml holo-rhLF gel over 14 days of encapsulation using live/dead assay.....	186
Figure 55. Schematic representation of the enzymatic crosslinking of gelatin-poly(ethylene glycol) tyramine (GPT) conjugates and the image of the in situ GPT hydrogel formation using a dual syringe. ....	194
Figure 56. Extent of phenolic group substitution in gelatin as a function of reaction time under the conditions used in the study.....	199
Figure 57. SEM images of 10-50 mg/ml gelatin gels.....	200
Figure 58. Average pore width and pore wall thickness of gelatin gels.....	201
Figure 59. Rheological testing of 10, 25 and 50 mg/ml gelatin gel.....	201
Figure 60. Photomicrographs of MC3T3 cells encapsulated in gelatin gels of different concentrations (10-50 mg/ml) as a function of time. <b>(A)</b> Gels prepared by dissolving gelatin in H <sub>2</sub> O. <b>(B)</b> Gels prepared by dissolving gelatin in 1:1 H <sub>2</sub> O:PBS solution. Images taken at 20x magnification. ....	204
Figure 61. Bioactivity of gelatin and modified gelatin.....	205
Figure 62. Alkaline phosphatase activity of MC3T3 cells treated with gelatin and holo-rhLF (modified and unmodified). ....	206
Figure 63. Calcium deposition of MC3T3 cells treated with gelatin and holo-rhLF (modified and unmodified). ....	206

Figure 64. Phosphorylation of Erk in MC3T3 cells encapsulated in 10 mg/ml gelatin gel.	208
Figure 65. Schematic showing cell encapsulation in holo-rhLF gel.	218
Figure 66. Various cell seeding densities of MC3T3 cells encapsulated in 10 mg/ml holo-rhLF gel.	222
Figure 67. 100 µg/ml holo-rhLF increases EdU incorporation and Ki67 protein expression in MC3T3 cells after 8 hours treatment.	224
Figure 68. Increased phosphorylation of Erk and increased Ki67 protein expression in MC3T3 cells treated with 100 µg/ml holo-rhLF.	225
Figure 69. Phosphorylation of Erk and Ki67 expression in (A) holo-rhLF gel—encapsulated MC3T3 cells. (B) Gelatin gels were dissolved in H <sub>2</sub> O (C) Gelatin gels were dissolved in 1:1 H <sub>2</sub> O:PBS solution	226
Figure 70. Cell number and h viability of MC3T3 cells encapsulated in 10mg/mL of holo rhLF gels as a function of time.	226
Figure 71. Akt phosphorylation in MC3T3 cells encapsulated in (A) 10 mg/ml holo-rhLF gel. (B) Gels were prepared by dissolving gelatin in H <sub>2</sub> O (C) Gels were prepared by dissolving gelatin in 1:1 H <sub>2</sub> O:PBS solution	227
Figure 72. Viability in MC3T3 cells encapsulated in (A) 10 mg/ml holo-rhLF gel during serum starvation. (B) Gels were prepared by dissolving gelatin in H <sub>2</sub> O (C) Gels were prepared by dissolving gelatin in 1:1 H <sub>2</sub> O:PBS solution Images taken at 20x magnification.	228
Figure 73. Live/dead assay of serum-starved encapsulated cells in the gels.	230
Figure 74. Phospho-Akt expression of serum-starved encapsulated cells in the gels.	231

Figure 75. Active $\beta$ catenin expression in MC3T3 cells encapsulated in (A) 10 mg/ml holo-rhLF gel and gelatin gel. (B) Gelatin gels were dissolved in H <sub>2</sub> O (C) Gelatin gels were dissolved in 1:1 H <sub>2</sub> O:PBS solution Images taken at 20x magnification. ....	232
Figure 76. Collagen 1 and OCN expression in MC3T3 cells encapsulated in 10 mg/ml holo-rhLF gel and gelatin gel. A. Gels prepared from gelatin dissolved in 1:1 H <sub>2</sub> O: PBS solution. B. Gels prepared from gelatin dissolved in H <sub>2</sub> O. Images taken at 20x magnification. ....	233
Figure 77. Tyramine Concentration Standard Curve. ....	261

## 1 Synopsis

The pursuit for bone tissue engineering has been prompted by clinical demands that may occur as a result of congenital anomalies, trauma and skeletal diseases (Geckil et al. 2010, Huang et al. 2011). The current gold standard for skeletal repair is autografts (Laurencin et al. 1999). However, this treatment has limitations, which include donor site morbidity and limited availability. Allografts are commonly used as an alternative option to autografts, however, it too is associated with significant limitations – delayed vascular penetration, slow bone formation, high incidence of non-union or delayed union and possibility of disease transmission (Delloye et al. 2007). A new avenue, namely bone tissue engineering, is currently being explored to overcome the limitations of these biological grafts. Tissue engineering uses cells, scaffolds, and biological factors alone or in combination toward the repair, restoration and replacement of bone tissues (Laurencin et al. 1999).

A major modality in tissue engineering is cell-based therapeutics, and its efficiency is based on successful delivery of cells to sites of repair or regeneration. Recently, various biomaterials have been employed to mediate localized cell delivery. *In situ*—forming gel scaffolds (i.e., injectable, crosslinked polymeric networks) are of great interest since they can be implanted simply by injection to fill irregularly shaped defects. These crosslinked networks allow for the accommodation of homogeneous incorporation of cells and bioactive molecules in a three-dimensional (3D) microenvironment. Moreover, protein-based gels are especially attractive since their bioactivity may encourage encapsulated cells to recognize and bind to specific sites within proteins. Recently, significant interest has grown towards developing biologically active gels that could modulate the functions of encapsulated cells for better regenerative outcome. Our lab has

previously developed a novel, *in situ*—forming, lactoferrin (LF) – based gel system that may utilize the biological functions of the native protein for the development of a bioactive biomaterial in order to modulate encapsulated cell functions. The rationale for developing a LF-based gel is multi-fold. 1) The gel is *in situ* forming, which allows for non-invasive implantation through injection. 2) The injectable gel may also be used as a cell delivery vehicle as it provides a mild water rich environment. 3) Due to the potential bioactivity of LF, the gel might present a bioactive environment for enhanced cellular performance.

Our preliminary studies discussed here demonstrated the bioactivity of bovine LF (bLF) gel. bLF was used to evaluate the bioactivity of the novel biomaterial since there is significant literature on the bioactivity of soluble bLF protein. The advent of the recombinant human protein technology, however, offers a cost-effective alternative and a foundation for producing consistent and predictable results for potential clinical applications. The goal of the present study aimed to evaluate the bioactivity of rhLF towards osteoblast cells, and develop a bioactive injectable cell delivery system based on rhLF.

We hypothesize that injectable rhLF gel can be formulated and this biomaterial will possess osteogenic activities. We further hypothesize that the cell survival activities of the rhLF gel are regulated upstream of PI3K/Akt and the osteogenic activities will be transduced via a  $\beta$ -catenin—dependent signaling pathway.



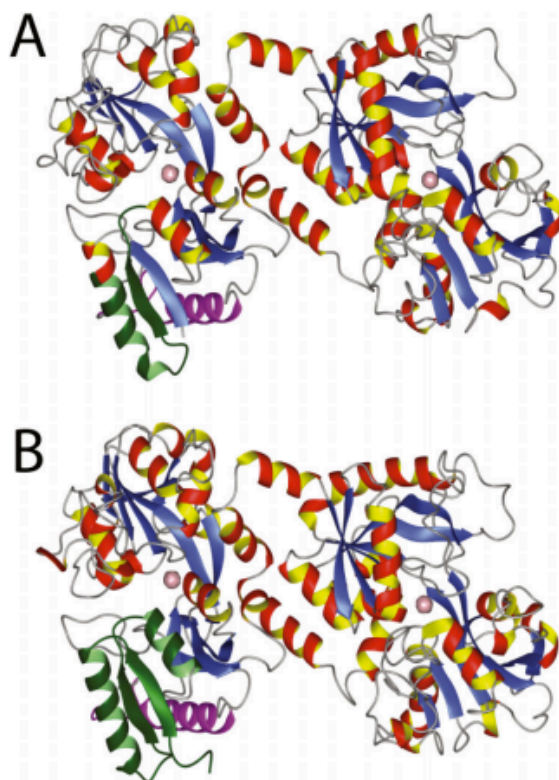


Figure 1. Crystal structure of (A) bLF of (B) hLF.

Each protein binds to two  $\text{Fe}^{3+}$  atoms (pink spheres) – one in each lobe of the protein. Image taken from (Vogel 2012).

Since there is only 69% species homology between the bLF and human LF (hLF) (van Berkel et al. 2002b) (Figure 1), we first confirmed the bioactivity of rhLF protein using *in vitro* cell models. We also investigated the biological effects of the various iron saturation forms of rhLF (apo-, pis- and holo-) on MC3T3 pre-osteoblast cells to understand the effect of iron concentration on rhLF bioactivity and identify the suitable polymer to develop injectable hydrogels for bone tissue engineering application. We performed a global gene analysis using microarrays to examine the effect of LF iron saturation on MC3T3 cells. MC3T3 cell line was selected to evaluate the bioactivities of rhLFs since it is a well-characterized murine osteoblast cell line (Sudo et al. 1983) that

has been used extensively as a model for osteoblasts *in vitro*. Next, we compared the effect of holo-rhLF on two *in vitro* culture systems: clonal MC3T3 cells and primary NHOst cell cultures. These comparative experiments were designed to confirm whether MC3T3 could act as a good model cell line to demonstrate the potential future clinical efficacy of the system. Further, the biological effects (cell survival, proliferation and osteogenesis) of holo-rhLF were tested using standard cell culture system. Molecular mechanism underlying LF's anti-apoptotic and osteogenic effects were probed using western blot analysis and PCR arrays, and confirmed using pharmacological inhibitor studies. Finally, after establishing the biological effects and molecular mechanisms of holo-rhLF protein on MC3T3 cells, our next aim was to characterize the physical properties of crosslinked holo-rhLF gel based on gelation time, water uptake, mechanical properties and morphology properties to be further employed as a regenerative skeletal biomaterial. In all these studies, enzyme-crosslinked injectable gelatin gel was used as the control. Biological effect of holo-rhLF on MC3T3 pre-osteoblasts was evaluated based on its ability to promote cell survival, proliferation and differentiation compared to the gelatin gel.

## **2 Literature review**

### **2.1 Injectable hydrogels for skeletal repair**

The pursuit to engineer bone and cartilage microenvironments are prompted by the clinical demand for skeletal tissue repair and replacement, which occur as a result of congenital anomalies, trauma and skeletal diseases (Geckil et al. 2010, Huang et al. 2011). Autografts, the current gold standard for bone and cartilage repair, presents itself with limitations, including donor site morbidity and limited availability. Although the use of allografts can overcome these limitations, they also have substantial limitations, which include delayed vascular penetration, slow bone formation, high incidence of non-union or delayed union and possibility of disease transmission (Burchardt 1987, Wozney et al. 1988). The avenue of tissue engineering explores the use of cells, scaffolds, and biological factors alone or in combination toward the repair, restoration and replacement of tissues (Laurencin et al. 2001). The opportunities and challenges for tissue engineering are extensive for both bone and cartilage.

The extracellular matrix (ECM) in natural tissue provides the structured microenvironment with mechanical, biochemical and physical cues that enable the cells to interact with each other and with the ECM to allow optimal cell function. ECM is a dynamic structure that consists mainly of fibrous proteins and some glycosaminoglycans, which self-assemble into nanofibrillar supramolecular networks (collectively called structural/physical signals) to provide structural architecture to support the resident cells (Nair, Laurencin 2006). The native microenvironment is not only composed of ECM, but also biomolecules (growth factors, chemokines and cytokines) and ions that are bound to the ECM. Growth factors bind to target cell receptors and induce intracellular

signal transduction that reaches the cell nucleus and determines the biological response (Devescovi et al. 2008). The main growth factors acting on the skeleton are bone morphogenetic proteins (BMPs), transforming growth factor  $\beta$  (TGF $\beta$ ), fibroblast growth factor (FGF), platelet-derived growth factor (PDGF), vascular endothelial growth factor (VEGF) and insulin-like growth factors (IGFs) (Linkhart, Mohan & Baylink 1996, Baylink, Finkelman & Mohan 1993). Each biological growth factor has specific roles in the growth, maintenance and repair of the skeleton. In summary, the multifunctionality of ECM is achieved through the biochemical signaling from the soluble factors along with the unique tissue specific matrix composition and hierarchical structural features. It is therefore pertinent to consider the structural features of ECM along with the biological principles that govern cell-cell and cell-matrix interactions while developing novel strategies to promote tissue regeneration. Successful fabrication of a biomimetic scaffold requires the biomaterial to be finely tailored toward the dynamic native microenvironment and to mimic the intricate and organized meshwork of extracellular matrix (ECM).

### **2.1.1 Hydrogels as skeletal ECM mimetic scaffolds**

Hydrogels are cross-linked, porous networks that exhibit high tissue-like water content and elastic properties. The potential of hydrogels as unique biomaterials was reported in the later half of the 20<sup>th</sup> century when non-degradable methacrylate gels were used for developing soft contact lenses. Subsequently, a wide range of hydrogels were developed using synthetic and natural hydrophilic polymers that are biodegradable or non-degradable for various biomedical applications in the form of drug/gene/protein delivery, as unique wound dressing materials as well as scaffolds for tissue engineering

(Peppas, Sahlin 1996). Synthetic hydrogels provide more chemically programmable and reproducible platform to systematically understand cell-matrix interactions. Poly(ethylene glycol) (PEG) is one of the most extensively investigated non-degradable, synthetic, hydrophilic polymer for biomedical applications due to its hydrophilicity, good tissue compatibility, non-toxicity and availability of reactive end groups for chemical functionalization. Several degradable synthetic polymeric systems have also been developed to form hydrogels. These include co-polymers of PEG with a variety of synthetic degradable polymers such as poly(lactic co-glycolic) acid (PLGA), poly(propylene fumarate) (PPF), poly(vinyl alcohol) (PVA), poly(propylene oxide) (PPO), polyanhydrides and polyphosphazenes (Joa, Engelb & Mikos 2000, Lee et al. 2007). Among the natural biodegradable hydrophilic macromolecules investigated for hydrogel formation, proteins and polysaccharides form the most prominent members (Coviello et al. 2007). This is due to various advantages such as non-toxicity, biocompatibility, availability in large variety of composition and properties, widely present in living organisms as well as due to the fact that they can be produced using recombinant DNA techniques (Coviello et al. 2007). Hydrogels made of naturally derived, polysaccharides for skeletal repair include agarose, alginate, chitosan and hyaluronic acid (Burdick, Prestwich 2011). Protein-based scaffolds, such as collagen, gelatin and fibrin, are very attractive for building bioactive scaffolds due to their ability to mimic the extracellular environment, biodegradability and inherent biochemical properties (Stenzel, Miyata & Rubin 1974, Dreesmann, Ahlers & Schlosshauer 2007, Liu et al. 2009, Spotnitz, Burks 2008). These biocompatible and biodegradable matrices due to their highly swollen three-dimensional environment with large pore sizes, porosity and

high water content provide temporary support for cell growth and maintenance as they facilitate the transfer of nutrients, gases, metabolic waste and cell signaling molecules. Furthermore, convenient tunability of these scaffolds allows for the incorporation of sophisticated biochemical cues in these networks to better mimic the native microenvironment.

In addition to preformed hydrogels, injectable *in situ* forming hydrogels are of significant interest for therapeutic and diagnostic applications. The ability to introduce the injectable *in situ* forming hydrogels via simple injection significantly increases patient compliance relative to preformed hydrogels, which must be crosslinked *in vitro* and then surgically implanted *in vivo*. The injectable hydrogels can be processed in the operating room, can be used to fill irregularly shaped defects as the implants are formed *in situ* at the defect site, can shorten surgical time, minimize surrounding tissue damage and reduce postoperative pain and scar size. Moreover, with injectable gels, the gelation takes place under very mild physiological conditions allowing for the successful encapsulation of cells and biologically active proteins or peptides for regenerative applications (Nguyen, Lee 2010).

The biological properties of bone and cartilage tissue are highly distinguished from each other with regards to physical structure, vascularity, growth factors and cell types. As a result of this uniqueness, there are distinct demands for design and use of biomaterials for the regeneration of these tissues. For cartilage regeneration, hydrogels may effectively able to serve as ECM mimics. However, due to the high mechanical strength and structural complexity of bone, hydrogels may be effectively used as carriers for biological growth factors and cells to aid bone regeneration.

### 2.1.2 *In situ* gelling hydrogel systems

Several criteria need to be met to develop an ideal *in situ*-forming injectable gel for biomedical applications. These include: 1. Solubility in aqueous media with gelation occurring in physiological conditions (temperature, pH and ionic concentration); 2. No release of harmful by-products upon gelation; 3. Gelation occur at a sufficiently rapid rate for clinical efficacy, however allow adequate time for proper mixing and injection of the solution in the presence of additives such as cells and/bioactive molecules (Ma, Elisseeff 2005).

Hydrophilic polymers that can undergo gelation in response to different types of stimuli have been developed either by modifying existing polymers or by specifically designing polymers with stimuli sensitive units along the polymer chain. The various stimuli of interest for biomedical applications include light (photo-polymerizing/photo-gelling systems), chemical agents (chemical and ionic crosslinking systems) as well as environmental stimuli from the physiological environment (temperature, pH and ionic strength). Physical and chemical crosslinking methods can be used to develop hydrogels. Physical crosslinking of the polymers is generally considered to be milder than chemical crosslinking reactions. Hydrogels formed by ionic and thermogelation are examples of those formed via physical crosslinking. On the downside, the instability and reversibility of many of these systems yields low mechanical properties (Nguyen, Lee 2011). Chemical crosslinking generally yields more stable hydrogels with better mechanical properties relative to those formed by physical crosslinking. The main drawback of chemical crosslinking is the need to incorporate reactive compounds and/or photoirradiation, which may lead to toxicity problems. However, recent advances in

chemical crosslinking methods led to the development of systems that undergo gelation under mild reaction conditions. Examples of various hydrogel materials and their crosslinking mechanism are listed in Table 1.

Table 1. Various hydrogel materials, crosslinking initiators and mechanism.

Material	Gel Precursors	Crosslink Mechanism	Reference
Pluronics	Macromer(s): PEO-PPO-PEO Initiator: temperature (37°C)	Physical	(Ruel-Gariepy, Leroux 2004)
Chitosan-Pluronics	Macromer(s): chitosan and pluronics Initiator: temperature (37°C)	Physical	(Weng et al. 2001)
Chitosan–AHP	Macromer(s): chitosan and AHP Initiator: temperature (37°C)	Physical	(Nair et al. 2007)
Chitosan-glycerol phosphate	Macromer(s): Chitosan and glycerol phosphate Initiator: temperature (37°C)	Physical	(Ahmadi, de Bruijn 2008)
PPF-co-ethylene glycol	Macromer(s): hydrophobic PPF and hydrophilic PEG Initiator: light	Covalent	(Fisher et al. 2004)
Hyaluronic acid	Macromer(s): tyramine substituted hyaluronic acid Initiator: HRP enzyme	Covalent	(Darr, Calabro 2009)
Hyaluronic Acid-Pluronics	Macromer(s): Hyaluronic Acid and pluronics Initiator: temperature (37°C)	Physical	(Jung, Park & Han 2010)
SMO-PCLA-PEG-PCLA-SMO copolymer hydrogel	Macromer(s): pH-sensitive SMOs and thermo-sensitive PCLA-PEG-PCLA Initiator: temperature (37°C) and pH (7.4)	Physical	(Shim et al. 2006)
oxidized alginate, gelatin and biphasic calcium phosphate	Macromer(s): oxidized alginate, gelatin and biphasic calcium phosphate	Covalent	(Nguyen, Lee 2011)

#### 2.1.2.1 Physically crosslinked hydrogels

Thermo-gelation is one of the most extensively investigated strategies to develop physically crosslinked *in situ* gelling polymers. N-isopropyl-acrylamides (NIPAAm), pluronics and various PEG based polymers are some of the most widely used non-degradable thermo-gels (Ruel-Gariepy, Leroux 2004). Aqueous solutions of triblock copolymers composed of PEO and PPO (PEO-PPO-PEO) exhibit sol-to-gel phase



transitions at physiological temperatures and are commercially known as Pluronics. Chondrocytes suspended in Pluronics "painted" onto a tissue engineered osseous surface resulted in a bone-cartilage interface for mandibular condylar reconstruction (Weng et al. 2001). Even though pluronics has advantages such as mild gelation, ability to increase the stability of encapsulated proteins, and good biocompatibility, the low mechanical integrity of the gel, non-degradability, limited gel stability with quick dissolution and high permeability limits its biomedical applications (Liu et al. 2007). This led to the development of several degradable block co-polymers with hydrolytically sensitive blocks such as poly(lactic acid/glycolic acid) or poly( $\epsilon$ -caprolactone) and pluronics/PEG/NIPAAm units as potential candidates for biomedical applications (Cohn et al. 2006, Jeong, Bae & Kim 2000, Chen, Singh 2005). Thermosensitive chitosan-pluronic hydrogel has proven itself to be a successful injectable cell delivery vehicle for cartilage regeneration (Park et al. 2009). Composite thermosensitive hydrogel using pluronic derivatives and crosslinked hyaluronic acid (X-HA) loaded with TGF $\beta$ 1 have been shown to increase benefits in the induction of chondrogenic differentiation of human adipose-derived stem cells in a full-thickness defect of rabbit knee articular cartilage model (Jung, Park & Han 2010).

A pH- and temperature-sensitive hydrogel of sulfamethazine oligomer, poly( $\epsilon$ -caprolactone-co-lactide)-poly(ethyleneglycol)-poly( $\epsilon$ -caprolactone-co-lactide) (SMO-PCLA-PEG-PCLA-SMO) pentablock copolymer was synthesized by adding pH-sensitive SMOs to either end of a thermo-sensitive PCLA-PEG-PCLA block copolymer. This copolymer solution forms stable gel under physiological conditions (pH 7.4 and 37°C), but not at high pH (pH 8.0) or at increased temperatures (ca. 70°C) (Shim et al. 2006).

pH/temperature-sensitive hydrogel of poly(beta-amino ester)-poly( $\epsilon$ -caprolactone)-poly(ethylene glycol)-poly( $\epsilon$ -caprolactone)-poly(beta-amino ester) (PAE-PCL-PEG-PCL-PAE) pentablock copolymer was evaluated as a sustained injectable insulin delivery system (Huynh et al. 2009). Insulin was ionically linked forming an insulin-PAE complex and was steadily released for 15 days in a Sprague-Dawley rat subcutaneous model (Huynh et al. 2009). The ability of these systems to undergo gelation under physiological conditions (pH 7.4 and 37°C) makes them strong candidates for therapeutic applications.

Apart from synthetic polymers, several natural polymers have also been used to develop thermogels mostly due to their innate thermo-sensitivity. Methyl cellulose, a biocompatible polysaccharide can undergo thermogelation around 37°C due to the hydrophobic interactions between molecules containing methoxy substitution. Ghanaati *et al.* evaluated the efficacy of an injectable composite bone substitute composed of  $\beta$ -tricalcium phosphate ( $\beta$ -TCP), methyl cellulose and hyaluronic acid. The presence of the polymeric phase decreased the degradation time of  $\beta$ -TCP and at the same time increased the vascularization of the construct (Ghanaati et al. 2011). Chitosan is another polysaccharide that is attracting significant attention as a biomaterial due to its biodegradability, biocompatibility and wound healing properties. We have developed an injectable thermo-gelling system based on chitosan using inorganic phosphate salts as the neutralizing and thermo-gelling agent (Nair et al. 2007). The *in situ* gelling system was developed by adding ammonium hydrogen phosphate (AHP) to chitosan solution at low temperature. The system has been found to be highly versatile with gelling time varying from 5 minutes to several hours at 37°C by varying the concentration of the phosphate

salt. The injectability of the system as well as the feasibility of using chitosan–AHP thermogels as a cell delivery vehicle has been demonstrated (Nair et al. 2007). Biocompatible, chitosan-glycerol phosphate hydrogels have also been demonstrated to stimulate mesenchymal stem cell proliferation as a potential vehicle for cell encapsulation (Ahmadi, de Bruijn 2008). Furthermore, chitosan molecules, which share glycosaminoglycan (GAG) structural features, have been crosslinked with proteins or other GAGs to promote chondrogenesis (Suh, Matthew 2000). Various reagents such as  $\beta$ -glycerophosphate, genipin and glyoxal have been investigated to develop composite injectable hydrogels of chitosan with proteins such as collagen (Wang, Stegemann 2010, Wang, Stegemann 2011). Hydroxy butyl chitosan (HBC), a water-soluble thermosensitive polysaccharide, can undergo physical gelation under physiological conditions and has also been investigated as a cell delivery vehicle (Dang et al. 2006).

Agarose, a polymer isolated from red algae and seaweed, crosslinked via hydrogen bonds has been shown to be well suited for 3D cell encapsulation, especially for chondrocytes (Benya, Shaffer 1982, Buschmann et al. 1992). BMP2-transduced mesenchymal stem cells (MSCs) form more cartilage-like tissue in agarose gels than in other matrices, such as collagen and alginate. This has been attributed to the tendency of agarose gel to resist blood vessel invasion resulting in low oxygen tension that facilitate cartilage tissue formation (Xu et al. 2005).

Alginic acid, another polysaccharide present in brown algae has also been extensively investigated for cell encapsulation. Alginic acid can undergo rapid ionotropic gelation in the presence of various divalent cations, including calcium, zinc and strontium (Wee, Gombotz 1998, Rowley, Madlambayan & Mooney 1999, Place et al. 2011).

Calcium-alginate gels are studied as a scaffold for encapsulating non-adherent cells such as chondrocytes as it does not mediate mammalian cell adhesion due to its poor binding of serum proteins (Smetana 1993). This will allow for maintaining the spherical morphology of chondrocytes in alginate gels. In comparison with the native cartilage tissue, the calcium-alginate hydrogels display slightly lower water content and compressive modulus but the tensile modulus of these hydrogels match well with that of the tissue (Wan et al. 2008). On the other hand, since osteoblasts may not thrive in a non-adhesive hydrogel environment, the chemistry of hydrogels may further be amended (i.e., covalent grafting of adhesion peptides (Hern, Hubbell 1998, Mann et al. 1999, Rowley, Mooney 2002) and tethering growth factors (Mann, Schmedlen & West 2001)). Hydrogels modified with cell surface adhesion peptides, such as arginine-glycine-aspartic acid (RGD), can improve osteoblast adhesion and matrix synthesis within the 3D polymer network (Burdick, Anseth 2002, Alsberg et al. 2001).

Gelatin is the denatured form of the ECM's main component, collagen, and has been used successfully as a cell vehicle in chondrogenesis studies (Ponticciello et al. 2000) and bone tissue engineering (Payne et al. 2002). Crosslinking of gelatin polymer has been demonstrated in various ways including physical crosslinking due to its thermosensitivity. However, the use of these biodegradable matrices formed via physical crosslinking is limited due to their weak structure at physiological temperature (Landers et al. 2002).

Self-assembled peptide-amphiphile (PA) molecules, which consist of a peptide segment coupled to a fatty acid chain, into 3D nanofiber networks have been shown to support cell processes, including cell migration, proliferation and differentiation within

the hydrogel (Paramonov, Jun & Hartgerink 2006, Silva et al. 2004, Hosseinkhani et al. 2006b). The formation of self-assembling gels is driven by the hydrophobic core, which is composed of closely packed alkyl tails, and the fibrous strands that build-on via hydrogen bonds between the amino acids of adjacent PA molecules. Self-assembly can be triggered upon mixture of PA solutions with cell culture media or other physiological fluids that contain polyvalent metal ions (Zhang 2002, Zhang 2003). The PA system presents a versatile platform, where in molecules can be designed and developed for specific applications. PA system has been developed that allows for mineral deposition (Hartgerink 2004), optimized cell adhesion (Harrington et al. 2006, Guler et al. 2006) and supports ectopic bone formation (Hosseinkhani et al. 2006b). Another interesting variation of PA systems includes the *in situ* hydrogel formation through ionic interactions between negatively charged PAs and a positively charged basic fibroblast growth factor (bFGF) (Hosseinkhani et al. 2006a). Although these types of self-assembling systems are inherently biocompatible and versatile, they may present difficulties for precisely controlling the gelation and mechanical properties.

#### **2.1.2.2 Covalently crosslinked hydrogels**

Visible or near ultra violet light induced photo-polymerization is one of the most extensively investigated *in situ* gelation process for developing injectable covalently cross-linked hydrogels. Biodegradable photocurable polymers form a versatile class of injectable biomaterials as the aqueous polymer solution can be introduced to the desired site *via* injection followed by photo curing *in situ* using fiber optic cables. The most extensively investigated route involved water-soluble polymers with acrylic/methacrylic side groups that can undergo photo-polymerization *via* a radical chain polymerization

mechanism initiated by appropriate photo-initiators. Moreover, photopolymerization allows for temporal and spatial control over scaffold formation, enabling the implantation of complex structures such as multilayered hydrogels in a minimally invasive manner with minimal heat production. Multilayered photopolymerizable hydrogels facilitate the encapsulation of multiple cell types in a stratified organization and also control of spatial presentation of bioactive factors within the scaffold. Zonal organization of articular cartilage is of structural and functional importance. To achieve zonal distribution of multiple cell types, researchers have combined cells with photosensitive polymers that could be injected and gelled *in situ* or photopolymerized in layers, reproducing the structures of articular cartilage and osteochondral tissue (Hunziker, Quinn & Hauselmann 2002, Hu et al. 2001).

Poly(propylene fumarate) (PPF), a biocompatible and biodegradable polyester that can be crosslinked through its fumarate double bond, undergoes cell-friendly biodegradation as one of its degradation products include fumaric acid, a substance which occurs naturally as a part of the Krebs's cycle (Kasper et al. 2009). Peter *et al.* used PPF to successfully produce chemically crosslinked hydrogels *in vivo* capable of acting as an injectable bone cement (Peter et al. 1997). Furthermore, a polymer-based system of copolymer PPF-co-ethylene glycol, formed from hydrophobic PPF and hydrophilic PEG, support chondrocyte survival and ECM production (Fisher et al. 2004). The versatility of PPF and its ease of modification lend itself to be an excellent candidate for bone and cartilage replacement. The material property allows it to be injected into irregularly shaped bone voids *in vivo* and provide good mechanical stability to support bone regeneration. Recently, osteoblasts have been added to the PPF construct to improve the

rate and extent of new bone formation (Payne et al. 2002). TGF $\beta$ -loaded PPF composite scaffolds was shown to act directly on cell migration and differentiation within the material (Peter et al. 2000, Lu, Stamatias & Mikos 2000, Lu, Yaszemski & Mikos 2001). Porter *et al.* has developed porous composites from PPF and tricalcium phosphates as scaffolds for bone regeneration. The moduli of the composites are on the order of magnitude of trabecular bone indicating that these composites are attractive candidates for use as a replacement scaffold for trabecular bone (Porter et al. 2000).

Photo-crosslinkable dendrimers, which are highly branched and regularly structured macromolecules composed of natural metabolites (i.e., succinic acid, glycerol, and beta-alanine), and non-immunogenic PEG have been synthesized using ester and carbamate forming reactions. Histological analysis of the photo-crosslinked macromer solutions in a rabbit osteochondral defect showed good attachment in the defect site and presence of collagen II and GAGs in contrast to the contralateral unfilled defects. The strong potential of these dendrimer-based, photocrosslinked hydrogels as scaffolds for osteochondral defect repair was illustrated by its good mechanical properties, lower water absorption, good adhesion to the defect site, and positive *in vivo* performance (Degoricija et al. 2008).

Even though degradable injectable photo crosslinkable systems presents unique advantages, the gelation process does present some limitations such as residual high molecular weight kinetic chains upon gel degradation, mild toxicity associated with the photo-initiators, limited control over the network evolution mechanism during chain-growth and also light attenuation by the initiators restricting the maximum attainable cure depth of only a few millimeters (Rydholm, Bowman & Anseth 2005).

To circumvent the limitations of photo-polymerization, crosslinking using thiolated polymers have been proposed. The thiolated polymers form degradable networks through Michael-addition type reaction when reacted with polymers containing acrylate, acrylamide or vinyl sulfone groups (Lutolf, Hubbell 2003, Vernon et al. 2003). The thiol based systems has shown to form crosslinked networks with better control over the crosslink density, eliminate high molecular weight degradation products as the degradable segments get incorporated throughout the network and allow samples to be cured to depths exceeding 10 cm and therefore have significant potential as an *in situ* gelling system for cell encapsulation (Rydholm, Bowman & Anseth 2005).

Polymeric aldehydes derived from polysaccharides having vic-diols using periodate chemistry are potential candidates for developing injectable fast gelling systems due to their chemical reactivity. An *in situ* gelling non-toxic system via the crosslinking of oxidized alginate and amino groups of gelatin has been reported (Balakrishnan, Jayakrishnan 2005). Recently, Nguyen *et al.* fabricated a composite gel consisting of oxidized alginate, gelatin and biphasic calcium phosphate as a bone graft substitute (Nguyen, Lee 2011). Covalent crosslinking of the composite was achieved via Schiff-base reaction between the aldehyde groups of oxidized alginate and amino groups of gelatin (Boanini et al. 2010, Liao, Zhang & Chen 2009). The osteogenic properties of the composite have been attributed to the calcium phosphate ceramics, which release calcium and phosphate ions upon degradation that are beneficial to bone formation. Furthermore, the system presents excellent tunability wherein the degree of crosslinking, water uptake and mechanical strength may be controlled by the degree of alginate oxidation. With



excellent biocompatibility and biodegradability, this composite is an example of a promising injectable biomaterial for bone regeneration.

#### 2.1.2.2.1 Enzymatically crosslinked hydrogels

Another emerging technique for developing *in situ* gelling system for biomedical applications is based on enzyme-catalyzed crosslinking reactions due to the mild, cell-friendly and natural crosslinking process involved (Table 2, Figure 3). Enzymatic crosslinking of hydrogels is an innovative alternative to other crosslinking methods, such as the photo-polymerization or physical crosslinking. Drawbacks to other crosslinking methods include cytotoxicity in photo-polymerized gels and insufficient mechanical strength in physically crosslinked gels. These limitations may be overcome through the use of enzymes to covalently crosslink polymers to form hydrogels. Transglutaminases and horseradish peroxidases (HRP) are highlighted as enzyme systems involved in hydrogel crosslinking.

Transglutaminase has been investigated as a biocompatible catalyst to crosslink polymers containing glutamine and lysine residues in a calcium-dependent reaction (McHale, Setton & Chilkoti 2005a, Yung, Bentley & Barbari 2010, Davis et al. 2010b). Tissue transglutaminase is naturally found *in vivo* during wound healing for the purpose of stabilization and organization of the ECM (Greenberg, Birckbichler & Rice 1991). Members of the transglutaminase family have been used to crosslink polymers, including PEG (Hu, Messersmith 2003, Ehrbar et al. 2007) and elastin-like protein polymers (McHale, Setton & Chilkoti 2005a) to form gels.

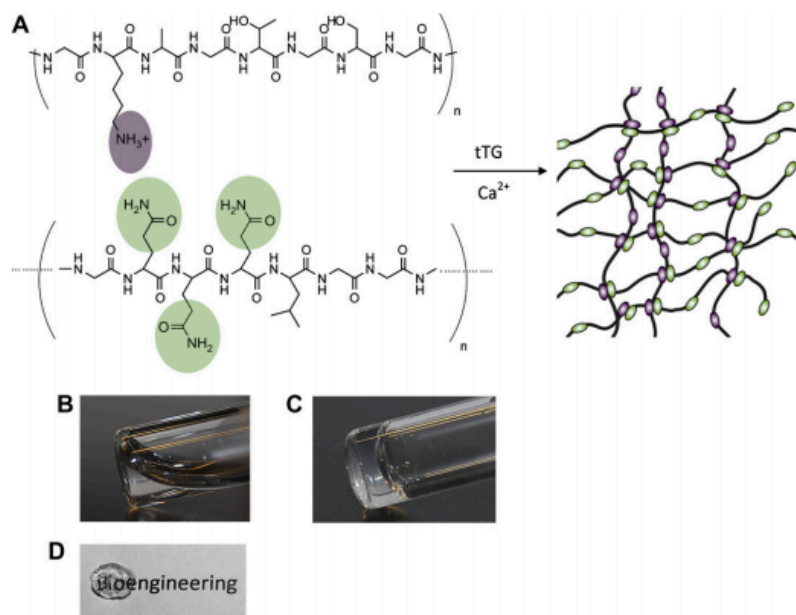


Figure 2. Enzymatically crosslinked recombinant protein by transglutaminase (TG) enzymatic crosslinking.

(A) Schematic of the protein hydrogel formation by tissue transglutaminase enzymatic crosslinking. (B&C) Photograph of the precursor solution before and after enzymatic gelation with tTG. (D) Photograph of a transparent hydrogel crosslinked by TG. Image taken from (Davis et al. 2010a)

Several synthetic and natural polymers functionalized with tyramine, tyrosine or aminophenol side groups are currently under development that can form *in situ* gels by phenol or aniline derivative coupling using hydrogen peroxide as an oxidant catalyzed by HRP (Kurisawa et al. 2005, Kobayashi, Uyama & Kimura 2001, Jin et al. 2007a, Lee, Wagoner Johnson & Murphy 2010). HRP-mediated crosslinking takes place at physiological pH and temperature and the gelation time can be modulated to a great extent by varying the reagent concentrations, making this a potential route to form injectable cell and protein delivery vehicles (Sakai et al. 2009, Hu et al. 2009). For example, tyramine substituted hyaluronic acid was developed to form injectable gels in the presence of HRP (Darr, Calabro 2009). The injectable system has several advantages

as the gelation time, equilibrium swelling and storage modulus of the gel may be adjusted by varying the degree of substitution of tyramine residues and polymer concentration. Furthermore, the mild enzymatic crosslinking has shown to be highly suitable for chondrocyte encapsulation as it allow for high viability of encapsulated chondrocytes, maintenance of the encapsulated cells' round morphology, increased production of glycosaminoglycans and collagen type II (Jin et al. 2010a).

**Table 2. Enzyme-catalyzed crosslinkable hydrogels and potential applications.**

*Table adapted from (Teixeira et al. 2012)*

Gel type/composition	Enzyme type	Potential applications	References
Fibrin gel	Factor XIIIa (transglutaminase isoenzyme)	Angiogenesis	(Eyrich et al. 2007, Hall, Baechi & Hubbell 2001)
		Bone and cartilage tissue repair	
8-arm PEG-peptide conjugates	Factor XIIIa (transglutaminase isoenzyme)	Drug delivery systems	(Ehrbar et al. 2007, Sala et al. 2010)
Elastin-like polypeptide gels	Tissue transglutaminase	Cartilage tissue repair	(McHale, Setton & Chilkoti 2005b)
PEG-peptide conjugates		Surgical tissue adhesives	(Hu, Messersmith 2005)
		Cartilage tissue repair	
Gelatin	Microbial transglutaminase	Scaffolds for tissue engineering	(Yung et al. 2007)
Gelatin	Calcium-independent microbial transglutaminase	Microfluidic biosensor systems	(Chen et al. 2003b)
Gelatin-chitosan conjugates	Tyrosinase	Tissue glue	(Chen et al. 2003a)
Gelatin-chitosan conjugates		Film biofabrication	(Wu, Bentley & Payne 2011)
Coil-chitosan bioconjugate		Protein immobilization	(Demolliens et al. 2008)
Coenzyme A-functionalized PEG	Phosphopantetheinyl transferase (surfactin synthetase)	Cell biology	(Mosiewicz, Johnsson & Lutolf 2010)

Supramolecular tyrosine-based hydrogel	Alkaline phosphatase	Assay platform for enzyme inhibitors	(Li et al. 2010)
Chitosan-glycolic acid conjugates modified with phloretic acid	Horseradish Peroxidase	Cartilage tissue repair	(Jin et al. 2009)
Hyaluronic acid-tyramine		Protein delivery	(Lee, Chung & Kurisawa 2009b, Kim et al. 2011)
		Cartilage tissue repair	
Carboxymethylcellulose		Biomedical applications	(Ogushi, Sakai & Kawakami 2007)
Dextran-tyramine conjugates		Protein delivery	(Jin et al. 2007b)
Dextran-hyaluronic acid conjugates		Cartilage tissue repair	(Jin et al. 2010b)
Dextran-heparin		Cartilage tissue repair	(Jin et al. 2011)
Tyramine-terminated PEG		Drug delivery	(Tran et al. 2010)

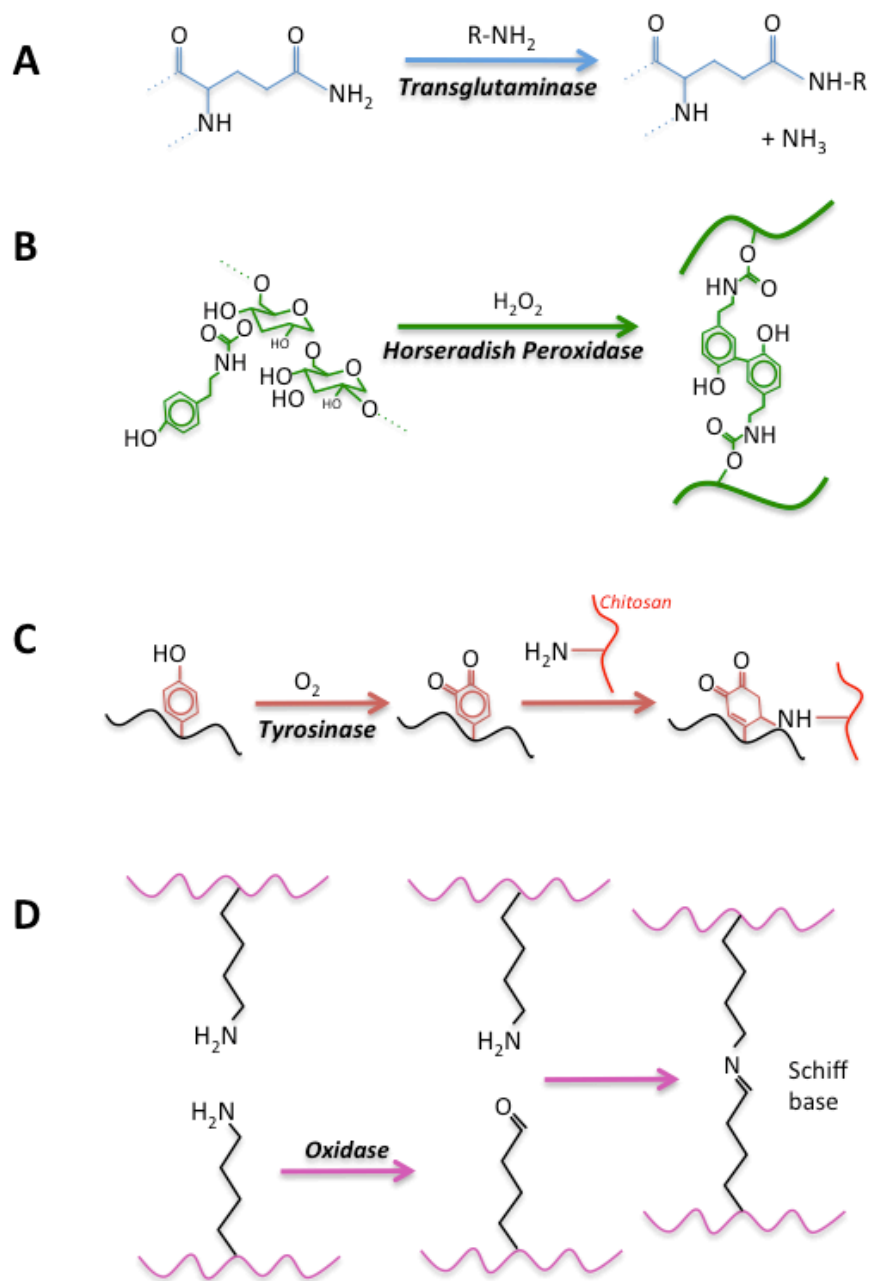


Figure 3. Schematic mechanism of the enzyme-mediated crosslinking systems.

A) *Transglutaminase*, B) *horseradish peroxidase*, C) *tyrosinase* and D) *oxidase* enzymatically crosslink polymer to form gels. Figure modified from (Teixeira et al. 2012)

### 2.1.3 Application of hydrogels

Hydrogels may be utilized as localized delivery vehicles by homogenously incorporating cells, growth factors and other bioactive compounds while concomitantly allowing diffusion of nutrients and metabolites. Hydrogels may serve as a transient biomimetic scaffold with suitable mechanical and viscoelastic properties in many applications such as cartilage regeneration, serve as a suitable vehicle to locally deliver appropriate growth factors and cells to facilitate regeneration of tissues such as bone. Physical, chemical and biological properties of hydrogels can be modulated by chemical and biological modifications by the incorporation of functional groups, cells or growth factors to facilitate tissue regeneration (Figure 4).

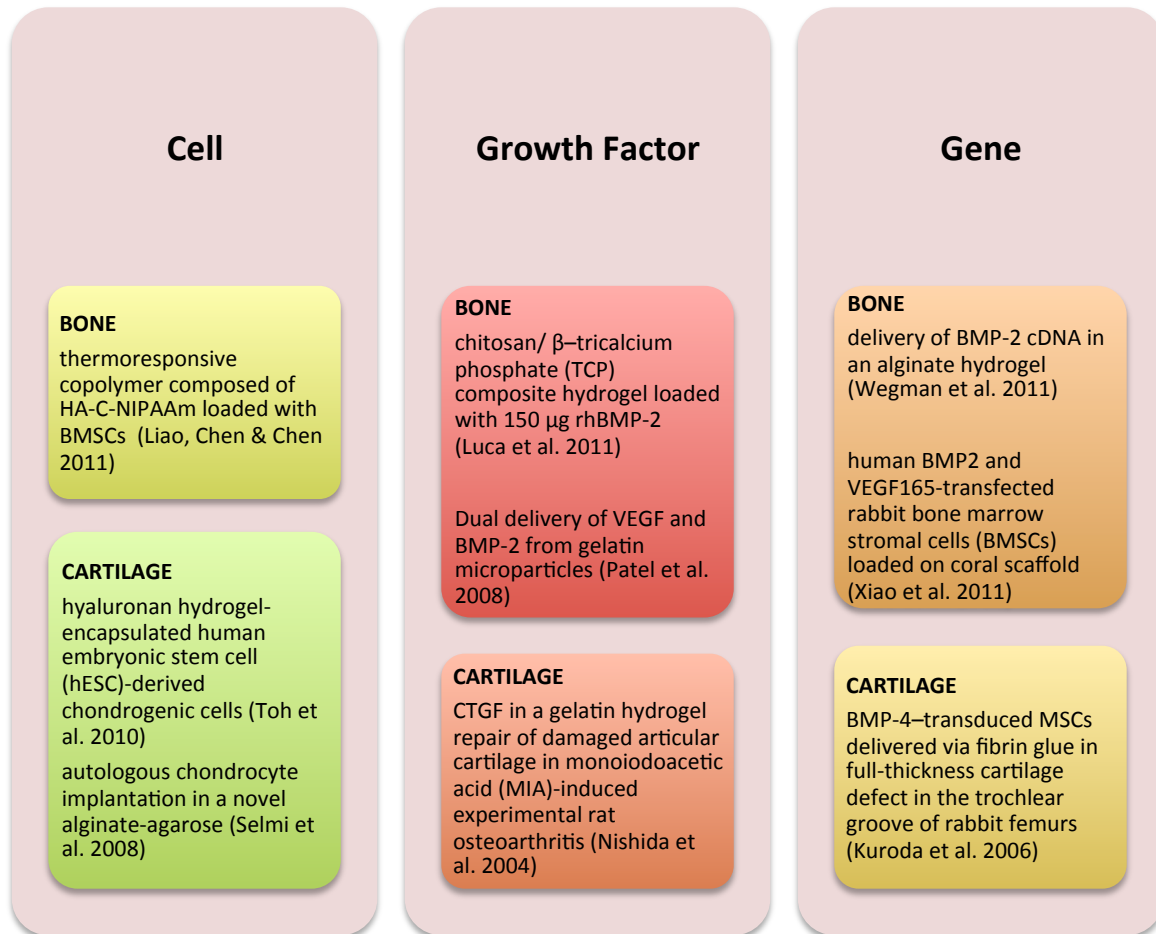


Figure 4. Examples of hydrogels as growth factor, gene and cell delivery systems.

#### 2.1.3.1 Enhancing mechanical properties and mineralization of hydrogels

As viscoelastic solids, hydrogels characteristically possess low static and dynamic moduli due to their high water content and high permeability for oxygen, nutrients and other water-soluble metabolites. Due to the limited mechanical strength of hydrogels, they have been widely considered to be excellent therapeutic delivery devices of cells and growth factors for soft-tissue engineering and ideal porous scaffolds when load-bearing support is unnecessary. The challenge of tissue-engineered grafts is to also match the mechanical properties of native bone or cartilage tissue (Hutmacher 2000). Recent

advances in polymer synthesis and processing made it possible to increase the mechanical strength of hydrogels in various ways, including addition of covalent crosslinks, increasing the crosslinking density, increase of monomer content, addition of fillers and biodegradable fibers and preculturing to allow embedded cells to generate functional tissue before implantation (Anseth, Bowman & Brannon-Peppas 1996, Kloxin et al. 2010, Salinas, Anseth 2009).

One approach commonly used to increase the mechanical properties of hydrogel for bone tissue engineering is to develop mineralized composite systems. Various strategies have been employed to induce mineralization in inert, non-mineralizing hydrogels for the use of bone tissue engineering (Gkioni et al. 2010). Major strategies for hydrogel mineralization include (1) the addition of inorganic particles, (2) the creation of nucleation sites by biomimetic methods, and (3) the derivatization of the polymeric hydrogel backbone with anionic functional groups. The addition of inorganic phase allows for the dispersed minerals to promote nucleation, subsequent hydroxyapatite formation and provides cell adhesion sites that enable integration with surrounding bone tissue (Rea, Best & Bonfield 2004). Finally, as the temporary hydrogel degrades the on-going mineralization will allow for replacement by new bone formation and thus increase mechanical stability.

#### **2.1.3.2 Enhancing biological properties by growth factor loading**

Bone regeneration is a coordinated cascade of spatio-temporal events regulated by several cytokines and growth factors. Biomaterial scaffolds are used to retain growth factors at the orthopedic defect site for an appropriate period of time to allow native cells to migrate to injury site, then proliferate and differentiate. A recent study used a



biopolymer chitosan/  $\beta$ -tricalcium phosphate (TCP) composite hydrogel loaded with 150  $\mu$ g recombinant human BMP2 (rhBMP2) in a 15 mm critical-size defect in the radius of a rabbit to demonstrate successful osteoinduction (Luca et al. 2011). However, many other studies have demonstrated that osteogenic factors alone may not be sufficient for optimal bone regeneration due to inadequate vascularization. Therefore, the combined delivery of osteogenic and angiogenic factors have been studied to enhance bone regeneration. Since VEGF and BMPs are key regulators of angiogenesis and osteogenesis during bone regeneration, various studies have investigated the effect of dose and temporal release of these growth factors from hydrogels on bone formation.

Dual delivery of VEGF and BMP2 from gelatin microparticles for bone regeneration in rat model having an 8 mm rat critical size defect led to synergistic effects on bone formation and enhancement of bone bridging and union of the critical size defect. At 12 weeks, the dual VEGF/BMP2 release showed bone formation within the scaffold pores and along the outer surfaces of the scaffold; osteoid secretion and mineralization were apparent, and new bone was often in close or direct contact with the scaffold interface (Patel et al. 2008). A supporting study demonstrated the delivery of VEGF and BMP2 to osteoprogenitor cell populations of human bone marrow stromal cells (HBMSC) positively effecting bone formation. HBMSCs seeded onto VEGF/BMP2 releasing, biodegradable composite composed of alginate and P(DL)LA significantly enhanced new endochondral bone matrix in a critical sized femur defect (Kanczler et al. 2010).

Since angiogenic growth factors are predominantly expressed during the early phases of regeneration for vascularity, whereas osteogenic growth factors are continuously expressed during bone formation and remodeling, the effect of sequential delivery of VEGF and BMP2 on bone formation was also investigated (Kempen et al. 2009). A composite scaffold which consisted of poly(lactic-co-glycolic acid) microspheres loaded with BMP2 embedded in a poly(propylene) scaffold surrounded by a gelatin hydrogel loaded with VEGF was used for the sequential release of the growth factors. The implantation of this scaffold resulted in a large initial burst release of VEGF within the first 3 days and a sustained release of BMP2 over the full 56-day implantation period. In the orthotopic defects, no effect of VEGF on vascularization was found, nor was bone formation higher by the combination of growth factors, compared to BMP2 alone. Contradictory to the previously mentioned growth factor delivery studies, this study demonstrates that a sequential release of VEGF followed by the sustained release of BMP2 may not be beneficial for bone regeneration relative to just BMP2 alone. Similarly, dual delivery of VEGF and BMP2 from porous PPF scaffolds incorporating gelatin microparticles on bone regeneration in a rat critical-size cranial defect model did not demonstrate that the addition of VEGF increased bone formation over BMP2 delivery alone (Young et al. 2009). An *in vivo* dose-dependent decrease in percentage of bone regeneration was observed for BMP2. The addition of VEGF was unable to reverse this decrease in bone formation, although improvements in the number of bridged defects did occur in some groups.

A significant shortcoming of hydrogel based growth factor delivery is high burst release leading to growth factor inactivation. To overcome this shortcoming and better

control the release kinetics, natural and synthetic materials have been functionalized with anchoring sites with affinity for the loaded growth factors. The repeated binding/interaction of growth factors to the functionalized recognizing species slows down their diffusion and prolongs release rate from the biomaterial. Key determinants of the growth factor release rate include the number of binding sites, the affinity of growth factor for the immobilized recognizing species, and the degradation rate of the hydrogel (Quaglia 2008). Heparin has been widely used as an interacting site due to the presence of heparin-binding domain on many growth factors. Heparinized collagen gels (Wissink et al. 2000, Steffens et al. 2004) and heparin-immobilized hydrogels based on thiol-functionalized PEGs (Nie et al. 2007) were synthesized and tested as growth factor delivery platform. More recently, heparin-immobilized macroporous PLGA scaffolds for the release of bFGF have been developed (Yoon et al. 2006). Another study utilized poly(L-lactide) and sucrose acetate isobutyrate-based coating around rhBMP2 – loaded collagen-chondrotin sulfate to extend rhBMP2 release period from 24 hour to 12 days (Keskin et al. 2005). The extended release of rhBMP2 from the biomaterial allowed for histologically well-organized bone formation.

As discussed before, articular cartilage has a poor healing capacity, and thus healing does not always entail cartilage regeneration. Studies have shown that controlled release of various pro-chondrogenic growth factors using hydrogel scaffolds may support articular cartilage regeneration. Intra-articular administration of collagen scaffolds loaded with BMP2 induces chondrogenic differentiation of marrow-derived MSCs (Mimura et al. 2011). RT-PCR results showed that the BMP2 administration enhanced chondrogenic differentiation. Another study demonstrated that the incorporation of

recombinant connective tissue growth factor (CTGF), a hypertrophic chondrocyte-specific gene product, in a gelatin hydrogel possessed the ability to repair damaged articular cartilage in monoiodoacetic acid (MIA)-induced experimental rat osteoarthritis. The repaired cartilage histologically looked similar to that of normal articular cartilage. Similar results were obtained using a 2 mm diameter, full-thickness rat articular cartilage defect treated with CTGF-loaded gelatin gel. At 4 weeks post treatment, new cartilage was found filling the defect (Nishida et al. 2004). The combined use of cells and growth factors loaded on to injectable hydrogels has proven to be constructive in the quest for optimal skeletal regeneration. PLGA microspheres loaded with IGF1 and TGF $\beta$ 1 and bovine articular chondrocytes were photoencapsulated in PEO-based hydrogels demonstrated statistically significant changes in GAG production and cell content compared to control gels either without microspheres or with blank microspheres after a 14 day incubation (Elisseff et al. 2001). These studies suggest that localized delivery of growth factors, such as BMP2, CTGF, IGF1 and TGF $\beta$ 1 via porous hydrogel scaffolds may be useful in therapeutic regeneration of articular cartilage.

#### **2.1.3.3 Enhancing biological properties by drug delivery**

Hydrogels may also be utilized to enhance the delivery and therapeutic efficacy of drugs. Biodegradable hydrogels have the potential to deliver a wide range of water-insoluble drugs. Recent studies have demonstrated that a biodegradable gelatin hydrogel can be used for the sustained release of water-insoluble simvastatin at a bone defect site (Tanigo, Takaoka & Tabata 2010). The release of biologically active simvastatin was accompanied by the biodegradation of hydrogel. In this study, simvastatin was water-solubilized by gelatin grafted with L-lactic acid oligomer and mixed with gelatin,

followed by chemical crosslinking to obtain gelatin hydrogels incorporating simvastatin. Bone healing of critical-sized nasal defects in rabbits by simvastatin in hydrogels has also been investigated (Mukozawa et al. 2011). At 2 and 4 weeks post-implantation, increased bone healing and BMP2 expression was seen in the animal groups with simvastatin delivered in the hydrogels. Other studies have also demonstrated the increased expression of BMP2, along with VEGF and Cbfa1 upon treatment with statin-loaded hydrogels (Wong, Rabie 2006). Thus, the delivery of drugs, such as statins, may be achieved via hydrogel delivery to enhance bone regeneration.

#### **2.1.3.4 Enhancing biological properties by gene delivery**

Another promising method of growth factor delivery in the field of bone-tissue engineering is the application of gene therapy (Caplan 2000, Chen 2001), which presents a simple approach to evade the difficulties involving the delivery of multiple growth factors. The transfer of genetic material into the genome of the target cell allows for high expression of bioactive factors from the local cells in the defect and delivering a more biologically active product that can be achieved by exogenous application of recombinant proteins. Gene therapy has the potential to provide control over the timing, distribution and level of multiple growth factors that can be either simultaneously or sequentially expressed in a tissue-specific manner; this approach may also provide a cure to diseases or offer transient growth and regeneration (Franceschi 2005).

The possibility of achieving osteogenic differentiation as a result of prolonged presence of BMP2 was investigated using plasmid DNA-based gene therapy. The delivery of BMP2 cDNA in an alginate hydrogel resulted in an increasing amount of biologically active BMP2 released from endogenous cells after 6 weeks of implantation

(Wegman et al. 2011). Combinatorial gene therapy has also been explored; human BMP2 and VEGF165-transfected rabbit bone marrow stromal cells (BMSCs) loaded on coral scaffold resulted in increased new bone formation, compared with any single factor in a critical-sized orbital defect rabbit model (Xiao et al. 2011).

#### 2.1.3.5 Enhancing biological properties by cell encapsulation

Numerous studies have utilized hydrogels as cell delivery vehicles for skeletal regeneration. Although hydrogels lack mechanical strength, they are extremely valuable and efficient in encapsulating and maintaining viable cells. Various cell types are available for engineering organized skeletal tissues. However, when selecting the optimal cell type for therapeutic application, one must consider a few different factors, including the *ex vivo* proliferative capacity of the cells, phenotypic stability and immunogenicity. Cell types that are currently considered for skeletal regeneration include fully differentiated cells, mesenchymal stem cells and embryonic stem cells.

Photoencapsulation of rat calvarial osteoblasts in injectable, non-adhesive PEG hydrogel modified with Arg-Gly-Asp (RGD) peptide for bone tissue engineering demonstrated increased mineral deposition (Burdick, Anseth 2002). However, a decrease in osteoblast viability of approximately 25% and 38% was seen after 1 day of *in vitro* culture when the macromer concentration was increased to 20 and 30wt%, respectively. A later study demonstrated collagen type I hydrogel allowed for the migration, proliferation and finally adoption of the osteoblastic fate of rat bone marrow stromal cells (rBMSCs) (Hesse et al. 2010). However, only about one third of the entire rBMSC population had the ability to actively migrate. Although this study contributes to the

development of novel bone grafts, it also presents current drawbacks of hydrogels as cell delivery vehicles for bone tissue engineering.

A recent study investigated the need for smart matrices in bone tissue-engineered grafts to provide an optimal environment for cells and retain osteoinductive factors for sustained biological activity. Slow-degrading, heparin-incorporated HA hydrogel loaded with primary osteoblasts and BMP2 facilitated the increase of bone-related genes after 8 weeks in rat femor. An arterio-venous loop provided an angiogenic stimulus and supported axial vascularization to provide nutrition for a bio-artificial bone graft. However, no significant increase in bone formation was observed histologically which might be explained by the absence of biomechanical stimulation as a result of the heterotopic isolation chamber. This suggests that optimization of osteogenic and angiogenic conditions are necessary to generate sufficient amounts of vascularized bone grafts for reconstructive surgery. This study also clearly demonstrated that the HA hydrogel supported growth and differentiation of osteoblasts *in vitro* and *in vivo* and allowed sustained release of BMP2 (Rath et al. 2011).

Also, while designing a cell delivery system, it must be noted that tissues are generally not homogenous from a cell perspective; they consist of multiple cell types in highly organized frameworks – termed microscale heterogeneity. For example, skeletal tissue consists of various cell types including osteocytes, osteoclasts, endothelial cells and chondrocytes. Engineering osteochondral tissues to have regulatory effects with each other, in turn, encourages more functional tissue development. Co-culture models of multiple cell types is especially exciting since different cells act cooperatively and bioactive factors secreted by one cell type provides cue for the action of its neighboring

cells. An important study that showed promise in bone regeneration and angiogenesis using a vascular endothelial cell/bone marrow MSC co-culture model (Sun et al. 2007). A later study went on to demonstrate the patterned microscale capability of 3D co-culturing endothelial cells and osteoblastic cells in a microchannel (Chueh et al. 2010). This simple and reversible hydrogel patterning method for 3D cell culture allowed for alginate gel to be formed in select regions of a microfluidic device through light-triggered release of caged calcium. Since microscale heterogeneity is central to cellular niches and tissue development, microscale engineering of hydrogels has proven to be a useful tool for tissue engineering (Sands, Mooney 2007). Furthermore, techniques to mimic the microscale heterogeneity of the ECM *in vitro* improve how scientists examine the interaction of cells.

Toti-potent embryonic stem cells possess the potential to differentiate into an unlimited array of cell types. Cartilage repair was seen using hyaluronan hydrogel-encapsulated human embryonic stem cell (hESC)-derived chondrogenic cells (Toh et al. 2010). In this study, hESC-derived chondrogenic cells produced ECM-enriched cartilaginous tissue construct when cultured in HA-based hydrogel. Furthermore, the use of this hydrogel/hESC system for the repair of rat critical-sized osteochondral defect resulted in an orderly spatial-temporal remodeling over 12 weeks into osteochondral tissue with good surface regularity and complete integration with the adjacent host cartilage. This study demonstrated the feasibility of using hESC-derived chondrogenic cells for cartilage tissue engineering.

Multi-potent mesenchymal stem cells have the ability to differentiate into several cell types to form new repair tissue. Bone marrow is a major source of mesenchymal



stem cells (BMSCs), which may contribute to the regeneration of bone and cartilage. Studies have investigated the biocompatibility of thermoresponsive copolymer composed of hyaluronic acid-g-chitosan-g-poly(N-isopropylacrylamide) (HA-C-NIPAAm) and its efficacy as a cell carrier for bone marrow stem cells (BMSCs). After 4 months of composite hydrogel/BMSCs implantation subcutaneously in nude mice, significant ectopic bone formation was confirmed via microCT analysis (Liao, Chen & Chen 2011).

The most widely studied synthetic gels for MSC encapsulation and cell delivery are based on PEG and PVA. PEG is biocompatible polyester that has been approved by FDA for many medical applications. Non-toxic, biodegradable PEG hydrogels are promising matrices for cell encapsulation (Sims et al. 1996, Chen et al. 2003) and has been shown to support BMSC chondrogenesis *in vitro* (Williams et al. 2003). Successful application of photopolymerizable PEG hydrogels towards the engineering of multilayered articular cartilage has been demonstrated (Alhadlaq, Mao 2005). MSCs were treated *ex vivo* for 3-4 days with either chondrogenic or osteogenic supplements and loaded into two hydrogel layers and cured via photopolymerization. Stratified layers of chondrogenesis and osteogenesis were observed after 4 weeks of implantation. In a recent study, swine auricular chondrocytes were photoencapsulated into two PEG dimethacrylate (PEGDM) copolymer hydrogels of different degradation profiles: degradable (PEG-4,5LA-DM) and nondegradable (PEGDM) macromers in molar ratios of 60:40 and 70:30. The less degradable PEGDM hydrogel supported higher glycosaminoglycan and hydroxyproline contents in the neotissue. This study demonstrated that PEGDM copolymer hydrogels can support *in vivo* chondrogenesis by photoencapsulating auricular chondrocytes (Papadopoulos et al. 2011). The control of

biomaterial degradation rate is essential for proper matrix synthesis of the encapsulated cells.

Autologous chondrocyte implantation is an established, FDA-approved method of treatment for cartilage repair. This treatment requires the removal of the chondrocytes from the patient's knee, expansion of the chondrocytes and subsequent implantation into the defect site. This procedure entails disadvantages such as donor site morbidity and also loss of chondrogenic phenotype during the cell expansion step. A recent study has utilized autologous chondrocyte implantation in a novel alginate-agarose hydrogel to demonstrate significant clinical improvement at follow-up at two years with predominantly hyaline cartilage-like repair tissue (Selmi et al. 2008). Another supporting study encapsulated bovine chondrocytes from corresponding zones of the femoral articular cartilage in photopolymerizing hydrogels to regenerate cartilage with zonal organization (Kim et al. 2003). However, the encapsulation of growth factors for modulation of chondrogenesis and osteogenesis may be necessary for further phenotypic maintenance of chondrogenic and osteogenic cells derived from MSCs *in vivo* (Lu, Yaszemski & Mikos 2001, Elisseeff et al. 2001).

Thusfar, no hydrogel biomaterial has been presented in literature to inherently increase cell survival, proliferation or osteogenesis (without the use of drugs, gene therapy or growth factors). Such bioactive biomaterial is warranted since these processes are necessary for successful bone formation and regeneration. The bioactivity of protein-based hydrogels in cell-based therapeutics may encourage encapsulated cells to recognize and bind to specific sites within proteins. The key for a successful regenerative biomaterial lies in its ability to interact with the surrounding environment and induce a

multitude of cell signaling pathways, including cell survival, proliferation and mineralization.

#### **2.1.4 Conclusions**

For optimal tissue regeneration, biomaterial scaffolds should not serve as a simple inert substrate; instead should serve as three-dimensional mediums for the dynamic extracellular signaling and facilitators for progenitor cell recruitment, growth and differentiation. Hydrogels may serve as excellent scaffolds for skeletal regeneration since their biomimetic properties and high water content presents a cell-friendly, natural microenvironment to support cell functions. The ability to conveniently control the chemistry and functionality of the hydrophilic polymers allow tailoring the physical and mechanical properties of hydrogels for bone and cartilage regeneration. The use of enzymatically-crosslinked hydrogels provides a mild, *in situ*-forming biomaterial system for the localized delivery of cells to support tissue regeneration. Our ability to incorporate specific and controlled biological activities in these hydrogels to modulate encapsulated cell performance can significantly increase their efficacy as scaffolds for skeletal tissue regeneration. Attempts have been made to increase the bioactivity of hydrogels by incorporating one or more growth factors in the gels. However, it is to be noted that tissue regeneration/healing is a complex process involving several bioactive molecules expressed under very tight spatio-temporal control. Since encapsulated cells are capable of producing these bioactive molecules, one attractive strategy will be to design and develop bioactive materials as injectable cell delivery vehicles that can induce the encapsulated cells to produce appropriate bioactive molecules for regeneration. We

explore the feasibility of developing such a novel injectable biomaterial system in the present study.

## 2.2 Lactoferrin as a biologically active molecule for bone regeneration

LF is described as a “moonlighting” protein as it possesses multifold functions (Gonzalez-Chavez, Arevalo-Gallegos & Rascon-Cruz 2009) (Figure 5) and its bioactivity is dependent on the specific physiological environment (Baker, Baker 2009). The regulation of LF synthesis, secretion and spatio-temporal distribution *in vivo* collectively play a part in determining its specific biological functions. Since successful skeletal tissue engineering requires concerted efforts of different cell types, the modulatory effect of LF on pluripotent cells, osteoblasts, osteoclasts and immune-modulating cells makes this glycoprotein a potential molecule to support skeletal tissue regeneration.

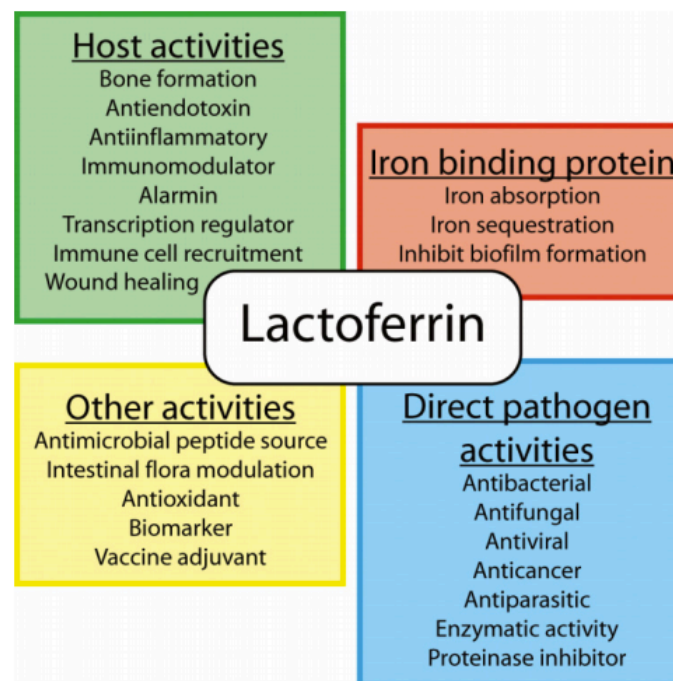


Figure 5. The wide range of beneficial functional properties described for LF.

*Image taken from (Vogel 2012).*

### 2.2.1 Molecular structure and composition

The structure and composition of a protein play very important roles in determining its biological functions. LF is a highly cationic protein with an isoelectric point of 8.0-8.5 (van et al. 2001). Structurally, it is a bilobal globular glycoprotein with a molecular weight of approximately 80 kDa. Anderson et al., reported the three dimensional structure of human diferric LF as comprising of two highly homologous globular lobes (N and C lobes), each containing one canonical trivalent ferric iron-binding site and one glycan, linked by an extended  $\alpha$ -helix (Anderson et al. 1987). The globular lobes of LF can bind to variety of cations such as trivalent  $\text{Fe}^{3+}$ ,  $\text{Ga}^{3+}$  and  $\text{Al}^{3+}$  and di- and trivalent transition metal ions  $\text{VO}^{2+}$ ,  $\text{Mn}^{3+}$ ,  $\text{Co}^{3+}$ ,  $\text{Cu}^{2+}$ , and  $\text{Zn}^{2+}$ . However, as the name suggests, LF has very high affinity for and is most commonly associated with trivalent ferric iron (Harrington 1992). For each cation bound to LF, one bicarbonate anion binds concomitantly and synergistically to the iron-binding crevice. The presence of the bicarbonate anion bound to LF is essential for metal binding and greatly increases the saturation of iron (Anderson et al. 1989).

Because of its ability to reversibly bind iron, LF can exist free of iron (apo-LF) or loaded with iron (holo-LF) (Schanbacher, Goodman & Talhouk 1993). As in the case of transferrins, the bound iron from LF can be released by the destabilization of the protein, which can be triggered perhaps by receptor binding *in vivo* and by lowering of the pH, reduction or the use of small-molecule chelating agents *in vitro*. The iron binding induces substantial structural changes of the globular lobes of LF, consistent with the closure or opening of the inter-domain cleft (Grossmann et al. 1992). The binding of the protein

ligands to the ferric iron and bicarbonate leads to the highly compact conformation of iron saturated-LF (Anderson et al. 1989). The presence of iron can also possibly affect the stability of the protein towards proteases. Studies have shown that the protein is more resistant to proteolysis, especially in its iron-saturated holo form (Brines, Brock 1983, Brock et al. 1976). However, species differences do exist and human apo-LF has been found to be more stable compared to bovine apo-LF (Brines, Brock 1983). It is important to note that the vast majority of the molecular surface remains the same when LF is “open” or “closed” state, therefore the surface receptor binding sites are likely to be unaffected by iron status. However, the structural dynamics of the open binding cleft of apo-LF provides additional sites for molecular interactions compared to holo-LF which implies possible differences in their biological functions (Baker, Baker 2009).

Another important structural component of LF is the nature and extent of glycosylation. All LFs are glycosylated although the glycosylation profile (the number and location of potential glycosylation sites and sites actually used) is species-specific. Bovine LF (bLF) has five potential glycosylation sites (Goodman, Schanbacher 1991), out of which only four sites are known to be glycosylated. Native human LF (hLF) contains three potential N-glycosylation sites, located at Asn138, Asn479, and Asn623. Two sites are glycosylated by complex-type *N*-glycans and the third putative site (Asn623) is unglycosylated (Spik et al. 1982, van Berkel et al. 2002a). Natural hLF contains complex highly branched, highly sialylated and highly fucosylated structures. The glycosylation patterns of LF have also been shown to be tissue/cell – specific. LF is often associated with secretion of mucosal tissues and with neutrophilic granules. Even though no significant differences in protein moiety have been reported between the

mucosal and neutrophilic LF, they show difference in molecular weight (Levay, Viljoen 1995b). It has been reported that the digestion of the two forms with N-glycanase resulted into a single protein band of approximately the same apparent molecular weight indicating that the difference in molecular weight is mainly due to difference in glycosylation (Hurley et al. 1993). Human milk lactoferrin glycan differs from the neutrophilic protein in the presence of  $\alpha$ -1,6 and  $\alpha$ -1,3 fucose residues and in the degree of sialylation (Levay, Viljoen 1995b). The recombinant forms of LF also show differences in the composition of carbohydrate chains and vary according to the specific species expression system. The glycosylation patterns of rhLF have been investigated in forms that were expressed in maize, tobacco, rice and cattle transgenic systems (Fujiyama et al. 2004, Samyn-Petit et al. 2003, Samyn-Petit et al. 2001, Yu et al. 2010). The recombinant form produced in the milk of transgenic clone cattle has been found to be approximately 2 kDa smaller than that of native form, due to the differences in N-glycosylation (Yu et al. 2010). As discussed before, neutrophilic LF, unlike the milk-derived protein, is not fucosylated – however, the difference in the molecular structure and functions of the two naturally occurring forms are not completely understood. On the other hand, rhLF, obtained from rice, contains N-glycans that are of high mannose, hybrid structures with low sialic acid and fucose, which are common post-translational modification patterns (van Berkel et al. 2002a, Nandi et al. 2005). A recent study investigated the difference in properties of glycosylated and non-glycosylated human LFs showed that deglycosylation did not affect its iron-binding and/ release as well as thermal stability (Baker, Baker 2009). However, based on some of the reported studies, it is

possible that the glycosylation pattern of LF might affect some of the biological activities of the protein such as immune-regulatory functions (Yu et al. 2010).

### **2.2.2 Role of lactoferrin in ferrokinetics**

LF is a pleiotrophic factor that exhibits a vast range of biological functions, including anti-microbial, anti-inflammatory, iron homeostasis, osteogenesis, angiogenesis and immuno-modulation (Gonzalez-Chavez, Arevalo-Gallegos & Rascon-Cruz 2009). Of the many biological functions credited to LF, the protein was initially well recognized for its ability to bind iron. Among the members of the transferrin family, LF has the ability to retain iron over a wide pH range. LF's possible role in ferrokinetics is attributed to its great affinity for free iron (Brock 2002). Homeostasis of iron is required at specific concentrations for metabolic functions of cells including cell proliferation and host defense. Elevated biological concentrations of iron are potentially deleterious; consequences include support of microbial growth, suppression of various defense mechanisms and cell injury induced by excessive hydroxyl or ferryl radicals. Iron loading conditions, such as hemochromatosis, have been positively correlated with a suppression of osteoblast formation and new bone synthesis (Weinberg 2006).

It is consensual that LF influences the iron availability (Levay, Viljoen 1995a), however, it is still not proven to be essential for normal iron homeostasis or intestinal iron delivery (Brock 2002, Ward, Paz & Conneely 2005). LF knockout (LFKO<sup>-/-</sup>) mice, which develop normally and display no overt abnormalities, demonstrated that LF is not essential for iron delivery during the postnatal period. Analysis of adult mice on a basal or a high-iron diet revealed no differences in transferrin saturation or tissue iron stores between wild-type and LFKO<sup>-/-</sup> mice on either diet, although the serum iron levels were



slightly elevated in LFKO<sup>-/-</sup> mice on the basal diet (Ward, Uribe-Luna & Conneely 2002). Collectively, these results support the notion that LF does not play a major role in the regulation of iron homeostasis unlike transferrins. However, the iron-binding function of LF may contribute to alterations in iron metabolism during infection, inflammation or other physiological functions (Brock 1995).

Among LF's physiochemical properties, which collectively contribute to its myriad of functions, are its reversible affinity for iron and resulting three-dimensional changes in structural conformation. Biological properties of LF have been described relative to its iron binding states, which differ significantly in structural conformation (Baker, Baker 2004). Apo-LF, the predominating *in vivo* form, is an "open" molecule that has been reported to increase VEGFA-mediated angiogenesis *in vivo* (Norrby 2004) and strongly modulate inflammatory response (Baveye et al. 1999). Holo-hLF has been reported to stimulate cell cycle progression through PI3K/Akt pathway (Lee et al. 2009). However, iron (FeCl<sub>3</sub>) supplementation did not significantly promote cell cycle progression indicating that the iron content does not induce the proliferative ability of holo-hLF, but instead holo-hLF possesses a noble growth regulatory function (Lee et al. 2009). Physiological concentrations of apo-LF and holo-LF have been demonstrated to result in a suppression of osteoclastogenesis (Cornish et al. 2006, Cornish et al. 2004, Lorget et al. 2002). Cornish *et al.* assessed the effects of iron-binding of bLF, compared to similar size cations (chromium and magnesium), in primary rat osteoblast-like cell cultures on cell proliferation. The rate of proliferation of cells exposed to chromium- and manganese-loaded LF was similar to iron-loaded and iron-unloaded LF. These studies indicate that the proliferative effect of LF on osteoblast is independent of cation type and

saturation (Cornish et al. 2006). Further studies are needed to elucidate the molecular mechanisms regarding potential differences in response to iron saturation of LF. Aside from its metal bound state, the potent activity of LF on bone cells at peri-physiological concentrations indicate that LF might have a physiological role in bone growth and thus may serve as a novel bone repair therapeutic.

### **2.2.3 Positive skeletal regulator**

Bone is continuously remodeled by the sequential activities of osteoclast-mediated bone resorption and osteoblast-mediated bone formation (Parfitt 1976). LF, as a multifunctional glycoprotein, is also shown to be a potent anabolic effector of the skeleton. LF's anabolic effect in bone morphogenesis is attributed to its strong dose-dependent proliferative and anti-apoptotic actions on osteoblasts and inhibition of osteoclastogenesis (Cornish et al. 2004) (Figure 6 & 7). At physiological concentrations, LF promotes proliferation of osteoblasts and cartilage cells *in vitro* at a magnitude that exceeds the response observed relative to other skeletal growth factors such as IGF1 and TGF $\beta$  (Cornish 2004).

A recent study analyzed the immuno-expression of LF in human bone tumors in comparison to normal fetal and adult bone tissue (Ieni et al. 2009). Immunoreactivity of this glycoprotein was seen in neoplastic fibroblast like stromal cells as well as multinucleated giant cells (MNGCs). Positive LF immuno-expression was found in osteoid osteomas, adamantinomas and chondroblastomas. Normal fetal bone tissue exhibited positive LF immuno-expression, where it was primarily localized in the osteoblasts, in the calcified cartilage area as well as the nucleus of chondrocytes in the cartilage matrix adjacent to the calcified area. No LF expression has been found in any

of the adult bone tissue samples most likely due to the decrease in osteoblast metabolic activity. The high LF immuno-expression in the human osteoblastic lineage or bone forming tumors as well as in human fetal bone supports its significant role in promoting bone formation.

The potency of LF's anabolic actions on the skeleton requires better understanding of its molecular mechanisms. However, the mechanisms and cell signaling pathways involved in the transduction of LF's growth-modulating effects on osteoblasts have not yet been comprehensively studied. Presently, LF's potent mitogenic effect is accredited to low-density lipoprotein receptor-related protein (LRP) 1, which signals the activation of mitogen-activated protein kinases (MAPKs) to confer increased cell mitogenesis (Grey et al. 2004, Naot et al. 2005). LRP1 and 2 are among the putative LF receptors (Ji, Mahley 1994, Meilinger et al. 1995, Vash et al. 1998, Willnow et al. 1992). LRP is a membrane glycoprotein that spans the cell membrane and consists of an extracellular 515 kDa heavy chain and an 85 kDa light chain (Herz, Gotthardt & Willnow 2000). The extracellular domain of LRP contains four ligand-binding clusters, where hLF interacts with the second and fourth cluster of class A cysteine-rich repeats (Neels et al. 1999). LRPs, found on hepatocytes, fibroblasts, immune cells, osteoblasts, and endothelial cells, functions as both endocytic receptors and signaling receptors (Herz, Gotthardt & Willnow 2000, Neels et al. 1999, Li, Cam & Bu 2001, Strickland, Gonias & Argraves 2002). The expression of LRP1 by human osteoblasts was demonstrated as a mechanism for delivery of lipoproteins and vitamin K<sub>1</sub> to bone (Niemeier et al. 2005). Although LRP1 is classically known for its involvement in the endocytic pathway, LF has also been demonstrated to transduce cell signaling pathways mediated by LRP1 independent

of the receptor's endocytic properties (Grey et al. 2004). LF's proliferative actions on osteoblastic cells via LRP1-dependent phosphorylation of p42/44 MAP kinases (Grey et al. 2004) suggests that this receptor may also mediate its anabolic effects in skeletal tissue.

LRP5 and 6, are multiligand, nonendocytic members of LRP receptor family and have been widely identified as crucial regulators of osteoblast function (Gong et al. 2001, Babij et al. 2003). Thus, it is of question whether these receptors possess overlapping functions with LRP1 in the increase of skeletal mass. Previous reports indicate that LRP1 cannot substitute LRP5/6 in the transmission of the Wnt canonical pathway (Tamai et al. 2000) and even represses the canonical Wnt pathway (Zilberberg, Yaniv & Gazit 2004). LRP1 cytoplasmic domain plays a crucial role in LRP1-mediated signal transduction (Howell, Herz 2001). Thus, to elucidate whether LRP1-mediated signaling events directly or indirectly leads to the repression of the canonical Wnt pathway, Zilberberg *et al.* demonstrated that mLRP4T100, a mini-receptor of LRP1, tailless mutant preserved its repressive effect on Wnt signaling. The study demonstrated that LRP1-mediated signaling events directly lead to the repression of the canonical Wnt pathway. Furthermore, this study excludes the possibility that this repression is attributed to LRP1-affected signaling pathways that cross-regulate the canonical Wnt pathway. On the contrary, another study has reported that LF causes the significant down-regulation of dickkopf homolog 1 (DKK1) mRNA, a Wnt antagonist, in human primary osteoblasts (Cornish, Naot 2010) possibly indicating the on-state of the canonical Wnt signaling pathway.

LF has been demonstrated to have potent anti-apoptotic effects on osteoblast cells, which may also contribute to its anabolic skeletal actions. At peri-physiological concentrations (1-10 $\mu$ g/ml), LF protects both primary rat osteoblast cells and SaOS2 cells from serum withdrawal-induced apoptosis (Grey et al. 2006). Studies have demonstrated that LF induce LRP1-dependent phosphorylation of Erk and PI3K-dependent phosphorylation of Akt (Grey et al. 2004, Grey et al. 2006). However, the ability of LF to promote osteoblast survival was found to be independent of both of these activities (Grey et al. 2006). Although studies indicate the activation of LRP1 can lead to the activation of both PI3K and Erk (Orr et al. 2003), this study clearly indicates the existence of unique signaling transduction pathways mediated by LF that subserve its anti-apoptotic actions on osteoblasts (Grey et al. 2006). Thus, collective studies demonstrate that LF's anti-apoptotic activities are not sufficiently explained by signaling via LRP1 and most likely mediated by more than one of LF's putative cell membrane bound receptors. This notion is further supported by the cationic nature of LF allowing it to interact with a heterogeneous array of receptors, cells and anionic molecules, including DNA (Elass-Rochard et al. 1995, Appelmelk et al. 1994b, Shimazaki et al. 1998, Mann, Romm & Migliorini 1994, Hutchens, Magnuson & Yip 1989).

Through the use of microarrays and low-density arrays to investigate the changes in gene expression induced by LF treatment in osteoblasts, a recent study indicate the significant upregulation of IGF1 mRNA (Cornish, Naot 2010). As an endocrine and paracrine regulator of skeletal homeostasis, IGF1 has been demonstrated to promote survival and proliferation in osteoblasts through parallel PI3K and p42/44 MAPK signaling pathways (Grey et al. 2003). IGF binding proteins (IGFBPs) modulate IGF

action by inhibiting or enhancing IGF binding to IGF receptors. Furthermore, LF has been indicated to be a high affinity, IGFBP3 binding protein (Baumrucker, Gibson & Schanbacher 2003). Interestingly, holo-LF showed slightly greater binding to IGFBP3 than the apo form (Baumrucker, Gibson & Schanbacher 2003). This interaction will free IGFs (both IGF1 and IGF2) from their association with IGFBP. Much remains to be learned about the interactions involving IGFs, IGFBPs and LF. The connections between the various regulatory signaling pathways need to be further explored to help elucidate LF's effects on modulating skeletal growth.

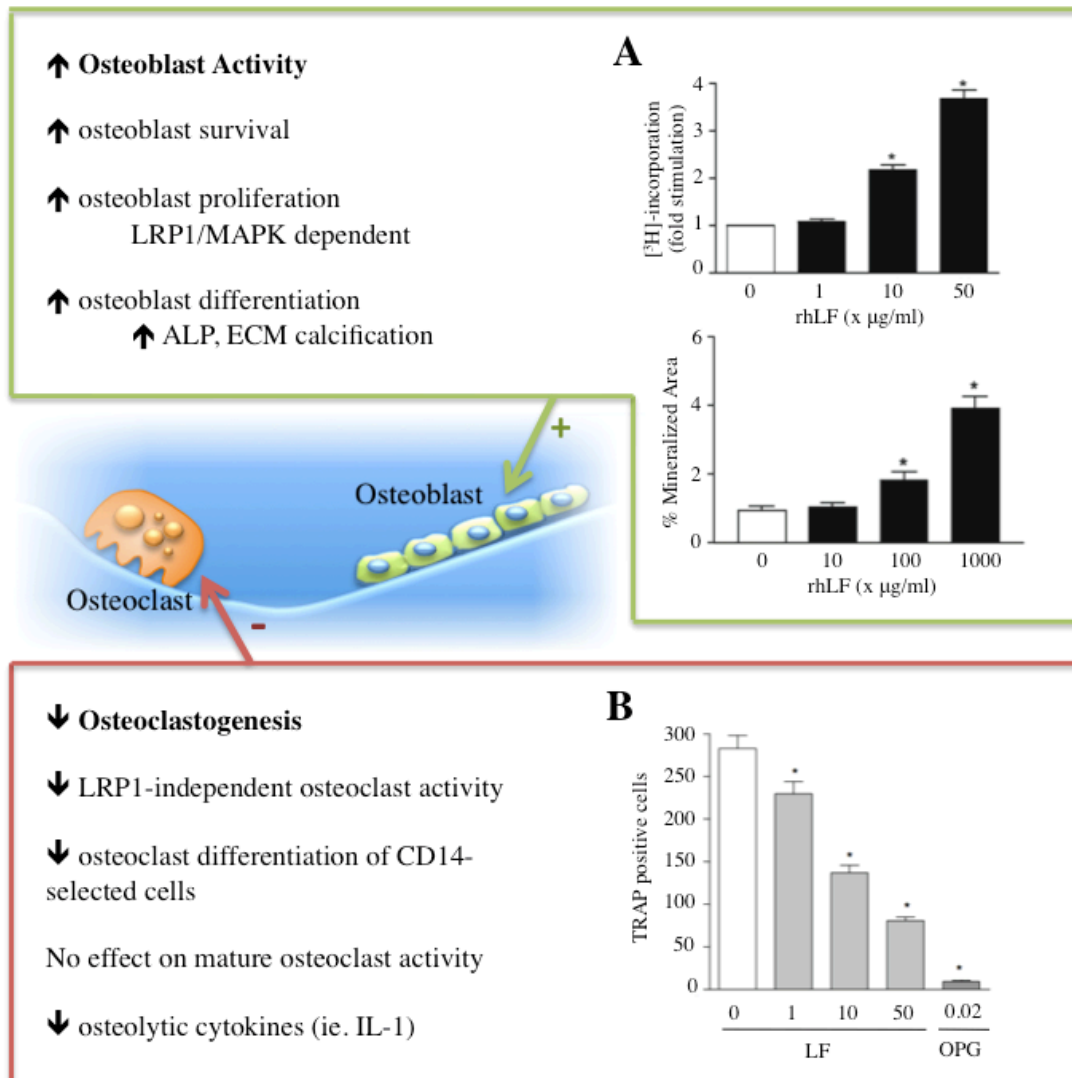


Figure 6. Through bidirectional signalling, LF enhances osteoblast activity and suppresses osteoclastogenesis.

A) Effects of lactoferrin on rat primary osteoblast proliferation and differentiation. Thymidine incorporation in primary cultures of rat osteoblast-like cells treated for 24 hours with increasing concentrations of rhLF. The effect of rhLF on areas of mineralized bone nodules as determined in primary cultures of rat osteoblast-like cells cultured over a period of 3 weeks. Cells were stained for mineral using Von Kossa stain. Image was adapted from (Cornish et al. 2004, Grey et al. 2004).

B) RAW264.7 cells, induced to differentiate to osteoclasts by the addition of 50ng/ml RANKL to the culture media, were treated with increasing concentrations of bLF (x µg/ml). TRAP positive multinucleated cells were counted on day 5. Osteoprotegerin (OPG) (0.02 µg/ml) was used as a positive control. Image was adapted from (Cornish, Naot 2010).

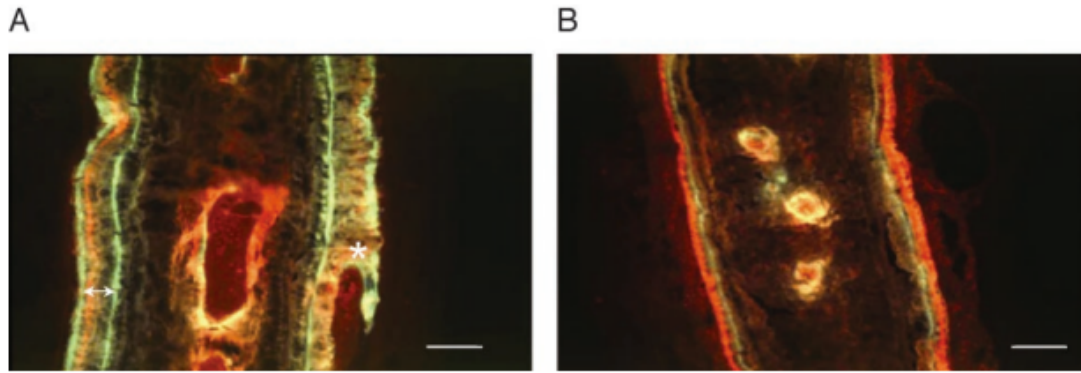


Figure 7. Anabolic effect on mouse hemi-calvaria in response to bLF after 10 days treatment.

*Photomicrographs of calvariae from animals treated with lactoferrin bLF) (4 mg) (A) and vehicle (B) for 5 days. Animals were killed 10 day later. Fluorochrome labels used: green, calcein; red, alizarin. Two calcein labels were given 13 day apart. The increased new bone growth in the 13-d period (i.e. distance between the two green calcein labels, arrowed) can be appreciated in the calvaria from the lactoferrin-treated animal. It can also be noted that there is new bone marrow formation occurring within the recently formed bone in the lactoferrin-treated calvaria. New bone formed on the injected side of the lactoferrin calvaria is partially woven (\*). This was seen only in the animals treated with the highest dose of lactoferrin and probably reflects the very high rate of matrix deposition. Horizontal bar, 50  $\mu$ m. Figure was taken from (Cornish et al. 2004).*

#### 2.2.4 Lactoferrin as an immunomodulatory protein

LF is a potent modulator of inflammation, innate and adaptive immune response (Legrand et al. 2005, Spadaro et al. 2008). The presence of LF in neutrophil granules indicates its important role in host defense. High affinity LF receptors have been identified on cells such as lymphocytes, monocytes and macrophages. The modulatory effects of LF have been attributed to its ability to interact with pro-inflammatory bacterial components as well as through interactions with epithelial and immune cells via specific cellular receptors even though the exact mechanisms have not been fully elucidated yet. At the cellular level, LF is known to modulate antigen presenting cells (monocytes, macrophages, dendritic cells) migration and activation as well as affects the expression of



soluble immune mediators such as cytokines, chemokines and other effector molecules. Several factors such as concentration of LF, iron content and composition have shown to have an effect on its immune-modulatory function.

The immunotropic regulation of LF in the innate immune system includes a multitude of host-protective effects against microbial infections, septic shock, inflammation, allergy and cancer (van Hooijdonk, Kussendrager & Steijns 2000). Supporting data indicates that patients with congenital or acquired LF deficiency are subjected to recurring infections (Breton-Gorius et al. 1980). Enhanced Th1 response to *Staphylococcus aureus* (*S. aureus*) infection was demonstrated in transgenic mice expressing human LF (Guillen et al. 2002). Oral LF administration demonstrates a protective effect during lethal bacteraemia and septic shock (Lee et al. 1998, Zagulski et al. 1989). Degree of iron saturation of LF has been demonstrated to play an interesting role in LF's ability to inhibit or promote *L. pneumophila* intracellular multiplication in mononuclear phagocytes at sites of inflammation (Byrd, Horwitz 1991). Apo-LF completely inhibited *L. pneumophila* multiplication in non-activated monocytes, whereas iron-saturated LF had no effect on the already rapid rate of *L. pneumophila* multiplication in non-activated monocytes. Increased levels of LF during inflammatory and immune responses target the monocytic cell line with high affinity ( $4.5 \times 10^{-9}\text{M}$ ) through a receptor-mediated mechanism (Bennett, Davis 1981, Birgens et al. 1983). However, lower affinity of LF is demonstrated for adherent mononuclear cells (Bennett, Davis 1981, Birgens et al. 1983) and alveolar macrophages (Campbell et al. 1992). Furthermore, LPS-induced TNF $\alpha$ , IL1 $\beta$ , IL6, and IL8 production is inhibited by LF in various human monocytic cell lines (Haversen et al. 2002). LPS-induced endotoxaemia

is associated with an up-regulation of nitric oxide synthase (Lauw et al. 2000). However, the inducible nitric oxide synthesized in response to *E. coli* infection is inhibited by the administration of LF (Zagulski et al. 1989). LF also promotes lytic cell activity by increasing the number of natural killer cells (Shimizu et al. 1996, Yamauchi et al. 1998), which results in a phagocytosis-enhancing effect (Szuster-Ciesielska, Kamiaska & Kandefer-Szersze, 1995, Wakabayashi et al. 2003). LF activating effect is also due to the modulation of natural killer cell cytotoxicity and an increased sensitivity of target cells to lysis (Damiens et al. 1998). LF-enhanced phagocytosis of pathogens could be due to its direct binding to PMNs and opsonin-like activity (Miyauchi et al. 1998). The adjuvant effect of LF in the generation of delayed-type hypersensitivity due to its binding on the mannose receptor of immature antigen-presenting skin cells is further supportive of its immunotropic activity (Zimecki, Kocieba & Kruzel 2002). The ability of LF to directly activate macrophages (Actor et al. 2002, Sorimachi et al. 1997) and also inhibit effector phases of cellular immune responses (Zimecki, Machnicki 1994) are contradictory and therefore require greater knowledge of the conditions during the administration of LF.

The anti-inflammatory properties of LF have been extensively studied. LF's anti-inflammatory properties may be partially explained by its iron-independent regulatory role during cytokine response to decrease pro-inflammatory cytokines, such as tumor necrosis factor  $\alpha$  (TNF $\alpha$ ), M-CSF, IL1 $\beta$ , IL6 and IL8 (Sawatzki, Rich 1989, Broxmeyer et al. 1987, Machnicki, Zimecki & Zagulski 1993, Kruzel et al. 2002) and to increase anti-inflammatory cytokines, such as IL4 and IL10 (Legrand et al. 2005, Togawa et al. 2002).

The anti-inflammatory activity of LF is applicable to infectious and non-infectious pathologies, such as allergies, rheumatoid arthritis, inflammatory bowel disorders and neurodegenerative disorders (Ward, Uribe-Luna & Conneely 2002). The effects of exogenous pro-inflammatory molecules, such as bacterial lipopolysaccharides (LPS) (Miyazawa et al. 1991) and bacterial unmethylated CpG-containing oligonucleotides (Britigan et al. 2001), are alleviated by LF. The binding of LPS to LF inhibits LPS signaling, in turn blocking the activation of the serum LPS-binding protein (LBP) and soluble CD14 (sCD14), as well as, membrane CD14 (mCD14) on monocytes and L-selectins on PMNs (Elass-Rochard et al. 1998, Baveye et al. 2000b). The strong interaction between LF and sCD14 interferes with the formation of the sCD14-LPS complex and ultimately inhibits the expression of endothelial adhesion molecules, E-selectin and ICAM-1 and reactive oxygen species production in neutrophils (Baveye et al. 2000a). Furthermore, the lactoferricin domain of LF was demonstrated as a high-affinity lipid A binding protein (Elass-Rochard et al. 1995, Appelmeik et al. 1994a). The charge-charge interaction that occurs between LF and lipid A can result in exposure of the unbound portion of lipid A to recognize LPS receptors, such as Toll-Like Receptor 4 (TLR4). This complex recognition would, in turn, activate macrophages. Potentially separate pathways for LF-mediated macrophage activation events are demonstrated by LF-induced, TLR4-dependent CD40 expression and the LF-induced, TLR4-independent IL6 secretion (Curran, Demick & Mansfield 2006).

In addition to inducing systemic immunity, *in vivo* studies show promotion of skin immunity and inhibition of allergic responses by LF (Elrod et al. 1997, Griffiths et al. 2001). Through dose-dependent inhibition of Langerhan cell migration and

accumulation of dendritic cells in lymph nodes, LF is able to protect the immune system against skin allergies. The overexpression of LF in patients with allergies (Zweiman et al. 1990) involves mast cell and basophil activation and IL1 $\beta$  and TNF $\alpha$ - induced migration of antigen-presenting cells. The interaction of LF and keratinocytes results in the inhibition of TNF $\alpha$  release by keratinocytes (Kimber et al. 2002).

Furthermore, the iron-dependent anti-inflammatory activity is associated with iron sequestration by apo-LF, which is released by neutrophils at the septic site. LF participates in detoxification by reducing the tissue-toxic hydroxyl radicals produced by the granulocytes. During inflammation, the Fenton/Haber-Weiss reaction produces damaging hydroxyl radicals as a result of free iron accumulation reacting with the reactive oxygen species released from the synovial macrophages. The chelation of iron by LF limits the concentration of radicals at the inflammation site and thus decreases lipid peroxidation and cell damage (Kruzel 2003).

Glycosylation patterns are known to impact immunogenicity and biological activity of various glycoproteins (Dwek 1995, Walsh, Jefferis 2006). Granulocytic LF, which is present in exocrine secretions and secondary granules of neutrophils, is known to have potent immunomodulatory functions. The two forms of LF show similar amino acid sequences and differ only in their glycosylation, indicating that glycosylation pattern can significantly affect LF's immunomodulatory functions. Recombinant human LF identical in glycosylation pattern to natural neutrophilic counterpart was recently bioengineered using *Pichia pastoris* expression system (Choi et al. 2008). The glycosylated recombinant protein showed potent immune regulatory properties and effectively reduce methotrexate induced suppression of secondary humoral immune

responses in sheep erythrocytes. The study also suggests that the terminal N-acetylneuraminic acid plays a significant role in LF mediated immune response. Even though the mechanism is not fully understood, it is suggested that the milk-derived, fucosylated LF has lower affinity to receptors that are responsible for signal transduction in immune cells.

Similarly, talactoferrin alfa (TLF), a recombinant human LF that differs from native human LF only in its glycosylation patterns, has been demonstrated to have potent immune modulatory functions (Engelmayer, Blezinger & Varadhachary 2008, de et al. 2008). TLF has recently been used as a therapeutic agent for several cancers and healing of diabetic wounds (Varadhachary et al. 2004, Wolf et al. 2007, Hayes et al. 2006). TLF rapidly mounts responses to pathogens by chemoattracting monocytes, promoting leukocytes and activating dendritic cells (de et al. 2008). The ability of TLF to recruit and activate antigen-presenting cells and to enhance antigen-specific immune responses are characteristic of alarmins, which are a group of endogenous mediators of the immune system that link innate and adaptive immune systems (de et al. 2008). The effects of TLF on macrophage function ultimately leads to attenuation of excessive inflammation and stimulation of host response against pathogen threats (Puddu, Valenti & Gessani 2009). Whether immunogenicity is affected by the different glycosylation pattern of rhLF as compared with the native form should be investigated further.

### **2.2.5 Lactoferrins's link to osteoimmunology**

The emerging heuristic field of osteoimmunology poses the interesting question of whether LF's regulation of bone homeostasis is a consequence of its cytokine modulation properties. The crosstalk and shared mechanisms between the skeletal and

immune systems is complex and multifold with shared cytokines, receptors, signaling molecules and transcription factors (Takayanagi 2005). For example, a mutation in *macrophage colony-stimulating factor (M-CSF)* gene produces a defect in both macrophage and osteoclast formation, indicating that immune and bone cells are derived from the same cell origin (Yoshida et al. 1990). Thus, the effect of molecules with osteoimmunological pleiotropy, such as LF, is not limited to modulation of inflammation and immune function, but also directly involved with associated inhibition of osteoclastogenesis.

LF has been shown to significantly decrease bone resorption (Lorget et al. 2002, Cornish 2004, Blais et al. 2009). At a concentration of 100 µg/ml, LF completely inhibits osteoclastogenesis in mouse bone-marrow culture. However, LF shows no effect on calvarial organ culture, implying LF does not affect mature osteoclast function (Cornish 2004). Collectively, data indicates that LF treatment decreases bone resorption by reducing osteoclast number formed from precursor cells. LF is able to directly inhibit osteoclastogenesis, independent of osteoblastic factors. Differentiation of murine macrophage RAW264.7 cells by the addition of receptor activator of NF-κβ ligand (RANKL) to the cell culture medium allows for a controlled study of LF effects on osteoclastogenesis independent of osteoblasts, as opposed to heterogeneous bone marrow derived culture systems. LF inhibits RANKL-induced osteoclastogenesis in RAW264.7 in a dose-dependent manner (Cornish, Naot 2010) measured by a significant decrease in TRAP positive multinucleated cells. Furthermore, the addition of LRP1-inhibitor RAP did not significantly alter LF-induced inhibition of osteoclasts (Cornish, Naot 2010), suggesting LRP1 is not involved in the LF-inhibition of osteoclasts.

The OPG/RANK/RANKL molecular triad is known to be a main regulator of osteoclastogenesis and osteoclast activity. Interestingly, it has been suggested that the mode of action of bLF in CD14—selected cells undergoing osteoclast differentiation, is independent of the RANK/RANKL/OPG molecular triad (Lorget et al. 2002). Osteoprotegerin (OPG), the physiological antagonist of RANKL, and RANKL mRNA was not detected either in the presence or absence of bLF. mRNA for RANK was detected in the CD14—selected culture system, however its expression was not modulated by bLF. This data is supported by previous studies that demonstrate mediators, other than the OPG/RANK/RANKL triad, are responsible for osteoclastogenesis. Proinflammatory cytokines, such as TNF $\alpha$  or IL1, induce osteoclast formation independent of the triad (Fox, Fuller & Chambers 2000, Fuller et al. 2002, Kudo et al. 2002). On the contrary, LF has been linked to the triad through the down-regulation of LPS-induced cytokine production in monocytic cells by NF $\kappa$ B. Haversen *et al.* demonstrated the capacity of LF to translocate to the nucleus and block NF $\kappa$ B activation, resulting in a decrease of the LPS-induced binding of NF $\kappa$ B to the TNF $\alpha$  promoter. This inhibition is also associated with LF's ability to inhibit LPS-induced IL6 and IL10 secretion in monocytic cells (Haversen et al. 2002).

Recent reports revealed significant LF-induced stimulation of *nuclear factor of activated T cells 1* (NFATc1) transcription, which is critical for lineage selection in T-cell differentiation, osteoblast differentiation and osteoclastogenesis (Cornish, Naot 2010, Zhao et al. 2010). NFATc1 is a master regulator of osteoclasts and plays a pivotal role in osteoclast activation via stimulation of various genes responsible for osteoclast adhesion, migration, acidification, and degradation of inorganic and organic bone matrix. The

calcineurin-NFAT signaling pathway is strongly implicated in osteoblast-mediated osteoclast differentiation and also in promoting osteoblast proliferation and differentiation (Stern 2006, Winslow et al. 2006). Constitutively active nuclear NFATc1<sup>nuc</sup> mutant mice showed an increase in osteoclast number and markers of osteoclast activity and increased bone resorption (Winslow et al. 2006). This regulation is independent of RANKL and OPG, which correlates to the negative osteoclast regulation of LF, also independent of the RANKL/OPG pathway (Lorget et al. 2002). Furthermore, mice expressing this NFATc1 variant displayed rapid Wnt-mediated osteoblastogenesis, independent of Runx2. The effect of rapid osteogenesis was suggested by histological analysis, which revealed that bone in mutant mice had a less organized appearance than normal tissue. The expression of the NFATc1 variant was found exclusively in osteoblasts, and the bone phenotype was marked by a significant increase in osteoblast number and bone volume. Furthermore, markers of osteoblast activity, serum osteocalcin and serum alkaline phosphatase, were greater than doubled. Other studies demonstrated NFATc1-activation of type 1 collagen through stimulation of Osterix suggesting the possibility of the formation of a novel NFATc1-Osterix complex. A contradiction in these sets of data includes LF's stimulation of *NFATc1* transcription, but reported decreases in osteoclastogenesis by this protein. Therefore, further exploration to elucidate this regulation may provide useful knowledge for the application of osteoclast-activated physiology and pathophysiology. These studies lend the question of possible LF signaling mediating osteoblasts and osteoclastogenic pathways through NFATc1.



#### 2.2.5.1 Lactoferrin and periodontitis-induced bone loss

The interplay between LF's immuno-modulation and bone homeostatic properties has recently been investigated using lipopolysaccharide (LPS)-induced periodontitis models (Yamano et al. 2010) (Figure 8). Periodontitis is an inflammatory disease instigated by infection with various oral plaque-associated periodontopathic bacteria, which includes *Aggregatibacter actinomycetemcomitans*, *Porphyromonas gingivalis*, and *Prevotella intermedia* and bacterial LPS. The induced inflammation ultimately leads to destruction of the periodontium, which includes the gingiva and the surrounding alveolar bone. This destruction is induced by pro-inflammatory cytokines, including TNF $\alpha$  and IL-1 $\beta$ , which subsequently leads to a significant increase receptor activator of NF $\kappa$ B ligand (RANKL)-induced osteoclastogenesis (Clowes, Riggs & Khosla 2005, Weitzmann, Pacifici 2007).

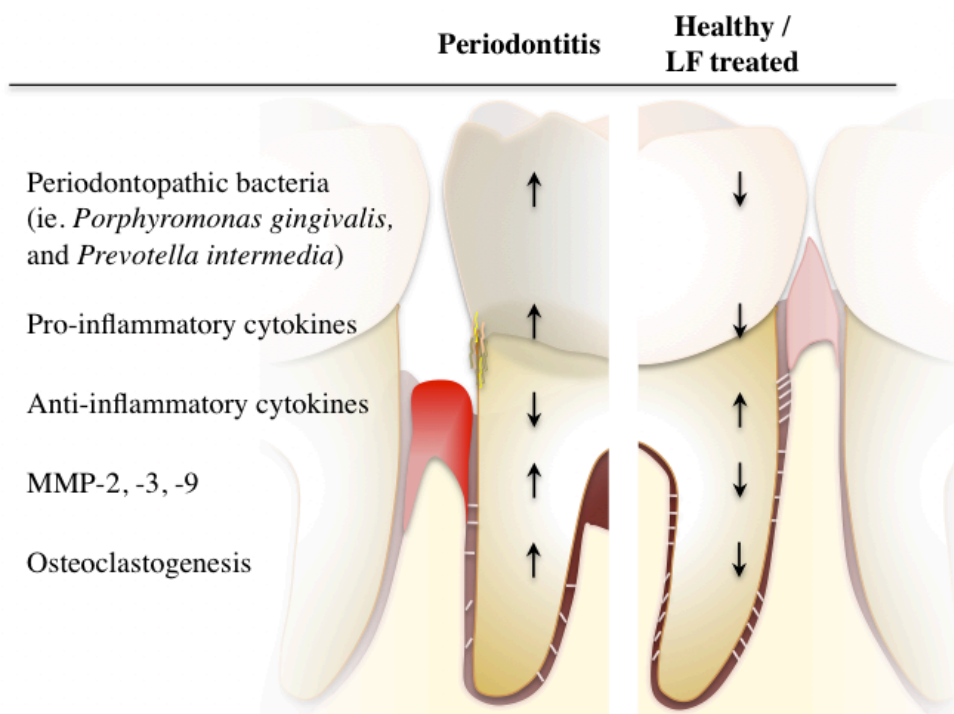


Figure 8. Comparison of periodontitis versus healthy/LF treated tissue.

LF is a component of exocrine secreted saliva and an important constituent of neutrophilic granules of leukocytes. This glycoprotein is seen to be an important immune defense factor against oral pathogens and periodontopathic bacteria and a good marker for periodontitis (Wakabayashi et al. 2003), since it is not synthesized in healthy gingival tissues and is produced by invading inflammatory cells in response to the inflamed periodontal tissue (Eberhard et al. 2006). LF has been reported to inhibit the LPS interaction with CD14 by competition with LPS-binding protein. Furthermore, LF may also bind directly to soluble CD14 receptor (Baveye et al. 2000a), which is expressed on the membrane of osteoclast precursors (Nicholson et al. 2000). *In vitro* assays have demonstrated that bLF inhibits LPS-induced osteoclastogenesis through the reduction of TNF $\alpha$  and RANKL expression and elimination of OPG suppression in osteoblastic cells

with LPS stimulation. Through liposomalization of bLF, which acts to increase protein stability, Yamano *et al.* demonstrated a significant inhibitory effect on LPS-induced osteoclastogenesis through orally administering this stabilized form of the protein (Yamano et al. 2010). Periodontal bone resorption occurs due to the significant increase in RANKL-stimulated osteoclastogenesis; on the other hand, LF causes an increase in osteoblast activity and inhibits osteoclastogenesis.

LF inhibits the growth of periodontopathic bacteria. As a major innate host defense factor, LF binds and sequesters LPS, thus preventing pro-inflammatory pathway activation, sepsis and tissue damage. LF may down-regulate LPS-induced cytokines following its internalization, nuclear localization and interference with NF $\kappa$ B activation (Haversen et al. 2002). Furthermore, this glycoprotein decreases pro-inflammatory cytokines, such as IL1 $\alpha$  and TNF $\alpha$ , and increases anti-inflammatory cytokines, IL4 and IL10. LF inhibits the adhesion of bacteria to fibroblasts and epithelial cells. MMPs, which are known to lead to periodontal ligament and tissue destruction in periodontitis, which have been demonstrated to be inhibited by LF in rabbit preterm delivery model (Mäkelä et al. 1994, Nakayama et al. 2008).

#### **2.2.5.2 Lactoferrin and osteoporotic bone loss**

Recent studies explored the crosstalk between LF's regulation of bone homeostasis and immuno-modulatory characteristics using ovariectomized animal models (Figure 9). Postmenopausal osteoporotic bone loss is regarded as a consequence of estrogen deficiency, which in turn increases osteoclastogenesis. Estrogen deficiency is known to increase pro-inflammatory cytokines, including TNF $\alpha$ , which, in turn, increases RANKL-

induced osteoclastogenesis. Due to the presence of LF in secretory granules of neutrophils, the production of LF is understood to be predominantly influenced by inflammatory stimuli. LF possesses strong immunomodulatory effects, including a decrease in the secretion of osteolytic cytokines, such as  $\text{TNF}\alpha$  and  $\text{IL1}\beta$ . Therefore, it is possible that this effect may contribute to its anabolic effects on the skeleton by counterbalancing the catabolic osteoclastogenesis caused by some of the mediators in the inflammatory bone turnover response.

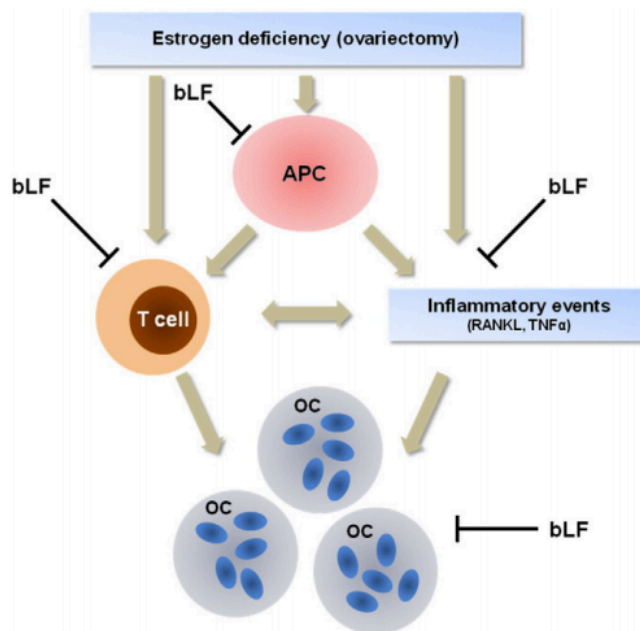


Figure 9. Schematic representation of the role of estrogen deprivation and bLF on bone loss and bone resorption markers through APC and T cell modulation.

*bLF can prevent osteoclastogenesis directly or indirectly by modulation of: i) T cell activation, ii) antigen presenting capacity (APC) and iii) Cytokines released in bone micro-environment particularly through a down-regulation of  $\text{TNF}\alpha$  release. Image was taken from (Malet et al. 2011).*

Recently, LF treatment was shown to improve bone status of ovariectomized mice *in vivo* and *in vitro* (Blais et al. 2009). Oral supplementation of LF to the diet dose-dependently improved bone mineral density and femoral failure load. Furthermore,

periphysiological concentrations of bovine LF treatment to primary cultures of murine bone cells was demonstrated to stimulate cell growth and differentiation of osteoblastic cells and inhibit the growth of preosteoclastic cells *in vitro* (Blais et al. 2009).

Milk basic protein (MBP) has been demonstrated to have positive bone effects *in vitro* and *in vivo* (Toba et al. 2000). Interestingly, a component of MBP that is responsible for anti-osteoclastic activity has recently been demonstrated to also possess pro-angiogenic activities due to its identical structure to 14 kDa milk angiogenin (Morita et al. 2008). In a recent study, a ribonuclease (angiogenin)-enriched LF supplementation improved bone-formation markers while reducing bone resorption markers in postmenopausal women (Bharadwaj et al. 2009). Due to its strong anabolic bone effects, LF can be considered as a potential molecule for bone regeneration.

### **2.2.6 Angiogenesis modulator**

Angiogenesis is a complex physiological process whereby new blood vessels form from pre-existing blood vasculature and is imperative for successful tissue regeneration. This complex process occurs during embryonic development, wound repair, and tumor growth. Basic fibroblast growth factor (bFGF) and vascular endothelial growth factor (VEGF) are two key mitogens involved in endothelial cell proliferation and migration, which are important components of the angiogenic processes. VEGF-A is stimulated during hypoxic condition and is key factor linking ischemia and collateral compensatory angiogenesis (Schaper, Ito 1996). Angiogenesis is essential in a variety of physiological and pathological processes, such as wound healing, tumor growth, metastasis and hypoxia (Isner, Asahara 1999).

Human and bovine LFs have been shown to modulate VEGF-A—mediated angiogenesis *in vivo*. Apo-hLF and apo-bLF exert specific and contrary angiogenesis-modulating roles in VEGF-A—mediated angiogenesis *in vivo*. Apo-hLF significantly enhances VEGF-A—mediated angiogenesis, but does not affect bFGF-mediated angiogenesis (Norrby 2004). These studies indicate that this endogenous protein by itself lacks angiogenesis-modulating activity, but apparently is able to enhance VEGF-A—mediated angiogenesis systematically. On the other hand, apo-bLF does not significantly affect IL1 $\alpha$ —mediated angiogenesis (Norrby et al. 2001), while it significantly suppresses VEGF-A—mediated angiogenesis (Norrby 2004). Furthermore, bLF administration, both orally and intraperitoneally, significantly suppressed tumor-induced angiogenesis in mice (Shimamura et al. 2004). The opposing effects of apo-hLF and apo-bLF on VEGF-A—mediated angiogenesis could be due to the differences in the three-dimensional structure of the protein, amino acid sequence and composition (Goodman, Schanbacher 1991, Spik et al. 1982).

Mechanistically, the actions of bLF on angiogenesis have been described in various lights. The investigation of bLF's inhibition of tumor-induced angiogenesis lead to the notion that bLF's inhibition of angiogenesis can be explained by the blocking of endothelial cell function and induction of IL18 production (Shimamura et al. 2004). In this study, bLF potently suppressed bFGF- or VEGF-induced proliferation of mouse endothelial KOP2.16 cells (Shimamura et al. 2004). Other studies have investigated bovine lactoferricin (LfcinB), a peptide fragment of iron- and heparin-binding LF, inhibits bFGF and 165-kd isoform of VEGF (VEGF<sub>165</sub>)-induced angiogenesis. LfcinB inhibits receptor-stimulated angiogenesis by complexing with heparin-like binding sites

on the endothelial cell surfaces that are involved in the binding of bFGF and VEGF<sub>165</sub> to their respective receptors (Mader et al. 2006).

VEGF-A is recognized by two receptors, KDR/Flk-1 and Flt-1, and thereby induces angiogenesis. In an attempt to elucidate the molecular mechanism underlying the effects of hLF on VEGF-A—mediated angiogenesis, Kim *et al.* (Kim et al. 2006) demonstrated that apo-hLF stimulates VEGF-mediated human umbilical vein endothelial cell (HUVEC) migration and proliferation through the up-regulation of KDR/Flk-1 mRNA expression and protein levels. Furthermore, exposure of apo-hLF to HUVECs was also correlated with a significantly increased VEGF-induced Erk MAPK phosphorylation and endothelial cell proliferation.

Pretreatment of endothelial cells with 5 µg/ml apo-hLF for 12 hours and subsequent exposure to 10 ng/ml VEGF stimulated cell proliferation approximately 3-fold over VEGF alone (Norrby 2004). However, it should be noted that apo-hLF did not induce endothelial cell migration by itself, but did so with the concurrent administration of VEGF-A. It was also observed that holo-hLF did not enhance HUVEC migration, even in the presence of VEGF-A. This data is consistent with a previous claim that apo-hLF, not holo-hLF, enhanced VEGF-A—mediated angiogenesis *in vivo* (Norrby 2004).

LF treatment of rodent osteoblast was reported to cause increased transcription of *prostaglandin-endoperoxide synthase 2* (*Ptgs2*), which is also known as *cyclooxygenase 2* (*Cox2*) (Cornish, Naot 2010). This transcription factor modulates angiogenesis by increasing the production of angiogenic factors, such as VEGF (Tsujii et al. 1998). However, it is important to note that the source and iron saturation of the LF used and the

time course was not specified in the above study making it difficult to derive definitive conclusion.

### **2.2.7 Candidate for bone regeneration applications**

An important goal of bone regeneration therapy is directed differentiation of heterogeneous populations of undifferentiated pluripotent mesenchymal cells to the osteoblastic lineage. Increased mRNA and protein expression of Runx2 and Sox9, tissue-specific differentiation markers for osteoblasts and chondroblasts, respectively, occurred in LF-treated pluripotent C2C12 mesenchymal cells. Levels of MyoD, a differentiation marker of skeletal muscle, and PPAR $\gamma$ , a critical transcription factor of adipocyte differentiation, significantly decreased upon LF treatment in this undifferentiated mesenchymal cell culture line (Yagi et al. 2009). This set of data suggests that LF appears to positively regulate undifferentiated mesenchymal cell population toward the osteoblastic and chondroblastic lineage, and inhibits myogenic and adipogenic differentiation.

The production of rhLF provides vast benefit for its use in regenerative bone tissue engineering, as it possesses similar physical, biochemical and biological characteristics from the native protein. The similarities that have been reported include anti-microbial and thermostability and ability to bind Fe<sup>3+</sup> (van Berkel et al. 2002a, Huang et al. 2008). The small difference in molecular mass between the recombinant and native form of hLF is accounted for in differential glycosylation patterns (van Berkel et al. 2002a). This cost-effective alternative provides a great option for regenerative therapeutic use of this protein. The use of the recombinant form of LF provides a foundation for producing consistent and predictable results.



Holo-rhLF, purified from rice, has been demonstrated to increase thymidine incorporation in primary rat osteoblast cultures. Holo-rhLF concentration of 100 µg/ml, almost doubled osteoblast proliferation over a 24 hour time course. A direct correlation between rhLF iron saturation levels and cell proliferation has been reported. It has been reported that holo-rhLF possesses stronger growth promoting effects compared to apo-rhLF (Huang et al. 2008) on HT-29 cells. On a commercial basis, this source of rhLF is now used as a growth factor for media to promote cell growth and cell productivity.

Since rhLF technology has made its way to the commercialized world as a nutritional supplement and as a clinical product with perceived benefits to the consumer. rhLF, expressed in milk, rice and microorganisms is now used commercially as a dietary supplement. Talactoferrin, an immunomodulatory rhLF preparation, has been demonstrated to be effective in the treatment of patients with diabetic neuropathic foot ulcers (Spadaro et al. 2008), non-small cell lung cancer therapy in combination with cisplatin treatment and renal cell carcinoma (Jonasch et al. 2008).

The potent modulating effects on the skeletal system support the prospect of rhLF application for regenerative bone tissue regeneration. The use of various biomaterials, such as type 1 collagen membrane (Takayama, Mizumachi 2009) and biodegradable gelatin hydrogels (Takaoka et al. 2011), have been used as carriers to provide a sustained localized release profile of LF. LF-embedded collagen membrane has been shown to promote osteogenic differentiation of MG63 human osteosarcoma-derived cells. Increased alkaline phosphatase activity and osteocalcin production was induced by the LF-embedded collagen membranes (Takayama, Mizumachi 2009). A recent study demonstrated significant bone regeneration at cranial defects following the implantation

of LF-incorporated gelatin hydrogels (Mäkelä et al. 1994, Takaoka et al. 2011). These studies concluded LF as a general osteogenic growth factor for bone tissue engineering.

### **2.2.8 Conclusions**

The bidirectional signaling of LF that suppresses osteoclastogenesis and enhances osteoblast proliferation and survival supports the notion that LF is a strong candidate for bone tissue engineering. This candidacy of the glycoprotein is further supported by the multifunctional ability of hLF to promote neovascularization and its key modulating role in inflammation. Although LF osteogenic research has made great strides, shortcomings of LF research includes the lack of detail in terms of procedure and specific forms of LF (iron saturation and source). Furthermore, the variations in preparation, which includes heat treatment and processing, may also account for inconsistencies in the reported LF data. Thus, it makes it difficult to compare and analyze published data thus far when lacking such indispensable information. It is imperative to investigate the effects of LF and report findings with specific details with regards to the molecular state of LF. Investigations should focus on the mechanisms by which LF concomitantly regulates the immune and skeletal systems. Such advances will provide a comprehensive understanding of LF's role in bone regeneration.

The studies discussed thusfar, provided great insights on the potential bioactivity of LF and well as its ability to increase bone regeneration. All these studies used soluble LF protein to evaluate the biological functions of the protein. However, to exploit the biological functions of the protein for regenerative application, it needs to be developed as a biomaterial that can be localized at the defect site to present an osteogenic microenvironment. The preliminary study discussed here examines the feasibility of

developing an injectable biomaterial from LF, which might serve as an osteogenic microenvironment to support bone regeneration.

### **3 Preliminary studies**

#### **3.1 Enzymatically—crosslinked bovine lactoferrin hydrogel as an osteogenic cell delivery vehicle**

##### **3.1.1 Introduction**

As discussed previously (section 2.2.3), the anabolic effect of bLF on osteoblasts and its potent inhibition of osteoclastogenesis *in vitro* suggests that bLF may have positive effects on bone mass *in vivo*. The administration of bLF over the right hemicalvaria of adult male mice resulted in a dramatic increases in bone area in the calvariae compared with PBS control. Four groups of mice were given daily injections of one of 3 doses of bovine lactoferrin (0.04 mg, 0.4 mg or 4 mg) or vehicle over the right hemicalvaria for 5 consecutive days. New bone formation was dose-dependently increased by bLF. Both 0.4 mg and 4 mg of lactoferrin produced an increase in new bone formation, however the 4 mg dose induced changes of 4-fold greater than those observed in control animals. Local injections of bLF also increased the mineral apposition rate and the bone formation rate (Cornish 2004). However, repeated injections of bLF over 5 consecutive days were used in this study to achieve the significant anabolic effect demonstrating that retention of the protein at the defect site for prolonged time may be required to activate the regenerative process.

In another recent study, murine preosteoblast MC3T3 cells revealed greater proliferation rates by the repeated addition of bLF compared to single addition of the

protein at the same dose (Takaoka et al. 2011). Attempts have been made to retain the protein at the defect site using a controlled protein delivery approach. Type 1 collagen membrane was used as a sustained delivery vehicle for bLF. Approximately 27% of bLF embedded on the collagen membrane was burst released within the first hour followed by a slower release (Takayama, Mizumachi & Takezawa 2002). The embedded bLF collagen membranes promoted MG63 cell calcium deposition, ALP activity and osteocalcin production (Takayama, Mizumachi & Takezawa 2002).

A recent *in vivo* study evaluated the efficacy of a sustained delivery vehicle in promoting bone formation. The study used biodegradable gelatin hydrogel to allow bLF release *in vivo* in a sustained fashion. Upon subcutaneous implantation into the dorsum of mice, the gelatin hydrogel incorporated with bLF demonstrated an extended retention of bLF at the site of implantation than that of bLF solution injection. The remaining radioactivity on days 1 and 3 of  $^{125}\text{I}$ -labeled LF solution injected subcutaneously was 2.96 and 0.82%, respectively. In contrast, the remaining radioactivity on days 1 and 3 of  $^{125}\text{I}$ -labeled LF in the hydrogel incorporated form was 10.14 and 5.26%. Upon implantation of gelatin hydrogels incorporating bLF into rat cranial defects, improved bone regeneration at the defect was observed than in control gelatin gel. The study demonstrated that the retention of bLF at the defect site enhanced bone regeneration (Takaoka et al. 2011) (Figure 10). However, a significant limitation of this study was that approximately 90% of the bLF incorporated in the gelatin gel was released within 24 hours. This necessitates the encapsulation of high concentrations of bLF since much of it will be lost due to burst release from the carrier gelatin gel. Furthermore, the high

concentration (30 mg) of bLF needed to induce significant bone growth may further induce negative systemic side effects.

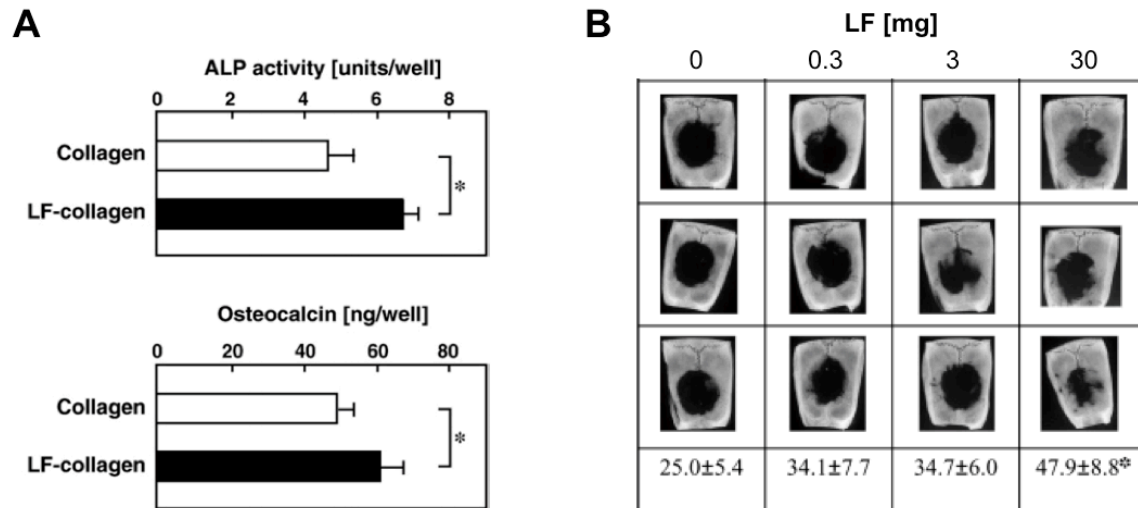


Figure 10. (A) Promoting effect of bLF—embedded collagen membrane on ALP activity and osteocalcin production in MG63 cells.

MG63 cells were plated onto a control collagen membrane (open bar) and a bLF embedded collagen membrane (closed bar). Upon confluence, the cells were shifted to osteogenic conditions for 2 weeks. ALP activity and osteocalcin production were calculated per well and values are represented as mean  $\pm$  standard deviation of three separate measurements. \* $p < 0.05$  significant difference. Image was adapted from (Takayama, Mizumachi & Takezawa 2002). (B) X-ray radiographs of rat calvarial defect 8 weeks after implantation of gelatin hydrogels incorporating 0, 0.3, 3 and 30 mg bLF. The lower stand value indicated the average percentage of area ossified in an 8 x 8 mm square around the bone defect. No statistical significant differences were observed between the bLF 0 and 0.3 mg group. \*  $p < 0.05$  significant difference from the percentage of ossified area in a square around the defect implanted with gelatin hydrogels without bLF (Takaoka et al. 2011).

A potential approach to overcome these limitations is to develop a biomaterial where in LF is immobilized. Such approach may significantly decrease the amount of LF introduced in the body as it can be used to localize the molecule for a prolonged time to induce maximum regenerative response. Considering the cell instructive properties of

LF, the ideal immobilization method might be to develop an injectable hydrogel, wherein cells can be encapsulated within the gel and can serve as a localized microenvironment for modulating the cell response. However, several challenges exist while developing such an approach. Even though the bioactivity of bLF is known, the mechanism of action of bLF is not completely known. Bioactive proteins may activate cellular processes through two different phenomenas – cell internalization/endocytosis or receptor-mediated signal transduction. It is therefore not known if an immobilized polymer, which is incapable of being endocytosed, will be bioactive or not. One study that supported our hypothesis determined that internalization of LF by osteoblastic cells is not necessary for activation of mitogenic signaling and that the endocytic function of LRP1 is independent of its signaling function (Grey et al. 2004).

For developing injectable biomaterials, we selected HRP-mediated, enzymatic crosslinking method of protein due to the reasons summarized below. As discussed before in section 2.1.2, hydrogels may be crosslinked through various mechanisms including photo-polymerization, covalent, ionic and enzymatic crosslinking. Enzymatic crosslinking, as previously discussed in section 2.1.2.2.1, involves a mild, cell-friendly and natural crosslinking process. Polymers functionalized with tyramine, tyrosine or aminophenol side groups can form crosslinked hydrogels by phenol derivative coupling – this reaction is driven by  $H_2O_2$ , as the oxidant, and HRP, as the enzyme (Kurisawa et al. 2005, Kobayashi, Uyama & Kimura 2001, Jin et al. 2007a, Amini, Nair 2012). HRP-mediated, enzymatic crosslinking was selected for developing LF-based injectable gels since this enzyme-mediated crosslinking may take place at physiological pH and temperature, making this a potential route to form injectable cell and protein delivery

vehicles (Sakai et al. 2009, Amini, Nair 2012, Lee, Chung & Kurisawa 2009a). Other advantages of these hydrogel injectable systems include the flexibility of gelation time, equilibrium swelling and storage modulus – which may be modulated by varying the degree of substitution of tyramine residues and reagent concentrations. The efficacy of the reaction has been demonstrated by various systems listed in Table 2.

Standard carbodiimide-mediated coupling of amino groups of tyramine with the carboxyl groups of LF was used to increase phenolic content of LF. Although LF contains phenolic amino acids, such as tyrosine, the phenolic content of LF is much lower than what is needed to develop an effectively cross-linked matrix via the enzyme-catalyzed coupling (Figure 11 & 12). The reaction of LF with tyramine increases polymer crosslinking by increasing the number of phenolic groups (Figure 13). Similar chemical reactions have been used to increase the phenolic content of other polymers such as chitosan and hyaluronic acid (Darr, Calabro 2009, Sakai et al. 2009, Lee, Chung & Kurisawa 2009a).

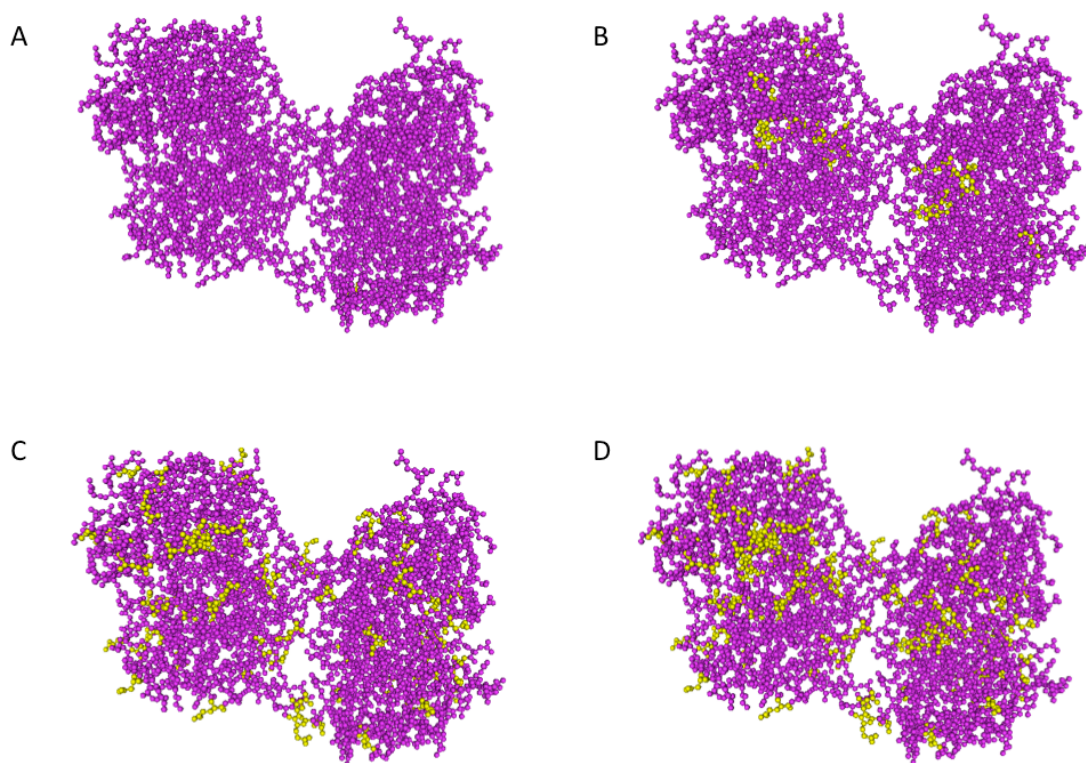


Figure 11. (A) Structure of Human LF. (B) Tyrosine amino acid groups contained in human LF. (C) Carboxylic acid containing amino acid groups (aspartate and glutamate) in human LF. (D) Theoretically available crosslinking amino acid sites after tyramine modification of human LF.

grrrsvqwct	vsqpeatkcf	qwqrnmrkvr	gppvscikrd	spiqciqaia	enradavtld
ggfiyeagla	pyklrpvaae	vvgterqprt	hyvavavvkk	ggsfqlnelq	glkschtglr
rtagwnvpig	tlrpflnwtg	ppepieaava	rffsascvpg	adkgqfpnlc	rlcagtgenk
cafssqepyf	sygafkclr	dgagdvafr	estvfedlsd	eaerdeyell	cpdntrkpv
kfkdechlarv	pshavvars	ngkedaiwnl	lrqagekfkg	dkspkfqlfg	spsgqkdllf
kdsaigfsrv	ppridsglyl	gsgyftaig	lrksveevaa	rrarvwcav	geqelrkcnq
wsglsegsvt	cssasttedc	ialvlkgead	amslaggvvy	tagkcglvpv	laenyksqqs
sdpdpncvdr	pvegylavav	vrrsdtsltw	nsvkgkksch	tavdrtagwn	ipmgllfnqt
gsckfdeyfs	qscapgsdpr	snlcalcigd	eqgenkcvpn	sneryvgitg	afrclaenag
dvaifvkdv	lqntdgnnne	awakdlklad	fallcldgkr	kpvtarsch	lamapnhavv
srmdkverlk	qvllhqakf	grngsdcpdk	fcflqsetkn	llfndnteccl	arlhgkttve
kylgpgqvag	itnlkkcsts	plleaceflr	k		

Figure 12. Amino acid sequence of human lactoferrin.

Tyrosine (y) amino acids are highlighted as they represent the possible crosslinking sites for LF gel. Glutamic acid (e) and aspartic acid (d) are also highlighted as they may be modified with phenolic groups and also serve as additional crosslinking sites.



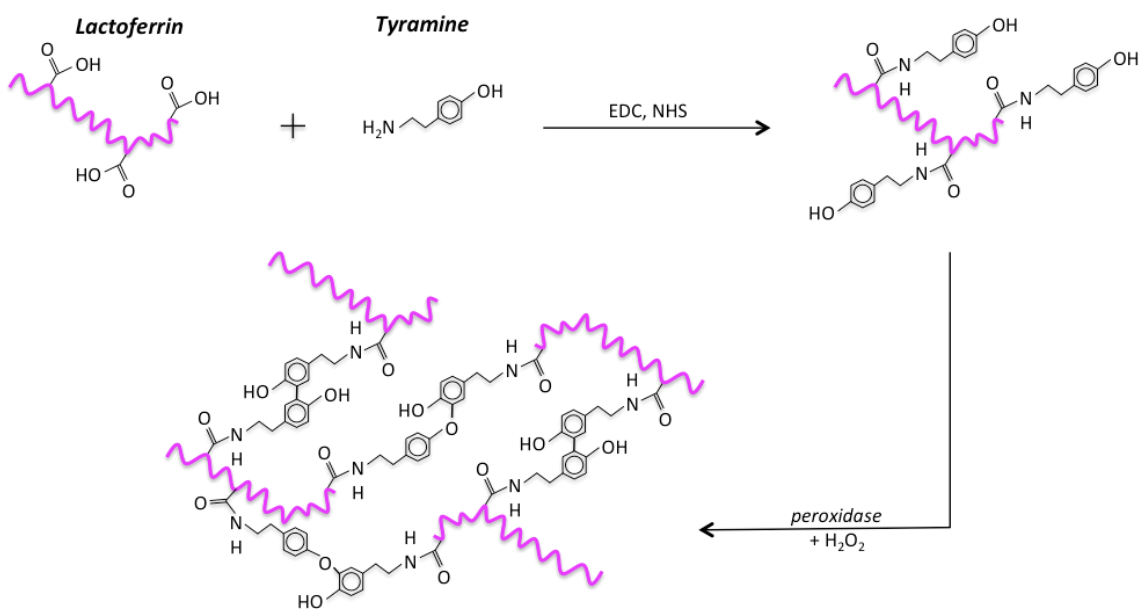


Figure 13. Schematic showing the modification of LF's acidic groups with tyramine to yield greater enzymatic crosslinking sites. Addition of HRP and H<sub>2</sub>O<sub>2</sub> yields a LF crosslinked gel.

The objective of our preliminary studies was to test the feasibility of crosslinking bLF using HRP-enzymatic reaction to be used as a localized delivery of bLF protein for increased osteoblast function. The second objective of the study was to test our hypothesis that the immobilized bLF based gel will be bioactive.

### 3.1.2 Methods

#### 3.1.2.1 Synthesis of bLF-tyramine conjugates (modified bLF)

bLF was tyramine modified for 1, 5, 15 and 24 hours (reaction time) as per the protocol described in the Appendix of Protocols (section 7.9.2.1.1).

### 3.1.2.2 Quantification of tyramine modification of bLF

Tyramine concentration of modified bLF was measured as described in Appendix of Protocols (section 7.9.2.1.1.1). A tyramine standard curve was used to determine the concentration of a tyramine in the modified bLF samples (Figure 77). Standard curve stock was made by diluting 10.5 mg tyramine in 2 ml MES buffer. 0 - 40  $\mu$ l of stock solution was diluted in increments of 5  $\mu$ l further in 900  $\mu$ l MES buffer (n=4) and diluted samples were measured by spectrophotometer at 275 nm.

### 3.1.2.3 Gelation time

Sol to gel time was determined via vial inversion method according to Appendix of Protocols (Section 7.9.2.2.1). The effect of modified bLF (10 – 50 mg/ml), HRP (10 – 50 U/ml) and 0.25% H<sub>2</sub>O<sub>2</sub> (1 - 10  $\mu$ l) concentration on gelation time was investigated. Variables were individually varied and tested for effect on gelatin time.

### 3.1.2.4 Morphology

The morphology of the bLF gels formed from modified bLF solutions of 10 mg/ml was visualized by scanning electron microscope to evaluate the gel microstructure. 10 mg/ml bLF gel was formed according to Appendix of Protocols (Section 7.9.2.1.2.2) on an SEM stub, flash frozen the samples using liquid N<sub>2</sub>, lyophilized and then visualized according to Appendix of Protocols (Section 7.9.2.2.3).

### 3.1.2.5 Protein expression analysis of encapsulated cells

#### 3.1.2.5.1 Western Blot Analysis

*Cells exposed to soluble bLF (2D studies):* MC3T3 cells were plated on 10 cm<sup>2</sup> tissue culture plates (200,000 cells/plate), grown to 90% confluence in basal media and then

serum starved for 6 hours. Cells were stimulated with 100 µg/ml of bLF or untreated (control) for 24 hours. *Cells encapsulated in bLF gel (3D studies)*: MC3T3 cells (2,000,000 cells/ml) were encapsulated in 1 ml of 10 mg/ml bLF. After 24 hours of incubation, total protein was lysed from cells and western blot analysis was performed as described in Appendix of Protocols (Section 7.2.2.3).

#### 3.1.2.5.2 Immunofluorescence

*Cells exposed to soluble bLF (2D studies)*: 50,000 cells were plated on 35 mm sterile glass bottom culture plates and then stimulated with 100 µg/ml of bLF or untreated (control) for 24 hours.

*Cells encapsulated in bLF gel (3D studies)*: MC3T3 cells were cultured on 35 mm sterile glass bottom culture plates. For 3D cell encapsulation studies, 500,000 cells/ml were encapsulated in 10 mg/ml bLF gels. bLF gel formation and cell encapsulation was performed according to Appendix of Protocols (Sections 7.9.2.1.2.2 and 7.9.2.4). The encapsulated cells were then maintained in basal media at 37°C for 2 days. Protein expression was analyzed via immunofluorescence according to Appendix of Protocols (Section 7.2.2.5).

### 3.1.3 Results

#### 3.1.3.1 Development of injectable gels from tyrosinated bLF

Figure 14a shows the phenolic content of tyramine modified and unmodified bLF as a function of reaction time under the described reaction conditions. The phenolic content of unmodified bLF is due to the presence of tyrosine. The study showed that the

extent of phenol group substitution significantly depends on the reaction time. The substitution of tyramine groups in bLF (modified bLF) and the phenolic content of the modified bLF after 24 hours was approximately 1.5 times higher than the unmodified bLF (0 hour reaction time).

bLF gels were prepared by the HRP-mediated oxidative coupling of modified bLF in the presence of  $H_2O_2$ . Various concentrations of modified bLF ranging from 10 mg/ml to 50 mg/ml were dissolved in 10 U/ml HRP (dissolved in  $H_2O$ ). Gelation was initiated by the addition of 0.25%  $H_2O_2$ . Figure 14b shows the gelation time of modified bLF at room temperature when treated with HRP and  $H_2O_2$ . As can be seen from the figure, the reaction time significantly effects gelation time. The 1 hour reacted bLF was found to behave similar to that of unmodified bLF, and unable to undergo gelation under the tested reacted conditions. The 5 hours reacted bLF underwent gelation in ~15 minutes and the gelation time significantly decreased for the 15 hours reacted samples. The 24 hours reacted sample underwent gelation in about 2 minutes, which falls in the clinically feasible injection time. This condition was therefore used for the rest of the studies.

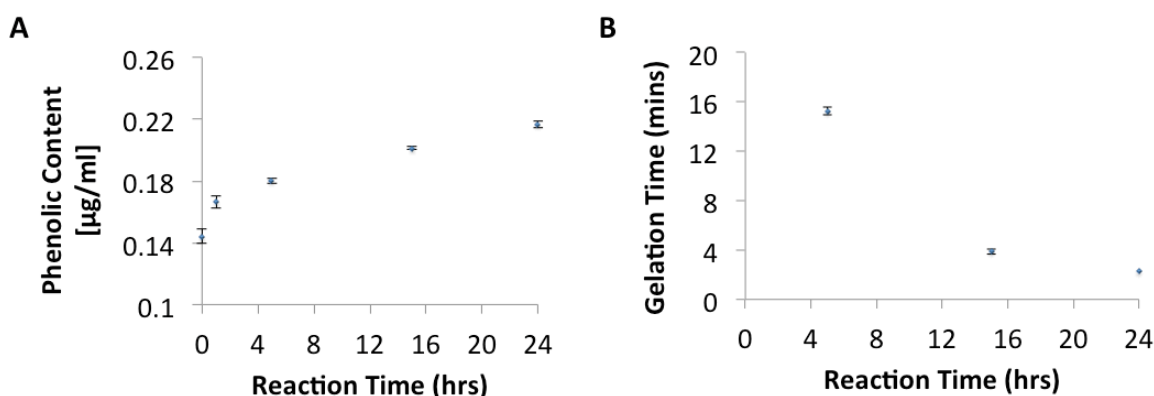


Figure 14. Effect of modification time on (A) bLF phenolic content and (B) gelation time.

The morphology of 10 mg/ml bLF gel after lyophilization was evaluated using SEM. Figure 15 shows the morphology of the gel at three different magnifications. The gels presented a flacky morphology with an open, irregular porous structure.

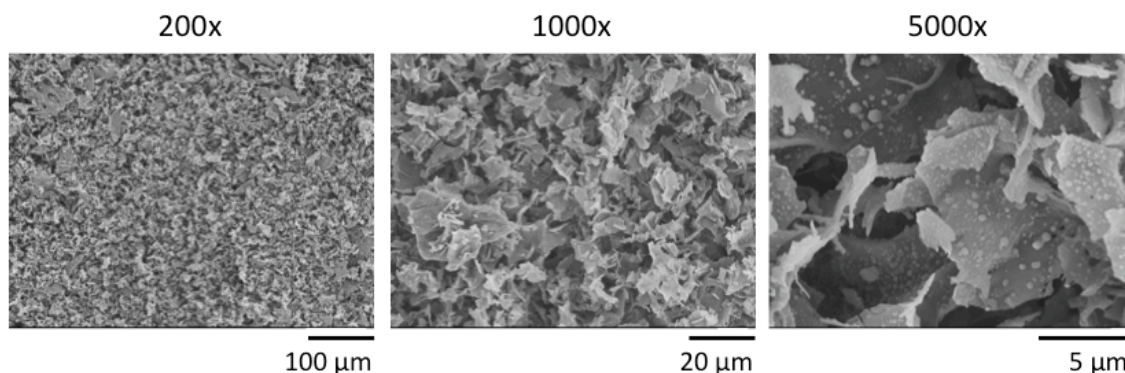


Figure 15. Morphology of 10 mg/ml bLF gel.

#### 3.1.3.2 Bioactivity of bLF gels

Figure 16a (lane 2) is a western blot showing the expression of phosphorylated Akt by MC3T3 cells when cultured in the presence of 100 µg/mL bLF compared to the untreated control (Figure 16a, lane 1). Cells that were not treated with bLF did not show positive expression of phosphorylated Akt, whereas, cells treated with bLF showed significant expression of p-Akt. Since soluble bLF can significantly upregulate phosphorylated Akt in MC3T3 cells after 24 hours in culture, the protein was used as a bioactive marker to test the bioactivity of bLF injectable gels. Figure 16a (lane 3) is a western blot showing the expression of phosphorylated Akt by MC3T3 cells encapsulated in injectable bLF gel (10 mg/ml). As in the case of soluble bLF, the bLF injectable gel also showed significant upregulation of phosphorylated Akt by the encapsulated MC3T3 cells indicating the

retention of bioactivity by the gel. Equal protein loading in the above experiments were confirmed by equivalent levels of tubulin in all lanes (Figure 16c).

The bioactivity of the injectable gel was further confirmed by following an osteoblast osteogenic marker (active  $\beta$  catenin). Similar to phosphorylated Akt, increased  $\beta$  catenin activation was seen in MC3T3 preosteoblast cells when treated with 100  $\mu$ g/ml soluble bLF after 24 hours of culture (Figure 16b; lane 2) relative to untreated MC3T3 cells (Figure 16b; lane 1). Due to the significant accumulation of  $\beta$  catenin in MC3T3 cells treated with soluble bLF, the same was tested in cells encapsulated in bLF gels. Figure 16b (lane 3) is the western blot showing the expression of active  $\beta$  catenin by MC3T3 cells encapsulated in injectable bLF gel (10 mg/ml). After 24 hours of culture, the encapsulated cells showed positive expression of active  $\beta$  catenin.

Our lab and others have shown the ability of bLF to induce MC3T3 cells to produce various osteogenic factors such as FGF2 and VEGF (Nakajima et al. 2011, James et al. 2011). The production of these cytokines by MC3T3 cells was followed by immunofluorescence. Figure 17 shows an immunofluorescence image of MC3T3 cells treated with soluble bLF and control PBS for 24 hours stained for VEGF and IGF2 expression. As can be seen, treatment of MC3T3 cells with bLF led to significant increase in expression of VEGF and IGF2 relative to untreated control. Figure 18 shows the immunofluorescence image of MC3T3 cells encapsulated in bLF gel (10 mg/ml) for 2 days. As in the case of soluble bLF, the encapsulated cells showed significant expression of these two proteins further confirming the cell instructive capability of bLF.

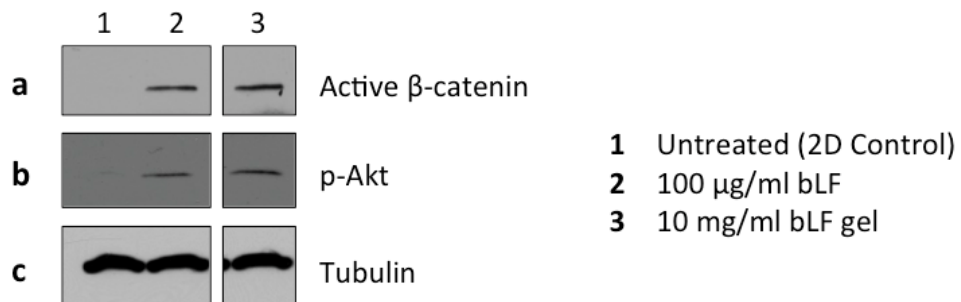


Figure 16. Increased stabilization of  $\beta$  catenin and phosphorylation of Akt in MC3T3 after 24 hour treatment of 100  $\mu$ g/ml bLF solution and encapsulation in 10 mg/ml bLF gel.

100  $\mu$ g/ml bLF treatment (lane 2) and 10 mg/ml bLF gel (lane 3) was compared to untreated (lane 1) MC3T3 cells.

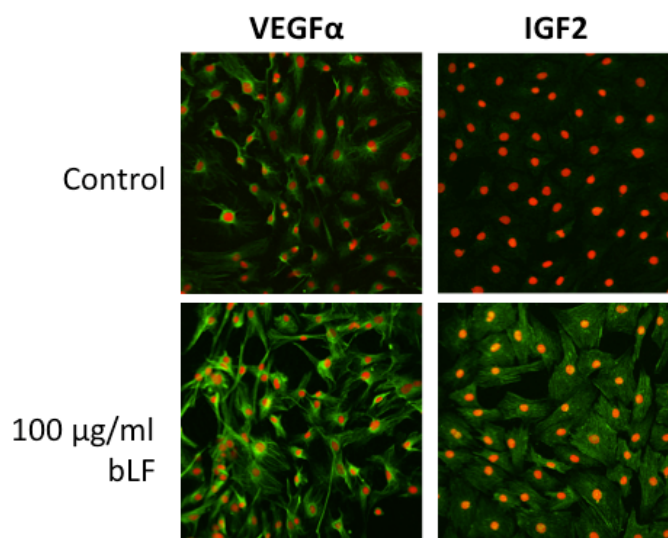


Figure 17. Effect of 100  $\mu$ g/ml bLF solution on MC3T3 protein expression after 24 hours treatment.

Expression of 100  $\mu$ g/ml bLF treated cells were compared to that of untreated control. Propidium iodide (red) was used to stain nuclei and FITC-tagged (green) secondary antibodies were used to visualize positive expression of protein.

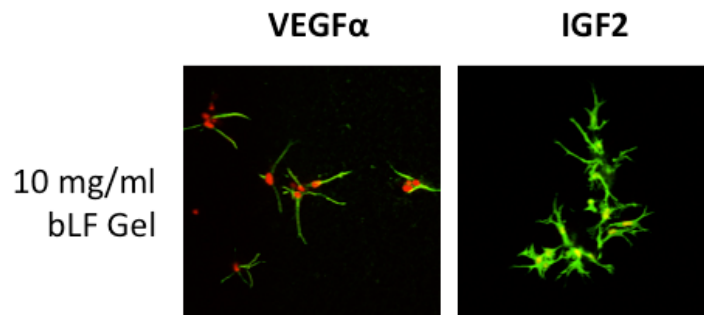


Figure 18. Increased IGF2 and VEGF $\alpha$  expression in 10 mg/ml bLF gel encapsulated MC3T3 cells after 2 days of culture.

*Propidium iodide (red) was used to stain nuclei and FITC-tagged (green) secondary antibodies were used to visualize positive expression of protein.*

### 3.1.4 Discussion

The efficiency of cell-based therapeutics in tissue engineering is based on successful delivery of cells to sites of repair or regeneration. Hydrogels allow for simple implantation via injection to fill irregularly shaped defects and accommodation of homogeneous incorporation of cells. Several hydrogel systems have been developed to localize cells at the defect site. In addition to localizing the cells, our ability to modulate cellular performance using these artificial matrices will be highly beneficial for positive regenerative outcomes. One method commonly used to modulate cellular performance is by encapsulating growth factors along with the cells as discussed before (section 2.1.3.2). Growth factor encapsulation, even though it has showed improved performance, has significant drawbacks. Hydrogels are highly permeable matrices and is associated with subsequent burst release of these growth factors upon implantation, and growth factors will not be available to the encapsulated cells for a prolonged time, which could significantly decrease the efficacy. Also, as discussed before, wound healing is a complex process involving several bioactive molecules expressed in a temporal and



spatial manner. Encapsulating one or two growth factors in the gel will not be able to recapitulate such a complex microenvironment. Cells are capable of producing much of the bioactive molecules required for the regenerative process. So the ideal approach will be to develop a cell-instructive, injectable hydrogel that could induce the production of these bioactive molecules by the encapsulated cells. Such a biomaterial does not exist so far. The preliminary studies discussed here aim to evaluate the feasibility of developing a cell-instructive biomaterial using bLF, which has shown to have bioactivities to support bone formation.

Natural bLF contains phenolic amino acids such as tyrosine. We first evaluated the feasibility of crosslinking bLF using the HRP-mediated enzymatic crosslinking using  $H_2O_2$ . However, we found that the phenolic content of natural bLF is much lower than what is needed to develop an effectively crosslinked matrix via the enzyme-catalyzed coupling. Therefore, attempts were made to increase the phenolic content of the bLF by chemically substituting the carboxyl groups of bLF with tyramine molecules to form modified bLF (Figure 11 & 13). The extent of tyramine substitution was analyzed using UV spectrophotometry at wavelength of 275 nm. The time of reaction was shown to have a significant effect on the extent of tyramine substitution with extent of substitution increasing with increase in reaction time. For clinical application of injectable gels as cells or factor delivery vehicles, a gelation time of 1-2 minutes is considered ideal (Miljkovic et al. 2009). Therefore, gelation time was used to determine the ideal concentration of phenolic group in modified bLF that will give the injectable solution a gelling time of ~1 minute. As indicated in Figure 14, the 24-hour modified bLF showed a gelation time in that range and was therefore used for the rest of the study.

The preliminary studies thus confirmed the feasibility of developing a clinically-relevant injectable hydrogel based on LF using the mild, enzymatic crosslinking method. The gel also showed a porous structure that might be conducive to support cell attachment and proliferation. However, before exploring the clinical applications of the biomaterial, it is important to confirm the bioactivity of the injectable gel, even though it is produced from a bioactive protein for reasons summarized below.

The bioactivities of the proteins are mostly governed by the composition as well as the three dimensional structure of the protein. Changes in the composition and or structure of the protein can significantly affect their bioactivities. Since only a very small amount of phenolic groups were substituted in modified bLF, we hypothesize that the modification might not completely alter the bioactivity of the protein. Similarly, previous studies have demonstrated the ability of bLF to improve osteoblast survival, proliferation and differentiation – however, the mechanism behind bLF's bioactivity is not completely understood. The role of LRP1 in mediating the bLF-induced signal transduction in promoting osteoblast proliferation has been shown to induce phosphorylation of MAP kinase signaling transduction cascade (Grey et al. 2004). Ligand-induced, receptor-mediated signal transduction are known to occur in an avidity-controlled manner, where 1) the extracellular ligands can activate the receptors without internalization, 2) it is consumption-controlled – meaning the extent of activation depends on the ability to internalize surface-bound ligand and 3) dual-sensitivity where both the avidity and consumption parameters are important. In the case of bLF, even though the exact mechanism is not known, a previous study revealed that the internalization of LF by LRP1 is not necessary for activation of mitogenic signaling (Grey et al. 2004). Thus, if

the internalization of bLF ligand is not required, then it is possible that the crosslinked injectable gel from bLF could show the same bioactivity as soluble bLF. The bioactivity of the injectable bLF was followed by determining the expression of several key signal transduction molecules and cytokines in MC3T3 cells induced by soluble bLF. Phosphorylated Akt is commonly considered as a marker for cell survival. Akt promotes cell survival by inhibiting apoptosis through phosphorylation and inactivation of several targets, including Bad, forkhead transcription factors, c-Raf, and caspase-9 (Cardone et al. 1998, Brunet et al. 1999, Zimmermann, Moelling 1999). bLF is known to increase the phosphorylation of Akt, however, a recent study demonstrated the anti-apoptotic action induced by bLF is not dependent on the phosphorylation of Akt (Grey et al. 2006). Although pAkt is known to play a critical role in cell survival and apoptosis, its function has also been reported to play an important role in glycogen metabolism and cell growth (Nave et al. 1999, Hajduch, Litherland & Hundal 2001). As shown in Figure 16a, similar to solution bLF, injectable bLF gel significantly upregulated the expression of pAkt in MC3T3 cells. Even though bLF has shown to significantly increase osteogenic differentiation markers, such as ALP, collagen 1, Runx2 and OCN (Ying et al. 2012), the molecular mechanism of the osteogenic effect of bLF has not yet been demonstrated. Our studies demonstrated the ability of soluble bLF to activate  $\beta$  catenin in MC3T3 cells. This is interesting from the context of bLF's ability to support osteoblast differentiation since the de-phosphorylation and subsequent accumulation of  $\beta$  catenin is a key step in osteogenic signaling pathway. The present study demonstrated that similar to soluble bLF, the injectable bLF gel may stabilize  $\beta$  catenin and promote its significant accumulation.

Bone regeneration is a coordinated cascade of spatio-temporal events regulated by an array of cytokines and growth factors (Amini, Nair 2011b). Bioactive biomaterials that are capable of locally inducing the production of endogenous cytokines and growth factors necessary for bone regeneration could serve as an excellent microenvironment to promote the regenerative process. These biomaterial scaffolds may serve as delivery vehicles to introduce donor cells at the defect site or can be used to allow native cells to migrate to the injury site, then proliferate and finally differentiate to regenerate the tissue. The combination of osteogenic and angiogenic growth factors have been shown to enhance bone regeneration (Kanczler et al. 2010, Patel et al. 2008).

For example, our studies demonstrated that bLF-crosslinked gel increased IGF2 protein expression in MC3T3 encapsulated cells after 2 days. As a member of the IGF signaling system, IGF2 plays an important role in prenatal growth and development (Randhawa, Cohen 2005). IGF2 activates various pathways including PI3K/Akt or MAPK signaling transduction pathways, via IGF receptors (O'Dell, Day 1998). Recent studies have also indicated that IGF2 potentiates BMP9-induced osteogenic differentiation and bone formation (Chen et al. 2010). Other studies reported that stimulated bone turnover via increased osteoblast number and function is directly and/or indirectly caused by local IGF1 and IGF2 production (Bouillon 1991). LF also activates the PI3K/Akt signaling pathway and increases mRNA levels of IGF1, but the functional significance of these remains to be determined (Cornish, Naot 2010).

Our studies also demonstrated a positive expression on VEGF in MC3T3 cells after 2 days of bLF gel encapsulation. Furthermore, previous LF study has reported that apo-hLF significantly enhances VEGF-A—mediated angiogenesis (Norrby 2004). VEGF is a

key mitogen involved in endothelial cell proliferation and migration, which are important components of angiogenesis (Schaper, Ito 1996). Angiogenesis is a complex physiological process whereby new blood vessels form from pre-existing blood vasculature and is imperative for successful tissue regeneration. This complex process occurs during embryonic development, wound repair, and tumor growth. Human and bovine LFs have been shown to modulate VEGF-A—mediated angiogenesis *in vivo*.

### **3.1.5 Conclusions**

The preliminary studies discussed here demonstrate the feasibility of developing an injectable biomaterial from bLF using the mild enzymatic crosslinking method. We also showed initial evidence regarding the ability of injectable biomaterial in retaining the bioactivities of soluble bLF. bLF, either in the soluble form or as injectable gel, was capable of regulating signal transduction molecules as well as inducing cytokine production which could play key roles in promoting osteoblast survival, proliferation and differentiation. These encouraging results formed the basis for exploring the development of novel injectable biomaterials based on recombinant human LF as a cell delivery vehicle, which will be discussed in sections 4 and 5.

## **4 Evaluation of the bioactivity of recombinant human lactoferrins**

### **4.1 Evaluation of the bioactivity of recombinant human lactoferrins (apo-, pis- and holo-) towards murine MC3T3 preosteoblast cells**

#### **4.1.1 Introduction**

LF protein, which belongs to the iron-binding transferrin family, is present in

exocrine secretions and is an important regulator of the levels of free iron in the body fluids (Gonzalez-Chavez, Arevalo-Gallegos & Rascon-Cruz 2009). LF harbors two iron-binding motifs, which are each responsible for the sequestration of a ferric  $\text{Fe}^{3+}$  molecule (Anderson et al. 1990, Anderson et al. 1989). The glycoprotein's degree of iron saturation has a pivotal influence on its physical structure (Baker, Baker 2009). When fully iron saturated (holo), LF presents as a stable “closed” structure, as opposed to its “open” iron-free state (apo) (Haridas, Anderson & Baker 1995, Grossmann et al. 1992). Furthermore, the structure of this protein, although differs throughout species (Anderson et al. 1989, Baker et al. 1991), retains essentially identical high affinity ( $K_D \sim 10^{-22}$  M) iron binding sites (Aisen, Leibman 1972).

The role of iron concentration and the resulting changes in protein conformation in modulating the bioactivity of LF is not clearly understood. Jiang *et al.* investigated the effect of apo- and holo-hLF on Caco-2 cell proliferation under standard cell culture conditions. The study demonstrated that even though both the proteins were internalized by LF receptor they differentially affected Erk-signaling and cell proliferation. Apo-hLF showed significant increase in cell proliferation and activation of Erk cascade compared to holo-hLF (Jiang et al. 2011). Similarly, a study using mouse crypt cells demonstrated the differential effects of apo- and holo-hLFs on cell functions. The proliferation of crypt cells was significantly enhanced by apo-hLF compared to holo-hLF. Moreover, different signaling pathways were involved in holo and apo-hLF mediated activation of the cells. Only apo-hLF was capable of activating the Erk signaling pathway, and both apo and holo-hLFs were capable of activating the PI3K/Akt pathway to modulate crypt cell proliferation (Jiang, Lonnerdal 2012). Francis *et al.* studied the iron dependent effect of

hLF on neutrophil survival (Francis et al. 2011) and concluded that only apo-hLF and not holo-hLF is capable of inhibiting neutrophil apoptosis. These studies indicate the possibility that iron concentration may play a significant role in LF bioactivity.

Cornish *et al.* investigated the effects of bLF's structure-activity relationship (Cornish et al. 2006) and reported that the degree of bLF iron saturation did not significantly affect the proliferation of primary rat osteoblasts. Furthermore, the substitution of bLF's iron with cations of similar size (i.e., magnesium and chromium) did not significantly change the extent of cell proliferation compared to iron (Cornish et al. 2006). Compared to the previous studies this data indicates that the iron content of bLF may not significantly affect the biological activities of this glycoprotein towards osteoblast. However, most of the studies reported thus far to understand the effect of LF on osteoblasts and osteoclasts were performed using LF isolated from bovine milk (bLF). Another important factor that may play an important factor in LF's bioactivity is its degree of glycosylation, as discussed in section 2.2.1.

Transgenic, rice-derived recombinant human LF (rhLF) has recently been made commercially available in three different iron saturation forms, ranging from apo-rhLF (iron depleted, <10% iron), pis-rhLF (partially iron saturated, ~50% iron), holo-rhLF (>90% iron saturated) (Huang et al. 2008). The advent of the recombinant human protein technology offers a cost-effective alternative and a foundation for producing consistent and predictable results for potential clinical applications. Biochemical and biophysical analyses indicate that rhLF is similar to native hLF and supports mammalian cell proliferation (Huang et al. 2008, Tang et al. 2010). Huang *et al.* reported a “bell shaped” dose response curve for the proliferative effect of apo-, pis- and holo-rhLF on HT-29

intestinal cells after 24-hour treatment. The maximal stimulatory effect was seen at a concentration of 1000 µg/ml for all three forms of rhLF. However, of the rhLF forms, holo-rhLF showed approximately 3.5 times greater proliferation as indicated by [<sup>3</sup>H]-thymidine incorporation over apo- and pis-rhLF. Furthermore, a dose-dependent increase in cell growth was seen in rat osteoblast with the treatment of holo-rhLF up to 100 µg/ml (Huang et al. 2008).

The objective of this study is to investigate the biological effect of apo-, pis- and holo-rhLFs on MC3T3 cells to understand the effect of iron concentration on rhLF bioactivity in order to identify the suitable polymer to develop injectable hydrogels for bone tissue engineering application. MC3T3 cell line was selected to evaluate the bioactivities of rhLFs since it is a well-characterized murine osteoblast cell line (Sudo et al. 1983) that has been used extensively as a model for osteoblasts *in vitro*. The dose and iron concentration dependent mitogenic activity of rhLF toward MC3T3 cells was evaluated using thymidine assay. The ability of rhLF to induce MC3T3 cells to activate transcription factors, signaling molecules, chemokines and cytokines were determined by following β-catenin activation, phosphorylation of Akt, VEGF and IL-6 expression. Protein and phosphorylation levels were followed using western blot and immunocytochemical analysis. Moreover, a global microarray analysis was performed to study the overall pattern of gene regulation in MC3T3 cells when cultured in the presence of different rhLFs for 24 hours.

#### **4.1.2 Methods**

##### **4.1.2.1 Cell proliferation**

The effect of varying concentrations of apo-, pis- and holo-rhLF on MC<sub>3</sub>T<sub>3</sub>-E1 cell



proliferation was measured through thymidine incorporation. MC3T3 cells were maintained in basal MEM $\alpha$  medium for 6 hours to allow proper cell adhesion and maintained in serum-free medium overnight. The cell culture was then performed upon supplementation with 0, 10, 100, and 1000  $\mu\text{g/ml}$  of apo-, pis- and holo-rhLFs and [ $^3\text{H}$ ] thymidine for 24 hour incubation at 37°C. Incorporation of [ $^3\text{H}$ ] thymidine radioactivity was performed as described in Appendix of Protocols (Section 7.6.2.2). Data was then normalized to untreated control sample and expressed as fold change over control.

#### **4.1.2.2 Protein expression analysis**

##### **4.1.2.2.1 Western blot analysis**

MC3T3 cells were plated on 10 cm tissue culture plates (200,000 cells/plate), grown to 90% confluence in basal media and then serum starved for 6 hours. Cells were stimulated with 100  $\mu\text{g/ml}$  of apo-, pis-or holo-rhLF or untreated (control) for 24 hours. Total protein was lysed from cells and western blot analysis was performed as described in Appendix of Protocols (Section 7.2.2.3).

##### **4.1.2.2.2 Immunocytochemistry**

MC3T3 cells were plated on glass-bottom tissue culture plates (50,000 cells/plate) to 90% confluence in basal media and then serum starved for 6 hours. Cells were either untreated (control) or stimulated with varying iron saturations of 100  $\mu\text{g/ml}$  rhLF for 24 hours. Immunocytochemistry was performed as described in Appendix of Protocols (Section 7.2.2.5).

#### 4.1.2.3 Microarray gene expression analysis

MC3T3 cells were plated on 10 cm tissue culture plates (200,000 cells/plate), grown to 90% confluence in basal media and then serum starved for 6 hours. Cells were stimulated with 100 µg/ml of apo-, pis- or holo-rhLF or untreated (control) for 24 hours. RNA extraction, purification and microarray analysis was performed as described in Appendix of Protocols (Sections 7.3.2.1 and 7.3.2.3). The ratio of the signal intensity of each experimental sample (100 µg/ml apo, pis, holo-rhLF treatment) and the signal intensity of untreated control was represented as the fold change relative to control (Table 3, 4 & 5).

#### 4.1.2.4 Statistical data analysis

All data is presented as mean  $\pm$  S.D. (standard deviation) for  $n = 3$ , unless stated otherwise. Statistical analyses were performed by t-test;  $p < 0.05$  was considered statistically significant.

### 4.1.3 Results

Figure 19 shows the effect of rhLF and iron concentration on the proliferation of MC3T3 cells after 24 hour treatment. Irrespective of the iron concentration, LF did not show significant increase in MC3T3 cell proliferation compared to control culture at a protein concentration of 10 µg/ml. However, significant increase in cell proliferation was observed when cells were cultured in rhLFs at concentrations of 100 and 1000 µg/mL rhLF treatment relative to untreated control. At any of the protein concentrations studied, no significant differences in cell proliferation was observed when cells were treated with apo-, pis- or holo-rhLF.

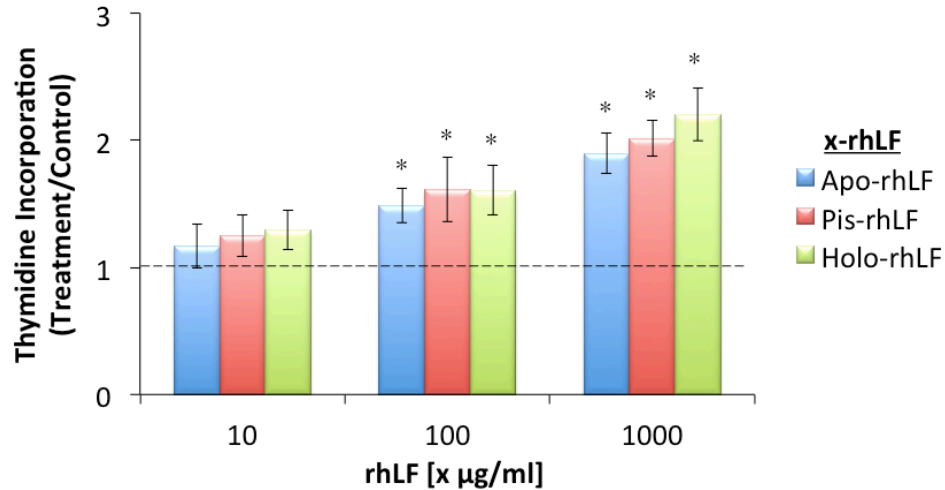


Figure 19. Effect of rhLF concentration and iron saturation on MC3T3 cell proliferation after 24 hour treatment measured by thymidine incorporation.

*Data is expressed relative to control and astrices represent statistical significance ( $p < 0.05$ ) relative to control and  $n = 4$  biological replicates.*

LF is a pleiotropic protein with multiple functions and is known to activate various cell signaling pathways in cells including osteoblast cells. In addition to the mitogenic effects, LF is known to increase cell survival, cause significant phosphorylation of Akt and support osteogenic differentiation. Bovine LF has been demonstrated to activate LRP1-independent, PI3K/Akt signaling in osteoblastic cells (Grey et al. 2006, Amini, Nair 2011c). Similarly, our studies demonstrated an increased Akt phosphorylation (Figure 20) and LRP1 expression (Figure 21) relative to untreated control by rhLF treatment in MC3T3 cells after 15 and 30 minutes irrespective of the iron concentration.

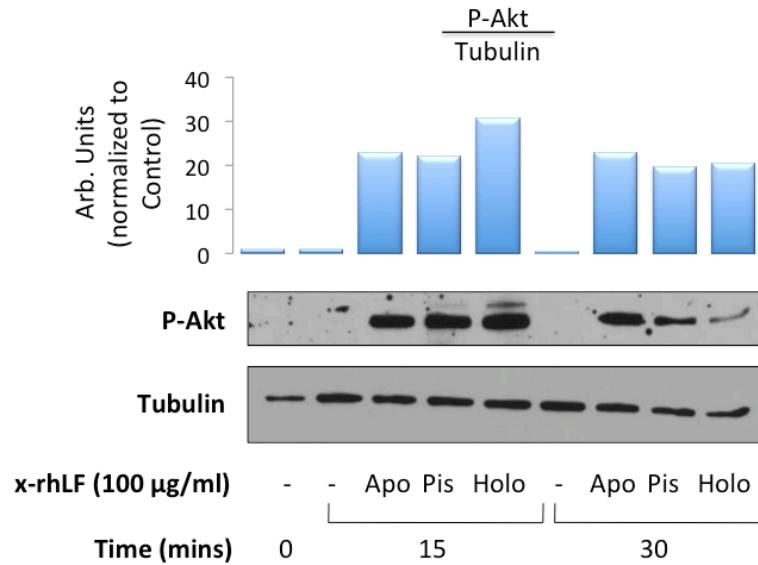


Figure 20. Effect of rhLF iron concentration on Akt phosphorylation in MC3T3 cells.

*Cells were treated for both 15 and 30 minutes in culture. Anti-tubulin was used as a gel loading control.*

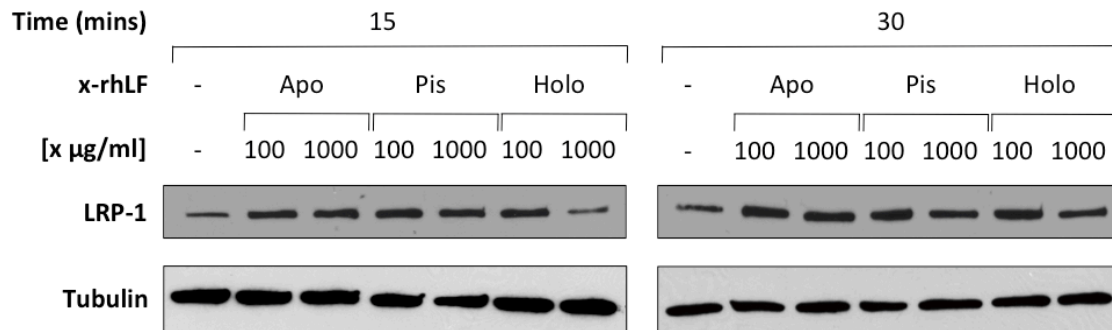


Figure 21. Effect of rhLF iron concentration on LRP1 expression in MC3T3 cells.

*Cells were treated for both 15 and 30 minutes in culture. Anti-tubulin was used as a gel loading control.*

The molecular mechanisms underlying the anabolic effects of LF have not yet been clearly elucidated.  $\beta$  catenin-dependent signaling pathway has been well documented as an osteogenic signaling pathway (Novak, Dedhar 1999). The

phosphorylation of Disheveled (Dsh) leads to the destabilization of the  $\beta$  catenin destruction/ubiquitination complex – which includes a series of events including Gsk3 $\beta$  phosphorylation. These actions ultimately lead to the stabilization of cytoplasmic  $\beta$  catenin. Irrespective of the iron concentration, all the rhLFs showed significant increase in phosphorylation of Dishevelled 2, Gsk3 $\beta$  and increased activation (de-phosphorylation) of  $\beta$  catenin relative to untreated control (Figure 22).

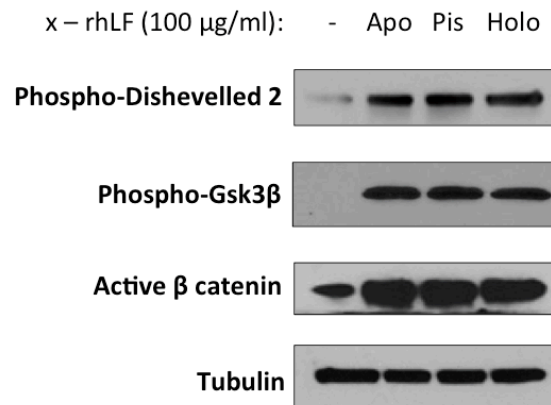


Figure 22. Effect of rhLF iron concentration on Dishevelled 2, Gsk3 $\beta$  phosphorylation and  $\beta$  catenin activation in MC3T3 cells.

*Cells were treated for 24 hours in culture. Anti-tubulin was used as a gel loading control.*

Furthermore, through immunocytochemistry, we demonstrated that the accumulation of  $\beta$  catenin in the cytoplasm resulted in the translocation of  $\beta$  catenin to the nucleus (Figure 23a) upon 100  $\mu$ g/ml apo- and holo-rhLF supplementation for 24 hours.

We also investigated the effect of iron concentration of rhLF in inducing the production of growth factors and chemokines by MC3T3 cells when cultured in the presence of apo, and holo-rhLFs. Immunocytochemistry studies were performed to

confirm the production of IL6 and VEGF by MC3T3 cells in the presence of apo- and holo-rhLF to evaluate whether the expression of the cytokines and chemokines is dependent on iron concentration. Figures 20b and c show the immunofluorescence images of MC3T3-E1 cells exposed to 100 µg/ml of apo and holo-rhLF indicating positive stains for both IL6 and VEGF. The data demonstrates that rhLF is capable of inducing the expression of IL6 and VEGF in MC3T3 cells and the effect is independent of the iron concentration.

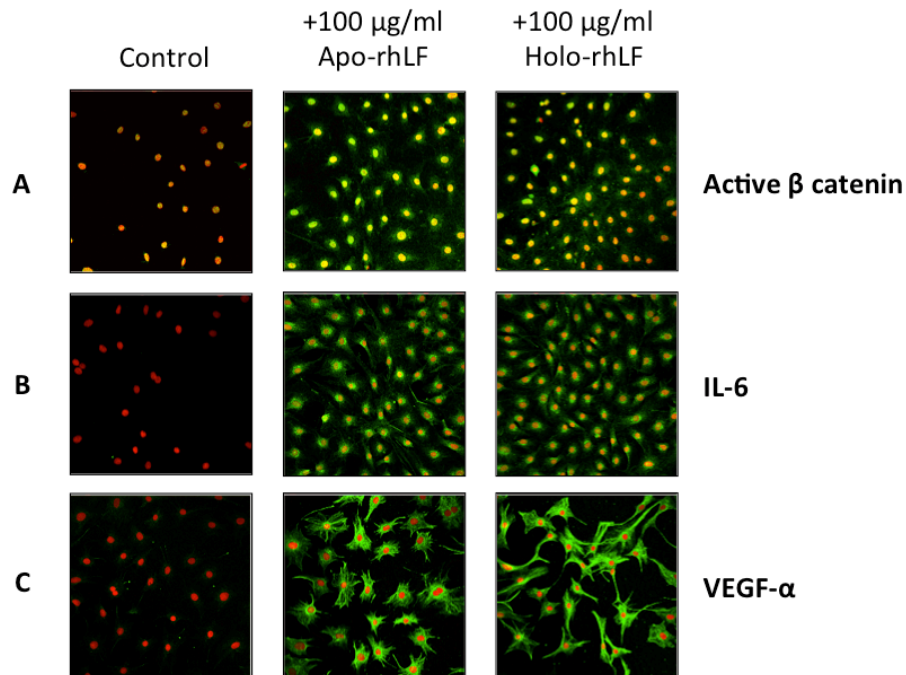


Figure 23. Immunocytochemistry analysis of (A) active β catenin, (B) IL6 and (C) VEGFα of 100 µg/ml of apo- or holo-rhLF treated + or untreated (control).

*Cells were treated for 24 hours in culture. Nuclei were detected using propidium iodide (red) and protein expression was detected using FITC-labelled (green) secondary antibodies.*

Microarray gene expression analysis was performed on MC3T3 cells treated with rhLF at the three varying iron saturations (apo, pis, holo) for 24 hours (Figure 24). Data

quality and reproducibility is supported by the use of three biological replicates per sample and also high level of bead-type redundancy (up to an average of 30 beads per probe) on each array. Of the 45,200 gene transcripts present in the gene array only 251 genes were significantly regulated by rhLF. We compared the relative expression of 251 regulated genes by rhLF of different iron concentrations normalized to untreated control. Approximately 94% of the 251 genes were regulated similarly by rhLFs irrespective of the iron concentration. Only 6% genes of the 251 statistically significant genes were found to be affected by rhLF iron concentration. For example, *Ccl7* was up-regulated 1.77-, 4.75-, and 3.48- fold over control respectively by apo-, partial- and holo-rhLFs. *Ccl2*, which is under the control of  $\text{NF}\kappa\text{B}$  and expressed by mature osteoclasts and osteoblasts (Matsuo, Irie 2008), was up-regulated 1.46-, 3.69-, 2.74-fold over control, respectively, by apo-, pis- and holo-rhLFs. *Nfkbiz*, a gene that encodes for  $\text{NF}\kappa\text{B}$  inhibitor zeta, was also positively regulated by rhLF. Interestingly, this cluster of genes – *Ccl7*, *Ccl2* and *Nfkbiz*, were all more up-regulated upon treatment with rhLFs with higher iron concentration (pis- and holo-) relative to the form with the lowest iron concentration (apo-). *Tfrc*, a gene that encodes for transferrin receptor, was the only gene found to be differentially regulated by the rhLFs with high (pis and holo) and low (apo) iron concentration. Iron-deficient (apo) rhLF up-regulated *Tfrc* 1.32-fold, whereas, pis- and holo-rhLF down regulated the gene by 1.20- and 1.26-fold, respectively. Table 3, 4 & 5, present the list of genes that were up-, down- or differentially-regulated in MC3T3 cells by 100  $\mu\text{g/mL}$  of rhLFs of three different iron concentrations after 24 hours in culture.

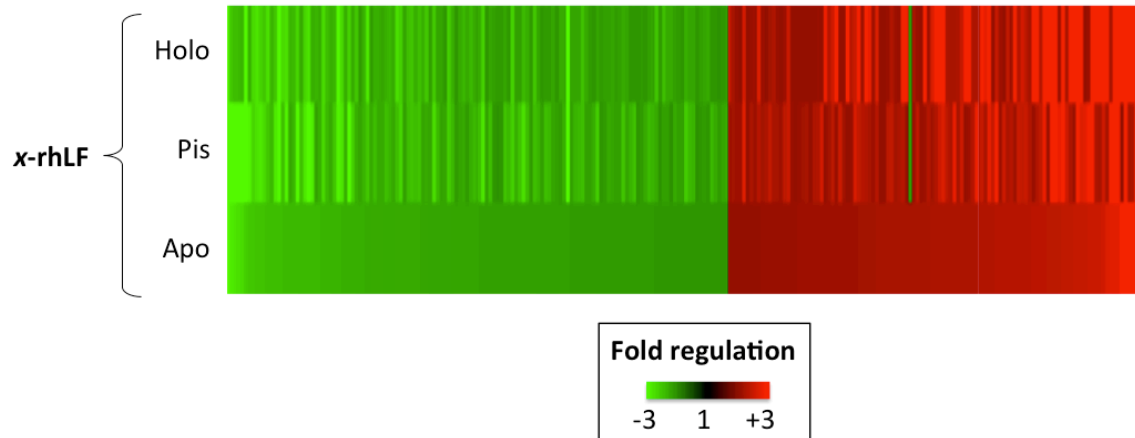


Figure 24. Global expression profiles in MC3T3 murine preosteoblasts treated with varying iron saturations of rhLF.

Cultures were treated for 24 hours with 100  $\mu\text{g/ml}$  apo-, pis- and holo-rhLF. Data is expressed as fold change over 24 hour untreated control sample. Red signifies up-regulation, and green signifies down-regulation. 251 genes had statistically significant regulation by the three iron saturated rhLFs relative to the untreated control sample.

Table 3. Genes up-regulated by rhLF of different iron concentrations.

		Fold change of 100 $\mu\text{g/ml}$ (x-rhLF) relative to untreated control		
PROBE_ID	Gene Symbol	Apo-rhLF	Pis-rhLF	Holo-rhLF
ILMN_1239230	<i>Aurkb</i>	1.308	1.161	1.161
ILMN_1229455	<i>D11Ertd759e</i>	1.272	2.677	1.166
ILMN_1259564	<i>Al481100</i>	2.027	5.613	1.166
ILMN_1229827	<i>St7</i>	1.237	1.162	1.174
ILMN_2420939	<i>scl0002624.1_576</i>	1.308	1.182	1.179
ILMN_1224855	<i>AA175286</i>	1.26	1.837	1.186
ILMN_2830661	<i>Top2a</i>	1.255	1.196	1.195
ILMN_1250410	<i>Prkr</i>	1.367	2.285	1.198
ILMN_1243129	<i>Slc11a2</i>	1.273	1.454	1.202
ILMN_2546272	<i>Gng12</i>	1.191	1.193	1.206
ILMN_2681232	<i>D12Ertd647e</i>	1.331	1.175	1.208
ILMN_2984828	<i>Ly6e</i>	1.321	2.467	1.213
ILMN_1257771	<i>Ifi205</i>	1.457	2.709	1.22
ILMN_2717127	<i>Ddx58</i>	1.462	2.47	1.222
ILMN_2956102	<i>Ncapd2</i>	1.242	1.18	1.231
ILMN_2924419	<i>H2-Q7</i>	1.518	2.832	1.234
ILMN_2688075	<i>Cyp51</i>	1.322	1.304	1.237
ILMN_1231392	<i>Melk</i>	1.232	1.193	1.238
ILMN_2431619	<i>Ube2l6</i>	1.264	2.154	1.24
ILMN_2711401	<i>3200002M19Rik</i>	1.299	1.276	1.244



ILMN_2770585	<i>BC027061</i>	1.194	1.24	1.249
ILMN_1230020	<i>Fmod</i>	1.171	1.527	1.249
ILMN_2661289	<i>Csprs</i>	1.334	2.892	1.25
ILMN_2593196	<i>Stat1</i>	1.427	2.531	1.257
ILMN_1243616	<i>Cdkn3</i>	1.228	1.165	1.26
ILMN_3161897	<i>Dync1li2</i>	1.183	1.21	1.267
ILMN_2511868	<i>2310002B06Rik</i>	1.184	1.159	1.272
ILMN_2630852	<i>Il7</i>	1.262	1.417	1.277
ILMN_3083163	<i>Cp</i>	1.369	2.168	1.277
ILMN_2739999	<i>B2m</i>	1.344	1.691	1.278
ILMN_1248132	<i>Stmn1</i>	1.404	1.277	1.28
ILMN_2708340	<i>1700029F09Rik</i>	1.27	1.195	1.282
ILMN_1229210	<i>2610318C08Rik</i>	1.245	1.175	1.285
ILMN_3096592	<i>Epb4.1l1</i>	1.204	1.243	1.287
ILMN_2816754	<i>Ndc80</i>	1.317	1.242	1.293
ILMN_1238000	<i>Srpx</i>	1.181	1.325	1.3
ILMN_1221817	<i>li</i>	1.706	3.788	1.3
ILMN_1234539	<i>Irgm</i>	1.587	2.834	1.304
ILMN_3135781	<i>Anxa3</i>	1.213	1.237	1.308
ILMN_2944666	<i>Ifit3</i>	2.17	10.802	1.309
ILMN_2625451	<i>Ankrd1</i>	1.359	1.367	1.318
ILMN_2757870	<i>Psmb10</i>	1.293	1.81	1.318
ILMN_1256257	<i>G1p2</i>	3.222	14.31	1.318
ILMN_2832219	<i>Cdca3</i>	1.255	1.181	1.324
ILMN_2755915	<i>Pet112l</i>	1.212	1.37	1.328
ILMN_1216746	<i>B2m</i>	1.39	1.777	1.331
ILMN_2737163	<i>Sqle</i>	1.318	1.213	1.348
ILMN_1237375	<i>Scd1</i>	1.352	1.304	1.35
ILMN_2588139	<i>H2-K1</i>	1.575	3.047	1.351
ILMN_2693940	<i>Psmb8</i>	1.49	2.104	1.353
ILMN_2773981	<i>0610007P14Rik</i>	1.211	1.164	1.358
ILMN_2657376	<i>Nipsnap3b</i>	1.191	1.237	1.36
ILMN_2696339	<i>Fgfr1op</i>	1.42	1.491	1.363
ILMN_1224110	<i>Bst2</i>	2.278	6.542	1.365
ILMN_2919433	<i>Cdc45l</i>	1.257	1.187	1.366
ILMN_1257574	<i>Esm1</i>	1.458	2.115	1.381
ILMN_1233449	<i>Ifi205</i>	1.344	2.391	1.383
ILMN_2636110	<i>Sgol2</i>	1.257	1.206	1.387
ILMN_2711772	<i>A930021H16Rik</i>	1.289	2.022	1.391
ILMN_2878355	<i>Kpna2</i>	1.447	1.296	1.409
ILMN_2866970	<i>Kif11</i>	1.337	1.27	1.411
ILMN_1225730	<i>Fdps</i>	1.37	1.37	1.413
ILMN_2914843	<i>Psmb10</i>	1.196	1.693	1.419
ILMN_1223045	<i>2810417H13Rik</i>	1.373	1.32	1.429
ILMN_2711075	<i>Mmp9</i>	1.303	1.672	1.433
ILMN_1260362	<i>LOC223594</i>	1.283	1.257	1.439
ILMN_2531281	<i>LOC271490</i>	1.427	1.265	1.447
ILMN_3122961	<i>Gbp2</i>	1.319	2.728	1.454
ILMN_3006767	<i>Mkl</i>	1.264	1.602	1.462

ILMN_2687156	<i>Galm</i>	1.347	1.342	1.465
ILMN_2711112	<i>Shcbp1</i>	1.231	1.258	1.467
ILMN_2612774	<i>Hrbl</i>	1.31	1.231	1.472
ILMN_1225718	<i>Hmgcr</i>	1.327	1.213	1.475
ILMN_2738921	<i>2410187C16Rik</i>	1.432	1.65	1.509
ILMN_2737302	<i>Cxcl12</i>	1.313	1.399	1.51
ILMN_2709478	<i>Sh3kbp1</i>	1.211	1.283	1.513
ILMN_1230065	<i>LOC245892</i>	1.458	1.421	1.513
ILMN_1256817	<i>Slpi</i>	1.277	1.903	1.515
ILMN_2701271	<i>Plscr1</i>	1.38	1.963	1.54
ILMN_1216764	<i>Ier3</i>	1.232	1.564	1.556
ILMN_1226839	<i>Hist1h2ag</i>	1.402	1.186	1.559
ILMN_2732795	<i>Mylc2pl</i>	1.443	1.473	1.567
ILMN_2528456	<i>LOC219106</i>	1.406	1.197	1.582
ILMN_2638548	<i>Atoh8</i>	1.428	1.417	1.583
ILMN_2662803	<i>Ptx3</i>	1.362	1.55	1.588
ILMN_2960214	<i>8430423A01Rik</i>	1.266	1.17	1.594
ILMN_2811737	<i>Casp4</i>	1.345	2.538	1.595
ILMN_2652857	<i>Ifi47</i>	1.608	2.837	1.621
ILMN_1235327	<i>Rbbp4</i>	1.484	1.329	1.623
ILMN_1217929	<i>LOC328752</i>	1.259	1.187	1.635
ILMN_2662802	<i>Ptx3</i>	1.275	1.579	1.667
ILMN_2930203	<i>Ugt1a10</i>	1.345	1.972	1.706
ILMN_1254561	<i>Csf1</i>	1.19	1.635	1.713
ILMN_2618918	<i>Slc2a6</i>	1.532	2.227	1.719
ILMN_1248830	<i>Hist1h2an</i>	1.533	1.174	1.769
ILMN_2459899	<i>Tsrc1</i>	1.392	2.178	1.781
ILMN_1238276	<i>Hist1h2ai</i>	1.472	1.231	1.799
ILMN_2725402	<i>Nsdhl</i>	1.353	1.329	1.799
ILMN_2594525	<i>Nsdhl</i>	1.37	1.361	1.831
ILMN_2856095	<i>Zc3h12a</i>	1.458	2.131	1.849
ILMN_1219574	<i>Hist1h2af</i>	1.556	1.225	1.912
ILMN_2759484	<i>C3</i>	3.17	9.662	1.993
ILMN_1228557	<i>Id2</i>	1.404	1.532	2.003
ILMN_1231814	<i>Ccl5</i>	4.426	26.037	2.045
ILMN_1255416	<i>Ly6a</i>	1.481	3.841	2.18
ILMN_1222543	<i>Ugt1a9</i>	1.564	2.528	2.248
ILMN_2493826	<i>Ugt1a10</i>	1.462	2.4	2.254
ILMN_2795040	<i>Hist1h2ad</i>	1.742	1.302	2.276
ILMN_2896200	<i>Tnn</i>	2.149	3.585	2.329
ILMN_2755008	<i>Nfkbiz</i>	1.758	3.666	2.599
ILMN_2835117	<i>Ccl7</i>	1.523	3.372	2.637
ILMN_1245710	<i>Ccl2</i>	1.463	3.685	2.736
ILMN_2771176	<i>Ccl7</i>	1.769	4.753	3.48

Table 4. Genes down-regulated byrhLF of different iron concentrations

Fold change of 100 µg/ml (x-rhLF)

relative to untreated control

PROBE_ID	Gene Symbol	Apo-rhLF	Pis-rhLF	Holo-rhLF
ILMN_1216322	<i>Hmgcs2</i>	-2.41	-2.60	-3.04
ILMN_1248998	<i>Xpnpep2</i>	-1.61	-2.03	-2.49
ILMN_2742426	<i>Selenbp1</i>	-1.44	-1.77	-2.29
ILMN_2944508	<i>Bglap2</i>	-1.80	-1.48	-2.25
ILMN_1220829	<i>Bglap2</i>	-1.83	-1.56	-2.19
ILMN_1233122	<i>Bglap-rs1</i>	-1.71	-1.40	-2.16
ILMN_2727309	<i>Selenbp2</i>	-1.38	-1.63	-2.10
ILMN_3101908	<i>Bglap1</i>	-1.73	-1.46	-1.98
ILMN_2445249	<i>Krt1-5</i>	-1.25	-2.05	-1.97
ILMN_2695085	<i>Sorcs2</i>	-1.45	-1.66	-1.95
ILMN_1245864	<i>Ifitm5</i>	-1.48	-1.94	-1.93
ILMN_1244099	<i>LOC386192</i>	-1.56	-1.38	-1.88
ILMN_2687165	<i>Chst2</i>	-1.40	-1.92	-1.88
ILMN_2724942	<i>Ptgis</i>	-1.47	-1.76	-1.86
ILMN_2816180	<i>Lbh</i>	-1.44	-1.37	-1.85
ILMN_2692244	<i>Itga10</i>	-1.52	-1.64	-1.83
ILMN_3162005	<i>BC054438</i>	-1.48	-1.57	-1.81
ILMN_1230648	<i>Rerg</i>	-1.44	-1.66	-1.80
ILMN_2479977	<i>1110065P19Rik</i>	-1.39	-1.68	-1.79
ILMN_2760254	<i>Mrgprf</i>	-1.28	-1.62	-1.77
ILMN_2980663	<i>Aqp1</i>	-1.53	-1.79	-1.76
ILMN_2633350	<i>Mfap4</i>	-1.27	-1.45	-1.75
ILMN_2643241	<i>Accn2</i>	-1.31	-1.59	-1.74
ILMN_1225348	<i>C230093N12Rik</i>	-1.51	-1.56	-1.71
ILMN_1229745	<i>Sertad4</i>	-1.43	-1.71	-1.70
ILMN_2980661	<i>Aqp1</i>	-1.55	-1.69	-1.66
ILMN_2829262	<i>Ltbp4</i>	-1.32	-1.62	-1.64
ILMN_1250569	<i>B230105J10</i>	-1.37	-1.36	-1.62
ILMN_2796472	<i>Vldlr</i>	-1.27	-1.64	-1.61
ILMN_2601833	<i>Plcg2</i>	-1.30	-1.61	-1.61
ILMN_1217102	<i>Tpcn1</i>	-1.24	-1.29	-1.61
ILMN_2746738	<i>Htra1</i>	-1.20	-1.37	-1.60
ILMN_2756486	<i>Aqp1</i>	-1.34	-1.79	-1.56
ILMN_2625197	<i>Ptprv</i>	-1.40	-1.41	-1.56
ILMN_3063340	<i>Ibsp</i>	-1.49	-1.75	-1.55
ILMN_1252294	<i>Eef2</i>	-1.27	-1.27	-1.54
ILMN_2695143	<i>Capn6</i>	-1.23	-1.33	-1.52
ILMN_2818294	<i>Srpx2</i>	-1.32	-1.49	-1.52
ILMN_2616164	<i>Itga3</i>	-1.27	-1.30	-1.52

ILMN_2939012	<i>1500012F01Rik</i>	-1.28	-1.36	-1.51
ILMN_1237485	<i>2310040A07Rik</i>	-1.32	-1.55	-1.51
ILMN_2744603	<i>2010323F13Rik</i>	-1.32	-1.72	-1.50
ILMN_1218264	<i>Vldlr</i>	-1.27	-1.55	-1.50
ILMN_1221178	<i>Pdlim2</i>	-1.33	-1.39	-1.50
ILMN_2954195	<i>Scyl1</i>	-1.45	-1.34	-1.50
ILMN_1230152	<i>Adamts4</i>	-1.22	-1.19	-1.50
ILMN_2770088	<i>lbsp</i>	-1.47	-1.69	-1.48
ILMN_2428931	<i>4631426J05Rik</i>	-1.32	-1.50	-1.48
ILMN_1221264	<i>Klf4</i>	-1.32	-1.36	-1.48
ILMN_1259339	<i>Cdk5r1</i>	-1.25	-1.50	-1.48
ILMN_1237421	<i>scl0003519.1_175</i>	-1.27	-1.35	-1.48
ILMN_1251301	<i>1200014P03Rik</i>	-1.28	-1.31	-1.47
ILMN_3139693	<i>Rab11fip5</i>	-1.26	-1.24	-1.47
ILMN_2438962	<i>2900054C01Rik</i>	-1.34	-1.39	-1.47
ILMN_1248099	<i>Col16a1</i>	-1.22	-1.28	-1.46
ILMN_2718096	<i>Sema3b</i>	-1.30	-1.39	-1.46
ILMN_1232884	<i>Sphk1</i>	-1.20	-1.31	-1.45
ILMN_2826816	<i>Ppox</i>	-1.27	-1.23	-1.45
ILMN_3141106	<i>lbsp</i>	-1.41	-1.48	-1.44
ILMN_2911520	<i>Hexdc</i>	-1.25	-1.32	-1.44
ILMN_2457408	<i>Zswim4</i>	-1.31	-1.30	-1.44
ILMN_3112922	<i>Hdac5</i>	-1.26	-1.23	-1.44
ILMN_1255166	<i>Ctxn</i>	-1.29	-1.32	-1.43
ILMN_2592823	<i>Cdc42ep5</i>	-1.19	-1.18	-1.43
ILMN_2604029	<i>Klf2</i>	-1.45	-1.46	-1.42
ILMN_1228385	<i>ltpr3</i>	-1.48	-1.42	-1.42
ILMN_3064283	<i>Pde4dip</i>	-1.26	-1.31	-1.41
ILMN_2966104	<i>Htra1</i>	-1.20	-1.31	-1.41
ILMN_1260064	<i>Pfn2</i>	-1.33	-1.43	-1.41
ILMN_2620145	<i>Plcd3</i>	-1.23	-1.19	-1.41
ILMN_2920736	<i>Bbc3</i>	-1.25	-1.30	-1.41
ILMN_2418426	<i>Wig1</i>	-1.22	-1.29	-1.41
ILMN_2622500	<i>B230208J24Rik</i>	-1.35	-1.40	-1.40
ILMN_2698728	<i>SrpX2</i>	-1.29	-1.44	-1.38
ILMN_2602185	<i>40795</i>	-1.43	-1.35	-1.37
ILMN_2490252	<i>Spred1</i>	-1.27	-1.27	-1.37
ILMN_2592093	<i>Ift20</i>	-1.25	-1.32	-1.37
ILMN_2696592	<i>C77080</i>	-1.24	-1.18	-1.36
ILMN_1214899	<i>Phospho1</i>	-1.36	-1.56	-1.36
ILMN_2648098	<i>Srgap2</i>	-1.39	-1.36	-1.36

ILMN_2909211	<i>Msrb2</i>	-1.21	-1.25	-1.35
ILMN_2618696	<i>D15Ert405e</i>	-1.34	-1.24	-1.35
ILMN_2750258	<i>Mea1</i>	-1.18	-1.17	-1.35
ILMN_2753323	<i>Eif4b</i>	-1.21	-1.53	-1.34
ILMN_1215524	<i>9330161C17Rik</i>	-1.22	-1.19	-1.34
ILMN_2815138	<i>Myom1</i>	-1.23	-1.26	-1.34
ILMN_2664155	<i>Pycr1</i>	-1.34	-1.36	-1.33
ILMN_2615559	<i>Dab2ip</i>	-1.34	-1.32	-1.33
ILMN_2744492	<i>D10Bwg0940e</i>	-1.29	-1.44	-1.33
ILMN_2925711	<i>Dusp6</i>	-1.41	-1.39	-1.33
ILMN_2871628	<i>Mapk8ip1</i>	-1.18	-1.23	-1.32
ILMN_2734391	<i>Ramp1</i>	-1.31	-1.57	-1.32
ILMN_1227494	<i>Egr3</i>	-1.46	-1.42	-1.32
ILMN_1237579	<i>1810062018Rik</i>	-1.33	-1.36	-1.32
ILMN_1234746	<i>AI790298</i>	-1.31	-1.26	-1.32
ILMN_1232621	<i>Ank</i>	-1.23	-1.31	-1.31
ILMN_2619767	<i>Pdlim2</i>	-1.23	-1.30	-1.30
ILMN_1226259	<i>Adamts2</i>	-1.26	-1.30	-1.30
ILMN_2907214	<i>Tcea3</i>	-1.29	-1.21	-1.30
ILMN_2650356	<i>Pthr1</i>	-1.32	-1.38	-1.30
ILMN_1241903	<i>Klf4</i>	-1.29	-1.34	-1.30
ILMN_2757916	<i>2810037C14Rik</i>	-1.30	-1.22	-1.30
ILMN_2450096	<i>Zfp30</i>	-1.18	-1.20	-1.30
ILMN_2617820	<i>Ppp3cc</i>	-1.28	-1.20	-1.29
ILMN_2483811	<i>2210408F11Rik</i>	-1.25	-1.29	-1.29
ILMN_1245549	<i>6330404C01Rik</i>	-1.44	-1.41	-1.29
ILMN_2701750	<i>2310061J03Rik</i>	-1.36	-1.23	-1.29
ILMN_2593774	<i>1190002H23Rik</i>	-1.21	-1.48	-1.28
ILMN_2643377	<i>Slc24a6</i>	-1.26	-1.19	-1.28
ILMN_2548010	<i>1110018K11Rik</i>	-1.30	-1.29	-1.28
ILMN_2594779	<i>5430431G03Rik</i>	-1.20	-1.22	-1.28
ILMN_1237061	<i>Dm15</i>	-1.21	-1.33	-1.28
ILMN_2509830	<i>A730063M14Rik</i>	-1.23	-1.24	-1.28
ILMN_2637714	<i>Rasa3</i>	-1.24	-1.33	-1.27
ILMN_2594031	<i>BC011468</i>	-1.24	-1.23	-1.27
ILMN_2443618	<i>2900026A02Rik</i>	-1.21	-1.22	-1.27
ILMN_1230145	<i>Acvr2b</i>	-1.23	-1.26	-1.26
ILMN_2476329	<i>Whrn</i>	-1.26	-1.20	-1.26
ILMN_1256950	<i>1190009E12Rik</i>	-1.32	-1.29	-1.26
ILMN_2599657	<i>Fmnl3</i>	-1.27	-1.24	-1.25
ILMN_2765047	<i>Chrd</i>	-1.19	-1.31	-1.24

ILMN_2732642	<i>Kptn</i>	-1.18	-1.17	-1.23
ILMN_1232146	<i>1700021C14Rik</i>	-1.22	-1.23	-1.23
ILMN_2799596	<i>Al662250</i>	-1.29	-1.33	-1.23
ILMN_2776619	<i>Ltbp3</i>	-1.23	-1.26	-1.23
ILMN_2490820	<i>2310005L22Rik</i>	-1.29	-1.19	-1.22
ILMN_1239386	<i>5230401C23Rik</i>	-1.25	-1.32	-1.22
ILMN_2890357	<i>2610027C15Rik</i>	-1.19	-1.28	-1.21
ILMN_2776283	<i>Tcea3</i>	-1.28	-1.29	-1.20
ILMN_2613306	<i>Efh1</i>	-1.19	-1.33	-1.20
ILMN_2704822	<i>Acaa2</i>	-1.27	-1.23	-1.19
ILMN_2687032	<i>Fbxo31</i>	-1.22	-1.17	-1.18
ILMN_3106053	<i>Slc39a7</i>	-1.24	-1.23	-1.18
ILMN_2754027	<i>Nit1</i>	-1.21	-1.23	-1.17
ILMN_2674575	<i>Mmd</i>	-1.20	-1.21	-1.17
ILMN_2671755	<i>Ceacam1</i>	-1.28	-1.22	-1.17
ILMN_2528440	<i>LOC380927</i>	-1.21	-1.32	-1.15

Table 5. Genes differentially regulated by rhLF of different iron concentrations

Fold change of 100 µg/ml (x-rhLF) relative to untreated control				
PROBE_ID	Gene Symbol	Apo-rhLF	Pis-rhLF	Holo-rhLF
ILMN_2619848	<i>Tfrc</i>	1.32	-1.20	-1.26

#### 4.1.4 Discussion

In this study, the effect of iron concentration on the biological activity of rice-derived rhLFs towards MC3T3 cells was examined. LF is a known pleiotropic factor with unique antimicrobial, antiviral, immunomodulatory properties and anabolic effects in bone at physiological concentrations. The molecular mechanisms behind the favorable pleiotropic properties of LF are largely unknown, however, the role of various cell surface receptors in mediating LF biological response have been identified. One of our long-term goals is to develop bioactive biomaterials using unique ligand molecules that

can activate specific receptor mediated signaling pathways. We have previously demonstrated the feasibility of developing LF-based biomaterials via an enzymatic process irrespective of the iron content of the protein (Amini, Nair 2011a, Amini, Nair 2012a). The aim of the present study was to evaluate whether the iron content of the protein can make a significant difference in the bioactivity towards pre-osteoblast cells, to determine the most effective protein to form LF based biomaterials to support bone regeneration.

Bovine LF has been shown to induce the proliferation of primary osteoblasts and osteoblastic cell lines. rhLF derived from rice has shown to have mitogenic effects towards a variety of cells types such as intestinal cells, hybridoma cells, osteoblast cells and embryonic kidney cells (Huang et al. 2008). Based on LFs mitogenic activity on different cell types two possible mechanisms have been suggested. The possibility of iron acting as a nutrient to support cell proliferation and LF regulated gene expression in cells through putative cell surface receptors. Statistically significant dose-dependent proliferation of MC3T3 cells cultured in the presence of 100 and 1000 µg/ml apo-, pis- and holo-rhLFs relative to untreated control demonstrated the significant mitogenic effect of rhLF towards MC3T3 cells. However, lack of difference in mitogenic effect between apo-, partial- and holo LFs at all the concentrations studied indicates that the mitogenic effect of rhLF towards MC3T3 is independent of iron concentration and therefore potentially mediated by modulation of gene expression via cell surface receptors. The observed results show a significant difference in behavior of rice-derived rhLFs towards HT-29 intestinal cells which might be due to the different receptors involved in the signaling cascade (Huang et al. 2008). The mitogenic effect of bLFs towards osteoblasts

is known to be mediated at least partially via LRP1 receptors, whereas in the intestinal cells, the ERK1/2 signaling cascades is mediated via lactoferrin receptor (LfR) (Jiang, Lonnerdal 2012). Interestingly, LF receptor mRNA has been found to be undetectable in osteoblastic cells (Naot et al. 2011).

Another unique bioactivity of lactoferrin is its ability to increase cell survival, even though the mechanism behind the anti-apoptotic activity of LF is unknown. Previous studies using osteoblasts have demonstrated the ability of bLF to induce PI3K-dependent Akt signaling independent of LRP1 receptor activation (Grey et al. 2006). MC3T3 cells cultured in presence of rhLFs showed significant increase in Akt phosphorylation irrespective of iron concentrations indicating that as in the case of mitogenic activity Akt phosphorylation of rhLF is mediated by a mechanism independent of iron concentration and potentially mediated through modulation of gene expression induced by the protein LF.

The  $\beta$  catenin-dependent signaling pathway has been documented as a potential osteogenic signaling pathway (Novak, Dedhar 1999). The phosphorylation of Disheveled (Dsh) leads to the destabilization of the  $\beta$  catenin destruction/ubiquitination complex – which includes a series of events including Gsk3 $\beta$  phosphorylation. These actions ultimately lead to the stabilization of cytoplasmic  $\beta$  catenin. Accumulation of  $\beta$  catenin in the cytoplasm prompts its translocation to the nucleus, where it interacts with members of the TCF/LEF family of transcription factors and induces the transcription of target genes. Figure 19 demonstrates that, irrespective of the iron concentration, rhLF increases phosphorylation of Dsh2, Gsk3 $\beta$  and activation (de-phosphorylation) of  $\beta$  catenin in MC3T3 cells relative to untreated control. The translocation of the stabilized  $\beta$  catenin to



the nucleus was confirmed by immunocytochemistry (Figure 20a). The stabilization of  $\beta$  catenin has been known to occur via Wnt-dependent as well as Wnt-independent pathways. Wnt and growth factor signaling can act through convergent pathways and possibly synergistically on GSK3 $\beta$  and  $\beta$  catenin (Jin, George Fantus & Sun 2008). Among Wnt proteins, Wnt3a has been extensively investigated as a potent molecule to induce stabilization of  $\beta$  catenin, which then cooperatively regulate gene expression with LEF/Tcf transcription factors (Mbalaviele et al. 2005, Chen, Alman 2009, Baron, Rawadi 2007). Signaling pathways affecting GSK3 $\beta$  (e.g. PI3K/Akt) can also modulate  $\beta$  catenin transcriptional activity. LRP6 phosphorylation by various protein kinases is considered another crucial factor for  $\beta$  catenin stabilization. In summary, the data shown here demonstrate the ability of rhLF to stabilize  $\beta$  catenin in preosteoblast cells and that the effect is independent of the iron concentration. More details on the possible mechanism of  $\beta$  catenin stabilization and the transcriptional activity will be discussed in section 4.3.3.2.1.

The pleiotropic functions of LF have also been attributed to its ability to induce the synthesis of growth factors, cytokines and chemokines by the cells. Cell signaling molecules, such as growth factors and cytokines, play an important part in the bone regenerative process. IL6, a pleiotrophic cytokine, has been demonstrated to be an important regulator for bone maturation during development (Yang et al. 2004). IL6, is also known to be involved in initiating signaling cascades required for bone regeneration following injury (Mountziaris, Mikos 2008). Immunofluorescence study demonstrated the expression of IL6 protein in MC3T3 cells after 24 hours in culture in the presence of 100  $\mu$ g/mL apo- and holo-rhLFs. The results concur with the up-regulation of *IL6* mRNA

in MC3T3 cells treated with 50 µg/ml bLF after 2 hours (Naot et al. 2011). Collectively, the results demonstrate that rhLF is capable of inducing IL6 expression in MC3T3 cells irrespective of the iron concentration.

VEGF $\alpha$  is another major angiogenic factor that has been demonstrated to be an essential component of skeletal development and repair. Recent studies demonstrated the ability of bLF in inducing the synthesis of the angiogenic factors VEGF and FGF2 in MC3T3 cells via the p44/p42 MAPK pathway (Nakajima et al. 2011, James et al. 2011). Other studies demonstrated the ability of hLF in stimulating VEGF $\alpha$  – mediated endothelial cell proliferation and migration (Kim et al. 2006). It has been demonstrated that exposure of human umbilical vein endothelial cells (HUVECs) to hLF significantly increased VEGF-induced Erk MAPK phosphorylation (Kim et al. 2006). Similarly, bovine milk LF induces synthesis of the angiogenic factors (VEGF) in MC3T3 cells via the p44/p42 MAP kinase pathway (Nakajima et al. 2011, Amini, Nair 2011a). Studies have also demonstrated that increased skeletal VEGF can enhance  $\beta$  catenin activity and results in excessively ossified bones (Maes et al. 2010). The present study demonstrates that rhLF is capable of inducing VEGF $\alpha$  expression in MC3T3 cells and the expression is also independent of rhLF iron concentration.

The global whole-genome array study was performed to understand the effect of iron concentration on the overall gene expression profile of MC3T3 cells. The regulated genes cover a broad range of functional activities of LF ranging from immunity, cell cycle progression and bone metabolism. The data reported to our knowledge is the first genetic profile of rhLF treated MC3T3 cells and provide better understanding of the molecular mechanism behind the pleiotropic effect of rhLF towards osteoblasts. Only a

limited number of genes with known osteoblast relevant functions are discussed here. A number of known genes regulated during osteoblast differentiation were found to be down-regulated in MC3T3 cells for 24 hours when cultured in basal media in the presence of rhLFs irrespective of the iron concentrations. These include mature osteoblast markers, *osteocalcin* (*Bglap*) and *bone sialoprotein* (*Ibsp*), transcription factors *parathyroid hormone receptor 1* (*Pthr1*) and *prostaglandin 12 synthase* (*Ptgis*). *Adamts2* (*A disintegrin and metalloproteinase with thrombospondin motifs 2*), which is responsible for processing several types of procollagen proteins (Wang et al. 2003), was also down-regulated approximately 1.28-fold by all iron saturation forms. Interestingly, FGF2-treated MC3T3 cells also showed similar results of significant down-regulation of osteoblast differentiation-associated genes (i.e., *BMP2*, *osteocalcin*, *Runx2* and *collagen 1*) at 24 hours in culture (Hughes-Fulford, Li 2011). On the other hand, *matrix metalloproteinase 9* (*MMP9*), a key regulator in the development of the growth plate during endochondral bone formation (Pratap et al. 2005), was stimulated by all iron saturation forms (apo-, pis-, holo-) by 1.30-, 1.67-, 1.43-fold, respectively.

The gene array however, demonstrated an up-regulation of early osteoblastic induction and proliferation markers. One example is *Cxcl12* (*chemokine (C-X-C motif) ligand 12*) or *SDF1* (*stromal cell-derived factor 1*), which is an early marker of osteoblastic induction modulated by growth factors, which include VEGF, PDGF and PTH (Jung et al. 2006). *Cell division cycle associated 3* (*Cdca3*), which is required for entry into mitosis, was also up-regulated an average of 1.25-fold across the three rhLF concentrations above untreated control.

Three genes that are significantly stimulated by rhLFs with higher iron concentrations

(pis and holo) are *Ccl7*, *Ccl2* and *Nfκβiz* (*NFκβ inhibitor zeta*). Studies have demonstrated *Nfκβiz* to be an activator of IL6 production and also involved in the induction of inflammatory genes activated through TLR/IL1 receptor signaling (Yamamoto et al. 2004). *Nfκβiz* is a gene that encodes for a family of proteins known to play a role in the inflammatory response to LPS by their interaction with NFκβ proteins (Eto et al. 2003). *Ccl2* is expressed by mature osteoblasts and is under the control of NFκβ (Li et al. 2007). Other studies demonstrated that Ccl2 mediates fibroblast survival through IL6 (Liu et al. 2007). The regulation of *Ccl7*, *Ccl2* and *Nfκβiz* were significantly affected by high iron saturation of rhLF, however this differential effect of rhLF iron saturation was not seen in IL6 protein expression. As discussed before, IL6 expression was found to be stimulated by 100 µg/ml of both apo- and holo-rhLF treatments relative to untreated control. Perhaps, this occurrence is due to the change in molecular confirmation in rhLF induced by iron saturation not significantly affecting the upregulation of IL6.

The only gene found to be differentially regulated by the iron concentration of rhLF is *Tfrc* (*transferrin receptor*) (Table 5). Interestingly, previous studies using cells such as monocytes and intestinal cells have demonstrated a binding site for LF different from the transferrin receptor. Only with high molar excess of both ligand proteins, (lactoferrin and transferrin), did a small percentage of the ligands cross-react with the receptor for the other. This most likely occur due to the structural similarity of the two glycoproteins (Roiron et al. 1989, Birgens et al. 1983, Hu et al. 1988). With regards to transferrin and iron, the transferrin family is known to be potent regulators of iron homeostasis (Cairo et al. 2002), and transferrin receptor 1 is the primary target of

transferrin in the iron transport system. It has been reported that low iron concentrations can lead to up-regulation of this protein (Lambert 2012) which may explain why *Tfrc* was differentially regulated by the iron unsaturated and saturated forms.

#### 4.1.5 Conclusions

The present study investigated the effect of rhLF iron saturation on pre-osteoblasts. Recombinant human LF was found to have a significant effect on MC3T3 cell proliferation, Akt phosphorylation,  $\beta$  catenin activation, Dishevelled 2 and Gsk3 $\beta$  phosphorylation at all iron concentrations studied over untreated control after 24 hour treatment. Up-regulation of chemokines and cytokines, such as VEGF and IL6, was induced by rhLF in MC3T3 cells independent of the iron concentration. Microarray analysis of the effect of various iron saturated rhLF forms on MC3T3 cells demonstrated only one gene, *transferrin receptor*, to be differentially regulated by the iron concentration of rhLF. Since there wasn't a significant difference of bioactivity of the various iron saturation forms of rhLF, we choose to use holo-rhLF for our future studies as this form is widely available.

### 4.2 Bioactivity of holo-rhLF towards MC3T3 murine preosteoblast cells and NHOst primary cells: a comparative study

#### 4.2.1 Introduction

*In vivo* studies allow for the analysis of biomolecules on a complete biological system with a vast array of cell types, growth factors and cytokines. However, in an isolated *in vitro* study, the effect of biomolecules is studied on a controlled, artificial

environment. Therefore, the selection of an isolated cell type to study the effect of a biomolecule on a particular system may result in pertinent or non-pertinent results. Thus, it is crucial to select a cell culture system that is pertinent to the organ of clinical interest and one that will also allow for the accurate study of a biomolecule's effect on that organ of interest.

To understand the biological activity of rhLF, we chose to use murine MC3T3 preosteoblast cells due to reasons summarized below. MC3T3 cells are clonal cells established from newborn mouse calvaria. Compared to primary calvarial cells that contain a limited percentage of osteoblast precursors capable of forming mineralized foci (Bellows, Heersche & Aubin 1990), confluent MC3T3 cells form a more continuous layer of cells and mineralized extracellular matrix (Sudo et al. 1983, Nakano, Addison & Kaartinen 2007, Wang et al. 1999). Moreover, studies have shown that MC3T3 cells have the capacity to differentiate into osteoblasts and osteocytes and to form calcified bone tissue *in vitro* (Sudo et al. 1983). With good culture maintenance, MC3T3 cells exhibit very high phenotype stability and biological reproducibility. In summary, MC3T3 cells have a long history of being used as a model osteoblast cell to understand osteoblast behavior (Sudo et al. 1983). However, while developing biomaterials to support tissue regeneration, it is important to confirm the translational potential of the material for applications in humans. Therefore, we compared the bioactivity of holo-rhLF towards MC3T3 cells and Normal Human Osteoblasts (NHOst) cells to confirm that rhLF is equally effective towards NHOst and MC3T3 cells. NHOst cells are primary cells isolated from human bone tissue. Therefore, the objective of the following studies

was to evaluate whether holo-rhLF would similarly affect MC3T3 and NHOst cell proliferation and differentiation.

## **4.2.2 Methods**

### **4.2.2.1 Proliferation assays**

#### **4.2.2.1.1 Thymidine incorporation**

The effect of varying concentrations of holo-rhLF on MC3T3 cell proliferation was measured through thymidine incorporation as described in Section 4.1.2.1. Briefly, the cell culture was then performed upon supplementation with 0, 10, 100, and 1000 µg/ml of apo-, pis- and holo-rhLFs and [<sup>3</sup>H]thymidine for 24 hour incubation at 37°C. Thymidine incorporation was analyzed; data was normalized to untreated control sample and expressed as fold change over control.

#### **4.2.2.1.2 MTS assay**

NHOst cells were plated at a density of 15,000 cells/well in a 48-well plate with basal media. After 24 hours, treatments were administered at various concentrations (n=4 biological replicates). The cell culture was then performed upon supplementation with 0, 10, 100, and 1000 µg/ml of holo-rhLF for 24 hour incubation at 37°C. The proliferation of NHOst cells was determined by MTS assay as described in Appendix of Protocols (Section 7.6.2.1). Data was then normalized to untreated control sample and expressed as fold changeover control.

#### **4.2.2.2 Differentiation assays**

##### **4.2.2.2.1 Alkaline phosphatase assay**

MC3T3 and NHOst cells were plated at a density of 50,000 cells/well in a 24 well plate with basal media. Cells were grown to confluence in basal medium and then changed to mineralization media. The cell culture was then performed upon supplementation with 0, 100, and 1000 µg/ml of holo-rhLFs (n=4 biological replicates). Mineralization media supplemented with and without rhLF treatments was changed every 3 days and samples were harvested on day 7, 14, 21 and alkaline phosphatase activity was determined as described in Appendix of Protocols (Section 7.7.2.1).

##### **4.2.2.2.2 Mineralization assay**

MC3T3 and NHOst cells were plated at a density of 50,000 cells/well in a 24-well plate with basal media. Cells were grown to confluence in basal medium and then changed to mineralization media. The cell culture was then performed upon supplementation with 0, 100, and 1000 µg/ml of holo-rhLF (n=4 biological replicates). Mineralization media with and without rhLFs was changed every 3 days and samples were harvested on day 7, 14, 21 days the extent of mineral deposition was followed as described in Appendix of Protocols (Section 7.7.2.2).

##### **4.2.2.3 Protein expression**

MC<sub>3</sub>T<sub>3</sub> and NHOst cells were plated at a density of 200,000 cells/plate on 10 cm tissue culture plates, grown to 90% confluence in basal medium. The cells were then maintained in basal serum-free medium overnight. The cell culture was then performed with supplementation with 0, 100 and 1000 µg/ml of holo-rhLF for 24 hours. Total



protein was lysed from cells and western blot analysis was performed as described in Appendix of Protocols (Section 7.2.2.3).

#### 4.2.3 Results

Thymidine incorporation and MTS assay, two traditional cell proliferation assays, were used to test the effect of holo-rhLF on MC3T3 and NHOst cells, respectively. Holo-rhLF led to a significant increase in proliferation of MC3T3 cells – concentration of 100 and 1000  $\mu\text{g/ml}$ . Similarly, holo-rhLF led to a significant increase in proliferation of NHOst cells – at all concentrations tested 10, 100, 1000  $\mu\text{g/ml}$  (Figure 25). Unlike MC3T3 cells, NHOst showed significant increase with 10  $\mu\text{g/ml}$  holo-rhLF treatment after 24 hours. 100  $\mu\text{g/ml}$  holo-rhLF treatment led to a 61% and 43% increase in proliferation over untreated control of MC3T3 and NHOst cells, respectively, after 24 hours treatment.

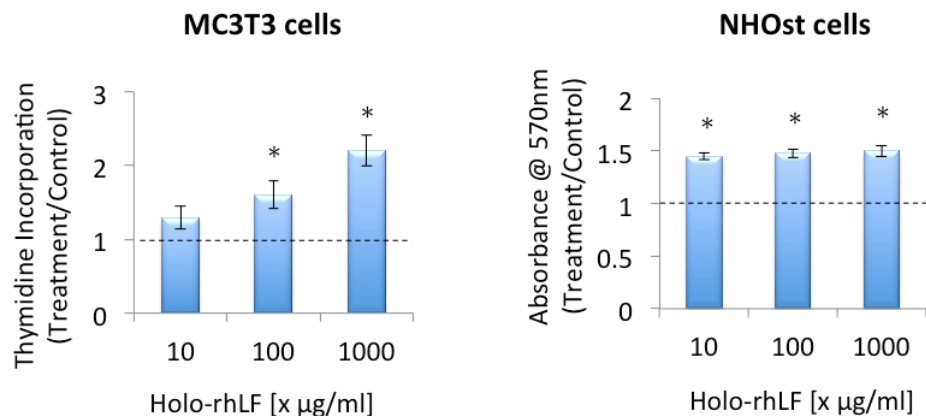


Figure 25. Effect of holo-rhLF treatment on MC3T3 and NHOst cell proliferation.

*Cells were treated for 24 hours in culture. Cell proliferation was measured in MC3T3 and NHOst cells by thymidine incorporation and MTS assay, respectively. Data was normalized to untreated control sample and expressed as fold change over control. Statistical significance ( $p < 0.05$ ) is represented as \* relative to appropriate control.*

Both cell types, MC3T3 and NHOst cells, demonstrated a significant increase in ALPase activity after 7, 14, 21 days of holo-rhLF treatment relative to untreated control samples (Figure 26). MC3T3 cells displayed a dose-dependent increase in ALP activity at 14 and 21 days. However, this effect was not seen in NHOst cells – 1000 µg/ml holo-rhLF induced a less significant increase in ALP activity relative to 100 µg/ml holo-rhLF at 14 and 21 days of culture. Significant increase in calcium deposition by MC3T3 and NHOst cells was measured by Alizarin Red staining after 14 and 21 days of holo-rhLF treatment (Figure 27). Trends in increase mineralization (Alizarin Red staining) were similar in MC3T3 and NHOst cells during the 21 day culture period.

An effect of holo-rhLF on signaling molecule production was exhibited by both MC3T3 and NHOst cells. As discussed before holo-rhLF can induce phosphorylation of Akt in MC3T3 cells. Holo-rhLF increase phosphorylation of Akt in MC3T3 cells (Figure 32) and NHOst cells (Figure 28a) after 24 hours treatment relative untreated control samples. Similarly, activation (de-phosphorylation) of  $\beta$  catenin was increased by holo-rhLF treatment relative to control in MC3T3 cells (Figure 22) and NHOst cells (Figure 28b) after 24 hours. Equal protein loading was confirmed in western blotting using anti-tubulin blot

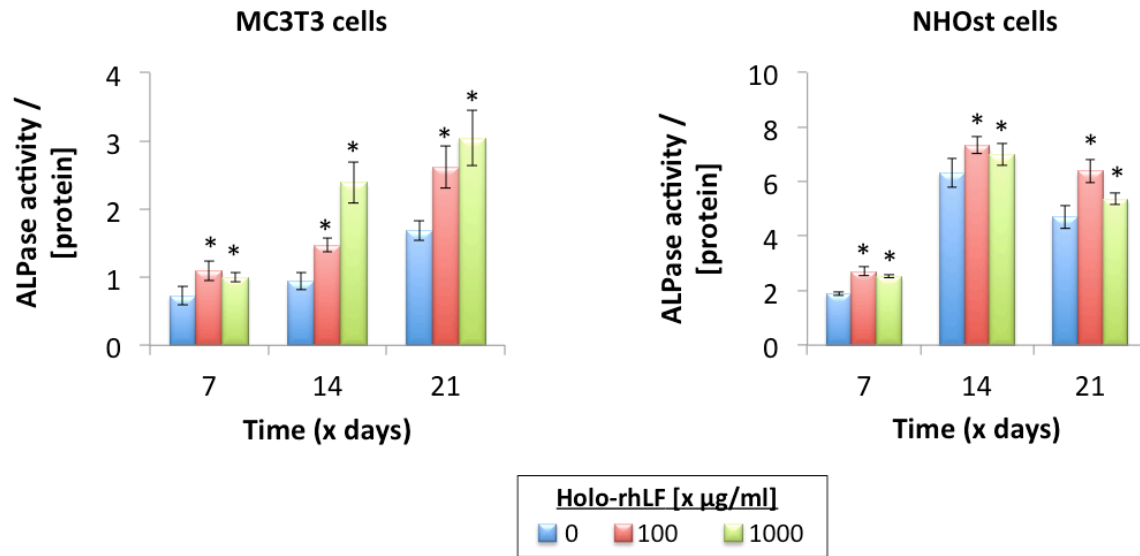


Figure 26. Alkaline phosphatase activity in MC3T3 and NHOst cells treated with holo-rhLF.

Alkaline phosphatase assay was performed on MC3T3 and NHOst cells maintained in mineralization media for 7, 14 and 21 days and treated with 100 or 1000 µg/ml holo-rhLF or untreated (-). Statistical significance ( $p < 0.05$ ) is represented as \* relative to appropriate control.

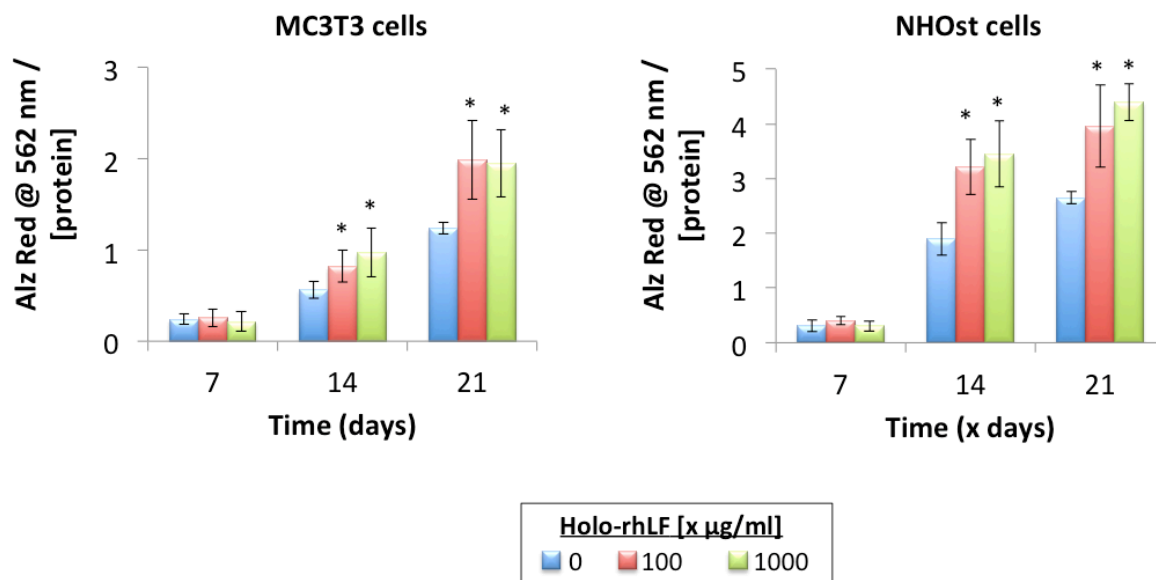


Figure 27. Mineral deposition by MC3T3 and NHOst cells treated with holo-rhLF.

*Alizarin Red assay was performed on MC3T3 and NHOst cells maintained in mineralization media for 7, 14 and 21 days and treated with 100 or 1000  $\mu\text{g/ml}$  holo-rhLF or untreated (-). Statistical significance ( $p < 0.05$ ) is represented as \* relative to appropriate control.*

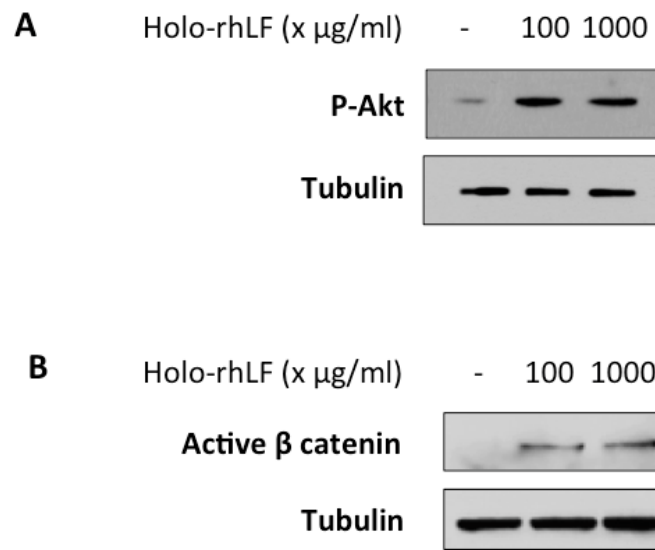


Figure 28. Holo-rhLF increases (a) phosphorylation of Akt and (b) activation of  $\beta$  catenin in NHOst cells after 24 hours of treatment.

#### 4.2.4 Discussion

Bone developmental sequence can be characterized in three stages: (1) osteoblast proliferation, (2) matrix maturation, and (3) mineralization (Siggelkow et al. 1999). This sequence has been most extensively studied in the rat calvarial cell system (Aronow et al. 1990b, Collin et al. 1992, Nefussi et al. 1997, Owen et al. 1991, Pockwinse et al. 1995) and murine MC3T3 cells (Quarles et al. 1992). Differentiation of human osteoblasts is not as widely characterized, however studies thusfar indicate an analogous process in developing human bone (Dodds et al. 1994, Mundlos 1994).

Fetal and neonatal rat calvaria cells are the most widely used source of primary osteoblasts. These calvarial cells are proteolytically released and in early passage are heterogeneous and not immortalized. However, enrichment of cultures for committed osteoblasts can be obtained by proper sub-confluent passaging and 0.1  $\mu$ M dexamethasone treatment (Aronow et al. 1990a). Cells released at later times of proteolytic digestion have increased osteogenic potential as they express osteoblast phenotypic markers and form mineralized nodules with time in culture (Kawaguchi et al. 1995).

Clonal osteoblast-like MC3T3 cell line, which is established from newborn C57B/6 mouse calvaria, provides an excellent *in vitro* model of bone development. This system resembles osteogenic cells in numerous ways as it undergoes the three orderly time-dependent phases characterized by proliferating pre-osteoblasts, hydroxyapatite crystal matrix deposition by differentiating osteoblasts, which results in the formation of multilayered bone nodules (Vary et al. 2000). This cell line provides one of the most convenient and physiologically relevant culture systems for osteoblast studies. The MC3T3 cell line is an immortalized cell line selected by the 3T3 passaging protocol (Sudo et al. 1983). At confluence, this cell line differentiates along the osteoblast lineage and sequentially expresses characteristic osteoblast phenotypic markers (including bone sialoprotein and osteocalcin) similar to that of primary calvarial osteoblasts cultures of fractions 3-5 (Vary et al. 2000, Franceschi, Iyer 1992, Franceschi, Iyer & Cui 1994). Moreover, post-confluent cultures of MC3T3 cells cultured in the presence of ascorbic acid and  $\beta$ -glycerolphosphate will mineralize and accumulate hydroxyapatite (Sudo et al. 1983). MC3T3 cell phenotype is very stable if the stocks are well maintained and

passaged accordingly before confluence. This cell line is a physiologically relevant model commonly used for studying osteoblasts – as it provides a model for signal transduction cascades and their interactions with osteoblast transcription factors.

MC3T3 and NHOst cells displayed all three stages of the bone developmental sequence in response to holo-rhLF treatment. A significant increase in MC3T3 and NHOst cellular proliferation induced by holo-rhLF treatment was measured by thymidine incorporation and MTS assay, respectively, after 24 hours of treatment. However, unlike MC3T3 cells, NHOst cells showed a significant increase in cell proliferation with only 10 µg/ml holo-rhLF treatment. Previous studies by Cornish *et al.* demonstrated similar effects of rhLF on rat primary osteoblast proliferation via thymidine incorporation after 24 hours treatment at concentrations of 10 and 50 µg/ml (Cornish et al. 2004). Although the response of MC3T3 cells to many growth factors and hormones mimics that of primary cultures of rodent osteoblastic cells (Delany, Canalis 1998), studies have demonstrated differential regulation of growth factors on osteoblast cells based on their differentiation stage. For example, FGFs induce immature osteoblastic cells to proliferate, whereas mature osteoblasts respond by unaltered or decreased proliferation (Hurley, Marie 2002). This reasoning may be used to explain the more sensitive response of primary NHOst cells to the lower concentration (10 µg/ml) of holo-rhLF relative to pre-osteoblastic MC3T3 cells.

Increased osteogenic differentiation was induced by holo-rhLF supplementation of mineralization media, which included 10 µg/ml L-ascorbic acid and 3 mM β-glycerophosphate. Osteogenic differentiation was assessed by increased alkaline phosphatase and mineralized matrix deposition at 7, 14 and 21 days. Choi *et al.*

reported the phenotypic increase of alkaline phosphatase activity during early matrix formation/maturation period (approximately day 10) (Choi et al. 1996). In our studies, MC3T3 and NHOst cells demonstrated a significant increase in ALP activity during early matrix formation period of day 7 and 14. This increase in alkaline phosphatase was further sustained in both cell types by holo-rhLF at 21 day culture. A previous study using MG63 osteoblast-like cells showed similar results as LF treatment led to significant increase in ALP activity at days 14 and 21 days (Takayama, Mizumachi 2008).

Similar to ALP activity, the presence of holo-rhLF significantly increased the mineral deposition by MC3T3 and NHOst cells at 14 and 21 days of culture in mineralization media. Other studies report that mineralization of extracellular matrix, which marks the final phase of osteoblast phenotypic development, begins approximately 16 days after culture (Quarles et al. 1992). Even at 21 days, the extent of mineralized matrix formed in the presence of rhLF was significantly higher than the control indicating the potential of rhLF to produce overall higher amount of matrix compared to control. Interestingly, there was no statistical significant increase in mineral deposition produced by 1000 µg/ml holo-rhLF treatment relative to 100 µg/ml. Thus, the concentration of 100 µg/ml of holo-rhLF is sufficient to induce significant mineral deposition in NHOst and MC3T3 cells.

These studies also showed similar response of MC3T3 and NHOst cells towards holo-rhLF treatment regarding Akt phosphorylation and  $\beta$  catenin activation. These results concur with results from our previous studies with MC3T3 cells (Section 4.1.3) and also previously published studies using primary rat osteoblasts and bLF to induce PI3K-dependent Akt signaling (Grey et al. 2006). The  $\beta$  catenin-dependent signaling

pathway has been documented as a potential osteogenic signaling pathway (Novak, Dedhar 1999).

#### **4.2.5 Conclusions**

The effect of holo-rhLF on the signaling and functional properties on NHOst and MC3T3 cells was compared to demonstrate the translational potential of rhLF-based materials. The study demonstrated NHOst followed the same pattern of transcriptional factor expression, cell proliferation and differentiation. The study confirmed that the bioactivities of rhLF may be reproduced in human cells similar to mouse clonal cells, thereby demonstrating the translational potential of rhLF based biomaterials.



### ***4.3 Evaluation of the mechanism behind the anti-apoptotic and osteogenic activity of rhLF towards MC3T3 cells***

#### **4.3.1 Introduction**

Cell-based bone tissue engineering encompasses the use of cells and biomaterials for the regeneration or repair of damaged bone tissue. The challenges in cell-based therapy are two-fold, which include biological and biomaterial obstacles. The biological challenges involve the survival of the implanted cells at the defect site (Manassero et al. 2012). The biomaterial challenge includes localizing the implanted cells at the defect site for prolonged time, positively modulating the activity of encapsulated cells in the microenvironment to support accelerated regeneration and maintain the survival of the cells. The significant cell death and decreased activity of cells after implantation at orthotopic sites have been demonstrated using various cell-based modalities in small animals, as well as human clinical trials. A recent study investigated the success of human mesenchymal stem cell survival after implantation to rat femoral defect. Unfortunately, less than 2% of the initial cell number was viable after 30 days of implantation (Figure 29) (Manassero et al. 2012).

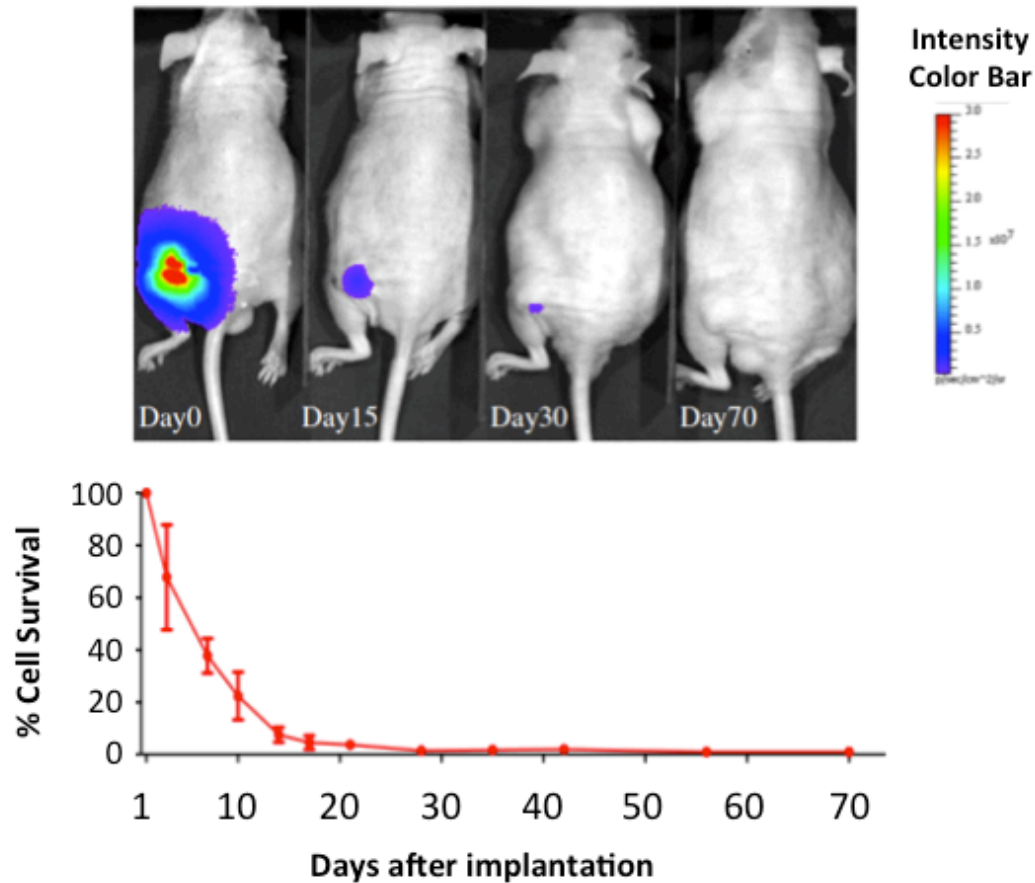


Figure 29. Representative bioluminescence imaging of a mice transplanted with human mesenchymal stem cells in a critical-size segmental femoral defect and *in vivo* kinetic cell survival quantification.

A recent human clinical trial investigated the potency of bone tissue engineering to reconstruct jaw defects. After 4 months of reconstructing an intra-oral bone defect, bone formation by implanted stem cells was shown to be feasible in only 1 out of 6 patients by the tissue-engineered construct (Meijer et al. 2008). To make bone tissue engineering techniques involving cells suitable for reconstructing an osseous defect, the problem of cell apoptosis and lack of osteogenic induction must be solved. Biomaterial with inherent anti-apoptotic and osteogenic properties would be highly beneficial as a cell-delivery vehicle as it would address the two major existing concerns in cell-based therapy.

LF has raised significant interest as a bioactive protein due to its wide array of physiological effects on many different cell types (Amini, Nair 2011c). The diverse list of LF's multifunctional roles includes immuno-modulatory, anti-cancer, anti-bacterial, and anti-viral properties (Spadaro et al. 2008, Legrand et al. 2005). Some of the recent studies have demonstrated LF as an effector molecule in the skeleton (Cornish, Naot 2010, Cornish 2004), due to its ability to increase osteoblast proliferation, survival and differentiation (Grey et al. 2006, Cornish et al. 2004, Cornish 2004) and decrease osteoclast survival (Lorget et al. 2002, Blais et al. 2009). Many of the biological activities of LF have been attributed to its ability to induce signal transduction pathways through cell surface receptors. LRP1 has been established as one of the putative receptors in osteoblasts. The activation of this receptor by bLF has been shown to induce MAPK-mediated osteoblast mitogenesis (Grey et al. 2004). However, the anti-apoptotic properties of this glycoprotein have been attributed to a PI3K/Akt-independent, and LRP1-independent pathway (Grey et al. 2006). The anabolic effect of bLF (Cornish 2004) has also been attributed to bLF's possible positive effects on osteogenic differentiation (Yagi et al. 2009). Yagi *et al.* demonstrated the ability of bLF to push the differentiation of pluripotent mesenchymal stems cells towards the osteoblastic or chondroblastic lineage, and prevent the differentiation towards myoblastic and or adipocytic lineages (Yagi et al. 2009). Furthermore, hLF stimulates keratinocytes proliferation via MAPK signaling cascade, which is a pathway similar to FGF2-stimulated mitogenesis, cell migration and cell survival implying its potential to promote wound re-epithelialization (Tang et al. 2010). Recent studies indicate the ability of bLF to promote FGF-2 and VEGF synthesis by osteoblasts via the p44/p42 MAP kinase

pathway (Nakajima et al. 2011, James et al. 2011). Additionally, bLF has been shown to inhibit osteoclastogenesis in primary culture of murine bone cells at a concentration as low as 10 µg/ml (Lorget et al. 2002). Collectively, these studies substantiate LF as a positive regulator of the skeleton.

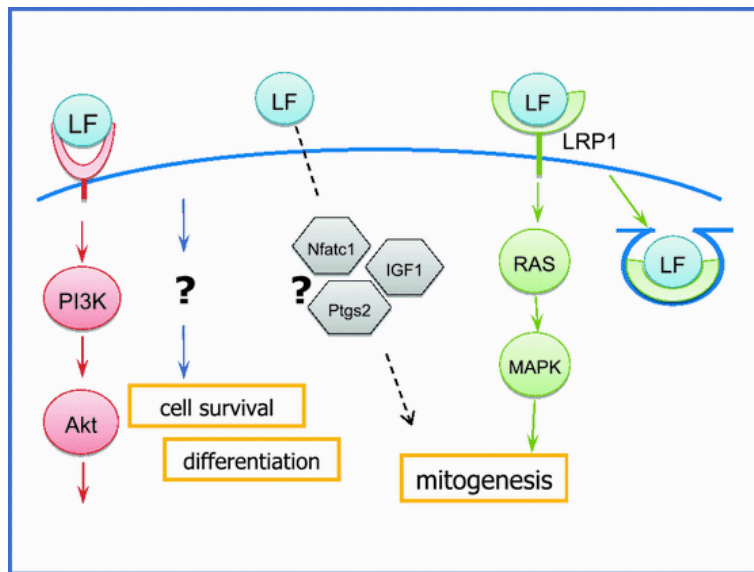


Figure 30. Schematic showing the summary of known mechanisms of action of LF in osteoblasts.

*Binding of LF to LRP1 receptor on osteoblasts induces endocytosis of the LF-LRP1 complex as well as activation of the p42/44 MAP kinases signaling pathway. Inhibition of the MAPK pathway blocks the mitogenic effect of lactoferrin in osteoblasts. LF also activates the PI3K/Akt signaling pathway and increases mRNA levels of IGF1, Nfatc1 and Ptgs2 but the functional significance of these remains to be determined. The mechanisms involved in the activities of LF as a survival factor and as a promoter of osteoblast differentiation are unknown yet. Image was taken from (Cornish, Naot 2010).*

Fetal bovine serum, the most widely used serum animal supplement, provides broad spectrum of macromolecules, carrier proteins, attachment and spreading factors, low molecular weight nutrients, and hormones and growth factors (Boone et al. 1971). Serum deprivation has been shown to efficiently induce apoptosis in several cell types (Aoki et al. 1997, Hara et al. 2012, Braun et al. 2011). Thus, serum deprivation model

was used to study holo-rhLF effect on cellular apoptosis. Furthermore, we investigated the osteogenic effect of holo-rhLF on MC3T3 cells. The objective of the following studies was to test the anti-apoptotic and osteogenic activity of holo-rhLF on MC3T3 cells to evaluate the efficacy of using holo-rhLF as a potential biomaterial to develop novel injectable cell delivery vehicles. We also went on to investigate the molecular mechanisms underlying holo-rhLF's anti-apoptotic and osteogenic effects to gain a better understanding of the signal transduction pathways induced by this bioactive molecule.

### **4.3.2 Methods**

#### **4.3.2.1 Cell viability/ survival assays**

##### **4.3.2.1.1 Serum starvation and cell viability assay**

MC3T3 cells were plated at a density of 50,000 cells/well in a 12-well plate with basal media for 24 hours. Cells were then maintained in serum-free basal media and the cell culture was then performed upon supplementation with 0 or 100 µg/ml of holo-rhLF. Live/dead viability assay was then performed as described in Appendix of Protocols (Section 7.5.2.1).

##### **4.3.2.1.2 Protein expression (Immunocytochemistry)**

MC3T3 cells were plated on glass-bottom tissue culture plates (10,000 cells/plate) for 2 days in basal media and then serum starved for 6 hours. Cells were either untreated (control) or stimulated with holo-rhLF 100 µg/ml for 24 hours. Immunocytochemistry was performed as described in Appendix of Protocols (Section 7.2.2.5).

#### 4.3.2.1.3 Wnt signalling pathway

MC3T3 cells were plated on 10 cm tissue culture plates (200,000 cells/plate), grown to 90% confluence in basal media and then serum starved for overnight. Cells were then maintained in serum-free basal media overnight and the cell culture was then performed upon supplementation with 0 or 100 µg/ml of holo-rhLF for 24 hours. RNA was extracted, purified and Wnt signaling pathway array was performed as described in Appendix of Protocols (Section 7.9.2.1).

#### 4.3.2.1.4 Inhibitor studies for signalling pathway probing

##### *4.3.2.1.4.1 Protein expression (Western blot analysis)*

MC3T3 cells were plated on 10 cm tissue culture plates (200,000 cells/plate), grown to 90% confluence in basal media and then serum starved for overnight. Inhibitor treatment of select inhibitors (10 µM LY294002 and 30 µM H-89) for 2 hours was followed by treatment with 100 µg/ml holo-rhLF or 100 ng/ml Wnt5a for 24 hours. Total protein was lysed from cells and western blot analysis was performed as described in Appendix of Protocols (Sections 7.2.2.3 and 7.8.2.1).

##### *4.3.2.1.4.2 Bioluminescent caspase-3 assay*

MC3T3 cells were plated on 10 cm tissue culture plates (200,000 cells/plate), grown to 90% confluence in basal media and then serum starved for overnight. Inhibitor treatment of select inhibitors (10 µM LY294002 and 30 µM H-89) for 2 hour was followed by treatment with 100 µg/ml holo-rhLF, 100 ng/ml Wnt5a or 100 ng/ml BMP2 for 24 hours. 50 µM Z-VAD-FMK was also used as a positive control apoptosis inhibitor. Total

protein was lysed from cells and caspase assay was performed as described in Appendix of Protocols (Section 7.5.2.2).

#### 4.3.2.1.5 Osteogenesis assays

##### 4.3.2.1.5.1 *Protein expression*

###### 4.3.2.1.5.1.1 *Total $\beta$ catenin expression*

###### 4.3.2.1.5.1.1.1 Canonical Wnt signaling pathway activation

MC3T3 cells were plated on 10 cm tissue culture plates (200,000 cells/plate), grown to 90% confluence in basal media. Cells were then maintained in serum-free basal media overnight and the cell culture was then performed upon supplementation with 0 or 100  $\mu\text{g/ml}$  of holo-rhLF or 10 mM LiCl for 15 minutes or 100 ng/ml Wnt3a for 6 hours. Total protein was extracted and western blot analysis was performed as described in Appendix of Protocols (Section 7.2.2.3).

###### 4.3.2.1.5.1.1.2 Time course of $\beta$ catenin expression

MC3T3 cells were plated on 10 cm tissue culture plates (200,000 cells/plate), grown to 90% confluence in basal media. Cells were then maintained in serum-free basal media overnight and the cell culture was then performed upon supplementation with 100  $\mu\text{g/ml}$  of holo-rhLF for 0, 0.25, 1, 3, 6 and 24 hours. Total protein was extracted and western blot analysis was performed as described in Appendix of Protocols (Section 7.2.2.3).

#### *4.3.2.1.5.1.2 Nuclear/cytoplasmic $\beta$ catenin expression*

##### *4.3.2.1.5.1.2.1 Western blot*

MC3T3 cells were plated on 10 cm tissue culture plates (200,000 cells/plate), grown to 90% confluence in basal media. Cells were then maintained in serum-free basal media overnight and the cell culture was then performed upon supplementation with 0 or 100  $\mu\text{g/ml}$  of holo-rhLF for 24 hours. Total protein was extracted, nuclear and cytoplasm fractions were separated and western blot analysis was performed as described in Appendix of Protocols (Sections 7.2.2.3 and 7.2.2.4).

##### *4.3.2.1.5.1.2.2 Immunocytochemistry*

MC3T3 cells were plated on glass-bottom tissue culture plates (10,000 cells/plate) for 2 days in basal media and then serum starved for 6 hours. Cells were either untreated (control) or stimulated with varying iron saturations of 100  $\mu\text{g/ml}$  rhLF for 24 hours. Immunocytochemistry was performed as described in Appendix of Protocols (Section 7.2.2.5).

#### *4.3.2.1.5.2 RNA expression*

MC3T3 cells were plated on 10 cm tissue culture plates (200,000 cells/plate), grown to 90% confluence in basal media. Cells were then maintained in serum-free basal media overnight and the cell culture was then performed upon supplementation with 0 or 100  $\mu\text{g/ml}$  of holo-rhLF for 0, 12 and 24 hours. RNA was extracted, purified and PCR analysis was performed as described in Appendix of Protocols (Section 7.3.2.2).



#### *4.3.2.1.5.3 Inhibitor studies for signaling pathway probing*

MC3T3 cells were plated on 10 cm tissue culture plates (200,000 cells/plate), grown to 90% confluence in basal media and then serum starved for overnight. Inhibitor treatment of select inhibitors (100 ng/ml DKK1 and 30  $\mu$ M H-89) for 2 hour was followed by treatment with 100  $\mu$ g/ml rhLF, 100 ng/ml Wnt5a or 100 ng/ml BMP2 for 24 hours. Total protein was lysed from cells and western blot analysis was performed as described in Appendix of Protocols (Section 7.2.2.3).

### **4.3.3 Results**

#### **4.3.3.1 Anti-apoptotic effect of holo-rhLF toward MC3T3 cells**

We investigated the ability of holo-rhLF to protect the cells against serum starvation–induced apoptosis. MC3T3 cell apoptosis was significantly reduced by 100  $\mu$ g/ml holo-rhLF over the course of 3 days, as evidenced by the increased ratio of live to dead cells in the holo-rhLF treated sample relative to control (Figure 31). Furthermore, holo-rhLF treatment (24 hours) increased Akt phosphorylation over control (Figure 32).

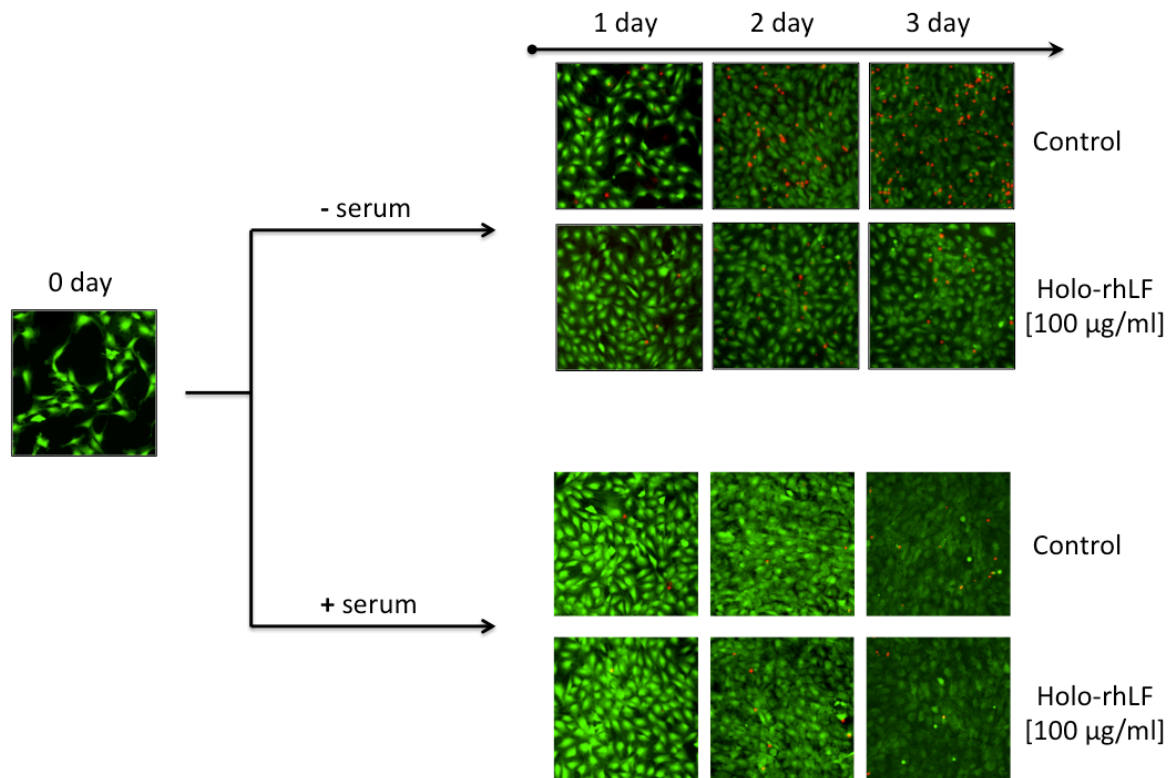


Figure 31. Viability of serum starved MC3T3 cells after holo-rhLF treatment.

*Viability assay demonstrates increased live (green) cells relative to dead (red) cells after 2 days in MC3T3 cells treated with 100 µg/ml holo-rhLF relative to untreated control during serum starvation.*

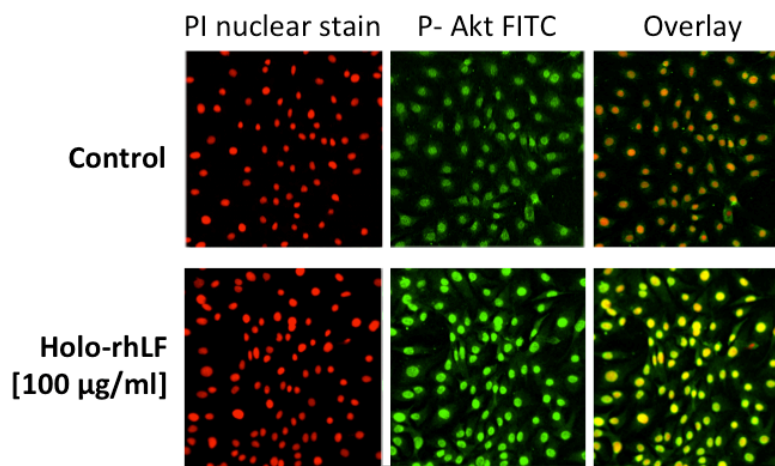


Figure 32. Increased phosphorylation of Akt in MC3T3 cells after holo-rhLF treatment.

*Immunofluorescence showing the phosphorylation of Akt (FITC-labeled secondary antibody) in MC3T3 cells treated with 100 µg/ml holo-rhLF treatment relative to untreated control after 24 hours. Nuclei are stained with propidium iodide.*

To elucidate the mechanism by which LF promotes cell survival, Wnt-mediated signaling transduction pathway array was used (Figure 33). Interestingly, Wnt5a was stimulated 3.8—fold upon 24-hour holo-rhLF treatment. A signaling pathway reported to be mediated by Wnt5a's anti-apoptotic effects is the protein kinase A (PKA)/ cAMP response element binding protein (CREB) (Torii et al. 2008). Next, we used PKA inhibitor, H89, and Akt inhibitor, LY294002, to probe these signaling pathways (Figure 34). We found that rhLF's increase phosphorylation of Akt was inhibited by both H89 and LY294002 – implicating the dependence of both pathways for holo-rhLF's phosphorylation of Akt. Caspase 3 activity, a marker of cellular apoptosis, was decreased upon rhLF treatment and then significantly increased upon H-89 inhibitor treatment – confirming the dependence of rhLF/PKA pathway for cell survival (Figure 35).

### WNT SIGNALING PATHWAY PCR ARRAY

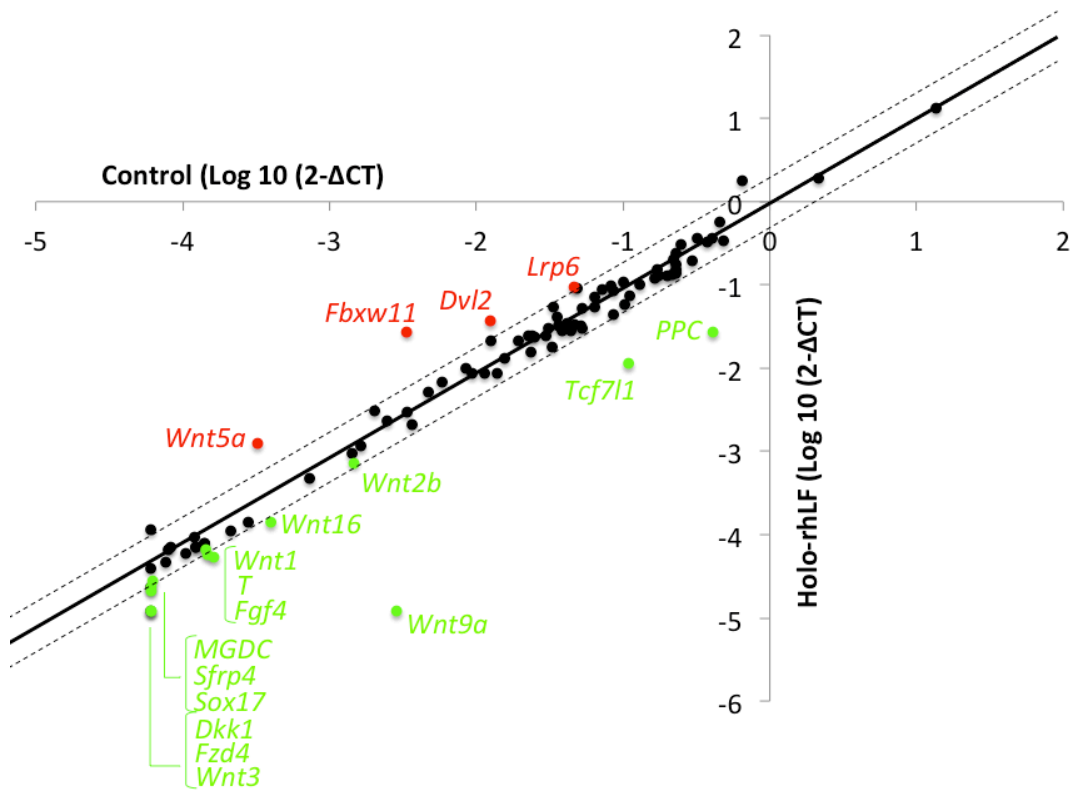


Figure 33. Regulation of Wnt signaling pathway in MC3T3 cells by holo-rhLF.

Wnt Signalling Array was utilized to examine the effect of 100  $\mu\text{g/ml}$  holo-rhLF treatment (y-axis) relative to untreated control (x-axis). Greater than or equal to 2-fold change over control was considered to be significantly regulated.

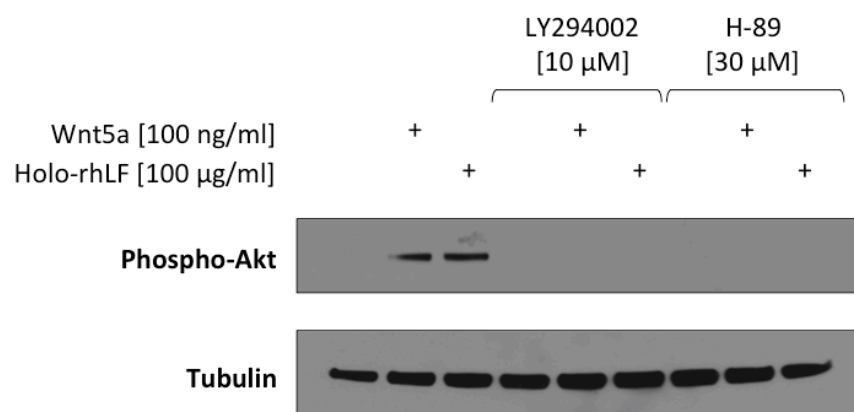


Figure 34. 30  $\mu$ M H89 and 10  $\mu$ M of LY294002 inhibited holo-rhLF-induced phosphorylation of Akt in MC3T3 cells after 24 hours.

*Wnt5a was used as a positive control. Anti-tubulin blot was used as a loading control.*

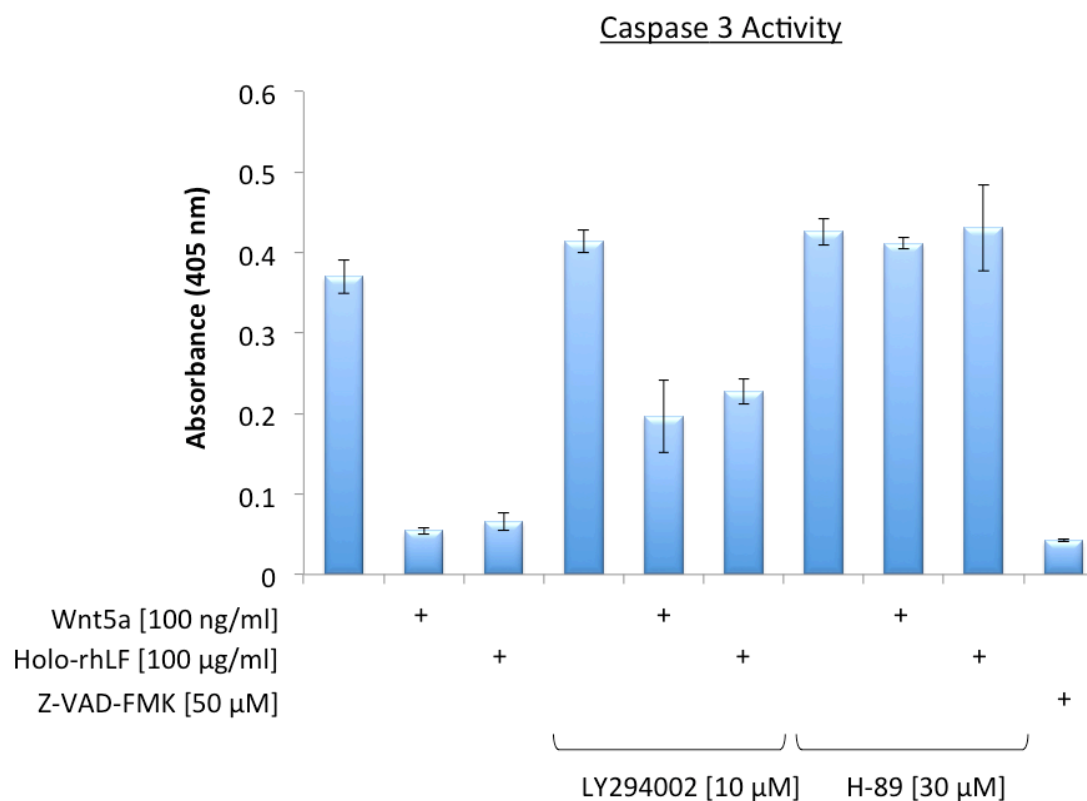


Figure 35. Caspase-3 activity after 24 hours of holo-rhLF treatment with signaling pathway inhibitors, H89 and LY294002.

*100 ng/ml Wnt-5a and 50  $\mu$ M Z-FAD-FMK were used as positive controls. Anti-tubulin blot was used as a loading control.*

#### **4.3.3.2 Osteogenic effect of holo-rhLF towards MC3T3 cells**

Osteoblast differentiation and mineralization is crucial for a bone regenerative biomaterial. Alkaline phosphatase activity, an early marker of osteoblast differentiation, was significantly increased by 100 and 1000  $\mu$ g/ml holo-rhLF treatment over 14 and 21 days of MC3T3 culture (Figure 26). Matrix deposition, a later marker of differentiation, was studied through calcium deposition – which also showed at 14 to 21 days of culture (Figure 27). Moreover, 100 and 1000  $\mu$ g/ml holo-rhLF treatment demonstrated a statistically significant increase during the late stage of culture, 14 and 21 days over the control.

##### **4.3.3.2.1 rhLF increases osteogenesis via $\beta$ catenin signaling pathway.**

The potency of LF's anabolic actions on the skeleton requires better understanding of its molecular mechanisms. However, the mechanisms and cell signaling pathways involved in the transduction of LF's growth-modulating effects on osteoblasts have not yet been comprehensively studied. We hypothesize osteogenic actions induced by rhLF is transduced via  $\beta$  catenin-dependent signaling pathway. Holo-rhLF treatment has also been demonstrated to increase phosphorylation of Disheveled 2 and Gsk3 $\beta$  (Figure 36). Furthermore, holo-rhLF significantly increased the activation (de-phosphorylation) of  $\beta$  catenin relative to untreated control (Figure 37). This accumulation of  $\beta$  catenin was seen in both the nuclear and cytoplasmic fractions (Figure 38 & 39).

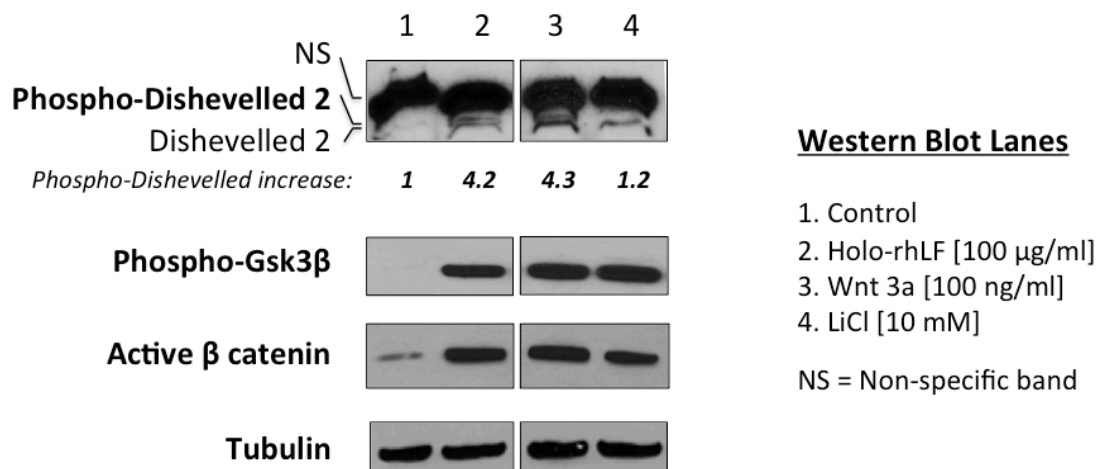


Figure 36. Increased  $\beta$  catenin signaling cascade by holo-rhLF treatment.

100  $\mu\text{g/ml}$  holo-rhLF increase Dishevelled 2, Gsk3 $\beta$  phosphorylation and  $\beta$  catenin activation in MC3T3 cells after 24 hour treatment. Anti-tubulin was used as a gel loading control. 100  $\text{ng/ml}$  Wnt 3a and 10  $\text{mM}$  LiCl were included as positive controls.

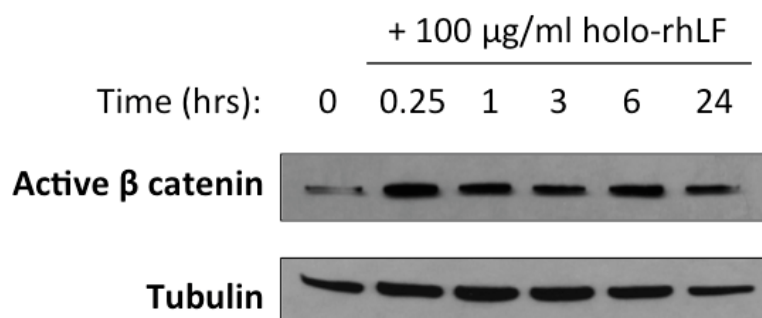


Figure 37. Active  $\beta$ catenin expression induced in MC3T3 cells by 100  $\mu\text{g/ml}$  holo-rhLF.

Cells were treated with 100  $\mu\text{g/ml}$  holo-rhLF for 0.25 – 24 hours of treatment in culture. Anti-tubulin blot was used as a loading control.

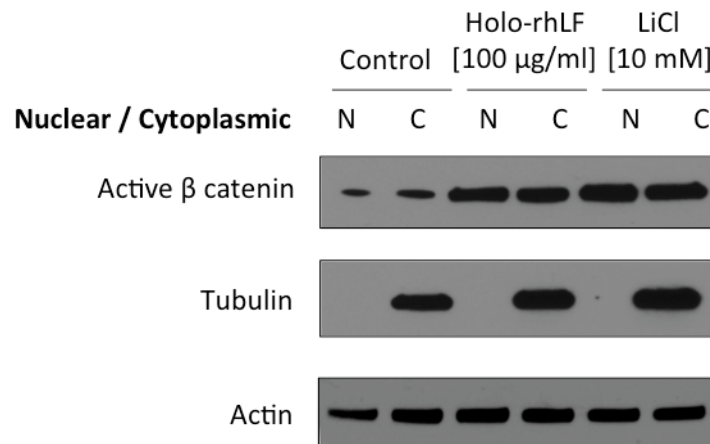


Figure 38. Increased accumulation/activation of  $\beta$  catenin in nucleus and cytoplasm of rhLF treated MC3T3 cells after 24 hours treatment.

*10 mM LiCl treatment was used as positive control of activation of  $\beta$  catenin. Anti-actin blot was used as a loading control. Anti-tubulin was used to test for nuclear/cytoplasmic contamination.*

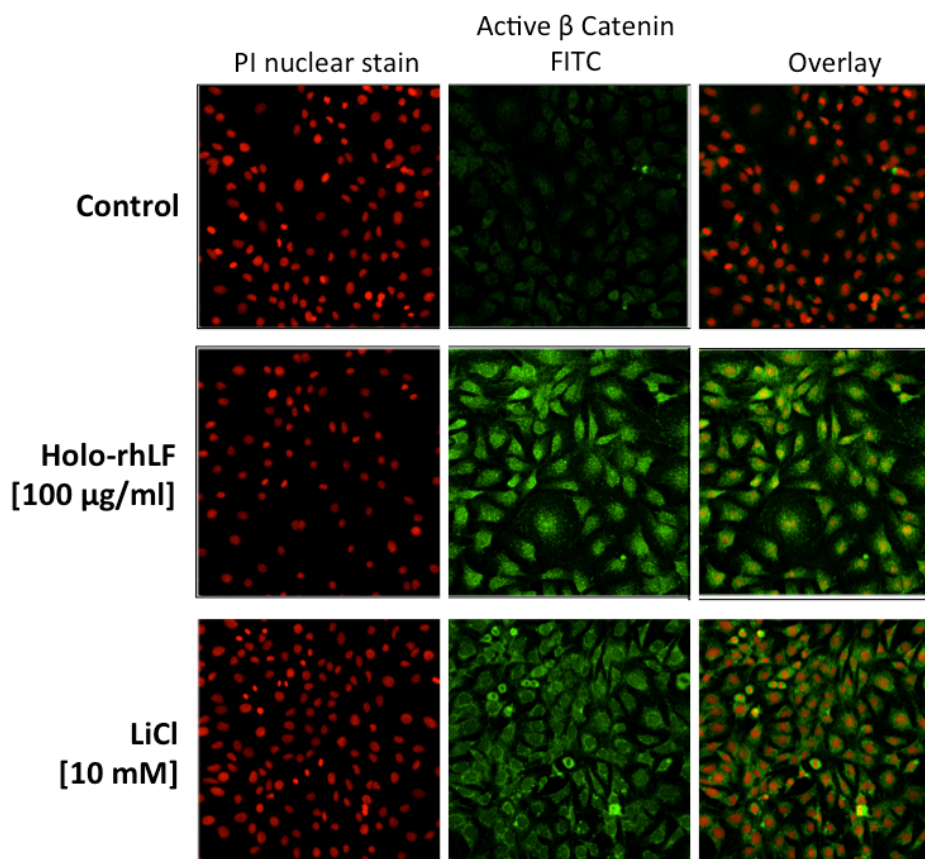


Figure 39. Increased  $\beta$  catenin in MC3T3 cells treated with 100 µg/ml holo-rhLF.



10 mM LiCl treatment was used as a positive control for activation of  $\beta$  catenin. Cells were treated for after 24 hours. Propidium iodide was used to stain cell nuclei.

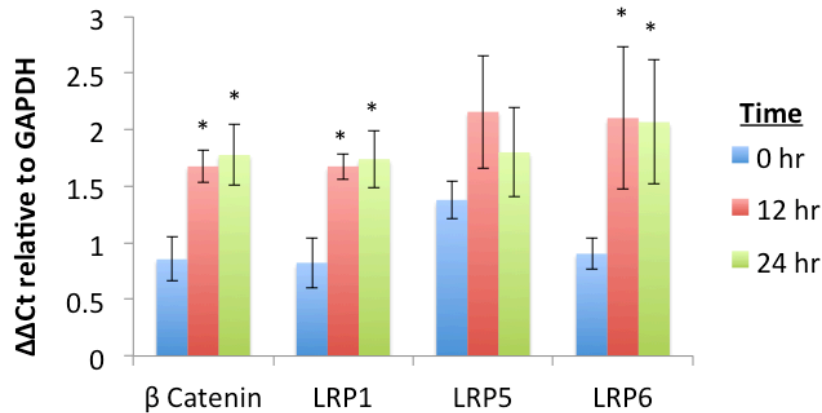


Figure 40. mRNA expression of LRP receptors after holo-rhLF treatment.

$\beta$  catenin, LRP1, LRP6 mRNA expression was significantly up-regulated by 100  $\mu$ g/ml holo-rhLF treatment after 24 hours.

Wnt-mediated signaling transduction pathway array demonstrated a significant increase in LRP6 and Dvl2 upon 24 hours of rhLF treatment relative to untreated control (Figure 33). Non-canonical Wnt5a was up-regulated, while canonical Wnts, Wnt2 and 3, were down-regulated by rhLF treatment. LRP6 up-regulation in MC3T3 cells was also demonstrated through PCR analysis after 24 hours of 100  $\mu$ g/ml holo-rhLF treatment (Figure 40). Similarly,  $\beta$  catenin and LRP1 (a known putative receptor of LF) were also up-regulated by holo-rhLF treatment. However, LRP5, a co-receptor of the canonical Wnt signaling pathway was not found to be significantly up-regulated (Figure 40).

In our next study, pharmacological inhibitors, DKK1, and H89 were used to inhibit the targeted pathways of LRP6 and PKA, respectively (Figure 41). rhLF's increased phosphorylation of LRP6 and activation of  $\beta$  catenin was inhibited by both

DKK1 and H89. This data suggests the activation of  $\beta$  catenin by rhLF to be dependent on PKA/LRP6 signalling pathway.

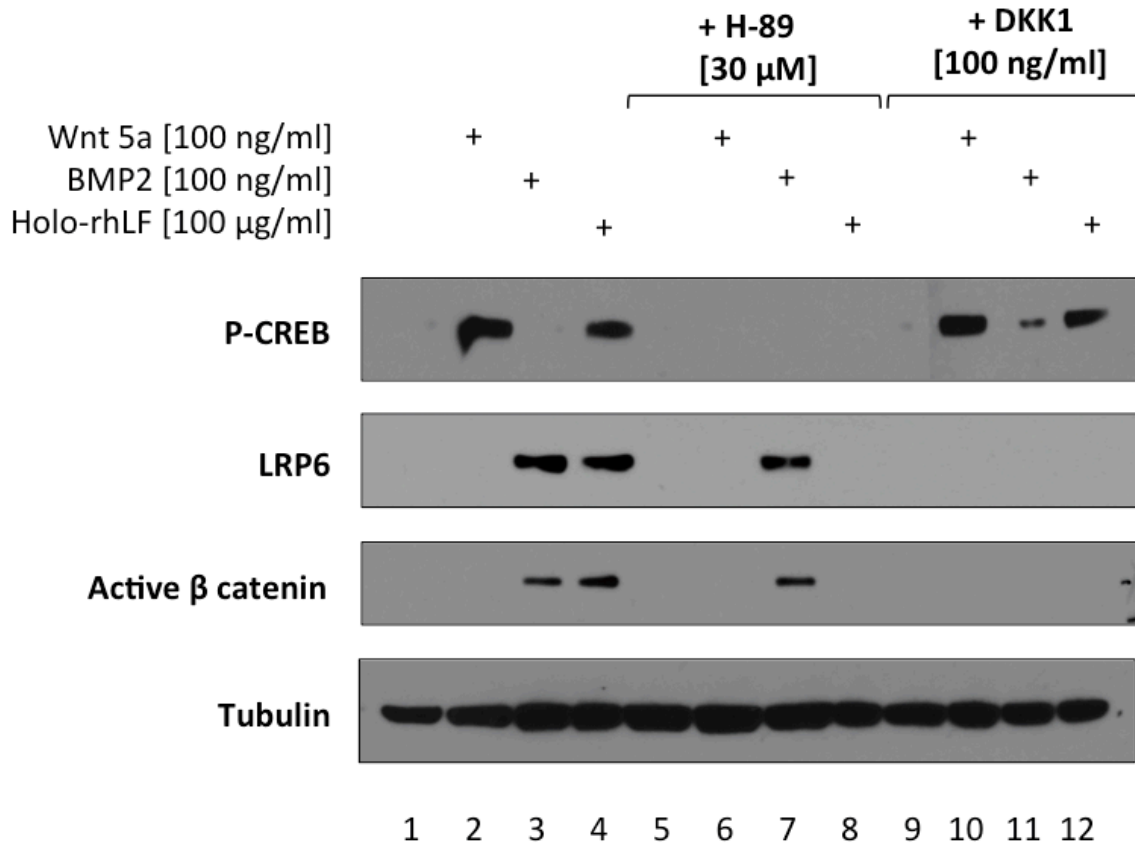


Figure 41. Inhibitor studies (30  $\mu$ M H89 and 100 ng/ml DKK1) to understand the osteogenic pathways and  $\beta$  catenin activation.

*Inhibitor experiments were performed for 24 hour stimulation of rhLF. Wnt5a and BMP2 were used as positive controls. Anti-tubulin blot was used a loading control.*

#### 4.3.4 Discussion

Our studies demonstrated strong protection against serum starvation-induced apoptosis by holo-rhLF treatment in MC3T3 cells after 3 days (Figure 31) and also increased phosphorylation of Akt (Figure 32). Akt was used as a marker of cell survival since a common mechanism by which growth factors promote cell survival is PI3K-

dependent, Akt phosphorylation. However, the anti-apoptotic properties of bLF have been demonstrated to increase LRP1-independent, PI3K/Akt phosphorylation (Grey et al. 2006). A previous study has reported that this increased phosphorylation of Akt is not required by LF to prevent programmed cell death (Grey et al. 2006). Thus, the mechanism by which LF prevents cellular apoptosis has not been clearly understood.

PI3K/Akt and PKA signaling transduction pathways are generally strongly associated anti-apoptotic pathways. Interestingly, previous studies have demonstrated PI3K/Akt pathway to be activated by Wnt5a treatment (Kawasaki et al. 2007). Furthermore, non-canonical Wnt5a has been shown to prevent serum starvation-induced osteoblast apoptosis via Src/Erk and PI3K/Akt-dependent mechanism (Almeida et al. 2005). LF promotes survival of osteoblasts *in vitro*, but these actions are independent of Erk/MAPK pathway, which subserves its proliferative actions (Grey et al. 2006).

The Wnt family is comprised of 19 secreted glycoproteins and play essential roles in embryonic patterning, cell apoptosis, proliferation and differentiation (Logan, Nusse 2004, Miller 2002, Moon et al. 2002, Wodarz, Nusse 1998). In our studies, we utilized a Wnt signaling array as a tool to elucidate the regulation of Wnts induced by holo-rhLF treatment in MC3T3 cells (Figure 33). This array was especially selected since the Wnt family of secreted growth factors are known to regulate developmental processes, including cell survival (Almeida et al. 2005). The only Wnt molecule that was found to be up-regulated upon holo-rhLF treatment in MC3T3 cells was Wnt5a. A signaling pathway reported to be mediated by Wnt5a's anti-apoptotic effects is the PKA/CREB (Torii et al. 2008). The use of H89 pharmacological inhibitor allowed for confirmation of holo-rhLF's regulation of PKA (Figure 34). We checked CREB phosphorylation, the

downstream signaling molecule of PKA, to confirm inhibition of PKA by H89 inhibitor. We included Akt inhibitor, LY294002, in our studies to confirm the previously published results by Grey *et al.* that reported that LF's anti-apoptotic properties are not dependent on Akt phosphorylation (Grey et al. 2006). Wnt5a was used as a positive control for Akt phosphorylation in MC3T3 cells. Interestingly, Akt inhibitor, LY294002, inhibited both holo-rhLF and Wnt5a phosphorylation of Akt. This data confirms that Wnt5a treatment of MC3T3 cells induces Akt phosphorylation – since cells that were co-treated with Wnt5a and LY294002 inhibitor did not display increased phosphorylation of Akt. Furthermore, PKA inhibitor, H89, also inhibited both holo-rhLF and Wnt5a phosphorylation of Akt. These results confirmed that upon Wnt5a treatment in MC3T3 cells, PKA activation signals downstream to phosphorylate Akt. Similarly, upon holo-rhLF treatment, PKA signals downstream to phosphorylate Akt. In our next experiment, we used *caspase 3* activity as an indicator for cellular apoptosis upon inhibition with LY294002 and H89 and stimulation with Wnt5a and holo-rhLF (Figure 35). This informative study demonstrated Wnt5a and holo-rhLF to be potent anti-apoptotic molecules. Furthermore, with LY294002 inhibition of Akt, a partial rescue of caspase 3 activity was induced by Wnt5a and holo-rhLF treatment. But with H89 inhibition, no rescue of caspase activity was induced by Wnt5a and holo-rhLF. This proved that cell survival mechanism of induced by both holo-rhLF and Wnt5a is dependent on PKA signaling.

The molecular mechanisms underlying the osteogenic properties of holo-rhLF has been long in question. Wnt molecules are secreted growth factors are known to regulate osteogenic pathways. Various combinations of Wnts and Fzds transduce two

distinct intracellular signaling pathways – “canonical” and “non-canonical” Wnt pathways. The canonical Wnt signaling pathway is centered on the regulation of cytoplasmic  $\beta$  catenin levels. Whereas, non-canonical Wnt pathway is typically characterized as  $\beta$  catenin-independent signaling often involving Fzd receptors, but not LRPs or TCF/LEF factors. Key Wnt members in the canonical pathway, which include Wnt 1, 3a and 8, transduce their signals and play a crucial role in controlling cell proliferation and differentiation. Central to the canonical pathway is the regulation of  $\beta$  catenin activity, which depends on its protein cytoplasmic abundance and nuclear localization. The activation of the canonical Wnt pathway is initiated with the activation of Disheveled, which leads to the inhibition of Gsk3 $\beta$  and subsequent stabilization of  $\beta$  catenin. Accumulation of  $\beta$  catenin in the cytoplasm prompts its translocation to the nucleus, where it interacts with members of the TCF/LEF family of transcription factors and induces the transcription of Wnt target genes. Canonical Wnt signaling controls gene expression by allowing  $\beta$  catenin to accumulate when Wnts are present and by reducing nuclear  $\beta$  catenin levels when Wnts are absent (Peifer, Polakis 2000, Chan, Struhl 2002, Sakanaka, Weiss & Williams 1998). Interestingly, in our studies, we found that rhLF treatment induced significant accumulation of  $\beta$  catenin but down-regulated canonical Wnts – Wnt2 and 3. Other canonical Wnts, which include Wnt1 and 8, were not found to be significantly regulated (< 2-fold change) in MC3T3 cells by holo-rhLF.

Non-canonical Wnt pathways are thought to involve Wnt/Ca<sup>2+</sup> (Veeman, Axelrod & Moon 2003, Kuhl et al. 2000, Ma, Wang 2006, Slusarski, Corces & Moon 1997) or the Wnt/planar cell polarity (PCP) (Veeman, Axelrod & Moon 2003, Adler, Lee 2001) or other less well-defined pathways (Logan, Nusse 2004, Miller 2002, Moon et al. 2002,

Wodarz, Nusse 1998, Veeman, Axelrod & Moon 2003). Wnt5a has been considered to be a representative non-canonical Wnt in several systems, which include stimulation of intracellular  $\text{Ca}^{2+}$  release and activation of PKC and CaMKII (Kuhl et al. 2000, Sheldahl et al. 1999). Non-canonical Wnt5a has also been suggested to antagonize canonical Wnt activity in mammalian cells (Torres et al. 1996, Olson, Gibo 1998, Ishitani et al. 2003). However, direct genetic evidence for this antagonistic interaction is lacking (Topol et al. 2003). Furthermore, even though Wnt5a signaling has been shown to support normal bone physiology, the biological significance of non-canonical Wnts in osteogenesis is essentially unknown. It has been just recently found that Wnt5a is a substantial constituent in BMP2-mediated osteoblast differentiation (Nemoto et al. 2012). Osteoblastic differentiation mediated by BMP2 is associated with increased expression of Wnt5a and Ror2 in MC3T3 cells. After silencing the gene expression of Wnt5a and Ror2 in MC3T3 cells, there was suppression of BMP2-mediated osteoblastic differentiation, which suggests that Wnt5a and Ror2 signaling are of substantial importance for BMP2-mediated osteoblastic differentiation (Nemoto et al. 2012).

Our studies demonstrated that LRP6 and Wnt5a were upregulated upon 24 hours of rhLF treatment relative to untreated control (Figure 33). Although Wnt5a and LRP6 were not previously thought to interact, recent reports have shown that LRP6 can affect typical non-canonical Wnt processes. These interactions have been shown to modulate Wnt5a-regulated processes in both *Xenopus* and mouse (Tahinci et al. 2007, Bryja et al. 2009). Furthermore, non-canonical Wnt signaling and  $\beta$  catenin signaling play a role in mechanically induced osteogenic cell fate (Arnsdorf, Tummala & Jacobs 2009). Wnt5a treatment has also been shown to increase integrin expression. Wnt5a enhances

osteogenesis through a positive feedback mechanism with integrins through BMP2 signaling (Olivares-Navarrete et al. 2011). In this study, scientists demonstrated the treatment of HMSCs with Wnt5a increases integrin expression and osteoblast differentiation. Furthermore, these results were confirmed using Wnt5a-knockdown HMSCs – where integrin expression on rough surfaces was decreased.

Biological growth factors, such as parathyroid hormone (PTH), has demonstrated PKA/LRP6-dependent signalling to increase bone formation in osteoblasts. Teriparatide, which has the identical sequence of biologically active region of recombinant human PTH, is FDA-approved as Forteo® for treatment of osteoporosis or high-risk fracture patients (Sibai, Morgan & Einhorn 2011). Studies have demonstrated the intermittent administration of PTH stimulates bone formation, but the precise mechanisms responsible for PTH responses in osteoblasts are incompletely understood. PTH, via the PTH/PTH-related protein receptor type 1 (PTH1R), couples to the PKA and the canonical Wnt/ $\beta$  catenin signaling pathway play important roles in bone formation. This study further utilized H89 inhibitor to confirm the involvement of PKA in PTH signalling, antagonized PTH stimulation of  $\beta$  catenin levels (Tobimatsu et al. 2006). Studies have also reported that PKA (Fang et al. 2000) has the ability to stabilize  $\beta$  catenin by phosphorylating Gsk3 $\beta$ . Furthermore, Fang *et al.* showed that PKA-mediated phosphorylation of serine 9 in Gsk3 $\beta$  activity and up-regulation of  $\beta$  catenin (Fang et al. 2000).

More recently, a study demonstrated that the binding of PTH to its receptor PTH1R induced association of LRP6 with PTH1R. The formation of the ternary complex containing PTH, PTH1R, and LRP6 then promoted rapid phosphorylation of LRP6,

which resulted in the recruitment of axin to LRP6, and stabilization of  $\beta$  catenin (Wan et al. 2008). This study demonstrated that activation of PKA is essential for PTH-induced  $\beta$  catenin stabilization. *In vivo* studies confirmed PTH treatment increases LRP6 phosphorylation and  $\beta$  catenin accumulation in osteoblasts with a concurrent increase in bone formation. These studies correspond with our findings of LF-induced, PKA/LRP6-dependent  $\beta$  catenin stabilization.

With the acknowledgment that osteoblast survival influences bone formation and skeletal integrity (Manolagas 2000, Weinstein et al. 1998), great likeliness is LF's anti-apoptotic activity plays a role in its ability to stimulate bone formation *in vivo* (Grey et al. 2006, Cornish et al. 2004). In our studies, we found LF's ability to activate  $\beta$  catenin and inhibit serum starvation-induced apoptosis to be both dependent on PKA signaling transduction pathway (Figure 42). However, the receptor through which LF is activating PKA pathway is still unknown.



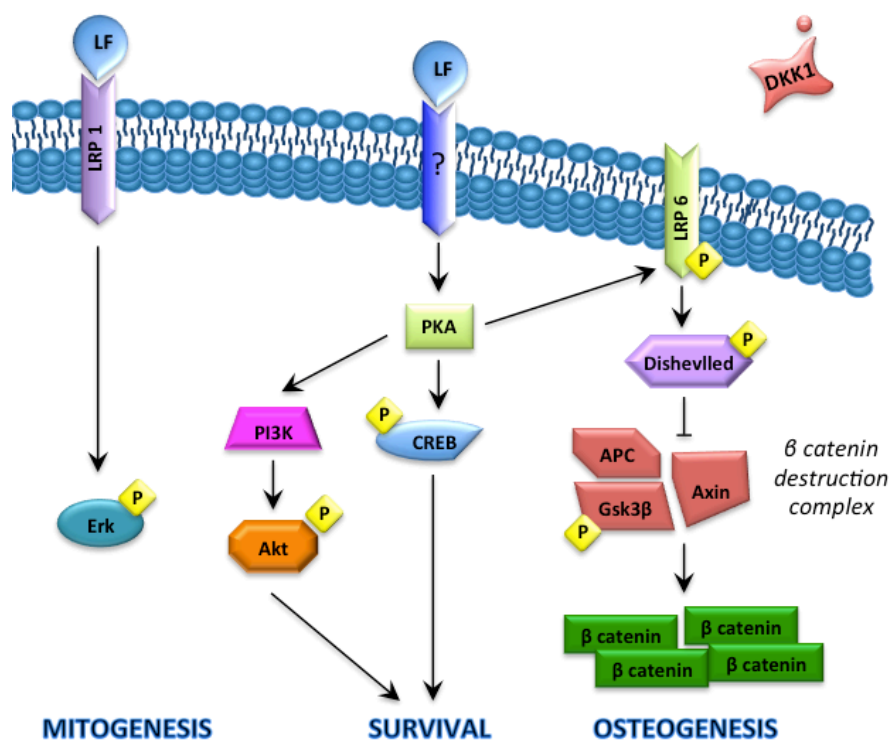


Figure 42. Schematic of signaling pathways induced by holo-rhLF in MC3T3 cells.

#### 4.3.5 Conclusions

The bioactivity of holo-rhLF was investigated in our *in vitro* cell culture model. Holo-rhLF treatment decreased cellular apoptosis in response to serum starvation. Furthermore, this bioactive protein up-regulated osteogenic markers, including collagen 1 and OCN, in MC3T3 cells. Our results demonstrated the novel discovery that holo-rhLF's anti-apoptotic actions and  $\beta$  catenin activation are dependent on PKA signaling cascade.

## **5 Preparation and characterization of injectable holo-rhLF and gelatin gels**

### **5.1 Development and characterization of bioactive holo-rhLF injectable gel via enzymatic crosslinking**

#### **5.1.1 Introduction**

Cell-based therapy has emerged as a promising strategy to repair and/regenerate lost, damaged or degenerative tissue using the principles of tissue engineering and regenerative medicine. Pluripotent and multi-potent cells along with tissue-specific cells are being investigated to develop novel cell based regenerative therapies. The therapeutic efficacy of local cell based strategies depends on several factors, including the ability to retain implanted cells at the defect site and present the cells in a three-dimensional manner without adversely affecting its performance (Zhao et al. 2011). Hydrogels are promising candidates due to their unique tissue-mimetic properties and their ability to allow gas and nutrient diffusion throughout the matrix, which is crucial for maintaining the viability of the encapsulated cells (Nicodemus, Bryant 2008, Annabi et al. 2010).

Eventhough both performed and injectable hydrogels have been considered for biomedical applications, injectable gels are preferred as cell delivery vehicles – as discussed previously in Section 2.1.2.2.1. Injectable scaffolds undergo mild and cytocompatible gelation, allow for homogeneous distribution of cells or molecules at the injection site, and have the ability to fill irregular defects (Slaughter et al. 2009). Moreover, they can be implanted by simple injection (Yu et al. 2008). Various polymers with stimuli sensitive properties and novel cross-linking chemistries are investigated to develop injectable hydrogels (Hennink, van Nostrum 2002). These include thermo-sensitive and pH-sensitive polymers, which can undergo sol-gel transition at or near

physiological conditions (Nair et al. 2007, Jiang et al. 2008), self-assembling peptides (Kopecek, Yang 2009), photo or thiol-mediated polymerization of acrylated polymers (Rydholm, Bowman & Anseth 2005) and enzyme-mediated crosslinking of polymers with appropriate functional groups (Davis et al. 2010). Polymers functionalized with tyramine, tyrosine or aminophenol side groups can form *in situ* gels by phenol or aniline derivative coupling using H<sub>2</sub>O<sub>2</sub> and HRP as the oxidant and enzyme, respectively (Kurisawa et al. 2005, Kobayashi, Uyama & Kimura 2001, Jin et al. 2007, Lee, Chung & Kurisawa 2009). This biologically compatible system has several advantages as the physical properties of the gel may be fine tuned by varying the degree of tyramine substitution, polymer and enzyme concentration (Jin et al. 2010, Sakai et al. 2009, Hu et al. 2009, Darr, Calabro 2009).

The objective of this study was to investigate the feasibility of developing injectable hydrogels from holo- rhLF gel and characterize the gel properties in terms of its gelation time, mechanical properties, water uptake and morphology. An understanding of the physical properties of gels is crucial for determining the range of their biomedical applications. Since LF-based biomaterials have been recently developed, the understanding of the structure-property relationships in this class of materials is limited. Such understanding would provide molecular design principles to tailor material properties, allowing the materials to be optimized for clinical applications or tuned systematically to address fundamental biological questions. Depending on various parameters, such as the gelation mechanism and polymer concentration, the gels can exhibit different mechanical properties. We hypothesize that varying concentrations of

the gel precursors, HRP, modified rhLF and  $\text{H}_2\text{O}_2$ , will directly affect the gelation rate, mechanical strength and morphology of the rhLF gels.

### **5.1.2 Methods**

#### **5.1.2.1 Synthesis of holo-rhLF tyramine conjugates (modified holo-rhLF)**

Modified holo-rhLF was prepared as described in Appendix of Protocols (Section 7.9.2.1.1).

#### **5.1.2.2 Preparation of holo-rhLF gels**

Holo-rhLF gels were prepared by the HRP-mediated oxidative coupling of modified holo-rhLF molecules in the presence of  $\text{H}_2\text{O}_2$  as described in the Appendix of Protocols (Section 7.9.2.1.2.2). Various concentrations of modified holo-rhLF ranging from 10 mg/ml to 50 mg/ml were dissolved in 10 U/ml HRP and gelation was initiated by the addition of 0.25% aqueous  $\text{H}_2\text{O}_2$ .

#### **5.1.2.3 Quantification of tyramine modification**

Holo-rhLF was modified with varying reaction times (0.5 – 24 hours) and tyramine concentration was then examined as a function of modification reaction time as described in Appendix of Protocols (Section 7.9.2.1.1.1). A tyramine standard curve was used to determine the concentration of a tyramine in the modified holo-rhLF samples.

#### **5.1.2.4 Gelation time**

Sol to gel time was determined via vial inversion method. The effect of modified holo-rhLF (10 – 50 mg/ml), HRP (10 – 50 U/ml) and 0.25%  $\text{H}_2\text{O}_2$  (1 - 10  $\mu\text{l}$ ) concentration on gelation time was investigated. 10mg/ml modified holo-rhLF in 100  $\mu\text{l}$  of 10/ml U HRP

+ 1  $\mu$ l of 0.25%  $\text{H}_2\text{O}_2$  represents the standard gelling conditions. Variables were individually varied and tested for effect on gelatin time.

#### **5.1.2.5 Soluble holo-rhLF protein release from holo-rhLF gel**

10 mg/ml holo-rhLF gel was incubated in PBS at 37°C. Aliquots were taken from each sample every 24 hours for 5 consecutive days and phenolic content was measured via UV spectrophotometer at 275 nm. Details of the protocol were described in Section 7.9.2.3.

#### **5.1.2.6 Percentage water uptake**

The percentage of water uptake of the injectable gels was determined as described in Appendix of Protocols (Section 7.9.2.2.4). Briefly, 400  $\mu$ l of holo-rhLF gel were prepared in 24-well plastic inserts (n=4).

#### **5.1.2.7 Morphology**

The morphology of the holo-rhLF gels formed from modified holo-rhLF solutions of different concentrations (10, 25, 50 mg/ml) was visualized by scanning electron microscope (JEOL 6335 Field Emission Scanning Electron Microscope) to evaluate the effect of solution concentrations on gel microstructure – as described in Appendix of Protocols (Section 7.9.2.2.3). Measurements (n=50) of pore size and pore wall width were obtained using Image J program.

#### **5.1.2.8 Rheological analysis**

A rheometer is an ideal instrument that may be used to measure the gel strength. The holo-rhLF gels were subjected to rheological measurements to assess the viscoelastic properties at varying component concentrations at 25°C and 37°C. Briefly, the modified holo-rhLF/HRP and  $\text{H}_2\text{O}_2$  mixture were introduced in a parallel plate rheometer (ARES-

LS, TA instruments). Stress sweeps at a constant frequency of 1 Hz were first performed to obtain the linear viscoelastic region for collecting subsequent data. Dynamic frequency sweeps were then performed in the linear viscoelastic region to determine values of the storage ( $G'$ ) and loss ( $G''$ ) modulus to compare the mechanical strength of gels with different concentrations of holo-rhLF.

#### **5.1.2.9 Biomaterial degradation in vivo**

Sprague Dawley rats (Charles River Laboratories, Wilmington, MA) (12-16 weeks) were used. 10 mg/ml holo-rhLF were injected subcutaneously to form the gels in situ. The animals were cared for according to the procedures approved by the Animal Care and Use Committee at the University of Connecticut Health Center, and following the guidelines established by the U.S. National Institutes of Health. At 4 and 12 weeks, rats were sacrificed and the tissue surrounding the injection sites were excised using blunt dissection technique. Samples were fixed in 10% formalin solution (Surgipath, USA) and embedded in paraffin, sectioned and hematoxylin and eosin (H&E) was performed.

#### **5.1.3 Results**

We investigated tyramine concentrations as a function of chemical modification time. The phenolic content of unmodified holo-rhLF is due to the presence of tyrosine. After 24 hours of tyramine modification, the phenolic concentration increased from 0.158  $\mu\text{g/ml}$  to 0.181  $\mu\text{g/ml}$ . This increase in phenolic concentration of the modified holo-rhLF led to decreased gelation time as in the case of bLF gel (Section 3.1.3.1) (Figure 43).

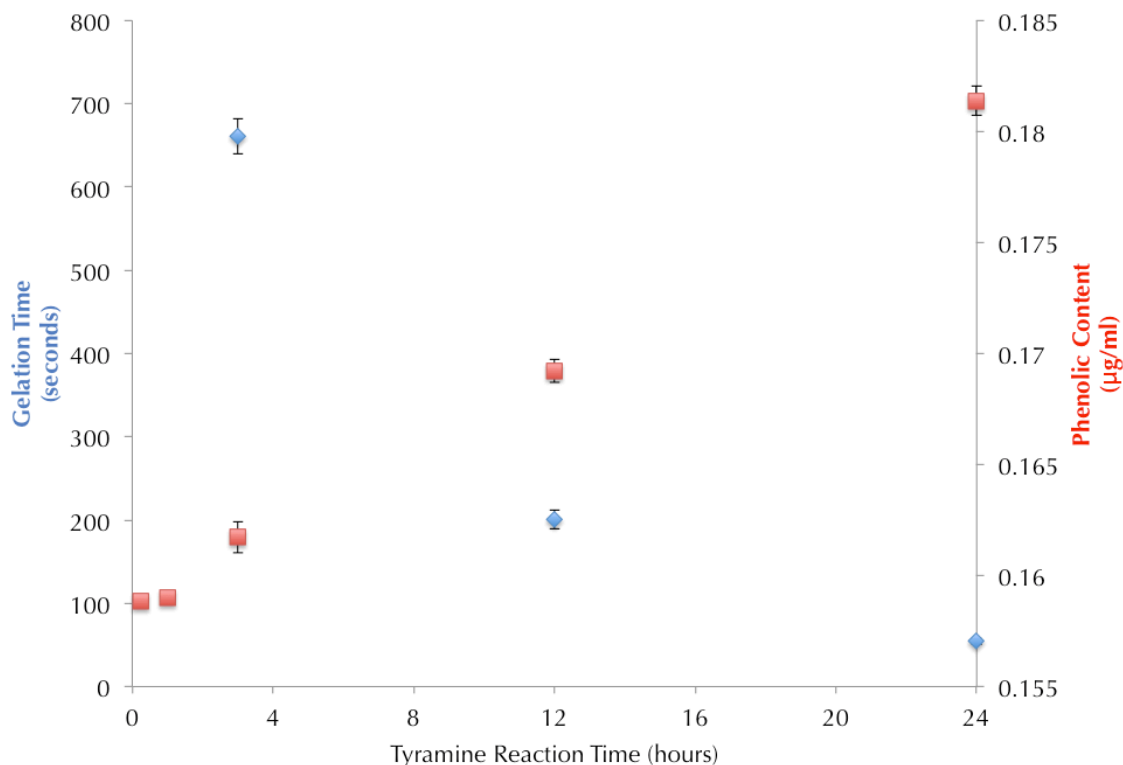


Figure 43. Inverse effect of tyramine modification time (over 24 hours) on phenolic content and gelation time of rhLF.

*The standard gel precursor concentrations, 10 mg/ml modified rhLF dissolved in 100 µl of 10 U/ml HRP plus 1 µl of 0.25% H<sub>2</sub>O<sub>2</sub>, were used to test gelation time.*

Sol-to-gel time of the holo-rhLF gels was determined via vial inversion method (Figure 44). The flexibility of fast or slow gelation time is possible through the manipulation of the concentration of the gel precursors – HRP, modified holo-rhLF and H<sub>2</sub>O<sub>2</sub> (Figure 45). HRP and holo-rhLF polymer concentration had a direct effect on gelatin time, whereas, H<sub>2</sub>O<sub>2</sub> concentration did not have this similar trend on gelation time. Lower amounts of H<sub>2</sub>O<sub>2</sub> (0.5-5 µl of 0.25% H<sub>2</sub>O<sub>2</sub>) decreased gelation time of holo-rhLF gel; whereas, higher amounts of H<sub>2</sub>O<sub>2</sub> (10 µl of 0.25% H<sub>2</sub>O<sub>2</sub>) actually increased the gelation time. Based on the study, the standard precursor concentrations was determined as follows: modified rhLF (10 mg/ml) dissolved in 100 µl of 10 U/ml HRP and 1 µl of

0.25%  $\text{H}_2\text{O}_2$  in water/PBS mixture– these conditions yielded a gelation time of approximately 1 minute.

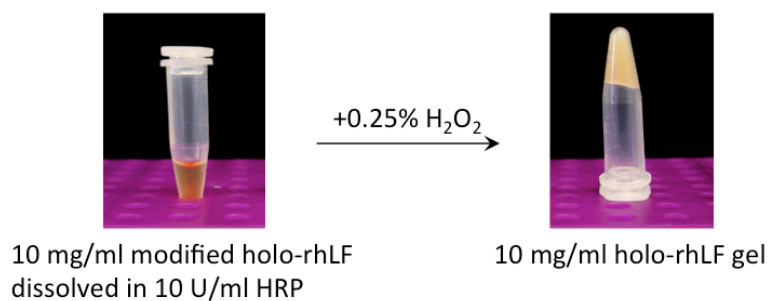
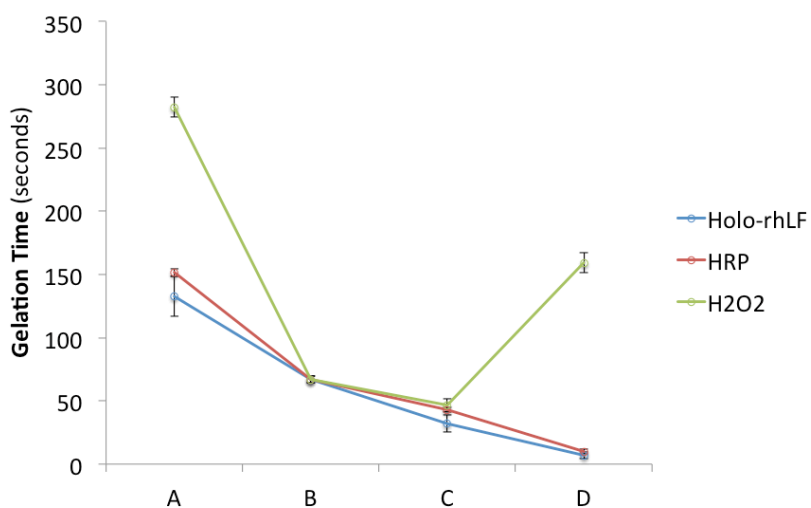


Figure 44. Gelation time of rhLF gel upon addition of dilute  $\text{H}_2\text{O}_2$  as determined by the vial inversion technique.



	Holo-rhLF [x mg/ml]	HRP [x U/ml]	$\text{H}_2\text{O}_2$ [x $\mu\text{l}$ 0.25%]
A	5	5	0.5
B	10	10	1
C	25	25	5
D	50	50	10

Figure 45. Effect of gel precursors (modified rhLF, HRP,  $\text{H}_2\text{O}_2$ ) concentration on gelation time.



*The standard conditions for approximately 1 minute gelation time is 10 mg/ml modified rhLF dissolved in 100  $\mu$ l of 10 U/ml HRP plus 1  $\mu$ l of 0.25%  $H_2O_2$ . To study the effect of each gel component, one component was varied and the concentrations of other components were held at the standard conditions.*

To test whether a substantial amount of polymer was un-crosslinked, we measured the amount of protein that was released (un-crosslinked polymer) from the gel into PBS buffer over 5 days at 37°C (Figure 46). After 24 hours, only 4.2 ng/ml of protein was released from 10 mg/ml holo-rhLF. By 5 days, a cumulative amount of 10.1 ng/ml of modified holo-rhLF protein was released in the PBS buffer. The study demonstrated that enzyme mediated crosslinking of modified rhLF lead to a fully crosslinked matrix

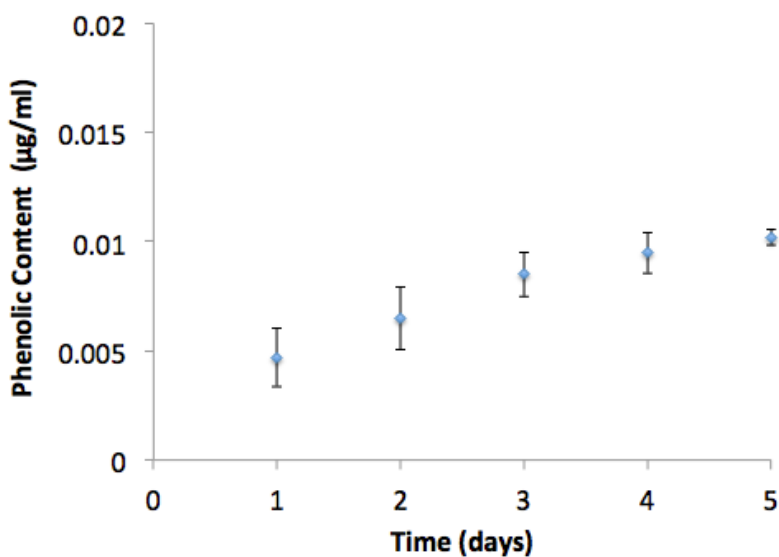


Figure 46. Soluble holo-rhLF release from crosslinked 10 mg/ml holo-rhLF gel as a function of time.

The crosslinked rhLF gel displayed a highly porous microstructure as indicated in Figure 47 and Figure 48). Changes in holo-rhLF polymer, HRP enzyme and  $\text{H}_2\text{O}_2$  oxidant concentrations did not result in a significant change in pore size of the crosslinked gel (Figure 48). The average pore size of holo-rhLF gels was  $8.51 \pm 2.97 \mu\text{m}$ . Figure 45 shows the storage modulus of the gel as a function of rhLF concentration. An increase rhLF polymer concentration led to corresponding increase in storage modulus,  $G'$  (Figure 49). rhLF gels with polymer concentrations of 10, 25, 50 mg/ml resulted in storage moduli of  $102.8 \pm 8.5$ ,  $429.2 \pm 31.8$ ,  $997.9 \pm 204.6$  Pa, respectively. We also investigated the effect of gelation temperature on the storage modulus of the gels. As shown in Figure 45b, the 50 mg/ml holo-rhLF gels formed at temperatures of  $25^\circ\text{C}$  and  $37^\circ\text{C}$  showed storage moduli of  $997.9 \pm 204.6$  Pa and  $899.8 \pm 93.4$  Pa, respectively, indicating that temperature of gelation does not have any effect on gel mechanical properties.

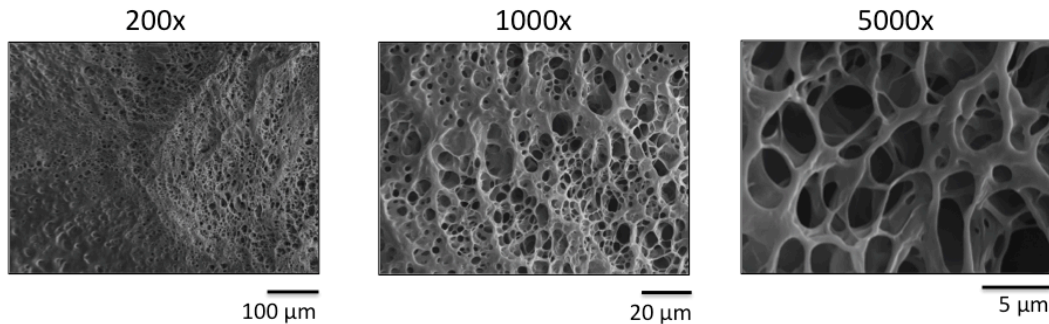


Figure 47. Morphology of 10 mg/ml holo-rhLF gel.

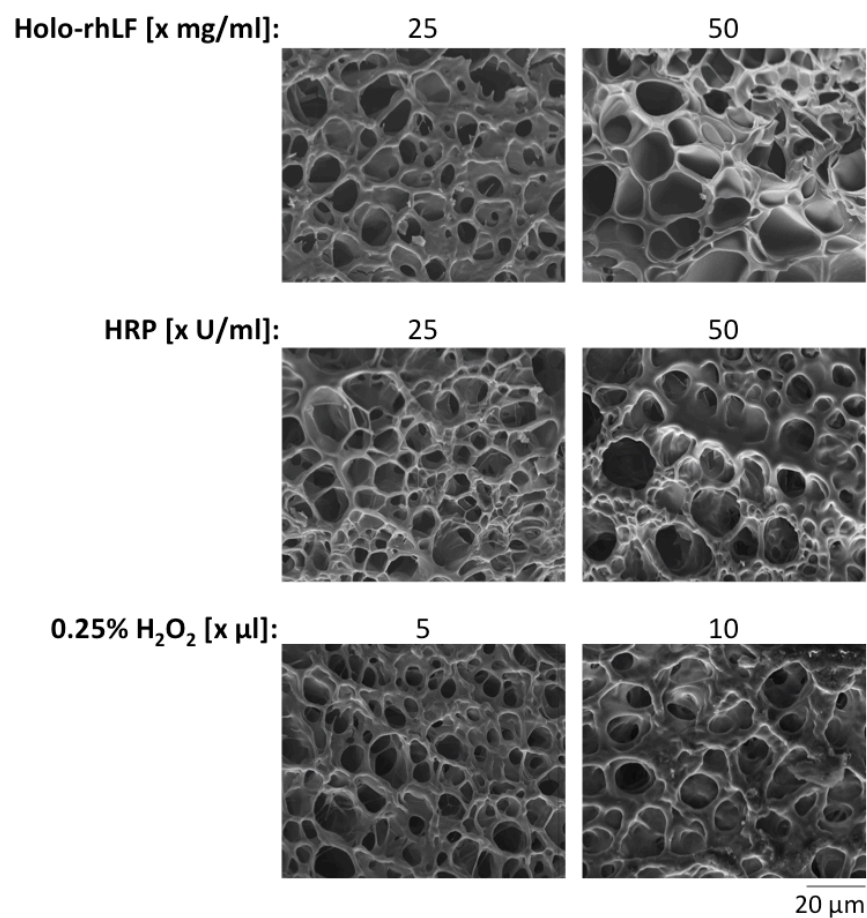


Figure 48. Morphology of holo-rhLF gel at various gel precursor concentrations

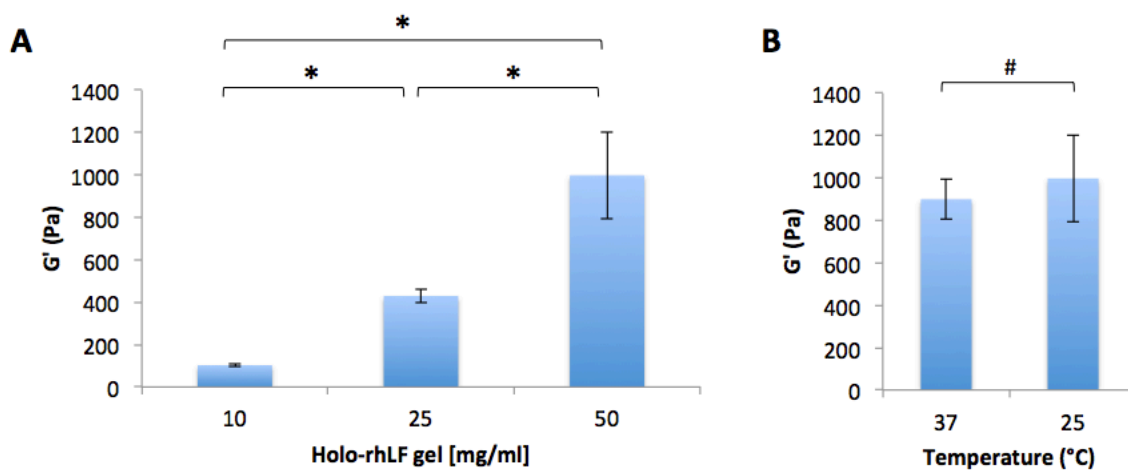


Figure 49. A) Effect of holo-rhLF polymer concentration on hydrogel mechanical strength as a function of storage moduli, G'. B) Effect of temperature (25°C vs. 37°C) on storage moduli, G', of 50 mg/ml holo-rhLF gel.

Data is expressed in Pascal (Pa). \* indicates  $p < 0.05$ ; # indicates  $p > 0.05$

Another physical property investigated was the extent of water uptake by the gels. Figure 50 shows the extent of water uptake of gels made from different polymer concentration. Although there was a trend towards increasing water uptake as the polymer concentration increased, there was no statistically significant differences between the weights of the gels at 0 day and after 8 days of incubation in buffer (Figure 50-52). Similar trends were observed with gels prepared at different HRP and  $H_2O_2$  concentration (Figure 51 & 52). No significant increase in water uptake was observed with any of the gels as a function of incubation time in PBS.

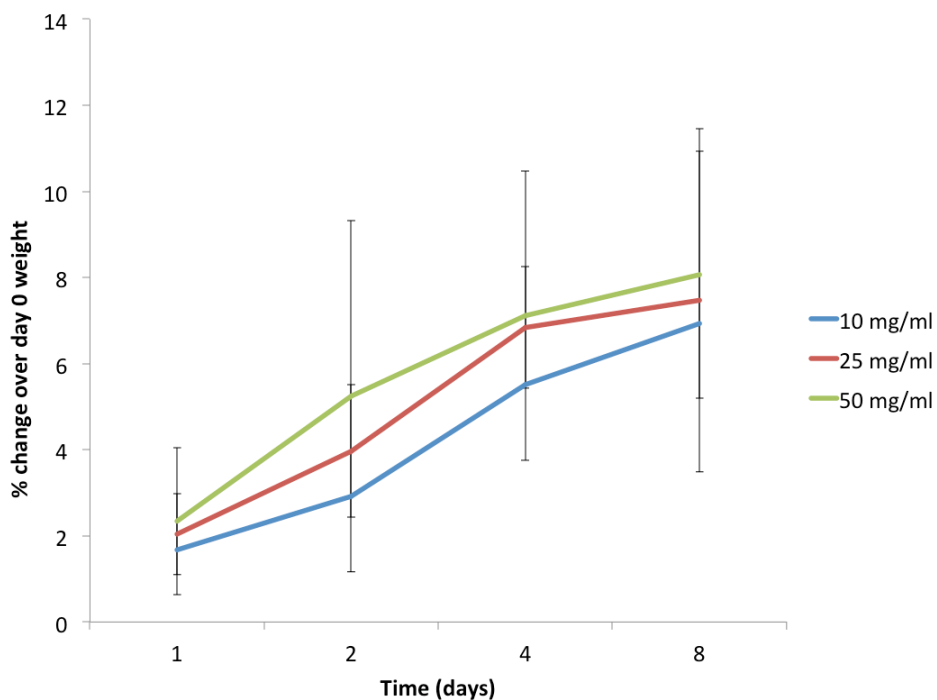


Figure 50. Effect of holo-rhLF concentration on holo-rhLF gel water uptake over 8 days.

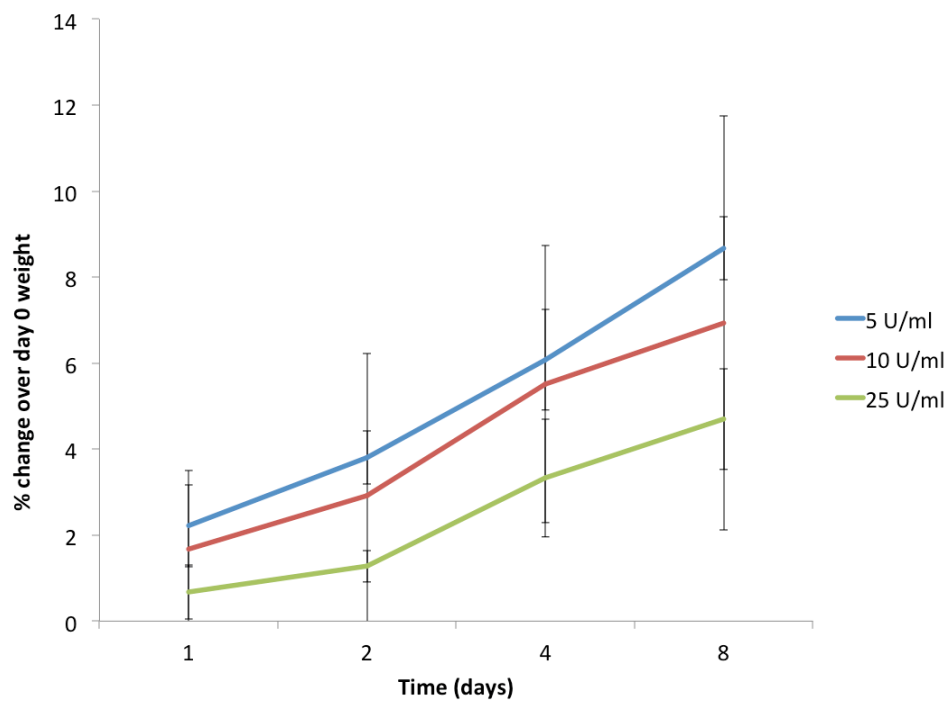


Figure 51. Effect of HRP concentration on holo-rhLF gel water uptake over 8 days.

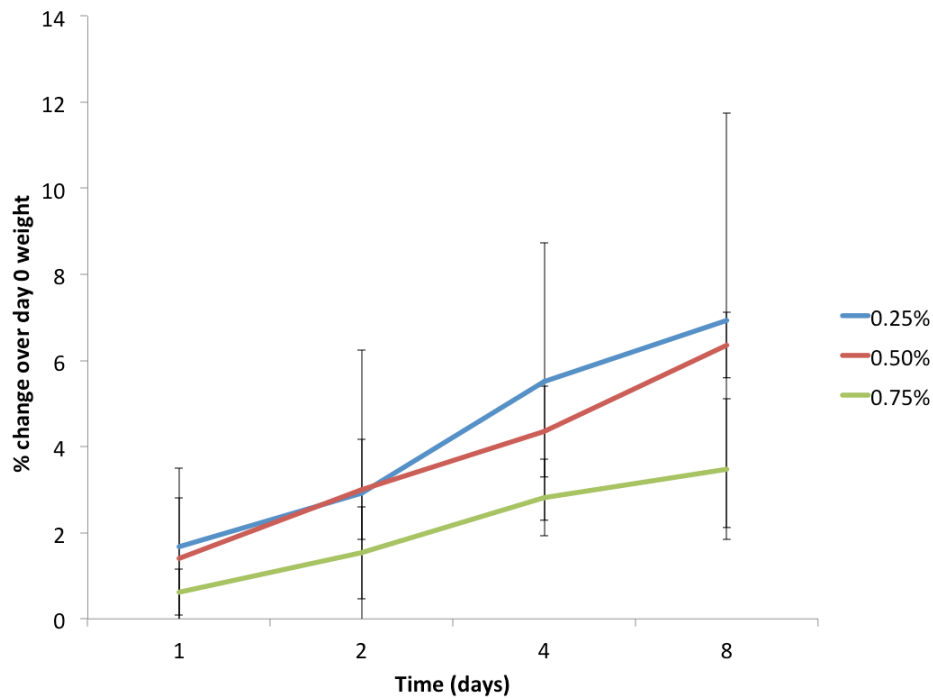


Figure 52. Effect of  $\text{H}_2\text{O}_2$  concentration on holo-rhLF gel water uptake over 8 days.

Figure 53 shows the H&E-stained subcutaneous tissue surrounding the gel (10 mg/ml holo-rhLF gel) implantation 4 and 12 weeks past implantation. At 4 weeks, the presence of injectable gel was evident at the site of injection. Significant cell infiltration mainly composed of macrophages and lymphocytes was observed within the gel. Interestingly, no sign of fibrous capsule formation was observed. At 12 weeks post implantation, the no evidence of gel was observed in the subcutaneous tissue indicating the complete degradation of the gel at that time point.

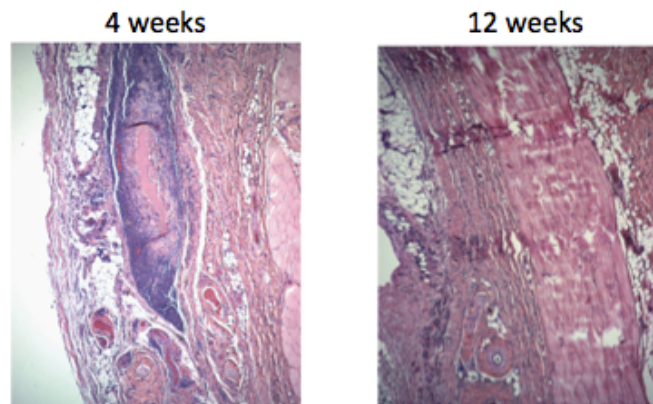


Figure 53. *In vivo* degradation of 10 mg/ml holo-rhLF gel in rat subcutaneous tissue after 4 and 12 weeks.

Attempts were also made to characterize the ability of rhLF gel to serve as a cell delivery vehicle. Cell delivery vehicle should be able to encapsulate cells under physiological condition, support cell adhesion, spreading and proliferation. Figure 54 shows the Live/Dead staining of MC3T3 cells encapsulated in holo-rhLF gels. Three different rhLF gel concentration was studied to understand the effect of polymer concentration on cell behavior. As shown in the figure, irrespective of the polymer concentration, rhLF gels were able to maintain MC3T3 cell viability. However, the extent of cell spreading and proliferation seems to be negatively affected by increase in

polymer concentration. Among the samples studied, 10 mg/ml holo-rhLF gel allowed for the most extensive cell spreading after 14 days of encapsulation.

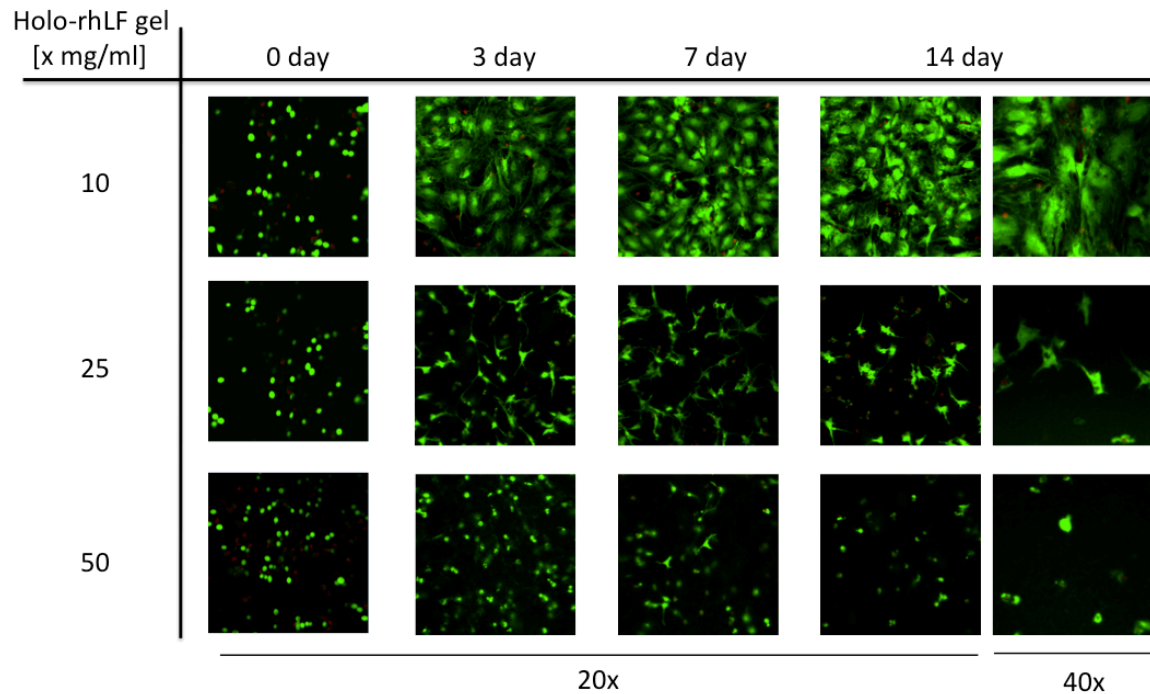


Figure 54. Cellular spreading in 10, 25 and 50 mg/ml holo-rhLF gel over 14 days of encapsulation using live/dead assay.

#### 5.1.4 Discussion

*In situ* formation of injectable biomaterials allows for the biomaterial to fill irregular 3D shapes of clinically relevant defects. The synthesis of our *in situ*—forming, biodegradable holo-rhLF crosslinked gel utilizes modified rhLF. Standard carbodiimide mediated coupling of amino groups of tyramine with the carboxyl groups of holo-rhLF was used to develop the modified rhLF (Sakai et al. 2009, Amini, Nair 2012b). Although holo-rhLF contains phenolic amino acids, such as tyrosine, the phenolic content holo-rhLF is much lower than what is needed to develop an effectively crosslinked matrix via

the enzyme-catalyzed coupling. The reaction of holo-rhLF with tyramine could increase the extent of polymer cross-linking by increasing the number of phenolic groups (Figure 11, Figure 12). Since there is significant species homology between bLF and hLF (van Berkel et al. 2002) (Figure 1), the substitution process of hLF similar to that used for developing bLF (section 3.1.3.1). Holo-rhLF gels were obtained by enzymatic crosslinking of the modified holo-rhLF in the presence of HRP, as the catalyst, and  $\text{H}_2\text{O}_2$ , as the oxidant (Figure 13). Enzymatic crosslinking driven by HRP and  $\text{H}_2\text{O}_2$  allows for a mild, cell-friendly gelation process. The advantages of HRP-mediated crosslinking include its ability to take place at physiological pH and temperature. Moreover, the gelation time can be modulated to a great extent by varying the reagent concentrations, making this a potential route to form injectable cell and protein delivery vehicles (Sakai et al. 2009, Hu et al. 2009, Amini, Nair 2012b).

Gelation time of HRP-mediated enzymatic crosslinking of holo-rhLF yields a protein-based hydrogel that may be controlled by the concentration of the reactants. Although increased concentration of modified holo-rhLF (polymer) and HRP (catalyst) led to decreased gelation time of holo-rhLF gel – this effect was not seen with the increase of  $\text{H}_2\text{O}_2$  (oxidant). It has been reported that HRP can be oxidized to an inactivated form upon exposure to an excess amount of  $\text{H}_2\text{O}_2$  (Arnao et al. 1990, Baynton et al. 1994). Moreover, the use of low amounts of  $\text{H}_2\text{O}_2$  is advantageous, since  $\text{H}_2\text{O}_2$  may give cytotoxicity problems. Fast gelation time is preferred especially for *in situ*—forming gels, since slow gelation *in vivo* may result in diffusion of gel precursors or bioactive molecules to the surrounding areas or failure of gel formation. The optimal gelation time was determined to be in the range of 1 minute.



Storage moduli of biomaterials has been shown to have an influence on several cellular behaviors, including cell adhesion, spreading, proliferation, morphology and differentiation of stem cells (Lo et al. 2000, Pelham, Wang 1997, Cukierman et al. 2001). Previous data reports a wide range in substrate stiffness with a soft gel (1 kPa), a stiff gel (8 kPa), and a rigid substrate (66 kPa) (Engler et al. 2004). The degree of stiffness in physiological human tissue varies dramatically between tissues: brain is about 0.1-1 kPa; striated skeletal muscle is approximately approximately 8-17 kPa and pre-calcified bone is 25-40 kPa (Engler et al. 2006, Tse, Engler 2010). Human bone exhibits unique mechanical properties – both elastic and semi-brittle behavior. There are two types of bone, compact or cortical, and cancellous or trabecular (spongy) bone. Compact and trabecular bone have mechanical strengths in the range of 131 - 224 MPa and 5 – 10 MPa, respectively (Yaszemski et al. 1996, Athanasiou et al. 2000, Currey 1998, Currey 1970, Currey 1999). However, the storage modulus of holo-rhLF gels (10-50 mg/ml) was in the range of 100-1000 Pa. The low storage modulus of holo-rhLF makes it an excellent cell delivery vehicle for non-load bearing applications and for load bearing applications with external support.

Another very important parameter that needs to be evaluated while developing an injectable biomaterial is the extent of water uptake of the formed gel once exposed to aqueous environment. Significant water uptake of the gel can adversely affect the performance of the injectable gel. As in the case of mechanical properties, several parameters, such as polymer concentration and cross-linking density, can directly affect the extent of water uptake. In our gel studies, holo-rhLF gels demonstrated water uptake percentage of about 10% of original gel weight after 8 days of PBS buffer incubation at

37°C physiological temperature. This percentage of water uptake did not seem to adversely affect the performance of the encapsulated cells.

Biomaterial morphology is an important characteristic to investigate when designing a cell delivery vehicle. Hydrogels are porous biomaterials that allow for *in situ*-delivery of encapsulated cells. Porous interconnectivity also allows for uniform cell seeding and necessary diffusion of nutrients and waste. In our studies, all concentrations of holo-rhLF gel that were investigated displayed a porous interconnected structure.

Osteoblasts require a delivery vehicle that not only maintains cell viability but also supports cell attachment and spreading for three-dimensional cellular organization. The highly porous structure of holo-rhLF gel allowed for cellular spreading, which was inversely regulated with polymer concentration of the gel (Figure 54). Decreased cell spreading at high polymer concentration gels may be attributed to the decreased cell proliferation at higher concentrations (Huang et al. 2008). Porous biomaterial hydrogels are favorable since they support vascular ingrowth for oxygen transport. Pore size of holo-rhLF gel (10-50 mg/ml) was averaged at approximately 5-10  $\mu\text{m}$ . However, the average size of an osteoblast is approximately 20-25  $\mu\text{m}$  (Puckett, Pareta & Webster 2008). Porosity and interconnected pores allow for the diffusion of nutrients and gases for enhancing cell viability. In our cell encapsulation studies, holo-rhLF gel allowed for high percentage of live to dead cell ratio. However, a decrease in cell spreading and density was seen in the MC3T3 cells encapsulated in 50 mg/ml holo-rhLF gel (relative to 10 and 25 mg/ml holo-rhLF gel). As described below, these results may be explained through a variety of different reasonings – decrease cell spreading and density due to 1) increased mechanical strength decreasing cell proliferation and spreading or 2) high

concentration holo-rhLF adversely affecting the encapsulated cell proliferation and spreading.

Hydrogels, which may act as the ECM that surrounds encapsulated cells, are known to contain biochemical information that may regulate cell functions, including adhesion, spreading, migration, proliferation, survival, and differentiation (Khatiwala, Peyton & Putnam 2006). A recent study reported an injectable HRP/H<sub>2</sub>O<sub>2</sub> hydrogel scaffold system with tunable mechanical properties for controlling the proliferation rate and differentiation of human mesenchymal stem cells (Wang et al. 2010). The scientists found that the hydrogel stiffness inversely affected the cell proliferation rates – an increase in stiffness led to a decrease in cellular proliferation.

Another possible reason for the decreased cell spreading in holo-rhLF gels of higher LF concentrations is that LF being a bioactive protein can adversely affect cellular behavior. In our studies, we only investigated the proliferative effect of 1000 µg/ml holo-rhLF, which showed an increase in cell proliferation (Figure 19). However, Huang *et al.* tested concentrations up to 50,000 µg/ml holo-rhLF in HT29 intestinal cells. In these studies, holo-rhLF increase thymidine incorporation in HT29 cells at concentrations of 10-1,000 µg/ml, however 10,000 and 50,000 µg/ml holo-rhLF treatment led to a significant decrease in thymidine incorporation (Huang et al. 2008). The decrease in cellular performance at high concentrations of holo-rhLF treatments in Huang's study may support our findings of decreased cell number and spreading at 50 mg/ml holo-rhLF gel.

### 5.1.5 Conclusions

The study demonstrated the feasibility of developing injectable rhLF gels by the enzymatic coupling of tyramine-modified rhLF. The gelation time of the gels significantly depended on the reagent concentrations. Through the optimization of the concentrations of the gel components, a clinically viable gelation time of ~1 minute was developed. However, the gel physical properties, such as morphology and water uptake, was not significantly affected by the change in reagent concentrations. Increase in rhLF concentration significantly increased the storage modulus of the gels. Based on the storage modulus, the gels were characterized as soft gels. rhLF-encapsulated MC3T3 cells in various concentrations of rhLF gel maintained high viability, demonstrating the cyto-compatibility of the gels. However, rhLF gels of higher concentration tended to decrease cell spreading and density. Since even 50 mg/ml rhLF showed a porous structure and storage modulus, the decreased cellular activity in rhLF gels with higher LF concentrations is presumed to be due to the bioactivity of the gels.

## ***5.2 Enzymatically crosslinked injectable gelatin gel as an osteoblast delivery vehicle***

### **5.2.1 Introduction**

The study discussed in section 5.1 demonstrated the feasibility of developing rhLF gel and the cytocompatibility of the gel as a potential cell delivery vehicle. Based on the demonstrated bioactivities of rhLF (sections 4.1- 4.3), we hypothesize that rhLF gels will retain the unique bioactivities of soluble rhLF protein and could serve as a bioactive cell delivery vehicle with anti-apoptotic and osteogenic properties. To demonstrate the bioactivity of rhLF gel towards encapsulated gel, a control gel system needs to be developed. The objective of the proposed study is to test if injectable gelatin gel may serve as a three dimensional control gel matrix to evaluate the bioactivity of rhLF gels.

Injectable hydrogels based on proteins are highly preferred as they can favorably interact with the encapsulated cells via specific peptide epitopes and also undergo cell-mediated enzymatic degradation (Nguyen, Lee 2010). Therefore, ECM-derived proteins, such as collagen, gelatin, laminin and elastins are potential candidates to develop cell delivery vehicles (Stenzel, Miyata & Rubin 1974). Compared to collagen, gelatin is more economical and possesses more integrin binding domains for cell attachment due to its less ordered structure. Furthermore, gelatin is a denatured protein, making it less immune-reactive than collagen (Dreesmann, Ahlers & Schlosshauer 2007, Liu et al. 2009, Spotnitz, Burks 2008). The good cell-adhesivity of gelatin is particularly useful in developing cell delivery vehicles for anchorage dependent cells such as osteoblasts, epithelial cells and smooth muscle cells (Kwon, Peng 2002).

Several preformed and injectable gelatin formulations have been developed (Young et al. 2005, Singh et al. 2010, Lai, Li 2010, Kuwahara et al. 2010, Chen et al. 2003). These include chemical cross-linking using the carboxyl or amino groups of gelatin with polymers having appropriate reactive groups (Balakrishnan, Jayakrishnan 2005), and photo cross-linking of acrylated gelatin either alone or in the presence of other biocompatible polymers. Yamamoto *et al.* used glutaraldehyde to crosslink acidic and basic gelatins with iso-electric points of 5.0 and 9.0, respectively (Yamamoto, Takahashi & Tabata 2006). The study demonstrated the ability of chemically crosslinked acidic gelatin gels to retain growth factors and function as a sustained delivery vehicle. The spatial and temporal control of the photo-curing process provides unique advantages for developing controllable *in vitro* systems. However, the need to use photo initiators and UV light has raised concerns with respect to *in vivo* applicability (Fukaya et al. 2009, Okino et al. 2002, Hoshikawa et al. 2006, Terao et al. 2003). As discussed before, enzyme-catalyzed reactions have recently gained interest due to the ability to use mild, cell-friendly natural processes to develop injectable gels. Several enzymatically-catalyzed reactions were developed to form gelatin gels. Transglutaminase cross-linked gelatin was developed as a cell delivery vehicle in which covalent N- $\epsilon$ ( $\gamma$ -glutamyl) lysine amide bonds are formed between the gelatin molecules in the presence of the enzyme (Yung, Bentley & Barbari 2010) (Figure 55). Cross-linking phenol derivatives of polymers in the presence of H<sub>2</sub>O<sub>2</sub> and HRP is another potential route to develop injectable gels (Lee, Chung & Kurisawa 2009, Sakai et al. 2009). Injectable gelatin gels using the HRP-H<sub>2</sub>O<sub>2</sub> oxidative coupling reaction has been reported (Sakai et al. 2009, Hu

et al. 2009, Park et al. 2011). Recently, gelatin–poly(ethylene glycol)–tyramine (GPT) injectable hydrogel was developed to support tissue regeneration (Sakai et al. 2009).

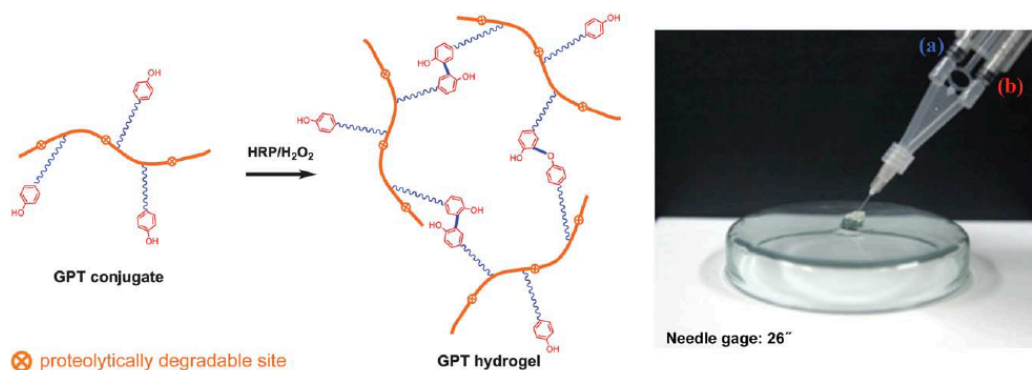


Figure 55. Schematic representation of the enzymatic crosslinking of gelatin–poly(ethylene glycol) tyramine (GPT) conjugates and the image of the in situ GPT hydrogel formation using a dual syringe.

*The dual syringe contained: (a) 3wt % GPT dissolved in 0.0025 mg/ml HRP in 0.01 M HRP and (b) 3wt% GPT dissolved in 0.0125wt % H<sub>2</sub>O<sub>2</sub> in 0.01 M PBS. Image adapted from (Park et al. 2011).*

Several parameters such as chemical and biological properties of the polymer, pore size, pore structure, stiffness and permeability of the scaffold are known to affect cell performance (Kim et al. 2010). In order to develop the appropriate control for rhLF gels, tyramine conjugated gelatin was used for HRP mediated crosslinking similar to rhLF gels. We evaluated the effects of gelatin concentration on the microstructure of the injectable gel and the long-term viability and spreading of encapsulated MC3T3 cells. The bioactivity of the modified and unmodified gelatin towards MC3T3 was evaluated by whether the protein can induce the phosphorylation of ERK and the expression of active  $\beta$  catenin and Runx2. Immunocytochemistry was used to investigate if the gel matrix can modulate the osteogenic functions of the encapsulated cells.

## **5.2.2 Methods**

### **5.2.2.1 Preparation of gelatin gel**

#### **5.2.2.1.1 Synthesis of gelatin tyramine conjugates (modified gelatin)**

Modified gelatins were prepared as described in Appendix of Protocols (Section 7.9.2.1.1). The extent of tyramine-substitution in modified gelatin was followed by UV-spectrophotometer at 275 nm and the concentration of the phenolic group in the solutions was determined from a standard curve.

#### **5.2.2.1.2 Preparation of gelatin gels**

Different concentrations of water-soluble modified gelatin (10, 25 and 50 mg/ml) were dissolved in HRP solution (10 U/ml) in distilled H<sub>2</sub>O and gelation was initiated by the addition of 0.25% H<sub>2</sub>O<sub>2</sub>.

### **5.2.2.2 Morphology**

The morphology of the gelatin gels formed from modified gelatin solutions of different concentrations (10, 25, 50 mg/ml) was visualized by SEM as described in Appendix of Protocols (Section 7.9.2.2.3).

### **5.2.2.3 Rheological analysis of gelatin gels**

The gelatin gels were subjected to rheological measurements to assess the viscoelastic properties at varying component concentrations at 25°C as described in Appendix of Protocols (Section 7.9.2.2.2). 50 µl of modified gelatin/HRP solution was first introduced in a parallel plate rheometer. Next, 50 µl of modified gelatin/H<sub>2</sub>O<sub>2</sub> solution was added during pre-shear step of 50 rad/second for 10 seconds. Dynamic frequency sweeps were then performed in the linear viscoelastic region to determine values of the



storage ( $G'$ ) and loss ( $G''$ ) modulus to compare the mechanical strength of gels with different concentrations of gelatin. Rheology testing conditions were as follows: angular frequency of 1 rad/second; 3% strain; 1000  $\mu\text{m}$  gap width; 100  $\mu\text{l}$  volume load.

#### 5.2.2.4 Cell encapsulation in gelatin gel

The water-soluble modified gelatin (10, 25 and 50 mg/ml) was dissolved in 10U/ml HRP in distilled water. Cell suspension on media (500,000 cells) were added and re-suspended in 100  $\mu\text{l}$  each of the modified gelatin/HRP solutions followed by the addition of aqueous  $\text{H}_2\text{O}_2$  (1  $\mu\text{l}$  of 0.25% solution). The encapsulated cells were then cultured in basal MEM $\alpha$  medium at 37°C.

The water/PBS soluble modified gelatin (10, 25 and 50 mg/ml) was dissolved in 10U/ml HRP in 50:50 water/PBS mixture. Cell pellet (500,000 cells) was added and re-suspended in 100  $\mu\text{l}$  each of the modified gelatin/HRP solutions followed by the addition of aqueous  $\text{H}_2\text{O}_2$  (1  $\mu\text{l}$  of 0.25% solution). The encapsulated cells were then cultured in basal MEM $\alpha$  medium at 37°C.

##### 5.2.2.4.1 Cell viability and spreading

500,000 cells/ml MC3T3 cell encapsulated in the two different types of gelatin gels were incubated at 37°C in basal medium for a time course of 21 days and then imaged every 7 days using live/dead viability assay as described in Appendix of Protocols (Section 7.5.2.1).

### **5.2.2.5 Bioactivity of gelatin and modified gelatin**

#### **5.2.2.5.1.1 Western blot analysis**

MC3T3 cells were plated on 10 cm<sup>2</sup> plates (250,000 cells/plate) and grown to 90% confluence in basal media. Cells were serum starved for 6 hours and treated with gelatin or modified gelatin (dissolved in PBS) or with PBS (control) for 15 minutes in serum-free media. For long time-course study, cells were plated at low density (200,000 cells/well) on 6-well plate and grown to 90% confluence in basal media and then treated with gelatin or modified gelatin or with PBS (control) for 21 days in mineralization media. Media and treatments were changed every 3 days. Total protein was lysed from cells and western blot analysis was performed as described in Appendix of Protocols (Section 7.2.2.3).

#### **5.2.2.5.1.2 Alkaline phosphatase activity**

For alkaline phosphatase studies, MC3T3 cells were plated on 24-well plates at a low density (10,000 cells/well) and grown for 1 day in basal media and then treated with gelatin or modified gelatin or with PBS (control) for 14 days in mineralization media (n=4) and samples were analyzed for alkaline phosphatase activity as described in Appendix of Protocols (Section 7.7.2.1).

#### **5.2.2.5.1.3 Mineralization assay**

For mineralization studies, MC3T3 cells were plated on 24-well plates at a low density (10,000 cells/well) and grown for 1 day in basal media and then treated with gelatin or modified gelatin or with PBS (control) for 14 days in mineralization media (n=4) and

samples were analyzed for calcium deposition using Alizarin Red staining method as described in Appendix of Protocols (Section 7.7.2.2).

#### **5.2.2.6 Bioactivity of gelatin gels**

MC3T3 cells (500,000 cells/ml) were encapsulated in 10 mg/ml gelatin gel dissolved in distilled water and were maintained in basal media for 2 days and the immunocytochemistry was used to detect the regulation of Erk phosphorylation and active  $\beta$  catenin. Soluble factors, 30 ng/ml insulin and 10 mM LiCl, were added separately to the medium of gelatin gel-encapsulated cell samples for 2 hours following 2 days incubation period. Immunocytochemistry was performed as described in Appendix of Protocols (Section 7.2.2.5).

#### **5.2.2.7 Statistical data analysis**

All data are presented as mean  $\pm$  SD (standard deviation) for  $n = 3$ , unless stated otherwise. Statistical analyses were performed by t-test, and  $p < 0.05$  was considered statistically significant.

### **5.2.3 Results**

#### **5.2.3.1.1 Synthesis of gelatin-tyramine conjugates**

Figure 56 shows the phenolic content of tyramine modified and unmodified water soluble gelatin as a function of reaction time under the described reaction conditions. The phenolic content of the modified gelatin was approximately four times higher than of the unmodified gelatin. Moreover, under the reaction conditions used, no significant increase in phenolic group was found after 25 minutes of reaction at room temperature.

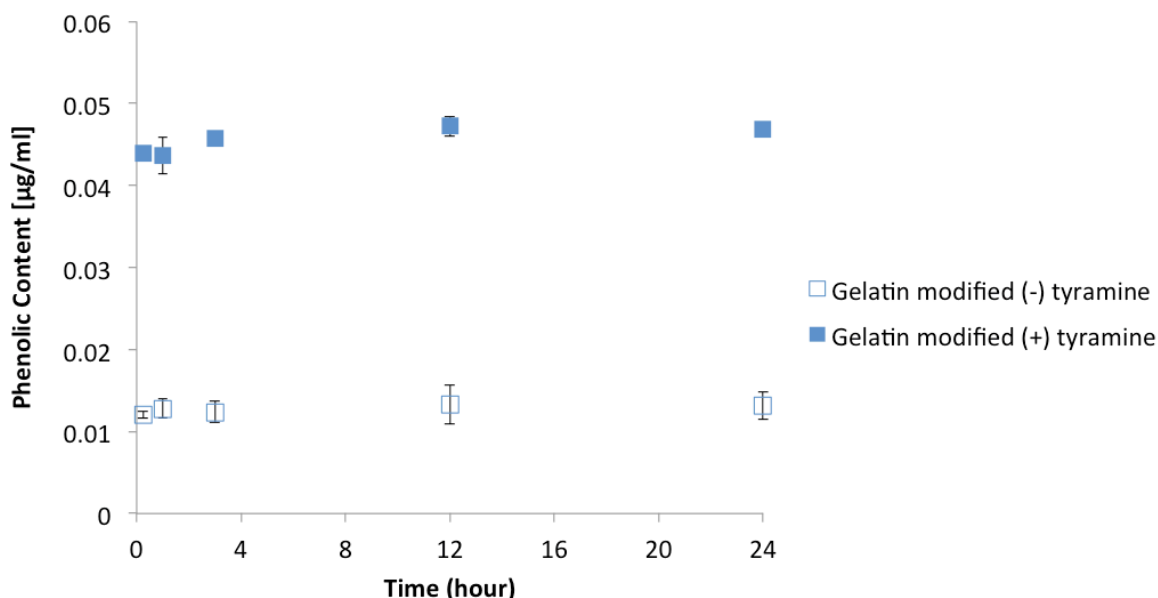


Figure 56. Extent of phenolic group substitution in gelatin as a function of reaction time under the conditions used in the study.

(■) Gelatin treated with tyramine in the presence of EDC; (□) Gelatin treated with EDC in the absence of tyramine.

#### 5.2.3.1.2 Preparation of gelatin gels

The concentrations of the reagents (modified gelatin,  $H_2O_2$  and HRP) play an important role in determining the gelation time as well as the properties of the resulting gel. Irrespective of the concentration of the water-soluble modified gelatin (10-50 mg/ml),  $H_2O_2$  (0.75-2  $\mu$ L of 0.25% w/v stock concentration) and HRP (5-10 U/mL) all the solutions gelled in less than 10 seconds. Unlike rhLF gels discussed in section 5.1.3, the reagent concentrations did not significantly affect the gelation time.

#### 5.2.3.1.3 Morphology

The morphology of flash frozen and lyophilized gels prepared from modified gelatin solutions of different concentrations are shown in Figure 57. The gels formed from 10

mg/ml and 25 mg/ml gelatin solutions presented a macro-porous structure with interconnected pores. Even though both 10 and 25 mg/ml presented a porous microstructure, the average pore width and pore wall thickness was significantly higher in the case of gels formed from 25 mg/ml solution compared to that formed from 10mg/mL (Figure 58). On the other hand, the highest concentration solution (50 mg/ml) presented a dense, less-porous structure. In order to investigate the effect of H<sub>2</sub>O<sub>2</sub> concentration on hydrogel morphology, gels were made from modified gelatin solutions of 50 mg/ml in the presence of different concentrations of H<sub>2</sub>O<sub>2</sub>. Irrespective of H<sub>2</sub>O<sub>2</sub> concentrations, the gels showed a dense less-porous structure at 50 mg/ml concentration. It is presumed that at 50 mg/ml concentration, the pore wall thickness increased to the extent that the matrix collapsed to form a structure with limited porosity.

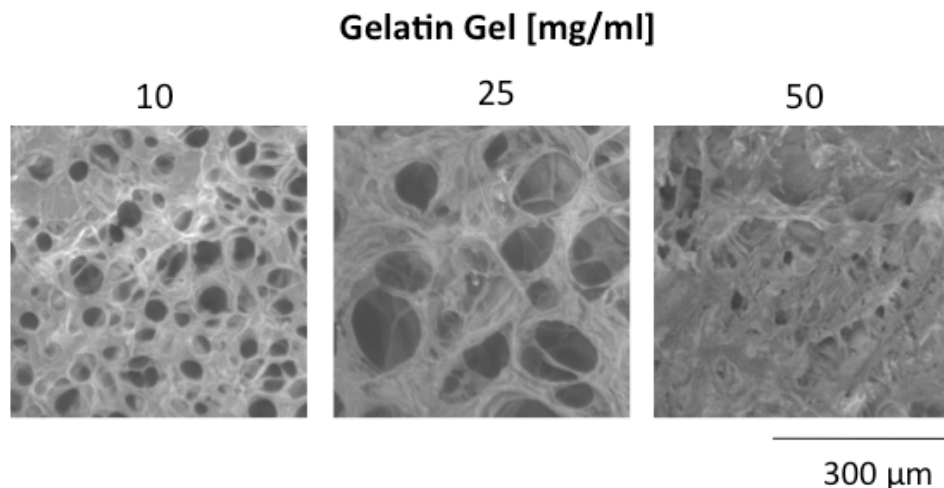


Figure 57. SEM images of 10-50 mg/ml gelatin gels.

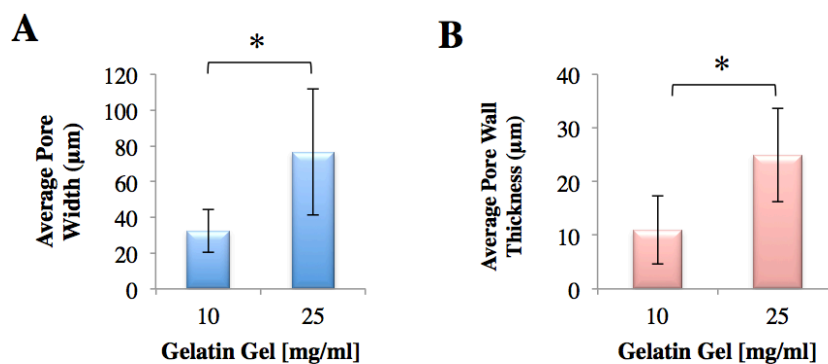


Figure 58. Average pore width and pore wall thickness of gelatin gels.

Gels were formed from solutions of 10mg/ml and 25mg/ml gelatin concentrations. A) Average pore width; B) Average pore wall thickness. \* indicates  $p < 0.05$  statistical significance.

#### 5.2.3.1.4 Rheological Analysis

Storage modulus of gelatin gels (10, 25 and 50 mg/ml) were measured –  $220.88 \pm 25.70$

Pa,  $1579.21 \pm 272.49$  Pa and  $5568.74 \pm 543.48$  Pa, respectively.

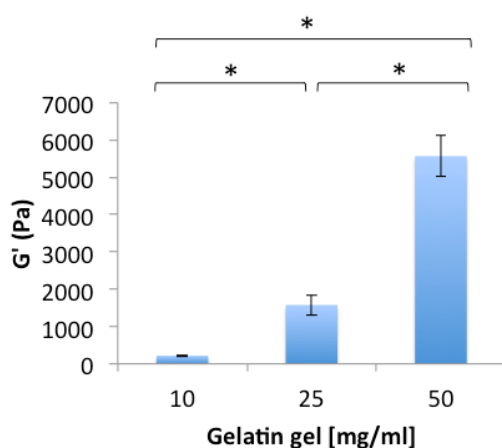


Figure 59. Rheological testing of 10, 25 and 50 mg/ml gelatin gel.

### 5.2.3.2 Cell-Gelatin Interactions

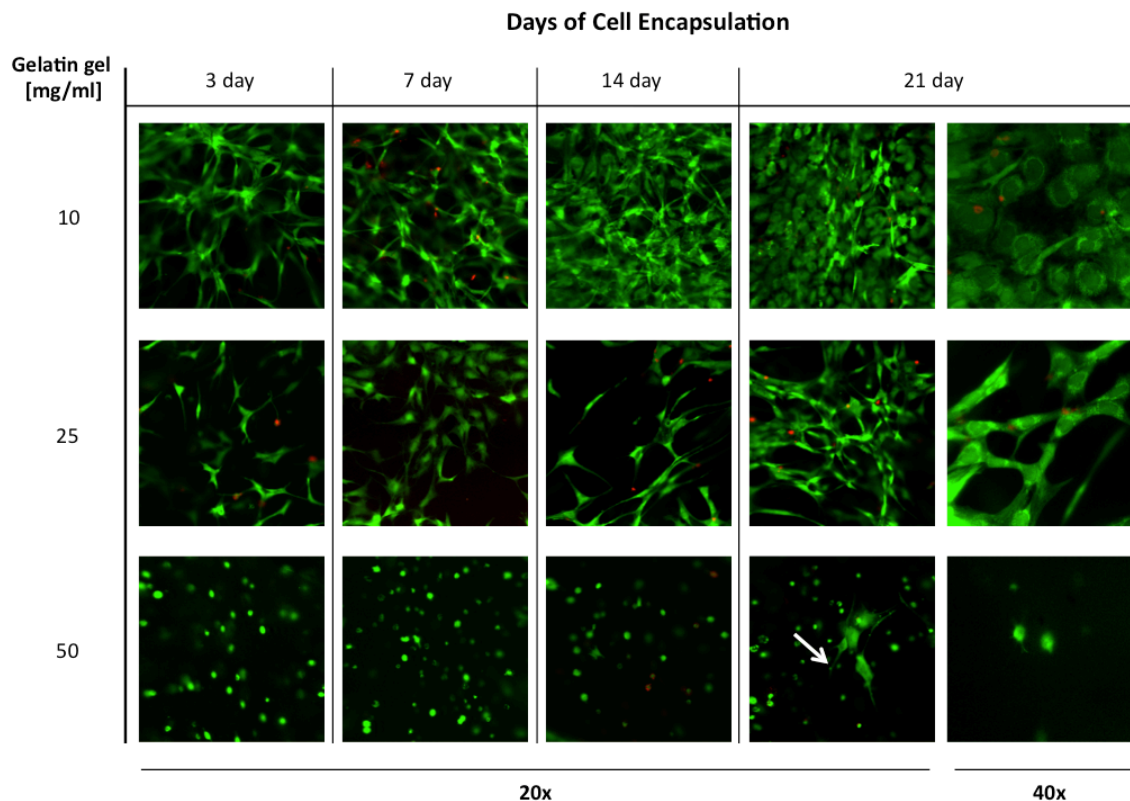
#### 5.2.3.2.1 Cell viability and spreading

In the present study, the effect of modified gelatin concentration on osteoblast viability and spreading in the gels as a function of encapsulation time was investigated. The viability and morphology of MC3T3 pre-osteoblast cells encapsulated in two different gelatin gels of different polymer concentrations and times in basal media are shown in Figure 60 A&B. The viable cells are indicated by green calcein fluorescent labeling and the dead cells by red ethidium homodimer-1 fluorescent labeling. Cell suspension encapsulated in water soluble gelatin gels (Figure 60A) exhibited high viability while the extent of cell spreading was dependent on the gelatin concentration. The MC3T3 cells encapsulated in 10 mg/ml gels with the lowest storage modulus displayed the greatest spreading and number of cells throughout the culture. The gels from 25 mg/ml gelatin also showed good cell spreading with extended filopodia rich morphology while cells encapsulated in 50 mg/ml gelatin had a round morphology with limited spreading throughout the 21 day culture. The increase in storage moduli of the gels prepared at 10, 25, 50 mg/ml gelatin concentrations was presumed to be one of the reasons for the limited spreading and lack of network formation by the cells in 50 mg/ml modified gelatin compared to the 10 and 25 mg/ml compositions. However, cells encapsulated in the 50 mg/ml gels started showing some cell spreading by day 21 (arrow, Figure 60A).

However, since the control gelatin gels were prepared to evaluate the biological activity of LF gel, we developed a modified protocol to develop gelatin gel that can be formed from a water/PBS mixture (similar to the LF gel protocol) and cell pellet was

encapsulated rather than cell suspension. Cell pellet were used in lactoferrin gel encapsulation studies to remove the contribution of FBS in the media which may exhibit some biological activity. The cell pellets encapsulated in gelatin gels prepared from water/PBS mixture also showed good cell viability, however, showed a lack of cell spreading (Figure 60B). Irrespective of the polymer concentration, none of the gels showed the potential of cell spreading over the 21 days culture period studied. Compared to the gelatin gel, cell pellet encapsulated in 10mg/mL of lactoferrin gel under similar culture condition showed good cell spreading within 24 hours.

**A.**





**B.**

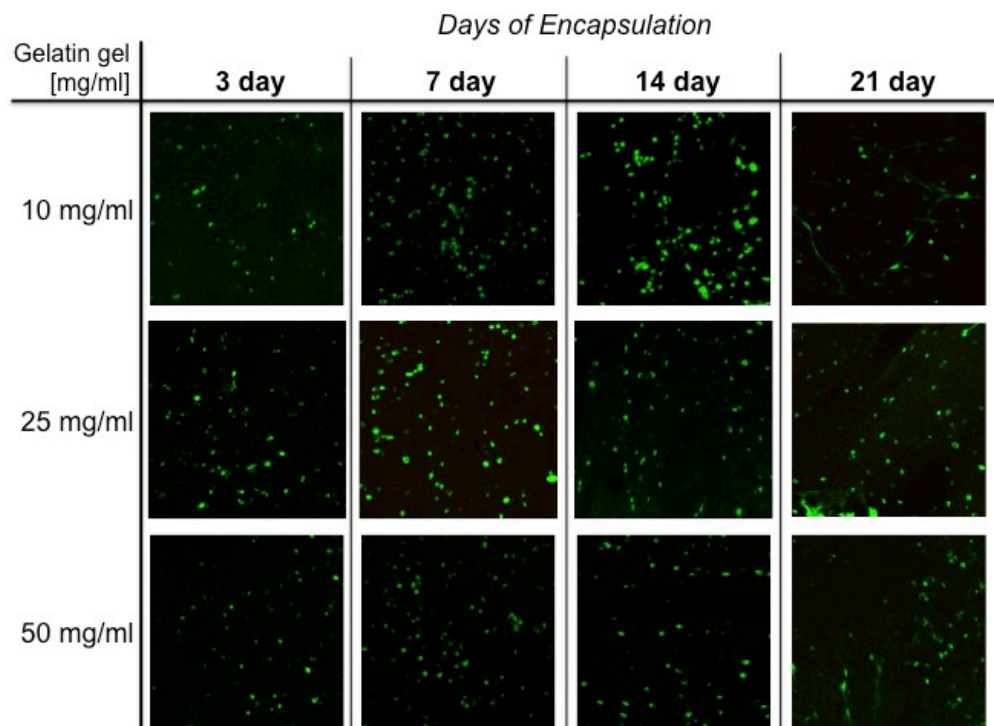


Figure 60. Photomicrographs of MC3T3 cells encapsulated in gelatin gels of different concentrations (10-50 mg/ml) as a function of time. **(A)** Gels prepared by dissolving gelatin in H<sub>2</sub>O. **(B)** Gels prepared by dissolving gelatin in 1:1 H<sub>2</sub>O:PBS solution. Images taken at 20x magnification.

*Cells were stained by a Live/Dead stain: green fluorescence indicating live cells and red fluorescence indicating dead cells.*

#### 5.2.3.2.2 Bioactivity of gelatin and modified gelatin

We probed different functional markers of osteoblasts, such as phosphorylation of Erk, activation of  $\beta$  catenin and phosphorylation of Runx2 after exposing the cells to media, media containing gelatin or media containing water soluble modified gelatin. The western blot analysis using specific phospho-Erk and active  $\beta$  catenin antibodies displayed no differences (Figure 61A) in phosphorylation of Erk or accumulation of active  $\beta$ -catenin in the cell lysate from cultures exposed to gelatin, modified gelatin or

control media. The non-osteogenic activity of the modified gelatin was further confirmed by the expression of Runx2 protein, an osteogenic marker after 21 days in culture in mineralization media (Figure 61B). No significant up-regulation of Runx2 was observed in cells exposed to gelatin or modified gelatin compared to cells given mineralization media alone. These studies clearly demonstrated the lack of inherent osteogenic activity of modified gelatin.

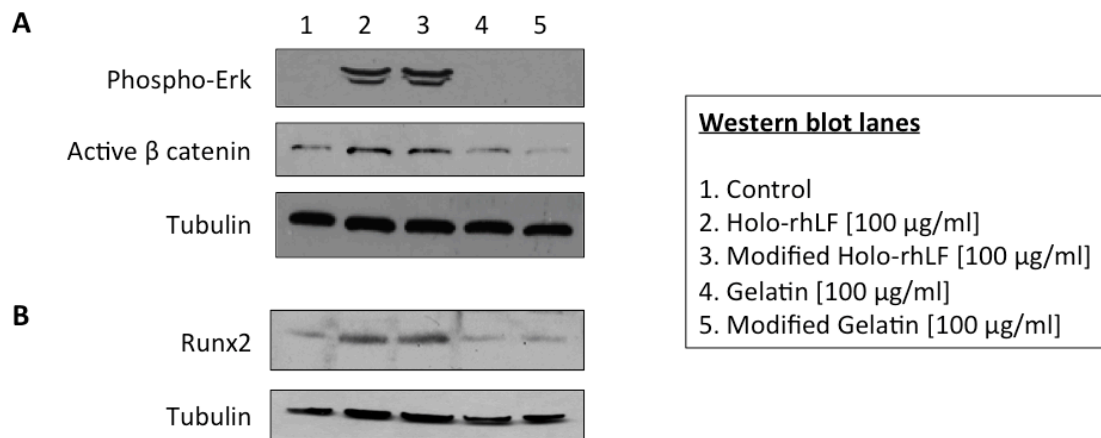


Figure 61. Bioactivity of gelatin and modified gelatin.

(A) MC3T3 cells were stimulated with 100 $\mu$ g/mL gelatin (+), modified gelatin (+\*) or PBS (-) for 15 min in basal media A) or for 21 days in mineralization media B). Anti-tubulin blots were used as loading controls.

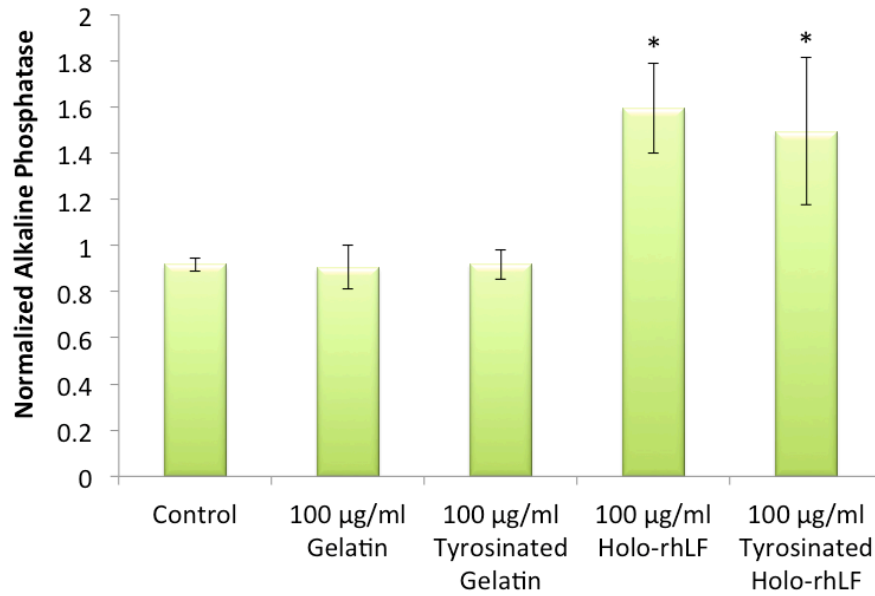


Figure 62. Alkaline phosphatase activity of MC3T3 cells treated with gelatin and holo-rhLF (modified and unmodified).

*Alkaline phosphatase assay was performed on samples maintained in mineralization media for 14 days. Statistical significance ( $p < 0.05$ ) is represented as \* relative to appropriate control.*

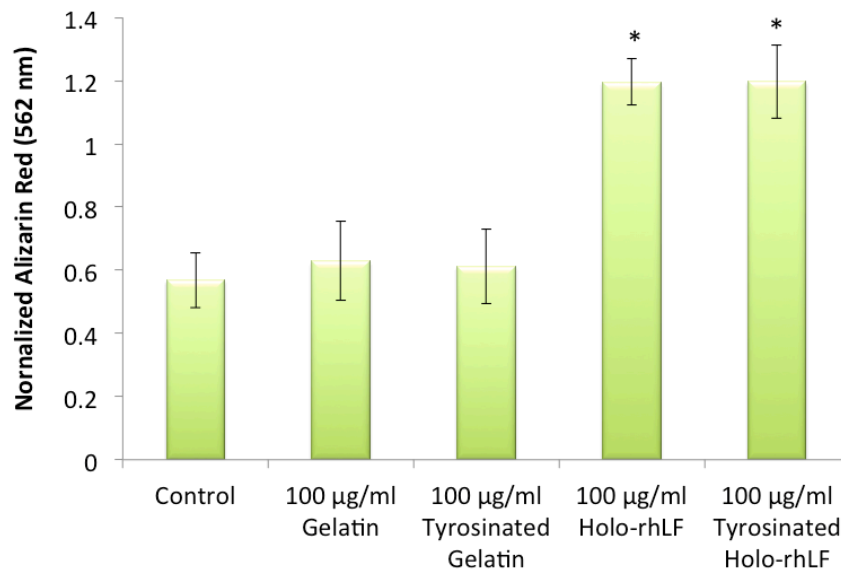


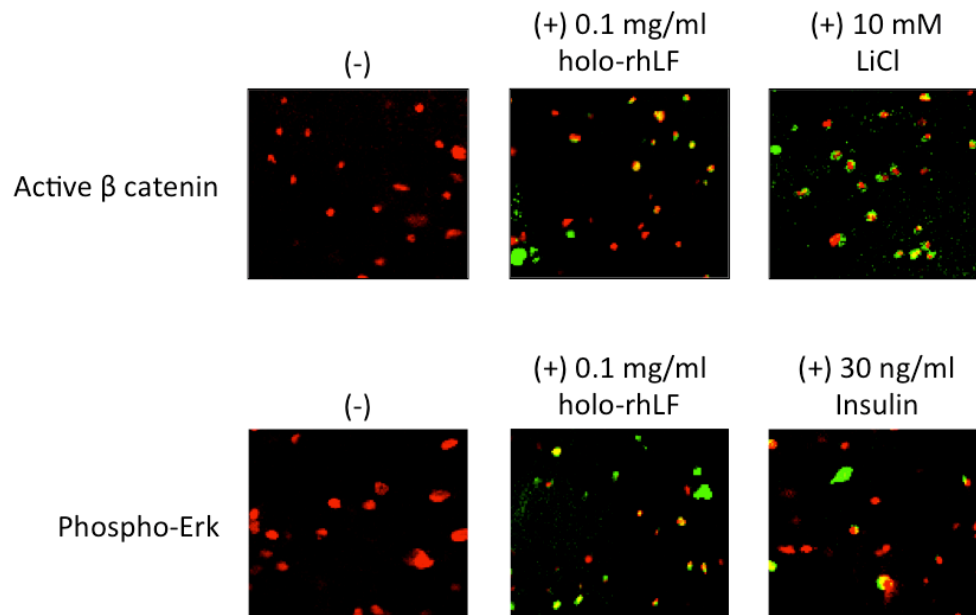
Figure 63. Calcium deposition of MC3T3 cells treated with gelatin and holo-rhLF (modified and unmodified).

*Alizarin red assay was performed on samples maintained in mineralization media for 14 days. Statistical significance ( $p < 0.05$ ) is represented as \* relative to appropriate control.*

#### 5.2.3.2.3 Bioactivity of injectable gelatin gels

We investigated the effect of three-dimensional encapsulation of MC3T3 cells in 10 mg/ml gelatin gel in cellular function by following the collagen I deposition as well as activating intercellular signaling by following the induction of Erk and  $\beta$ -catenin activation using immunocytochemistry. Propidium iodide (red) was used to label the cell nuclei and secondary antibodies were FITC-conjugated (green). Shown in Figure 64 A&B, no positive antibody staining (green) of active  $\beta$  catenin and Erk phosphorylation was observed in the MC3T3 cells encapsulated in water soluble and water/PBS gelatin gels. The addition of soluble molecules, 30 ng/mL insulin and 10 mM LiCl, to the media of the gelatin gel—encapsulated cells, led to the expression of active  $\beta$  catenin and phospho-Erk, after only a 2 day treatment. These studies confirmed that although the enzymatically cross-linked gelatin gel at 10mg/ml supported the adhesion, spreading, proliferation and collagen deposition of MC3T3 cells, the three dimensional organization of the osteoblast cells in the gel did not induce the phosphorylation of Erk or activation of  $\beta$  catenin indicating a lack of inherent osteogenic activity. However, the increased expression of active  $\beta$  catenin and phospho-Erk by the cells cultured in the presence of bioactive molecules indicated that the porous structure of this matrix allowed diffusion of soluble bioactive molecules to activate intercellular signaling pathways in the encapsulated cells.

A.



B.

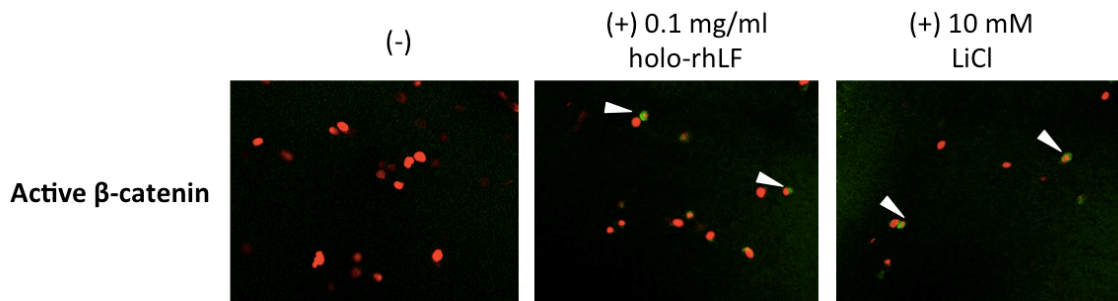


Figure 64. Phosphorylation of Erk in MC3T3 cells encapsulated in 10 mg/ml gelatin gel.

MC3T3 cells were encapsulated in 10 mg/ml gelatin gel and maintained in basal media 2 days. Activation of  $\beta$  catenin and phosphorylation of ERK were probed using immunocytochemistry. FITC-labeled secondary antibodies (green) and propidium iodide (red) were used to detect positive antibody staining and nuclei, respectively. Gelatin gel-encapsulated MC3T3 cells did not express activation of  $\beta$ catenin or phospho-Erk after 2 days of encapsulation (absence of green fluorescence). Positive expression of activation of  $\beta$ -catenin and phospho-ERK occurred after the addition of 10 mM LiCl or 30 ng/mL insulin, respectively, for 2 hours to the medium following 2 day encapsulation of MC3T3 cells in gelatin gel.

A) Gels were prepared by dissolving gelatin in H<sub>2</sub>O B) Gels were prepared by dissolving gelatin in 1:1 H<sub>2</sub>O:PBS solution Images taken at 20x magnification.

#### 5.2.4 Discussion

Gelatin possesses several desirable features for tissue engineering applications such as excellent biocompatibility, biodegradability and low immunogenicity. Standard carbodiimide mediated coupling of amino groups of tyramine with the carboxyl groups of gelatin was used to modify gelatin (Sakai et al. 2009). Natural gelatin contains phenolic amino acids, such as tyrosine, depending on its origin and purity. However, the phenolic content of natural gelatin has been reported to be much lower than what is needed to develop an effectively crosslinked matrix via enzyme-catalyzed coupling. The reaction of gelatin with tyramine or hydroxyphenylpropionic acid enhances polymer cross-linking by increasing the number of phenolic groups in gelatin (Sakai et al. 2009, Hu et al. 2009). Several methods such as colorimetric, spectrophotometric and chromatographic methods can be used to detect the phenolic content of polymers such as gelatin (Cobbett, Kenchington & Ward 1962). In our studies, we detected phenolic concentration of gelatin after tyramine concentration via spectrophotometry. Phenolic content of the modified gelatin increased over 24 hours of reaction time with tyramine.

Pore size and structure of the scaffold has an affect cell performance when cells are seeded on microporous hydrogels. Betz *et al.* cultured human mesenchymal stem cells on a porous hydrogel (100-250  $\mu\text{m}$  pore size) up-regulated BMP2 expression which favored osteogenic differentiation Betz et al. 2010). The viability and proliferation of cells is presumed to be favorably influenced by the microporous structure of the scaffold due to increased nutrient and gaseous permeability (Hwang et al. 2010). The enzymatic crosslinking of 10 mg/ml gelatin gel led to microporous structures of approximately 30  $\mu\text{m}$  pore size, which is sufficient since the average size of an osteoblast is approximately

20-25  $\mu\text{m}$  (Puckett, Pareta & Webster 2008). In our cell encapsulation studies, gelatin gel allowed for high percentage of live to dead cell ratio. However, a decrease in cell spreading and density was seen in the MC3T3 cells encapsulated in 50 mg/ml gelatin gel (relative to 10 and 25 mg/ml holo-rhLF gel). These results may be explained through a variety of different reasons – decrease cell spreading and density due to 1) increased mechanical strength decreasing cell proliferation and spreading or 2) collapsed pore structure adversely affecting the encapsulated cell proliferation and spreading. Although gelatin has cell adhesive domains, several three-dimensional hydrogel matrices developed from gelatin show poor cell viability and spreading (Hoshikawa et al. 2006, Grinnell et al. 2003). Other parameters, including storage moduli and pore structure, may also be playing crucial roles in determining the fate of the encapsulated cells.

Mechanical testing revealed significant storage modulus increases upon increased polymer concentration. The storage moduli of the gelatin gels were measured to range from approximately 200 – 5000 Pa for gelatin polymer concentrations of 10-50 mg/ml. As mentioned previously in section 5.1.4, hydrogel stiffness inversely affected the cell proliferation rates (Wang et al. 2010). Perhaps the significant storage moduli of 50 mg/ml gelatin gel resulted in a decrease proliferation rate of the encapsulated cells.

Unlike porous 10 mg/ml and 25 mg/ml gelatin gels, SEM analysis of the 50 mg/ml gelatin gel revealed a collapsed gel structure. This collapsed structure may not present as a conducive environment for cellular spreading and proliferation of the encapsulated cells. However, cells encapsulated in the 50 mg/ml gels started showing some cell spreading by day 21 (Figure 60). This may be presumably due to some cell

mediated degradation of the matrix, as gelatin has the same biodegradable epitopes as collagen (Atkinson et al. 1992).

Since the modified lactoferrin solutions were made in water/PBS mixture, modified gelatins were prepared that are highly soluble in water/PBS mixture. Cell pellets instead of cell suspension were used for cell encapsulation in LF gels to prevent the potential biological activity of serum in the media. The cell pellets encapsulated in LF gels maintained high cell viability. However, the absence of serum completely prevented cell spreading in gelatin gels. The poor cell spreading observed with higher gelatin concentrations in the previous study (Figure 60A) as well the present study (Figure 60B) can therefore be attributed to the inferior properties of aqueous gelatin solution in the absence of serum. Thus, the lack of cell spreading in gelatin gel presents limitation in using gelatin gels as proper 3D control systems for LF based gels. Future studies need to focus on developing appropriate inert control gels that can support cell adhesion similar to lactoferrin gels to quantitatively evaluate the increase in biological activity of lactoferrin gels.

An ideal cell delivery vehicle should allow for homogeneous mixing of cells within the solution before the sol-gel transition and promote favorable cell-matrix interactions particularly for anchorage dependent cells, such as osteoblasts (Wang, Varshney & Wang 2010). Gelatin is derived from natural extracellular matrix and exhibits a wide range of bioactivity (Alvarez-Perez et al. 2010, Peng et al. 2010). Previous studies report favorable effects of gelatin on cell adhesion. Furthermore, some of the recent studies have indicated that an increase in MC3T3 cell proliferation and differentiation via the activation of the Erk signaling pathway may be induced by gelatin



or chemically/biologically modified gelatin (Lee et al. 2010, Ge et al. 2007). Recently, the ability of gelatin nanostructures to induce Erk activation and the expression of cell adherent molecules, focal adhesion kinase, secreted protein acidic and rich in cysteine (SPARC) and VEGF in MC3T3 cells was reported (Ge et al. 2007). Similarly, the efficacy of micro-porous hydrogels in up-regulating osteogenic signal expression when cells are seeded on the gel was reported (Betz et al. 2010).

Unlike modified LF, our studies did not indicate any increased bioactivity in MC3T3 cells treated with gelatin, tyramine modified gelatin and gelatin gel. We investigated the bioactivity of soluble gelatin and its tyramine-modified form to test whether tyramine modification affects gelatin's bioactivity on MC3T3 cells. In our studies, we probed different functional markers of osteoblasts, including phospho-Erk,  $\beta$  catenin, Runx2, ALP activity and mineral deposition. Our analysis displayed no differences in the regulation of the functional markers from MC3T3 cell cultures exposed to gelatin, modified gelatin or control media (Figure 61). Furthermore, holo-rhLF and tyramine-modified holo-rhLF samples were included in these studies as positive controls. There was no significant difference in bioactivity induced by holo-rhLF and modified holo-rhLF. In summary, this study confirmed positive bioactivity of holo-rhLF and inert bioactivity of gelatin. Moreover, it demonstrated that tyramine modification did not alter the bioactivity of gelatin or holo-rhLF. In our next study, we investigated the bioactivity of gelatin gel-encapsulated MC3T3 cells. No positive expression of our functional markers (phospho-Erk and  $\beta$  catenin) were expressed in the gelatin gel-encapsulated MC3T3 cells. These studies also demonstrated that exogenous bioactive factors such as

insulin, LiCl and LF may be used to increase bioactivity of inert gels. These results demonstrate the applicability of gelatin gel as an inert osteoblast cell delivery vehicle.

### **5.2.5 Conclusions**

Gelatin, an ECM-derived protein, is an excellent candidate for developing cell delivery vehicle due to its biocompatibility and biodegradability. The use of aqueous gelatin solutions in developing enzymatic gels presented limitations in terms of cell spreading. The absence of inherent osteogenic activity of the modified gelatin and gelatin gel indicated the need to include exogenous bioactive molecules to modulate the functions of the encapsulated cells.

## 5.3 Evaluation of the bioactivity of holo-rhLF gel as a novel cell delivery vehicle

### 5.3.1 Introduction

As a highly specialized and complex organ, the skeleton is composed of extensive vasculature, bone cells and mineralized organic matrix. Bone possesses the intrinsic capacity for regeneration and remodeling – a constant formation and resorption of 5-15% total bone mass per year under normal physiological conditions (Davies, Hosseini 2000). Growth factors, cytokines, hormones, bone matrix proteins and mechanical forces act as modulators of essential homeostatic cellular functions, including cell survival, proliferation and differentiation, through the induction of specific cell signaling pathway cascades. The lengthy list of essential signaling molecules during bone regeneration include IL1, IL6, TNF $\alpha$ , TGF $\beta$ , PDGF, BMP, FGF, IGF, MMP, VEGF and angiopoietin (Fernandez-Tresguerres-Hernandez-Gil et al. 2006, Devescovi et al. 2008).

The temporal release of signaling molecules and activation of signaling pathways are responsible for the coordinated biological processes involved in bone regeneration – which include cell mitogenesis, survival and differentiation. Precise regulation of Wnt/ $\beta$ -catenin signaling plays a disparate role in the facilitation of pluripotent mesenchymal stem cell differentiation into osteoblasts and enhancing bone formation (Silkstone, Hong & Alman 2008, Chen et al. 2007). Erk, a member of the MAPK family, is activated by growth factors, such as FGF2, to increase osteoblast proliferation (Chaudhary, Avioli 2000, Lai, Cheng 2002, Xiao et al. 2000). Multiple signaling pathways, including ERK, have been shown to converge and lead to the activation and phosphorylation of osteoblast-specific transcription factor, *Runt-related transcription factor 2* (*Runx2*) (Franceschi et al. 2003), which plays a fundamental role in osteoblast differentiation and

bone formation (Komori 2002). *Runx2* induces osteoblast and chondrocyte differentiation and enhances their migration by coupling with PI3K-Akt signaling (Fujita et al. 2004), which has been implicated as a critical pathway for the differentiation and cell survival of skeletal component cells including chondrocytes, osteoblasts, myoblasts, and adipocytes (Kaliman et al. 1996, Sakaue et al. 1998, Ghosh-Choudhury et al. 2002, Hidaka et al. 2001).

In the case that bone is not able to self heal, bone tissue engineering is needed to regenerate the damaged bone (Rose, Oreffo 2002). Autologous transplantation, the current gold standard procedure for bone repair, holds significant drawbacks including possible donor site morbidity. Tissue-engineering strategies utilize biocompatible scaffolds with specific combinations of cells and bioactive factors (Vaccaro 2002, Carson, Bostrom 2007). Tissue regeneration may be enhanced by the introduction of biochemical signals, in the form of growth factors, cytokines and genetics, which directs cellular responses. However, administration of growth factors also present with significant shortcomings. For example, recombinant human BMP2 (rhBMP2) (Infuse®), the first approved complete bone graft substitute for spinal fusion, presents drawbacks as a regenerative bone factor since the proteins have the propensity to denature, may lead to ectopic bone formation, entail high cost, requires high doses to induce adequate bone formation, and possesses large variations in response among patients (Hawkins 2010).

Due to the multitude of growth factors and cell-cell interactions involved in bone regeneration, scientists have begun to investigate novel bioengineering systems that have the ability to release or bind to multiple growth factors. For example, dual delivery of VEGF and BMP2 from gelatin microparticles for enhanced angiogenesis and

osteogenesis in critical-sized defect bone regeneration (Patel et al. 2008). This multifactorial technique has presented itself with strong limitations including lack of spatial and temporal control of growth factor release from biomaterial scaffold. Thorough testing of the pharmacokinetics of the released agents and elucidation of the efficacy of the carrier systems must be performed on this type of bioengineering approach. Even so, each *in vivo* biological system presents its own individuality. Therefore, even with complete characterization of the bioengineering system, it still may not be fit for different biological systems.

In summary, the current biomaterials systems present a cytocompatible microenvironment to support cell adhesion and growth, they lack specific bioactivities to modulate the host/donor cell functions. Attempts were made to increase their bioactivity by incorporating biological molecules such as growth factors, cytokines and chemokines. However, those approaches also present various limitations. These include issues regarding inability to retain these bioactive molecules at the defect site due to the uncontrolled diffusion of protein from the matrices as well as the inability to present multiple bioactive molecules in a spatial and temporal controlled manner which plays a very important role in achieving optimal regenerative outcome (as described in section 2.1.3.2).

As discussed previously in section 2.1.3.5, cell-based strategies, on the other hand, are raising significant interest lately due to the ease of isolation of autologous mesenchymal stem cells and their ability to undergo osteogenic differentiation. Several other potential cell sources with good regenerative ability are also currently being investigated. Despite encouraging results from extensive preclinical studies on cell-based

bone tissue engineering, key biological and engineering challenges still need to overcome for its successful clinical translation. Some of the critical challenges include poor cell survival and inability to control cellular processes such as proliferation and differentiation due to the inability to present appropriate microenvironment with bioactive molecules to the transplanted cells (as described in section 4.3). Nevertheless, such transient bioactive microenvironments are expected to be necessary for the successful regeneration of functional tissue. Thus, the key for a successful regenerative biomaterial for bone regeneration lies in its ability to interact with the surrounding environment and activate specific cell signaling pathways to support cell survival and functions. LF's influential role in bone morphogenesis has been accredited to its wide array of effects on bone cells – including proliferative and anti-apoptotic actions of osteoblasts and inhibition of osteoclast function (Amini, Nair 2011, Cornish 2004, Cornish et al. 2004, Gonzalez-Chavez, Arevalo-Gallegos & Rascon-Cruz 2009). Based on the unique biological activities of LF, we hypothesize that an injectable biomaterial developed from rhLF will retain its bioactivities (as described in section 4) and will be able to present an artificial microenvironment capable of modulating encapsulated cell functions. The objective of the studies described in this chapter is to evaluate the biological activities of injectable holo-rhLF gel compared to the gelatin gel (which has shown to have no osteoblast-specific bioactivity towards encapsulated cells as discussed in section 5.2 to understand its efficacy as a bioactive cell delivery vehicle. Cellular proliferation analysis methods were investigated in the 2D model using EdU incorporation and Ki67 protein expression. Ki67 protein expression was then used to investigate cellular proliferation in MC3T3 encapsulated cells (3D model).

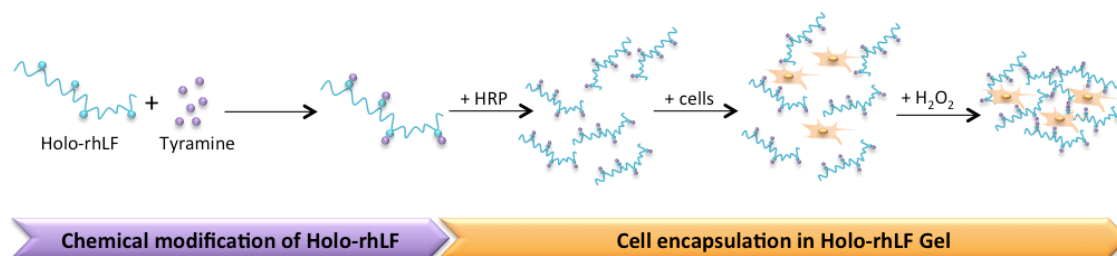


Figure 65. Schematic showing cell encapsulation in holo-rhLF gel.

*Chemical modification of holo-rhLF using standard carbodiimide reaction. Followed by the homogenous mixture of HRP and cells plus H<sub>2</sub>O<sub>2</sub> to yield cell-laden holo-rhLF gel.*

### 5.3.2 Methods

#### 5.3.2.1 Determination of optimal cell seeding density for cell encapsulation in hydrogel

MC3T3 cells of various cell-seeding densities ( $2.5 \times 10^6$  cells/ml,  $1.25 \times 10^6$  cells/ml and  $0.5 \times 10^6$  cells/ml) were encapsulated in 100  $\mu$ l of 10 mg/ml holo-rhLF gel as described in Appendix of protocols (Section 7.9.2.4). Holo-rhLF gel component concentrations: 100  $\mu$ l of 10 mg/ml holo-rhLF gel, 10 U/ml HRP, 0.75  $\mu$ l of 0.25% H<sub>2</sub>O<sub>2</sub>. Cells were then maintained in basal media for 1 day and imaged using live/dead assay as described in Appendix of protocols (Section 7.5.2.1).

#### 5.3.2.2 Mitogenic Activity

##### 5.3.2.2.1 EdU incorporation

MC3T3 cells were plated on glass-bottom tissue culture plates (50,000 cells/plate) and then serum starved for 6 hours. Cells were either untreated (control) or stimulated with holo-rhLF 100  $\mu$ g/ml for 8 hours. Click-it EdU Cell Proliferation Assay was performed as described in Appendix of Protocols (Section 7.6.2.3).

#### 5.3.2.2.2 Protein expression (2D Immunocytochemistry)

MC3T3 cells were plated on glass-bottom tissue culture plates (10,000 cells/plate) for 2 days in basal media and then serum starved for 6 hours. Cells were either untreated (control) or stimulated with holo-rhLF 100 µg/ml for 24 hours. Immunocytochemistry was performed as described in Appendix of Protocols (Section 7.2.2.5).

#### 5.3.2.2.3 Protein expression (3D Immunocytochemistry)

MC3T3 cells (500,000 cells/ml) were encapsulated in 100 µl of 10 mg/ml holo-rhLF gel as described in Appendix of protocols (Section 7.9.2.4). Holo-rhLF gel component concentrations: 100 µl of 10 mg/ml holo-rhLF gel (10 U/ml HRP, 0.75 µl of 0.25% H<sub>2</sub>O<sub>2</sub>). Immunocytochemistry was performed to investigate the phosphorylation of Erk and Ki67 expression as described in Appendix of protocols (Section 7.2.2.5).

#### 5.3.2.2.4 Long term culture of encapsulated cells in the gels

MC3T3 cells (500,000 cells/ml) were encapsulated in 100 µl of 10 mg/ml holo-rhLF gel as described in Appendix of protocols (Section 7.9.2.4). Cells were then maintained in basal media for 20 days and imaged using live/dead assay as described in Appendix of protocols (Section 7.5.2.1).

### 5.3.2.3 Anti-apoptotic effect of rhLF gels

#### 5.3.2.3.1 Serum starvation-induced apoptosis

500,000 cells/ml in 100 µl of 10 mg/ml holo-rhLF and gelatin gel (10 U/ml HRP, 0.75 µl of 0.25% H<sub>2</sub>O<sub>2</sub>). Cells were encapsulated and then grown in basal medium for 24 hours. Cells were then maintained in serum free media to induce apoptosis and imaged using live/dead assay as described in Appendix of protocols (Section 7.5.2.1).



#### 5.3.2.3.2 Protein expression

MC3T3 cells (500,000 cells/ml) were encapsulated in 100 µl of 10 mg/ml holo-rhLF and gelatin gels as described in Appendix of protocols (Section 7.9.2.4). Holo-rhLF gel component concentrations: 100 µl of 10 mg/ml holo-rhLF gel (10 U/ml HRP, 0.75 µl of 0.25% H<sub>2</sub>O<sub>2</sub>). Gelatin gel component concentrations: 100 µl of 10 mg/ml gelatin gel (10 U/ml HRP, 1 µl of 0.25% H<sub>2</sub>O<sub>2</sub>). Immunocytochemistry was performed as described in Appendix of protocols (Section 7.2.2.5).

#### 5.3.2.3.3 Holo-rhLF/ gelatin composite gels

The protocol for the following gel biomaterials is described below: 10 mg/ml gelatin gel + 10 mg/ml holo-rhLF; 10 mg/ml gelatin gel + 10 mg/ml tyrosinated holo-rhLF; and 10 mg/ml holo-rhLF gel + 10 mg/ml tyrosinated holo-rhLF. Encapsulated cells were maintained in basal media for 6 hours and then serum starved for 2 days. Viability was tested using live/dead assay as described in Appendix of protocols (Section 7.5.2.1). Phosphorylation of Akt was examined using immunocytochemistry as described in Appendix of protocols (Section 7.2.2.5).

##### **10 mg/ml gelatin gel + 10 mg/ml holo-rhLF gel**

- To make 1 ml of 10 mg/ml gelatin/HRP solution: dissolve 10 mg modified in 1ml of 10 U/ml HRP (dissolved in H<sub>2</sub>O) and then mix well.
- To make 1 ml of 10 mg/ml holo-rhLF/HRP solution: dissolve 10 mg tyrosinated holo-rhLF in 500 µl of 10 U/ml HRP (dissolved in H<sub>2</sub>O) and then mix well. Add 500 µl of 10 U/ml HRP (dissolved in PBS).

- Mix 50  $\mu$ l of gelatin/HRP solution and 50  $\mu$ l of holo-rhLF/HRP solution. Add 500,000 cells/ml and mix well to a 35 mm glass bottom plate. Next, add 1  $\mu$ l of 0.25%  $H_2O_2$  to gel.

#### **10 mg/ml gelatin gel + 10 mg/ml holo-rhLF (non-tyrosinated)**

- To make 1 ml of 10 mg/ml gelatin/HRP solution: dissolve 10 mg modified in 1ml of 10 U/ml HRP (dissolved in  $H_2O$ ) and then mix well.
- Next, add 10 mg holo-rhLF to gelatin/HRP solution.
- Add 500,000 cells/ml to 100  $\mu$ l gelatin/olo-rhLF/HRP solution and mix well to a 35 mm glass bottom plate. Next, add 1  $\mu$ l of 0.25%  $H_2O_2$  to gel.

#### **10 mg/ml holo-rhLF gel + 10 mg/ml holo-rhLF (non-tyrosinated)**

- To make 1 ml of 10 mg/ml holo-rhLF/HRP solution: dissolve 10 mg tyrosinated holo-rhLF in 500  $\mu$ l of 10 U/ml HRP (dissolved in  $H_2O$ ) and then mix well. Add 500  $\mu$ l of 10 U/ml HRP (dissolved in PBS).
- Next, add 10 mg holo-rhLF to holo-rhLF/HRP solution.
- Add 500,000 cells/ml to 100  $\mu$ l holo-rhLF/HRP solution and mix well to a 35 mm glass bottom plate. Next, add 1  $\mu$ l of 0.25%  $H_2O_2$  to gel.

### **5.3.2.4 Cell differentiation**

#### **5.3.2.4.1 Protein Expression**

500,000 MC3T3 cells/ml were encapsulated in 100  $\mu$ l of 10 mg/ml holo-rhLF gel (10 U/ml HRP, 0.75  $\mu$ l of 0.25%  $H_2O_2$ ) and 100  $\mu$ l of 10 mg/ml gelatin gel (10 U/ml HRP, 7.5  $\mu$ l of 0.025%  $H_2O_2$ ). Cell culture was maintained in basal medium for 1 day and then changed to mineralization media and cultured for 21 days. Immunocytochemistry was performed as described in Appendix of protocols (Section 7.2.2.5).

### 5.3.3 Results

We first tested the optimal cell seeding density for biomaterial encapsulation. MC3T3 cells were encapsulated in 10 mg/ml holo-rhLF gels at densities of 2,500,000 cells/ml 1,250,000 cells/ml and 500,000 cells/ml (Figure 66). Optimal cell seeding density was determined after 24 hours of incubation in basal media using live/dead assay. 500,000 MC3T3 cells/ml allowed for distinct cell imaging and therefore was determined to be the optimal cell seeding density for biomaterial encapsulation for evaluating the expression of transcription factors, growth factors and matrix deposition.

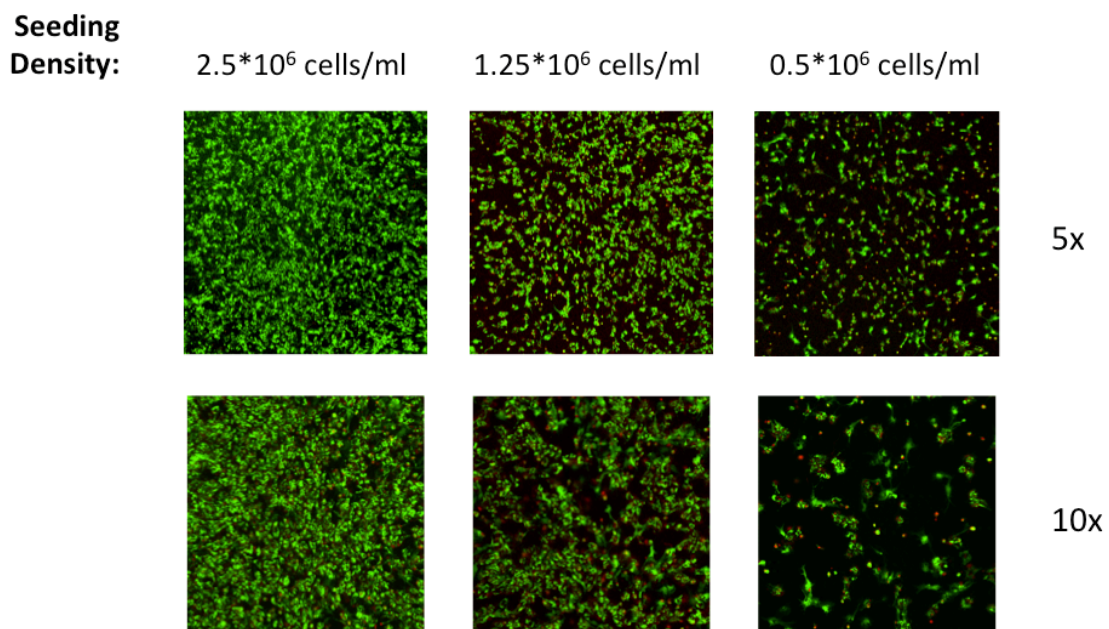


Figure 66. Various cell seeding densities of MC3T3 cells encapsulated in 10 mg/ml holo-rhLF gel.

*Imaged after 24 hours of encapsulation using live/dead assay using confocal microscopy (5x and 10x magnification).*

#### 5.3.3.1 Effect of holo-rhLF and holo-rhLF gel encapsulation on MC3T3 cell proliferation

Previous findings have reported rhLF to increase thymidine incorporation in primary rat osteoblast cultures (Huang et al. 2008). Similarly, our studies demonstrated holo-rhLF to significantly increase MC3T3 and NHOst cell proliferation at concentrations of 100 and 1000  $\mu\text{g/ml}$  (Figure 25). Different proliferation markers, including Ki67, pErk, EdU and thymidine incorporation were used to follow the extent of cell proliferation cultured in the presence and absence of holo-rhLF. We found increased Ki67 protein expression and EdU incorporation by MC3T3 cells significantly increased after 8 hours of rhLF treatment (Figure 67) relative to control. Since one cycle of MC3T3 cell division typically takes 24 hours, we chose to use an earlier time point (8 hours) to visualize cell proliferation rate via EdU incorporation. As seen in top left panel of Figure 67, 100  $\mu\text{g/ml}$  holo-rhLF treatment increased EdU incorporation. Furthermore, p42/p44 Erk phosphorylation and Ki67 expression increased after 24 hours of 100  $\mu\text{g/ml}$  holo-rhLF treatment (bottom left panel of Figure 67, Figure 68). In these immunocytochemistry figures, nuclei (first panel) was stained using propidium iodide (red), protein expression (second panel) was visualized using FITC-label secondary antibodies (green) and the merged/overlayed images are displayed in the third panel – which demonstrates cytoplasmic/nuclear protein localization.

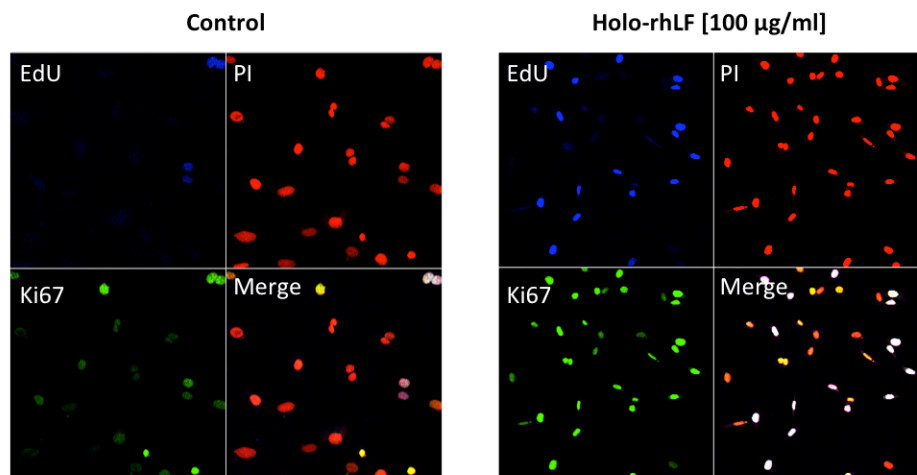
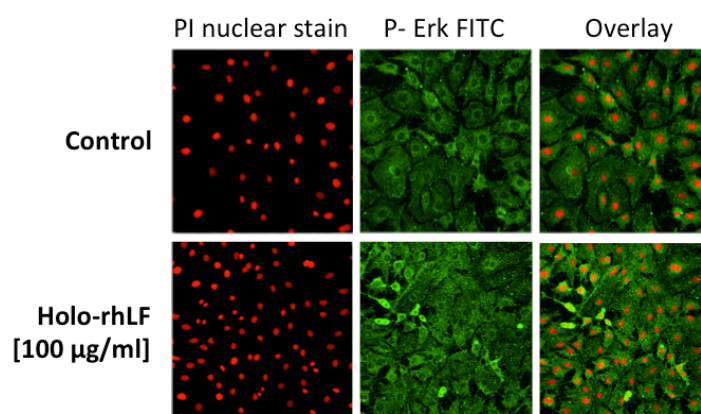


Figure 67. 100 µg/ml holo-rhLF increases EdU incorporation and Ki67 protein expression in MC3T3 cells after 8 hours treatment.

*Cells were treated for 8 hours in culture. The images of EdU incorporation (blue; top left panel), PI nuclei staining (red; top right panel), Ki67 protein expression (FITC-green, bottom left panel) were merged to yield bottom right panel.*



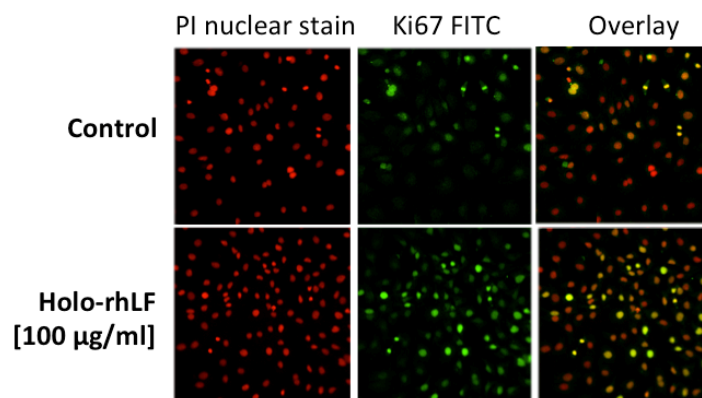


Figure 68. Increased phosphorylation of Erk and increased Ki67 protein expression in MC3T3 cells treated with 100 µg/ml holo-rhLF.

*Cells were treated for 24hours and protein expression was compared relative to untreated control MC3T3 cells. Propidium iodide was used to stain the cell nuclei.*

Figure 69 shows the pERK and Ki67 expression of cells encapsulated in rhLF gels (left panel) and gelatin gels (middle and right panels). As demonstrated in the figure, the proliferative effect of holo-rhLF on MC3T3 cells was retained by the crosslinked gel form. Cell proliferation was counted using live dead assay and Image J program after culturing the cells in the holo-rhLF gel for an extended culture period. 11.2—fold increase of cell number occurred after 20 days of encapsulation in holo-rhLF gel (Figure 70).

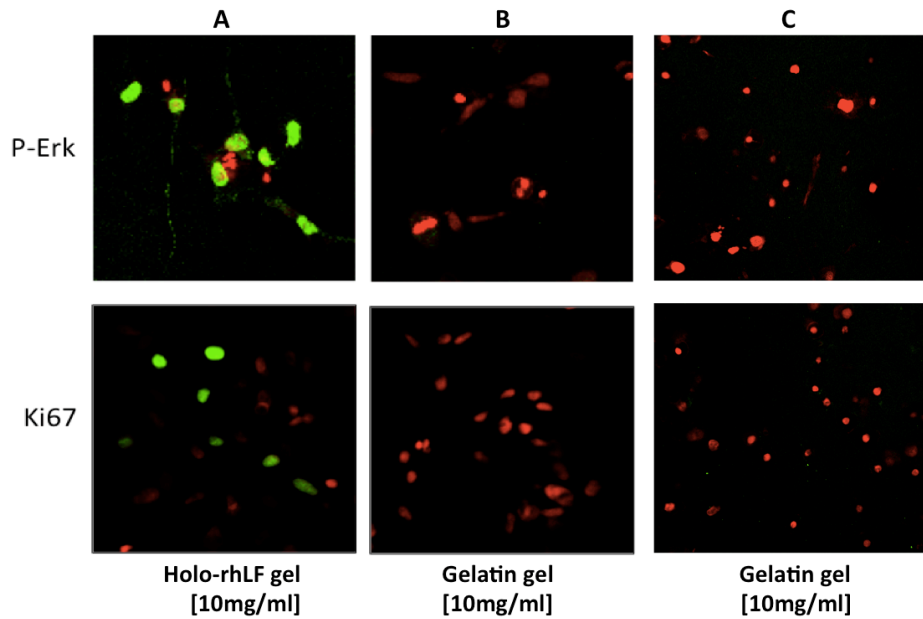


Figure 69. Phosphorylation of Erk and Ki67 expression in **(A)** holo-rhLF gel—encapsulated MC3T3 cells. **(B)** Gelatin gels were dissolved in H<sub>2</sub>O **(C)** Gelatin gels were dissolved in 1:1 H<sub>2</sub>O:PBS solution

*Cells were encapsulated for 2 days in culture. Protein expression was compared to that of gelatin gel—encapsulated cells. Propidium iodide was used to stain the cell nuclei.*

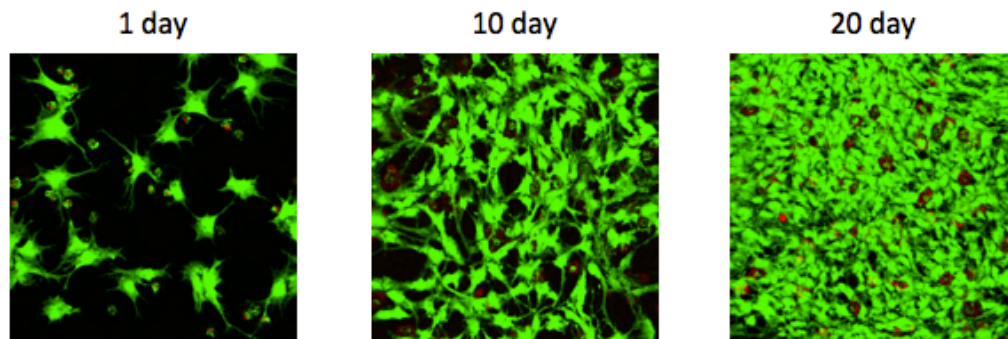


Figure 70. Cell number and h viability of MC3T3 cells encapsulated in 10mg/mL of holo rhLF gels as a function of time.

*Live/dead assay was used to investigate cell viability.*

### 5.3.3.2 Anti-apoptotic effect of holo-rhLF gel

Holo-rhLF gel encapsulated MC3T3 cells demonstrated stimulation of Akt phosphorylation after 2 days, which is a common marker in the survival signaling cascade (Figure 71). P-Akt protein expression of MC3T3 cells-encapsulated in holo-rhLF and gelatin gel was visualized using FITC-labeled secondary antibody (green). Cell nuclei were stained with propidium iodide (red). In the following experiment, we encapsulated MC3T3 cells in holo-rhLF and gelatin gels and then exposed them to serum-free media to investigate the ability of holo-rhLF gel to protect against serum starvation-induced cellular apoptosis. Significant cell survival was seen using live/dead assay in MC3T3 cells encapsulated in holo-rhLF gel after serum starvation for 3 days (Figure 72). After 3 days of serum starvation – induced apoptosis, MC3T3 cells encapsulated in holo-rhLF gel exhibited a 76% live (green) to dead (red) cells.

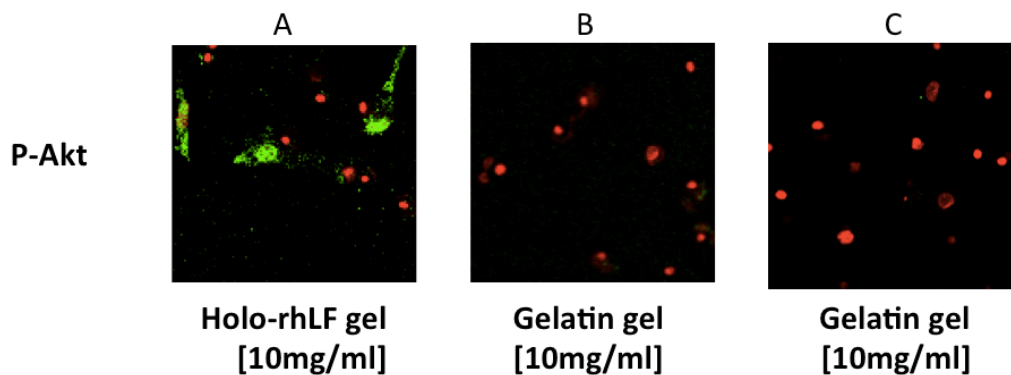
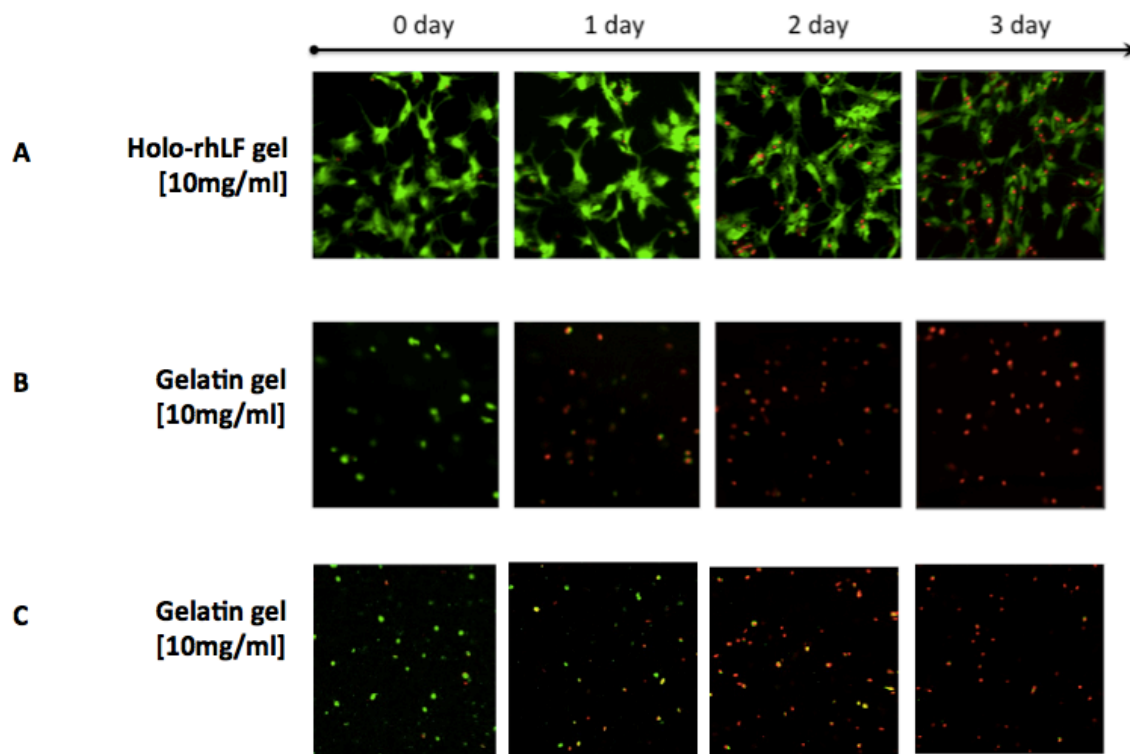


Figure 71. Akt phosphorylation in MC3T3 cells encapsulated in (A) 10 mg/ml holo-rhLF gel. (B) Gels were prepared by dissolving gelatin in H<sub>2</sub>O (C) Gels were prepared by dissolving gelatin in 1:1 H<sub>2</sub>O:PBS solution

*Immunofluorescence testing the phosphorylation of Akt (FITC-labeled secondary antibody) in MC3T3 cells treated with 10 mg/ml holo-rhLF treatment relative to untreated control after 24 hours. Nuclei are stained with propidium iodide.*





*Figure 72. Viability in MC3T3 cells encapsulated in (A) 10 mg/ml holo-rhLF gel during serum starvation. (B) Gels were prepared by dissolving gelatin in H<sub>2</sub>O (C) Gels were prepared by dissolving gelatin in 1:1 H<sub>2</sub>O:PBS solution Images taken at 20x magnification.*

*Live/dead assay was used to investigate cell viability.*

Since a certain number of crosslinking sites are required for crosslinking, the concentration of bioactive may be higher than what is needed for optimal bioactivity. Composite gels of bioactive holo-rhLF and inert gelatin allow manipulation of concentration of bioactive holo-rhLF in the gel encapsulating cells. To test this hypothesis, we made a composite gel of 1:1 ratio of 10 mg/ml tyrosinated holo-rhLF and 10 mg/ml tyrosinated gelatin to yield a 10 mg/ml holo-rhLF/gelatin composite gel which contained only half as much bioactive tyrosinated holo-rhLF protein as pure 10 mg/ml

holo-rhLF gel. In other words, we were able to maintain sufficient crosslinking sites (total polymer concentration) while we decreased the amount of bioactive, tyrosinated holo-rhLF protein by replacing it with inert, modified gelatin. Interestingly, 10 mg/ml holo-rhLF/gelatin composite gel also supported cell survival as visualized by live/dead assay (Figure 73c) and phosphorylation of Akt (Figure 74c) after 2 days of encapsulation. However, the addition of holo-rhLF (non-tyrosinated) to gelatin gel did not support cell survival (Figure 73b) and phosphorylation of Akt (Figure 74b) after 2 days of encapsulation. This observation supports the notion of tyrosination of holo-rhLF increases crosslinking and retention of the bioactive protein surrounding the encapsulated cells.

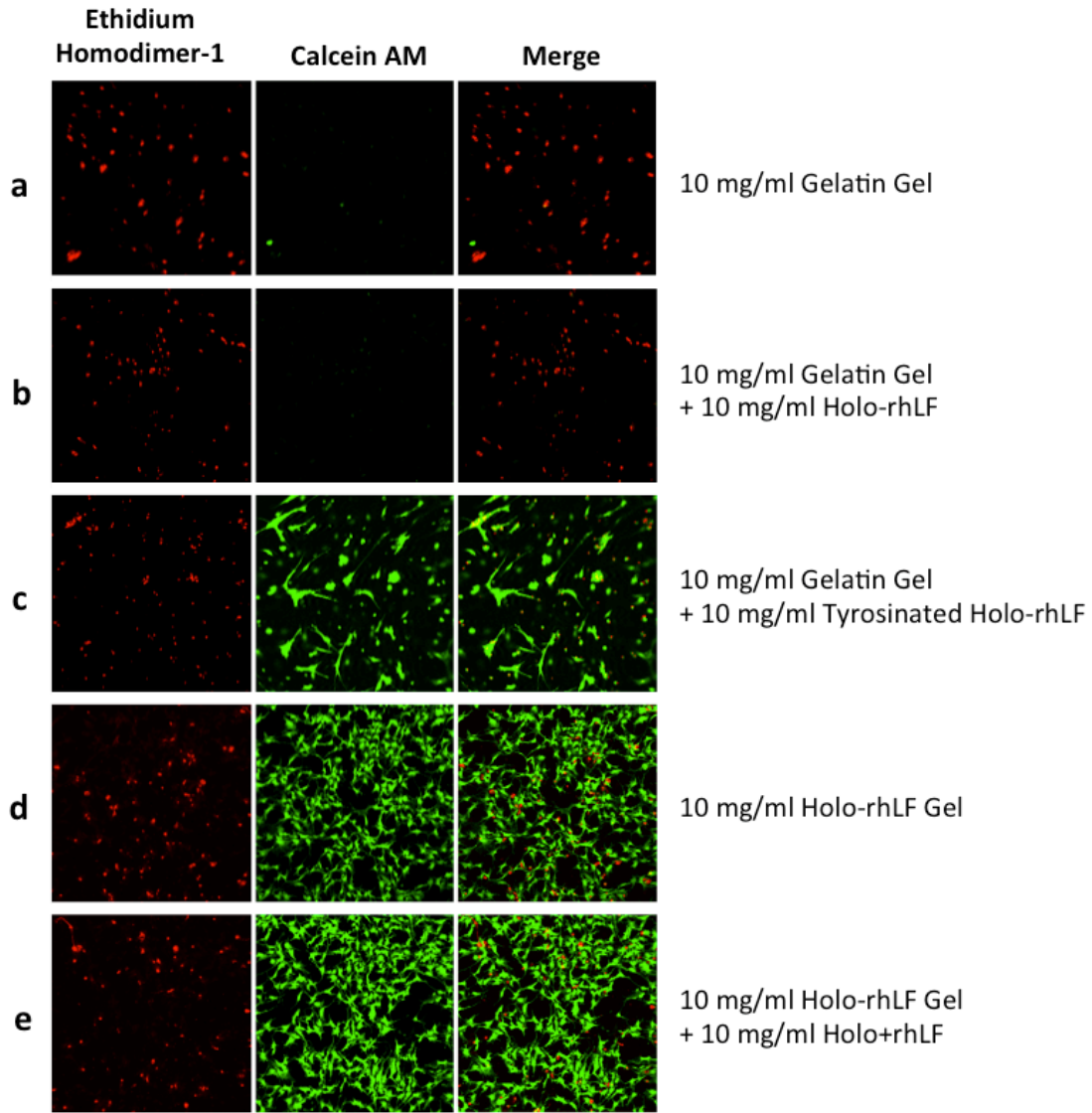


Figure 73. Live/dead assay of serum-starved encapsulated cells in the gels.

*Imaged on day 2 of serum starvation via confocal microscopy (10x magnification). Dead cells (first column) were visualized using ethidium homodimer (red) and live cells (second column) were stained using calcein AM (green). The first and second column images were merged to yield the third column to visualize the live/dead ratio.*

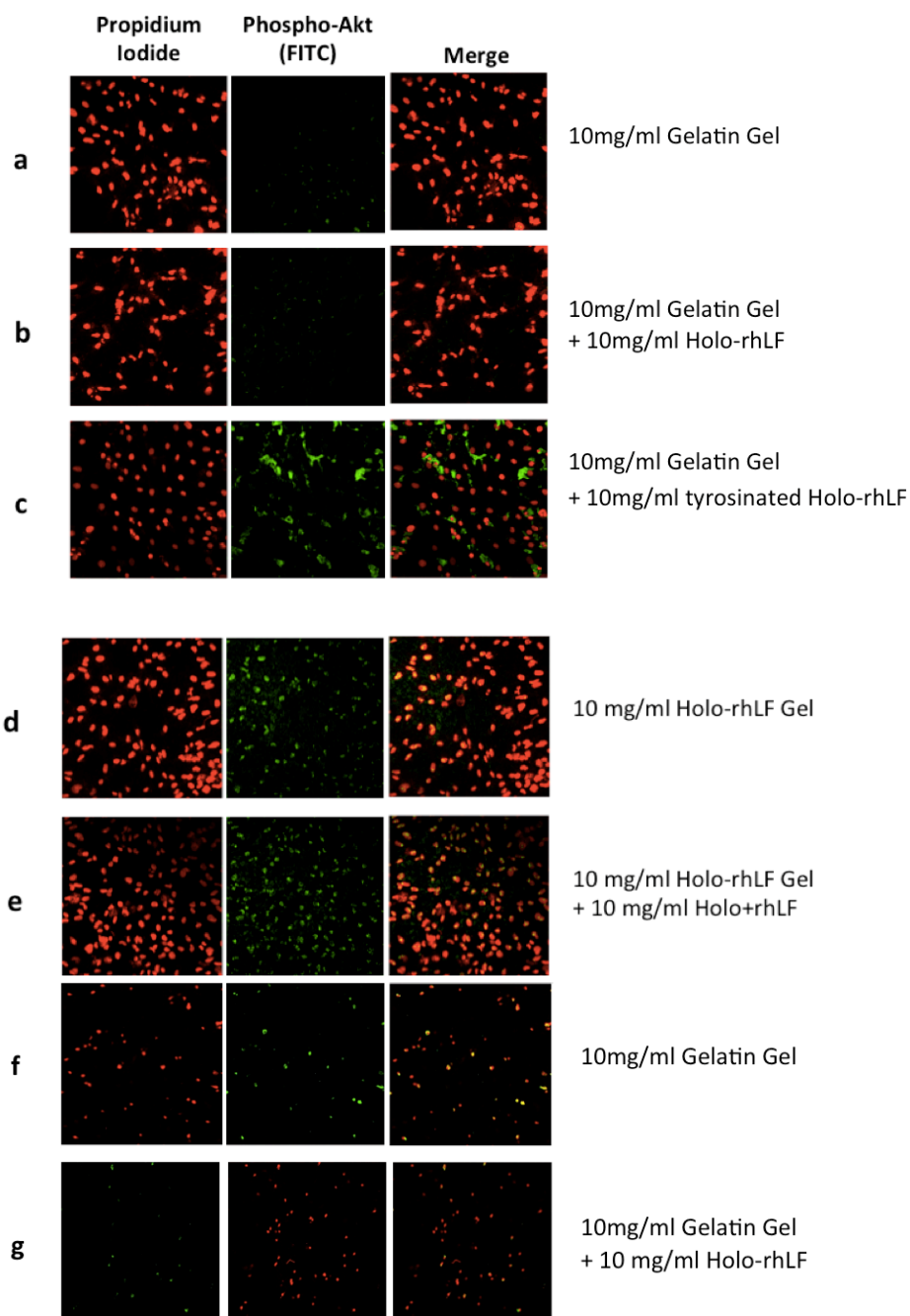


Figure 74. Phospho-Akt expression of serum-starved encapsulated cells in the gels.

*Imaged on day 2 of serum starvation via confocal microscopy (20x magnification). Cell nuclei (first column) were visualized using propidium iodide (red) and pAkt expression (second column) were stained using FITC-labeled antibody (green). The first and second column images were merged to yield the third column to visualize the localization of the pAkt protein expression in the encapsulated MC3T3 cells. (A-C) Gels prepared from gelatin dissolved in H<sub>2</sub>O. (F-G) Gels prepared from gelatin dissolved in 1:1 H<sub>2</sub>O:PBS solution Images taken at 20x magnification.*

### 5.3.3.3 Effect of holo-rhLF gel encapsulation on MC3T3 cell osteogenesis

Holo-rhLF gel biomaterial retained the osteogenic properties of the protein. The activation of  $\beta$  catenin was retained by the gel crosslinked form of holo-rhLF. (Figure 75). Collagen 1 and osteocalcin protein expression (Figure 76) were observed in cells encapsulated in holo-rhLF gel and cultured for 21 days in mineralization media.

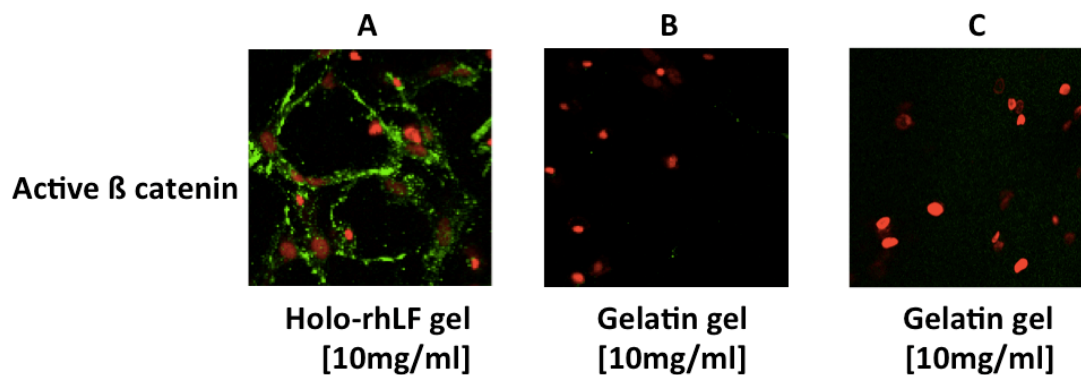


Figure 75. Active  $\beta$  catenin expression in MC3T3 cells encapsulated in (A) 10 mg/ml holo-rhLF gel and gelatin gel. (B) Gelatin gels were dissolved in H<sub>2</sub>O (C) Gelatin gels were dissolved in 1:1 H<sub>2</sub>O:PBS solution Images taken at 20x magnification.

Nuclei are stained with propidium iodide. Cells were encapsulated for 2 days.

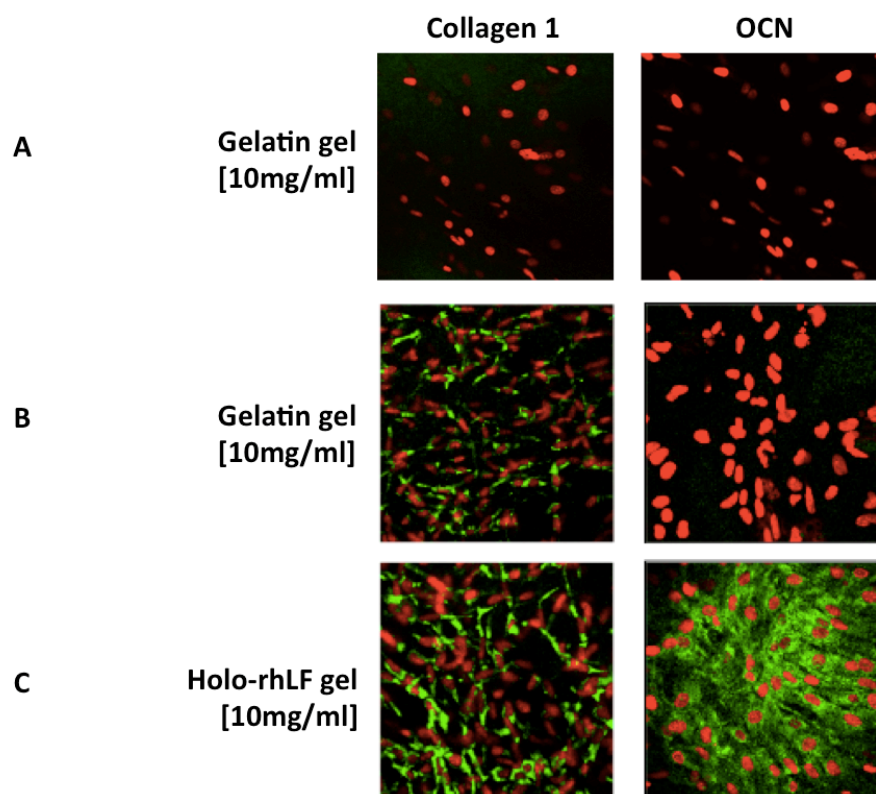


Figure 76. Collagen 1 and OCN expression in MC3T3 cells encapsulated in 10 mg/ml holo-rhLF gel and gelatin gel. A. Gels prepared from gelatin dissolved in 1:1 H<sub>2</sub>O: PBS solution. B. Gels prepared from gelatin dissolved in H<sub>2</sub>O. Images taken at 20x magnification.

*Nuclei are stained with propidium iodide. Cells were encapsulated for 21 days.*

### 5.3.4 Discussion

The challenges of this chapter stemmed from the porous structure of the rhLF biomaterial gel and also the strong affinity of LF to negatively charged molecules. Conventional methods were not selected due to the physical structure and porosity of the gels inhibiting accurate measurements of mineralization and proliferation. Therefore, the methodologies for this aim were selected carefully and took these points in to

consideration. Cellular proliferation was measured via Ki67 and pErk protein expression instead of thymidine incorporation as used in the 2D studies for soluble rhLF treatment on MC3T3 cells. Protein expression of collagen 1 and OCN, two key specific osteogenic markers, were used to evaluate osteogenic differentiation rather than conventional Alizarin Red, which was used for the 2D studies of holo-rhLF on MC3T3 cells. Furthermore, cell number for gel encapsulation was optimized to 500,000 cells/ml of gel since this cell density allowed for distinct cell imaging for evaluating the expression of transcription factors and growth factors.

Based on the previous gel characterization studies (section 5.1), 10 mg/ml holo-rhLF gel concentration was in our biological studies of the gel. This gel concentration yielded a clinically-feasible gelation time of approximately 1 minute. Also, 10 mg/ml holo-rhLF gel allowed for excellent cell spreading and viability and also provided sufficient mechanical strength to serve as an encapsulating cell delivery vehicle.

The mitogenic effects of LF have been clearly reported in our previous studies (Figure 25) and also previously published studies (Huang et al. 2008). However, it was not clear whether the crosslinked matrix would retain the properties of the soluble protein. Since bioactive proteins may activate cellular processes cell internalization or receptor-mediated signal transduction – it is therefore not known if an immobilized polymer, which is incapable of being endocytosed, will be bioactive or not. Grey *et al.* reported that LF internalization by osteoblastic cells is not necessary for activation of mitogenic signaling (Grey et al. 2004). Therefore, we could conclude that the crosslinked matrix has the potential to retain the protein's inherent bioactive activity.

Different proliferation markers, including Ki67, pErk, EdU and thymidine incorporation were used to follow the extent of cell proliferation cultured in the presence and absence of holo-rhLF. Ki67 protein expression is a marker that is expressed by proliferating cells in all phases of active cell cycle (G1, S, G2 and M phase). pErk is a signaling marker that is often seen in proliferating cells. In addition to following mitogenic markers, viable cell number in the gel after long-term culture was followed as a function of time by fluorescent live/dead staining. Our previous data (Figure 25) indicated increased cell proliferation in MC3T3 cells treated with holo-rhLF. Similarly, our long-term culture of the MC3T3 encapsulated cells in holo-rhLF gel demonstrated that this gel presents a conducive microenvironment to promote cell proliferation. This data shows that rhLF gel is mitogenic towards the encapsulated MC3T3 cells and immunocytochemistry is a very good tool to follow the mitogenic activity.

Our previous data demonstrated that holo-rhLF has potent anti-apoptotic effect on MC3T3 cells serum-starved in culture (Figure 31). Cornish *et al.* found pAkt, a common signaling molecule activated during cell survival events, to be increased by LF treatment. However, they also reported that this phosphorylation event is not required for LF-induced cell survival (Grey et al. 2006). In our studies, we discovered that this biological property of holo-rhLF to be dependent on PKA signaling pathway (section 4.3.3.1). Cells encapsulated in holo rhLF gels showed good viability upon serum starvation for 3 days. The cells in gelatin gel however did not show cell survival even at 24 hours. This can be attributed to the lack of biological activity of gelatin as well as the inability of the gel to support cell spreading. Future studies need to compare the



antiapoptotic effect of lactoferrin gels to control gels that allow cell spreading (Figure 72).

To address the question of whether it is the crosslinked holo-rhLF matrix that is showing bioactivity or some remaining/uncrosslinked holo-rhLF we measured the amount of protein that was released (un-crosslinked polymer) from the gel into PBS buffer over 5 days at 37°C (Figure 46). By 5 days, a cumulative amount of 10.1 ng/ml of modified holo-rhLF protein was released in the PBS buffer. However, in Figure 19, we demonstrated that a minimum of 100 µg/ml rhLF was required for statistically significant thymidine incorporation (Cornish et al. 2004). Therefore, we concluded the bioactivity induced in the MC3T3 cells encapsulated in holo-rhLF was a result of the crosslinked matrix not the small amount of un-crosslinked, modified holo-rhLF protein. To further confirm our theory, we designed an experiment where modified and unmodified holo-rhLF was encapsulated in gelatin gel. In this experiment, the modified holo-rhLF became crosslinked in the gelatin gel – forming a bioactive, holo-rhLF/gelatin crosslinked composite matrix. However, the unmodified holo-rhLF was not crosslinked in the gelatin gel and therefore did not induce any bioactivity in the encapsulated MC3T3 cells – as measured by pAkt expression and also live/dead assay upon serum starvation.

After confirming the mitogenic and anti-apoptotic effect of the holo-rhLF gel, attempts were made to understand the osteogenic activity of holo-rhLF. Thus far, no previously published data has revealed any molecular mechanisms underlying LF's osteogenic effects. In our studies, we found LF increases Disheveled/ Gsk3β / β catenin signaling cascade. Furthermore, through inhibitor studies, we discovered LF-induced PKA/LRP6 is responsible for β catenin accumulation. The cells encapsulated in holo

rhLF gels showed a positive expression for  $\beta$  catenin as well as express osteogenic markers – collagen I and OCN – after 21 days culture in osteogenic media.

There is a great need for a bioactive, biocompatible cell delivery vehicle. Furthermore, in the field of orthopedics there no existing biomaterial that provides effective cell delivery, survival, proliferation and increased osteogenesis. Current paradigms in tissue engineering involve the synthesis of novel biomaterials that mimic essential aspects of the physiological niche. Ideally, scaffold design is tailored towards reproducing required signals to foster and direct cellular attachment, proliferation and specific cellular differentiation. To accomplish that several factors must be taken in to account, including the fabrication and implantation of scaffolding material, the physical structures and their biological activity. To date, no studies report cells differentiating into osteogenic lineage without any exogenous soluble differentiation factors using hydrogel biomaterials *in vitro*. As demonstrated in the rpresent study, the enzymatically crosslinked LF gel presents a conducive environment to support cell viability, proliferation and differentiation and support phosphorylation/dephosphorylation of proteins demonstrating a potential avenue for developing cell instructive injectable materials.

### 5.3.5 Conclusions

The proposed studies were aimed to increase our understanding of the effect of holo-rhLF in modulating skeletal cells and further establish holo-rhLF crosslinked gel as an excellent candidate for a skeletal regenerative biomaterial. In our studies, the bioactive holo-rhLF gel matrix is used as a cell delivery vehicle and further promotes cell survival,

proliferation, differentiation and mineralization. The positive effects of holo-rhLF gel on cellular processes supports the notion that holo-rhLF gel is a strong candidate for bone tissue engineering.

## **6 Future studies**

### **6.1 Molecular mechanism underlying LF**

Grey *et al.* confirmed that LRP1 is a mitogenic receptor for LF in osteoblastic cells (Grey *et al.* 2004) and that LF inhibits osteoblast apoptosis via a LRP1-independent pathway (Grey *et al.* 2006). Several questions still remained unanswered such as what pathways are involved in LF's anti-apoptotic effects in osteoblasts. Our recent studies have demonstrated that LF induces PKA-dependent survival in MC3T3 preosteoblast cells. However, the mechanism and receptor by which LF induces PKA is still unknown.

Numerous studies have reported LF's osteogenic effects (Cornish *et al.* 2004). Our studies confirmed the activation of  $\beta$  catenin as it is the penultimate osteogenic signaling molecule. Further investigation revealed that PKA upregulation and LRP6 phosphorylation. Identification of LRP6 as LF's osteogenic receptor should be confirmed through DKK1 inhibitor studies and also knockout model. LRP6-knockout mice develop to term (Kelly, Pinson & Skarnes 2004) and therefore would allow for the investigation of its role in LF's osteogenic induction. Testing of osteogenic differentiation potential of primary osteoblast cells from LRP6 knockout mice by LF would confirm the LF's dependence on LRP6 for osteogenic differentiation.

### **6.2 LF composite gels**

For sufficient number of available crosslinking sites, LF gels required approximately 10 mg/ml of tyrosinated LF. However, in order to study concentration-

dependent effects of LF on the encapsulated cells, lower concentrations of LF should be used. Composite mixture with inert proteins or polymers (ie. gelatin) will allow for the study lower concentrations of crosslinked LF gels. Furthermore, addition of other polymers to LF gel may be used to modify the physical properties such mechanical strength and gelation time.

### **6.3 *Holo-rhLF gel bone regeneration study in vivo***

Maintenance of the skeletal system consists of a dynamic interplay between bone-forming osteoblasts and bone-resorbing osteoclasts. LPS-induced periodontitis models provide an excellent way to study the interactions between immune and bone cells (Yamano et al. 2010). This inflammatory disease ultimately leads to increased osteoclastogenesis and destruction of the periodontium (Clowes, Riggs & Khosla 2005, Weitzmann, Pacifici 2007). LF may affect this model multifold: inhibition of osteoclastogenesis, increased osteoblast activity and inhibition of periodontopathic bacteria growth. We hypothesize that localized LF gel injections will decrease the inflammation and thus inhibit osteoclastogenesis and destruction of the periodontium. Inflammatory markers, such as IL1 $\alpha$  and TNF $\alpha$ , from the saliva may be used to monitor the inflammatory state of the animal model. Alveolar bone levels may be monitored through live x-ray scanner. Calcein green labeling may be used to monitor new bone growth as described previously (Cornish et al. 2004).

## **7 Appendix of Protocols**

### **7.1 Cell culture**

#### **7.1.1 Materials**

- MC3T3-E1 Clone 4 cells (ATCC CRL-2593)
- MEM $\alpha$  medium (Gibco; Grand Island, NY)
- 10% FBS (Gibco; Grand Island, NY)
- 1% Pencillin/Streptomycin (Gibco; Grand Island, NY)
- 2.5% Trypsin/EDTA (Gibco; Grand Island, NY)
- L-ascorbic acid (Fisher Scientific; Pittsburg, PA)
- $\beta$ -glycerophosphate (Sigma-Aldrich; St. Louis, MO)
- Clonetics Normal Human Osteoblasts (NHOst) cells (Lonza; Walkersville, MD)
- Osteoblast Basal Medium (Lonza; Walkersville, MD)
- Single Quots (Lonza; Walkersville, MD)
- ReagentPack Subculture Reagents (Lonza; Walkersville, MD)
- Differentiation SingleQuots (Lonza; Walkersville, MD)
- Bovine LF, native hLF and LiCl (Sigma; St. Louis, MO)
- rhLFs (endotoxin level: <1.5 EU/mg) (InVitria; Fort Collins, CO)
- Gelatin Type A (MP Biomedicals; Solon, OH)
- rhWnt3a, rhWnt5a and rhBMP2 (R&D Systems; Minneapolis, MN)

## **7.1.2 Methods**

### **7.1.2.1 MC3T3 cell culture**

MC3T3-E1 (passages 18-35) were maintained 37°C, 5% CO<sub>2</sub> humidified incubator. MC3T3 cells were plated on 75cm<sup>2</sup> flasks at the recommended density of 5,000 cells/cm<sup>2</sup> with 0.2 ml/cm<sup>2</sup> basal media consisted of MEM $\alpha$  medium supplemented with 10% FBS and 1% Pencillin/Streptomycin. At 80% confluency, the MC3T3 cells were subcultured using 2.5% Trypsin/EDTA. Mineralization media consisted of supplemented MEM $\alpha$  media additionally supplemented with 10  $\mu$ g/ml L-ascorbic acid and 3 mM  $\beta$ -glycerophosphate.

### **7.1.2.2 Human osteoblast cell culture**

Clonetics Normal Human Osteoblasts (NHOst) cells (passages 2-4) were maintained 37°C, 5% CO<sub>2</sub> humidified incubator. NHOst cells were plated on 75 cm<sup>2</sup> flasks at the recommended density of 5,000 cells/cm<sup>2</sup> with 1 ml/ 5 cm<sup>2</sup> Osteoblast Basal Medium supplemented with Single Quots, which includes FBS, Gentamycin and Ascorbic Acid. At 80% confluency, the NHOst cells were subcultured using ReagentPack Subculture Reagents, which includes Trypsin/EDTA, Trypsin Neutralizing Solution and HEPES-BSS. To differentiate the NHOst cells to mineralizing bone cells, the supplemented Osteoblast Basal Medium were further supplemented with Differentiation SingleQuots, which includes Hydrocortisone-21-hemisuccinate (200 nM final concentration) and  $\beta$ -Glycerophosphate (10 mM final concentration).

## 7.2 Protein analysis

### 7.2.1 Materials

- CellLytic M and Protease Inhibitor (Sigma; St. Louis, MO)
- Western blot analysis reagents (BioRad; Hercules, CA)
- BCA Protein Assay Reagent (Peirce; Rockford, IL)
- ReadyPrep Cytoplasmic/Nuclear Protein Extraction kit (Fisher Scientific; Pittsburg, PA)
- Glass bottom culture plates, 35 mm uncoated (MatTek; Ashland, MA)

• Primary Antibodies	Company, Catalog number	Dilution
Phospho-Akt (Ser473)	Cell Signalling 4060	1:1000 (western)
Phospho-p44/42 MAPK (Erk1/2)	Cell Signalling 4370	1:1000 (western)
Phospho-p44/42 MAPK (Erk1/2)	Millipore 05-481	1:100 (immunocytochemistry)
anti-phospho-CREB (Ser133)	Millipore-06-519	1:1000 (western)
LRP1 (5A6)	Santa Cruz sc57351	1:1000 (western)
Phospho-LRP1	Upstate 30628	
LRP5/6 (1A12)	Abcam ab257250	1:1000 (western)
LRP5/6 (1A12)	Santa Cruz sc57354	
Phospho-LRP6	Millipore 07218	1:1000 (western)
VEGF	Santa Cruz sc65617	1:1000 (western)
VEGF	Abcam ab1316	1:100 (immunocytochemistry)
IL6	Abcam ab6672	1:100 (immunocytochemistry)
Phospho-Dishevelled 2	Millipore ab5972	1:1000 (western)
Phospho-Gsk3 $\beta$	Millipore ab05643	1:1000 (western)
$\beta$ catenin	BD 610153	1:2000
Active $\beta$ catenin	Millipore 05-665	1:1000 (western)
Runx2 (C-19)	Santa Cruz sc8566	1:1000 (western)
Runx2	Santa Cruz sc10758	
Runx2	Abcam ab76956	1:100 (immunocytochemistry)
Osteocalcin (FL-95)	Santa Cruz sc30045	1:100 (immunocytochemistry)
Collagen 1	Abcam ab292	1:100 (immunocytochemistry)
Tubulin	Millipore 05661	1:1000 (western)
$\beta$ - actin	Abcam ab8227	1:1000 (western)
Ki67	Abcam ab15580	1:100 (immunocytochemistry)
Anti-Lactoferrin	Santa Cruz SC-14434	1:1000 (western)



Secondary Antibodies		
Goat Anti-Rabbit IgG Conjugate	KPL #474-1516	1:3000 (western)
Goat Anti-Mouse IgG Conjugate	KPL #474-1806	1:3000 (western)
Goat Anti-Rat IgG Conjugate	KPL #474-1612	1:3000 (western)
Donkey Anti-Goat IgG-FITC	Abcam sc-2024	1:200 (immunocytochemistry)
Goat Anti-Rabbit IgG-FITC	Abcam ab6717	1:200 (immunocytochemistry)
Goat Anti-Mouse IgG-FITC	Abcam ab6785	1:200 (immunocytochemistry)

Table 6. Primary and secondary antibodies used for western blot and immunocytochemistry studies.

## 7.2.2 Methods

### 7.2.2.1 Extraction

Media was aspirated from cells and washed briefly with PBS. 500 µl of CellLytic M and Protease Inhibitor at a 1000:1 ratio were added to cells and then incubated at 4°C for 30 minutes. Cells were removed by mechanical scrapping and spun down at 10,000 rpm for 5 minutes.

### 7.2.2.2 Bicinchoninic Acid (BCA) total protein assay

Protein concentrations were measured using BCA Protein Assay Kit. BCA Protein Assay Reagent (Bicinchoninic Acid) contains BCA Reagent A (500 mL), BCA Reagent B (25 ml), Albumin Standard (2 mg/ml). Working BCA reagent was prepared by mixing 50 parts of BCA reagent A with 1 part of BCA reagent B. 10 µl of each unknown sample or standard (i.e., diluted with 1% Triton X100 solution) was pipette to a 96 well plate. 90 µl of the working reagent was then added to each well and plate was mixed thoroughly. The absorbance of the samples were measured at 562 nm after 30 minute incubation at 37°C. BSA standards were calculated according to Table 7.

Vial	Volume of diluent (μl)	Volume & Source of BSA	Final BSA concentration
A	450	150 μl of stock	500 μg /ml
B	300	300 μl of A	250 μg /ml
C	300	300 μl of B	125 μg /ml
D	360	240 μl of C	50 μg /ml
E	300	300 μl of D	25 μg /ml
F	320	80 μl of E	5 μg /ml
G	400	0	blank

Table 7. Diluted albumin (BSA) standards.

### 7.2.2.3 Western blot analysis

Each sample was prepared with Laemmli Sample Buffer and samples were boiled for 5 minutes. 25 μg of each sample were run on 4-15% Tris-HCl Ready Gels for western blot protein electrophoresis. Mini-PROTEAN Tetra System, 10x Tris/Glycine/SDS Buffer, Precision Plus Protein Dual Color Standard were used and gels were run at a constant 100 Volts. Gels were transferred at a constant 100 Volts for 2 hours using 10x Tris/Glycine Buffer, Mini Trans-Blot Electrophoresis Transfer Cell, Blot Papers and 0.2 μm Nitrocellulose Membrane. Membranes were blocked for 2 hours at 4°C in 10% milk/TBS-T solution (10x Tris-Buffered Saline, 0.1% Tween-20). Membranes were washed with TBS-T solution after each incubation. Membranes were incubated overnight with primary antibodies diluted in 5% milk/TBS-T solution at 4°C. Next, membranes were incubated for 45 minutes with secondary antibody diluted in 5% milk/TBS-T solution at 4°C and then washed three times with TBS-T. List of primary and secondary antibodies used for western blot are contained in Table 6. Super Signal West Pico Chemiluminescent Substrate was used for detection, and CL-XPosure Film was used for exposure of the membranes.

#### 7.2.2.4 Nuclear/ cytoplasmic protein extraction

ReadyPrep Cytoplasmic/Nuclear Protein Extraction kit enabled the stepwise separation and preparation of cytoplasmic and nuclear extracts from cell samples. Cells were harvested with trypsin-EDTA and then centrifuged at  $500 \times g$  for 5 minutes. Cells were washed by suspending the cell pellet with PBS.  $1-10 \times 10^6$  cells were transferred to a 1.5 mL microcentrifuge tube and pelleted by centrifugation at  $500 \times g$  for 2-3 minutes. A pipette was used to carefully remove and discard the supernatant, leaving the cell pellet as dry as possible. This protocol was scaled depending on the cell pellet volume and the volume ratio of CER I: CER II: NER reagents was maintained at 200:11:100  $\mu\text{L}$ , respectively (

Packed cell volume ( $\mu\text{L}$ )	CER I ( $\mu\text{L}$ )	CER II ( $\mu\text{L}$ )	NER ( $\mu\text{L}$ )
10	100	5.5	50
20	200	11	100
50	500	27.5	250
100	1000	55	500

Table 8).

Packed cell volume ( $\mu\text{L}$ )	CER I ( $\mu\text{L}$ )	CER II ( $\mu\text{L}$ )	NER ( $\mu\text{L}$ )
10	100	5.5	50
20	200	11	100
50	500	27.5	250
100	1000	55	500

Table 8. Reagent volumes for different packed cell volumes.

Ice-cold CER I was added to the cell pellet. The tube was vigorously vortexed on the highest setting for 15 seconds to fully suspend the cell pellet and then incubated on ice for 10 minutes. Ice-cold CER II was added to the tube and then vortexed for 5 seconds on the highest setting, followed by 1 minute incubation on ice. Samples were centrifuged for 5 minutes at maximum speed in a microcentrifuge ( $\sim 16,000 \times g$ ). The supernatant

(cytoplasmic extract) was then transferred to a clean pre-chilled tube and samples were placed stored at -80°C until use. The insoluble (pellet) fraction, which contains nuclei, was suspended in ice-cold NER and vortex on the highest setting for 15 seconds. The samples were placed on ice and continued vortexing for 15 seconds every 10 minutes, for a total of 40 minutes. The samples were then centrifuged at maximum speed ( $\sim 16,000 \times g$ ) in a microcentrifuge for 10 minutes. The supernatant (nuclear fraction) was then immediately transferred to a clean pre-chilled tube and stored at -80°C until use.

#### 7.2.2.5 Immunocytochemistry

Cells were cultured on sterile glass bottom culture plates, 35 mm uncoated. Washed briefly with PBS and then fixed using -10°C methanol for 5 minutes. Next, methanol was aspirated and allow to air dry. Samples were washed in three changes of PBS. Sufficient reagent was used to cover the specimen (approximately 200  $\mu$ l per slide). Samples were incubated in 10% normal blocking serum in PBS for 20 minutes to suppress non-specific binding of IgG. Blocking serum ideally should be derived from the same species in which the secondary antibody is raised and then washed with PBS. Next, the samples were incubated with primary antibody overnight in 1% normal blocking serum. Washed with three changes of PBS for 5 minutes each. Incubated in dark chamber for 45 minutes with fluorochrome-conjugated secondary antibody diluted to in PBS with 1% normal blocking serum and washed with three changes of PBS. List of primary and secondary antibodies used for immunocytochemistry are contained in Table 6. Mounted coverslip with Vectashield Mounting Medium with Propidium Iodide (nuclear stain) and imaged via confocal microscopy.

## **7.3 Gene expression analysis**

### **7.3.1 Materials**

- Clontech Sprint RT Complete cDNA synthesis kit (Clontech; Mountain View, CA)
- BioRad MyiQ2 Two-Color Real-Time PCR Detection System, 2x iQ real-time PCR Supermix (BioRad; Hercules, CA)
- TaqMan® Gene Expression Assay Probes (Applied Biosystems; Carlsbad, CA)
- Microseal 96-Well PCR Plates (BioRad; Hercules, CA)
- Illumina TotalPrep RNA Amplification Kit (Ambion, Carlsbad, CA)
- Illumina MouseWG-6 v2.0 Expression BeadChip (Ambion, Carlsbad, CA)

### **7.3.2 Methods**

#### **7.3.2.1 RNA extraction and purification**

RNeasy Mini RNA Isolation kit was used to isolate and purify the RNA. Cells were first disrupted by adding Buffer RLT and removed by mechanical scrapping. Lysate was homogenize for 30 seconds using a rotor–stator homogenizer. 1 volume of 70% ethanol was added to the homogenized lysate, and mixed well by pipetting and then added to an RNeasy spin column placed in a 2 ml collection tube and centrifuged for 15 seconds at  $\geq 8000 \times g$ . Flow-through was discarded. 700  $\mu$ l Buffer RW1 was added to the RNeasy spin column and then centrifuged for 15 seconds at  $\geq 8000 \times g$  to wash the spin column membrane. Flow-through was discarded. 500  $\mu$ l Buffer RPE was added to the RNeasy spin column and samples were centrifuged for 15 seconds at  $\geq 8000 \times g$  to wash the spin column membrane. Flow-through was discarded. 500  $\mu$ l Buffer RPE was added to the RNeasy spin column and centrifuged for 2 min at  $\geq 8000 \times g$  to wash the spin column

membrane. RNeasy spin column was placed in a new 1.5 ml collection tube. 30–50  $\mu$ l RNase-free water was added directly to the spin column membrane and centrifuged for 1 minute at  $\geq 8000 \times g$  to elute the RNA.

#### **7.3.2.2 Real time PCR analysis**

For cDNA synthesis, 2  $\mu$ g total RNA was used as a template for Clontech Sprint RT Complete cDNA synthesis kit in a total volume of 20  $\mu$ l. For quantitative real time PCR, BioRad MyiQ2 Two-Color Real-Time PCR Detection System, 2x iQ real-time PCR Supermix, TaqMan® Gene Expression Assay Probes were loaded in Microseal 96-Well PCR Plates. Each well contained 10  $\mu$ l of iQ real-time PCR Supermix, 1  $\mu$ l of TaqMan® Gene Expression Assay probe and 9  $\mu$ l of diluted cDNA. Threshold cycle values of target genes was standardized against GAPDH expression and normalized to the expression in the control culture. The –fold change in expression was calculated using the  $\Delta\Delta C_t$  comparative threshold cycle method.

#### **7.3.2.3 Microarray analysis**

Three biological replicates were tested for each sample (n=3). Illumina TotalPrep RNA Amplification Kit was used for RNA amplification. RNA Nano Chip on Agilent 2100 Bioanalyzer was used to detect quality of RNA and labelled cRNA. Samples were hybridized to Illumina MouseWG-6 v2.0 Expression BeadChip. The multi-sample format includes 45,200 transcripts and six samples simultaneously on a single BeadChip, which dramatically increases throughput while decreasing experimental variability. The MouseWG-6 beadchip exhibits a dynamic range of  $> 3$  logs; detectable fold change  $< 1.35$  fold and reproducibility CV  $< 10\%$ . The ratio of the signal intensity of each

experimental sample and the signal intensity of untreated control was represented as the fold change relative to control.

#### **7.3.2.4 Mouse Wnt signaling pathway array**

Quantitative real time PCR was employed to assess the influence of the 100 µg/ml holo-rhLF (n=3) on Wnt signaling pathway in MC3T3 preosteoblast cells. Total RNA was isolated using the Qiagen RNeasy Mini Kit according to the manufacturer's instructions. For cDNA synthesis, 2 µg total RNA was used as a template for Clontech Sprint RT Complete cDNA synthesis kit in a total volume of 20 µl. BioRad MyiQ2 Two-Color Real-Time PCR Detection System was utilized to measure expression profiles of 84 genes related to WNT-mediated signal transduction on cells treated with of holo-rhLF relative to untreated control. The RT<sup>2</sup> Profiler™ PCR Arrays includes built-in positive control elements for the proper normalization of the data, for the detection of genomic DNA contamination, for the quality of RNA samples, and for general PCR performance.

### **7.4 Cell Imaging**

#### **7.4.1 Materials**

Alexa Fluor 488 phalloidin (Molecular Probes; Grand Island, NY)

#### **7.4.2 Methods**

##### **7.4.2.1 Cell morphology**

##### **7.4.2.1.1 Actin staining via Alexa Fluor 488 phalloidin**

Cells were cultured on sterile glass bottom culture plates, 35 mm uncoated (MatTek P35G-1.0-14-C). Washed briefly with PBS and then fixed using 4% paraformaldehyde for 30 minutes at 37°C. Next, aspirate and rinse with PBS. Incubate samples in 0.1%

Triton X-100 in PBS for 3 to 5 minutes. Wash two or more times with PBS. Samples were then stained with Alexa Fluor 488 phalloidin to visualize the actin filaments. To prepare the stock solution of Alexa Fluor 488 phalloidin, the vial was dissolved in 1.5 mL methanol to yield a final concentration of 200 units/mL, which is equivalent to approximately 6.6  $\mu$ M. When staining with any of the fluorescent phallotoxins, dilute 5  $\mu$ L methanolic stock solution into 200  $\mu$ L PBS for each coverslip to be stained. To reduce nonspecific background staining with these conjugates, add 1% bovine serum albumin (BSA) to the staining solution. Place the staining solution on the coverslip for 20 minutes at room temperature in dark incubator. Wash two or more times with PBS. Image via confocal microscopy (excitation/emission: 495nm/518nm).

#### 7.4.2.1.2 Nuclear staining via propidium iodide

To stain the nuclei, mount coverslip with Vectashield Mounting Medium with Propidium Iodide (nuclear stain) and image via confocal microscopy (excitation/emission: 535 nm/ 617 nm).

## 7.5 *Cell survival and viability*

### 7.5.1 Materials

- Live/Dead Viability/Cytotoxicity Kit (Molecular Probes; Grand Island, NY)
- CaspACE assay (Promega; Madison, WI)

### 7.5.2 Methods

#### 7.5.2.1 Live/Dead Viability assay

Samples were stained using Live/Dead Viability/Cytotoxicity Kit to test viability of the cells. 2  $\mu$ M calcein AM and 4  $\mu$ M Ethidium homodimer-1 was added to PBS. The



polyanionic dye calcein was used since it is well retained within live cells, producing an intense uniform green fluorescence in live cells (excitation/emission: 495 nm/ 515 nm). EthD-1 was included since it enters cells with damaged membranes and undergoes a 40-fold enhancement of fluorescence upon binding to nucleic acids, thereby producing a bright red fluorescence in dead cells (excitation/emission: 495 nm/ 635 nm). Zeiss LSM 510 Confocal Microscope was utilized to image the samples.

#### **7.5.2.2 Colorimetric CaspACE assay**

CaspACE assay was used to measure the activity of caspase-3, a member of the cysteine aspartic acid-specific protease family. Grow cells on 10cm tissue culture plates to 90% confluence. Add serum-free media to MC3T3 cells as a positive (induced apoptosis) control. For inhibited apoptosis samples, add the Z-VAD-FMK inhibitor to the cells (final concentration of 50  $\mu$ M). Prepare negative controls using untreated cells. Incubate overnight at 37°C in a humidified, 5% CO<sub>2</sub> atmosphere. Cells were harvested by centrifugation at 450 x g for 10 minutes at 4°C. Keep the cell pellet on ice. Wash 1X with ice-cold PBS, and resuspend in Cell Lysis Buffer at a concentration of 10<sup>8</sup> cells/ml. Lyse cells by freeze-thaw, then incubate on ice for 15 minutes (repeat freeze thaw cycles as needed to ensure complete cell lysis). Cell lysates were centrifuged at 15,000 x g for 20 minutes at 4°C, and the supernatant fraction was collected. Caspase-3 activity was measured in cell extracts from at least 1 x10<sup>6</sup> cells/assay. Cell extracts were used as an enzyme source. In a flat-bottom, clear polystyrene 96-well plate 20  $\mu$ l of cell extract (75  $\mu$ g total protein) was added to each reaction. Prepare replicate wells (n=3) containing blank (no cell extract), negative control (extract from untreated cells), induced apoptosis (extract from induced cells) and inhibited apoptosis (extract from induced, inhibitor-

treated cells) samples (according to Table 9). Add 2 µl of DEVD-pNA Substrate (10mM stock) to all wells. Samples were incubated at 37°C overnight and then the absorbance was read at 405 nm.

	Blank	Negative Control	Induced Apoptosis	Inhibited Apoptosis
<b>Caspase Assay Buffer</b>	32 µl	32 µl	32 µl	32 µl
<b>DMSO</b>	2 µl	2 µl	2 µl	2 µl
<b>DTT, 100 mM</b>	10 µl	10 µl	10 µl	10 µl
<b>Untreated cell extract</b>	-	20 µl	-	-
<b>Induced apoptosis extract</b>	-	-	20 µl	-
<b>Inhibited apoptosis extract</b>	-	-	-	20 µl
<b>Deionized water to final volume</b>	98 µl	98 µl	98 µl	98 µl

Table 9. Caspase assay control sample preparation.

## 7.6 Proliferation assays

### 7.6.1 Materials

- Click-it EdU Cell Proliferation Assay Kit (Invitrogen; Carlsbad, CA)
- MTS assay (Promega; Grand Island, NY)

### 7.6.2 Methods

#### 7.6.2.1 MTS assay

Cells were plated at a density of 15,000 cells/well in a 48-well plate with basal media. After 24 hours, treatments were administered at various concentrations (n=4 biological replicates). The proliferation of MC<sub>3</sub>T<sub>3</sub> cells was determined by MTS assay. 1000 µl of culture medium was incubated with 200 µl of Cell Titer 96 AQueous One Reagent for 2 hours at 37°C and the absorbance was measured at 492 nm.

#### 7.6.2.2 Thymidine incorporation

Cells were plated and then incubated at 37°C for 6 hours to allow proper cell adhesion and maintained in serum-free medium overnight. The cell culture was then performed with supplementation of treatments and [<sup>3</sup>H]thymidine for 24 hour incubation (n=4 biological replicates). Incorporation of [<sup>3</sup>H]thymidine radioactivity was counted for 30 seconds in a liquid scintillation counter and expressed as disintegrations per minute (dpm) per microgram of DNA. Data was then normalized to untreated control sample and expressed as fold change over control.

#### 7.6.2.3 EdU incorporation

Click-it EdU Cell Proliferation Assay Kit protocol involves 4 main steps: preparation of stock solutions, EdU labeling, EdU detection and counter nuclear staining.

##### 7.6.2.3.1 Preparation of stock solutions

10 mM stock solution of EdU (Component A) was prepared by adding 2 mL of DMSO (Component C) to EdU (Component A). Next, a working solution of the Alexa Fluor® azide (Component B) was prepared by adding 70 µL of DMSO (Component C) to Component B. A working solution of 1X Click-iT® EdU reaction buffer (Component D) was prepared by diluting the 4 ml of Component D to 36 ml of deionized water. A 10X stock solution of the Click-iT® EdU buffer additive (Component F) was made by adding 2 mL of deionized water to the Component F vial.

##### 7.6.2.3.2 EdU labeling

Cells were cultured on sterile glass bottom culture plates, 35 mm uncoated and allow cells to adhere for 6 hours in basal media. 2X working solution of EdU (Component A) was prepared in serum free basal media from the 10 mM stock solution. A suggested

starting concentration is 10  $\mu$ M. An equal volume of the 2X EdU solution was added to the volume of serum free basal media containing cells to be treated to obtain a 1X EdU solution (final EdU concentration = 10  $\mu$ M). Concurrently, we added 0 or 100  $\mu$ g/ml holo-rhLF to the cell cultures. The time of EdU exposure to the cells allowed for direct measurement of cells synthesizing DNA. After incubation, media was removed and 1 mL of 3.7% formaldehyde in PBS was added to each sample and incubated for 15 minutes at room temperature. Next, the fixative was removed and the cells were washed well twice with 1 mL of 3% BSA in PBS. Next, 1 mL of 0.5% Triton® X-100 in PBS was added to each well and incubated at room temperature for 20 minutes.

#### 7.6.2.3.3 EdU detection

First, 1X Click-iT® EdU buffer additive was prepared by diluting the 10X solution 1:10 in deionized water. Click-iT® reaction cocktail was prepared according to Table 10. Click-iT® reaction cocktail was used within 15 minutes of preparation (as recommended).

Reaction components	Number of samples						
	1	2	4	5	10	25	50
1x Click-iT reaction buffer	430 $\mu$ l	860 $\mu$ l	1.8 mL	2.2 mL	4.3 mL	10 mL	21.4 mL
CuSO <sub>4</sub>	20 $\mu$ l	40 $\mu$ l	80 $\mu$ l	100 $\mu$ l	200 $\mu$ l	500 $\mu$ l	1 mL
Alexa Fluor azide	1.2 $\mu$ l	2.5 $\mu$ l	5 $\mu$ l	6 $\mu$ l	12.5 $\mu$ l	31 $\mu$ l	62 $\mu$ l
Reaction buffer additive	50 $\mu$ l	100 $\mu$ l	200 $\mu$ l	250 $\mu$ l	500 $\mu$ l	1.25 ml	2.5 ml
Total volume	500 $\mu$ l	1 ml	2 ml	2.5 ml	5 ml	12.5 ml	25 ml

Table 10. Click-iT reaction cocktails.

Permeabilization buffer was removed and the cells were washed twice with 1 mL of 3% BSA in PBS. Remove the wash solution. Next, 0.5 mL of Click-iT® reaction

cocktail was added to each sample and incubated for 30 minutes at room temperature, protected from light. The reaction cocktail was removed and then the samples were washed with 1 mL of 3% BSA in PBS.

#### **7.6.2.3.4 Counter DNA stain**

Samples were covered with Vectashield Mounting Medium with Propidium Iodide (nuclear stain) and image via confocal microscopy (excitation/emission: 535/617nm). Alexa Fluor® 647 EdU staining may be image via confocal microscopy (excitaton/emission: 650/670 nm).

### **7.7 Cell differentiation assays**

#### **7.7.1 Materials**

- Alkaline Phosphatase Substrate Kit (BioRad; Hercules, CA)

#### **7.7.2 Methods**

##### **7.7.2.1 Alkaline phosphatase assay**

Alkaline phosphatase activity was determined using the Alkaline Phosphatase Substrate Kit. In this assay, the early phenotypic marker ALP, from osteoblasts in culture, converts p-nitrophenyl phosphate (p-NPP) into p-nitrophenol (p- NP). The rate of p-NP formation is directly proportional to the ALP activity and can be measured colorimetrically.

At the end of each timepoint, the samples were washed twice with PBS to remove any unattached cells. The samples then incubated in 1% Triton X100. For a volume of 100  $\mu$ L of cell lysate, a 400  $\mu$ L of p-NPP substrate solution and buffer mixture was added and incubated at 37 °C for 30 min. The reaction was stopped by adding 500  $\mu$ L of 0.4 N

NaOH. Subsequently, the ALP induced p-NP production can be estimated by measuring the absorption at 405 nm the TECAN. The results of ALP activity was normalized to the total protein content (i.e., BCA assay) from each individual sample.

#### **7.7.2.2 Alizarin red (Calcium staining)**

Calcium deposition was determined using Alizarin Red staining.

Reagents were first prepared as follows.

**4 M Alizarin Red** –1.369 grams of alizarin red powder dye was dissolved in 100 ml of DD1 H<sub>2</sub>O; 1 N NaOH was used to adjust pH to 4.32

**10mM Na<sub>2</sub>PO<sub>4</sub>** –0.142 grams was dissolved in 100ml H<sub>2</sub>O

**10% (w/v) Cetylpyridinium Chloride (CPC)** –10 grams was dissolved in 100ml of 10mM Na<sub>2</sub>PO<sub>4</sub>; 1N HCl was used to adjust pH to 7.0

Mineralized matrix synthesis was analyzed with Alizarin Red staining method for calcium deposition. This technique used a colormetric analysis based on stabilizing the red matrix precipitate with Cetylpyridinium Chloride (CPC) to yield a purple solution. Briefly, the protocol is as follows: cells were rinsed twice with PBS- to remove any unattached cells and then fixed with 70% ethanol for 1 hour at 4°C. Ethanol was then removed and cells were air-dried and then rinse with DDI water. Cells were then incubated with 4 M Alizarin Red for 10 minutes at room temperature. Samples were wash five times with DDI water and then incubated with 10% CPC for 15 minutes at room temperature. Sample absorbance was read at 562 nm.

### **7.8 Signalling pathway probing**

#### **7.8.1 Materials**

- H-89 (Cell Signaling; Danvers, MA)

- LY294002 (Cell Signaling; Danvers, MA)
- DKK1 (R&D Systems; Minneapolis, MN)

## 7.8.2 Methods

### 7.8.2.1 Pharmacological pathway inhibitors

Cells were pretreated with pharmacological inhibitors (10  $\mu$ M LY294002, 30  $\mu$ M H-89 or 100 ng/ml DKK1) for 2 hours and then stimulated with treatment of choice for 24 hours.

### 7.8.2.2 Wnt signalling array

\*See above protocol section 7.3.2.4.

## 7.9 Biomaterial studies

### 7.9.1 Materials

- 2-(N-morpholino) ethanesulfonic acid (MES) buffer (Sigma-Aldrich; St. Louis, MO)
- *N*-(3-Dimethylaminopropyl)-*N'*-ethylcarbodiimide hydrochloride (EDC) (Sigma-Aldrich; St. Louis, MO)
- *N*-Hydroxysuccinimide (NHS) (Sigma-Aldrich; St. Louis, MO)
- Tyramine (Sigma-Aldrich; St. Louis, MO)
- Standard Regenerated Cellulose Dialysis Tubing MWCO 10,000 (Spectrum Labs; Rancho Dominguez, CA)
- UV-Vis Spectrophotometer (Thermo Scientific Evolution 60)
- 100U/ml HRP (Sigma-Aldrich; St. Louis, MO)
- 30% H<sub>2</sub>O<sub>2</sub> (Sigma-Aldrich; St. Louis, MO)
- PBS (Gibco; Grand Island, NY)

- ARES-LS Parallel plate rheometer (TA Instruments; New Castle, DE)
- JEOL 6335 Field Emission Scanning Electron Microscope (JEOL; Peabody, MA)

## 7.9.2 Methods

### 7.9.2.1 Formation of protein crosslinked hydrogels

#### 7.9.2.1.1 Synthesis of protein-tyramine conjugates

LF-tyramine conjugates were synthesized by a carbodiimide/active-ester coupling reaction. 500 mg protein was dissolved in 50 ml of 1 M MES buffer. To this solution, 500 mg of EDC, 150 mg NHS and 300 mg tyramine were added. The mixture was allowed to react for 24 hours at room temperature under gentle stirring. The modified polymer was purified by dialysis against excess deionized water using Standard Regenerated Cellulose Dialysis Tubing MWCO 10,000. Following dialyzation to remove unreacted tyramine, EDC, NHS, the remaining solution was subsequently frozen at -20°C and then lyophilized to give LF-tyramine conjugates.

Water soluble gelatin-tyramine conjugates were synthesized by the carbodiimide/active-ester coupling reaction. 500 mg protein was dissolved in 50 ml of 1 M MES buffer. To this solution, 500 mg of EDC, 150 mg NHS and 300 mg tyramine were added. The mixture was allowed to react for 24 hours at room temperature under gentle stirring. The modified polymer was purified by dialysis against excess deionized water using Standard Regenerated Cellulose Dialysis Tubing MWCO 10,000. Following dialyzation to remove



unreacted tyramine, EDC, NHS, the remaining solution was subsequently frozen at -20°C and then lyophilized to give the water soluble gelatin-tyramine conjugates.

Water/PBS soluble gelatin-tyramine conjugates were also synthesized by the carbodiimide/active-ester coupling reaction. 875 mg protein was dissolved in 55 ml of 1 M MES buffer and 20 mL of H<sub>2</sub>O. To this solution, 510 mg of EDC, 150 mg NHS and 510 mg tyramine were added. The mixture was allowed to react for 24 hours at room temperature under gentle stirring. The modified polymer was purified by dialysis against excess deionized water using Standard Regenerated Cellulose Dialysis Tubing MWCO 10,000. Following dialyzation to remove unreacted tyramine, EDC, NHS, the remaining solution was subsequently frozen at -20°C and then lyophilized to give gelatin-tyramine conjugates.

#### *7.9.2.1.1 Quantification of tyramine modification*

Protein was modified with varying reaction times and tyramine concentration was then examined as a function of reaction time. Tyramine concentration was measured at 275 nm using UV-Vis Spectrophotomer. A tyramine standard curve was used to determine the concentration of a tyramine in the modified bLF samples (Figure 77). Standard curve stock was made by diluting 10.5 mg tyramine in 2 ml MES buffer (n = 4 biological replicates). 0 - 40 µl of standard curved stock was diluted in increments of 5 µl further in 900 µl MES buffer (n=4) and diluted samples were measured by spectrophotomer at 275 nm.

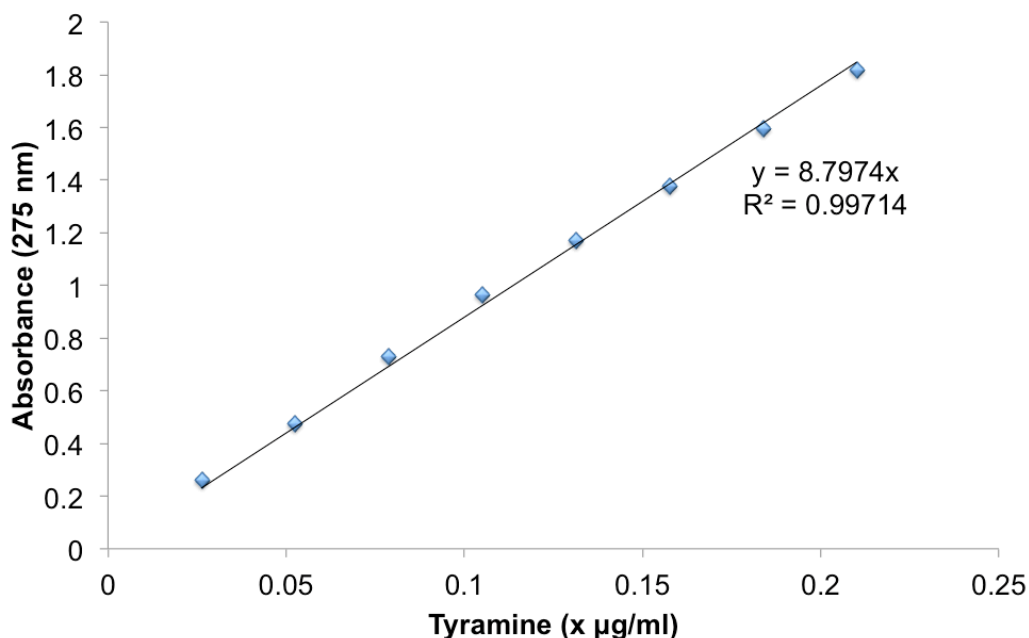


Figure 77. Tyramine Concentration Standard Curve.

#### 7.9.2.1.2 Preparation of protein crosslinked gels

Hydrogels were prepared by the HRP-mediated oxidative coupling of protein-tyramine conjugated molecules in the presence of dilute H<sub>2</sub>O<sub>2</sub>. Hydrogel samples were prepared in vials at 25°C. 100 U/ml HRP and 30% H<sub>2</sub>O<sub>2</sub> were individually dissolved at varying concentrations in PBS or DDI H<sub>2</sub>O. HRP solution was added at desired concentrations with sufficient agitation and time to ensure the rhLF-Tyr solution was fully hydrated.

##### 7.9.2.1.2.1 Gelatin gel

###### 7.9.2.1.2.1.1 Gelatin Gel (dissolved in H<sub>2</sub>O)

To make gelatin gel, first dissolve tyramine-modified gelatin in 10 U/ml HRP (diluted in H<sub>2</sub>O) and mix well. To form gel, add diluted H<sub>2</sub>O<sub>2</sub> and mix well. For example, the following is the protocol to make 10 mg/ml gelatin gel. To make 1 ml of 10 mg/ml

gelatin/HRP solution: dissolve 10 mg modified in 1 ml of 10 U/ml HRP (dissolved in H<sub>2</sub>O) and then mix well. Finally, to make 10 mg/ml gelatin gel: 100 µl of gelatin/HRP solution + 1 µl 0.25% H<sub>2</sub>O<sub>2</sub>.

#### *7.9.2.1.2.1.2 Gelatin Gel (dissolved in 1:1 PBS:H<sub>2</sub>O ratio)*

To make gelatin gel, first dissolve tyramine-modified gelatin in 10 U/ml HRP (diluted in 1:1 PBS:H<sub>2</sub>O ratio) and mix well. To form gel, at diluted H<sub>2</sub>O<sub>2</sub> and mix well. For example, the following is the protocol to make 10 mg/ml gelatin gel. To make 1 ml of 10 mg/ml gelatin/HRP solution: dissolve 10 mg modified in 1 ml of 10 U/ml HRP (diluted in 1:1 PBS:H<sub>2</sub>O ratio) and then mix well. Finally, to make 10 mg/ml gelatin gel: 100 µl of gelatin/HRP solution + 1 µl 0.25% H<sub>2</sub>O<sub>2</sub>.

#### *7.9.2.1.2.2 LF gels*

To make LF gels, first dissolve tyramine-modified LF in half the total volume of 10 U/ml HRP (dissolved in H<sub>2</sub>O) and mix well. Next, add the second half of the total volume of 10 U/ml (dissolved in PBS) and mix well. To form gel, at diluted H<sub>2</sub>O<sub>2</sub> and mix well. For example, the following is the protocol to make 10 mg/ml LF gel. To make 1 ml of 10 mg/ml LF/HRP solution: dissolve 10 mg modified LF in 500 µl of 10 U/ml HRP (dissolved in H<sub>2</sub>O) and then mix well. Add 500 µl of 10 U/ml HRP (dissolved in PBS). Finally, to make 10 mg/ml LF gel: 100 µl of LF/HRP solution + 1 µl 0.25% H<sub>2</sub>O<sub>2</sub>.

### 7.9.2.2 Characterization of hydrogels

#### 7.9.2.2.1 Gelation time

Sol to gel time was determined via vial inversion method (Menger, Caran 2000). 10 mg/ml protein-tyramine conjugate in 100  $\mu$ l of 10 U/ml HRP + 1  $\mu$ l of 0.25%  $H_2O_2$  represents the standard gelling conditions for LF and gelatin gels. Variables were individually varied and tested for effect on gelatin time.

#### 7.9.2.2.2 Rheological testing

A rheometer is an ideal instrument that may be used to measure the gel strength. The holo-rhLF gels were subjected to rheological measurements to assess the viscoelastic properties at varying component concentrations at 25°C. Briefly, the 150  $\mu$ l of modified holo-rhLF/HRP and 1  $\mu$ l  $H_2O_2$  mixture was mixed together in an eppendorf tube and then immediately introduced in a parallel plate rheometer and started the rheological testing program. Dynamic frequency sweeps were then performed in the linear viscoelastic region to determine values of the storage ( $G'$ ) and loss ( $G''$ ) modulus to compare the mechanical strength of gels with different concentrations of holo-rhLF. Rheology testing conditions were as follows: angular frequency of 1 rad/sec; 3% strain; 1000  $\mu$ m gap width; 100  $\mu$ l volume load.

#### 7.9.2.2.3 Gel morphology

The morphology of the hydrogels was visualized by scanning electron microscope to evaluate the effect of solution concentrations on gel microstructure. The gels were flash frozen by immersing in liquid nitrogen for 1 minute followed by 24 hour lyophilization and then observed under the SEM. Prior to imaging, the samples were mounted on

aluminum stubs and samples were platinum coated for improved conductivity. The samples were viewed at an accelerating voltage of 10kV and 12  $\mu$ A. Measurements (n=30) of pore size were obtained using Image J program (U.S. National Institutes of Health, Bethesda, MD).

#### 7.9.2.2.4 Percentage of water uptake

The percentage of water uptake of the injectable gels (n=4 biological replicates) was determined as follows. Briefly, holo-rhLF gels were prepared in plastic inserts, flash frozen with liquid nitrogen and then lyophilized. The weight of the samples was determined ( $W_1$ ) before incubating them in phosphate buffer solution at 37°C. At each time point, the samples were taken out, dabbed dry with a paper towel and their wet mass ( $W_{wet}$ ) was determined. The percentage water uptake of the samples was determined as  $[\% \text{ water uptake} = [(W_{wet} - W_1)/W_1] \times 100]$ .

#### 7.9.2.2.5 Degradation of holo-rhLF biogels *in vivo*

Sprague Dawley rats (Charles River Laboratories, Wilmington, MA) (12-16 weeks) were used 10 mg/ml holo-rhLF were injected subcutaneously to form the gels *in situ*. The animals were cared for according to the procedures approved by the Animal Care and Use Committee at the University of Connecticut Health Center, and following the guidelines established by the U.S. National Institutes of Health. At 4 and 12 weeks, rats were sacrificed and the tissue surrounding the injection sites were excised using blunt dissection technique. Samples were rinsed with PBS solution, washed with deionized water, fixed in 10% formalin solution (Surgipath, USA) and embedded in paraffin, sectioned and hematoxylin and eosin (H&E) was performed.

#### **7.9.2.3 Soluble holo-rhLF protein release from holo-rhLF gel**

100 µl of 10 mg/ml holo-rhLF gel was formed in a 1.5 ml eppendoff tube (n=5). 1 mL PBS was added above the holo-rhLF gel and incubated at 37°C. 150 µl aliquots were taken from each sample every 24 hours for 5 consecutive days. Phenolic content was measured via UV Spectrophotometer at 275 nm.

#### **7.9.2.4 Cell encapsulation in hydrogel**

Protein-tyramine conjugate was dissolved in 10 U/ml HRP. Appropriate number of cells were resuspended in protein-tyramine conjugate/HRP solution followed by the addition of H<sub>2</sub>O<sub>2</sub>. The encapsulated cells were then maintained in medium at 37°C.

## 8 References

Actor, J.K., Hwang, S.A., Olsen, M., Zimecki, M., Hunter, R.L. & Kruzel, M.L. 2002, "Lactoferrin immunomodulation of DTH response in mice", vol. 2, pp. 475-486.

Adler, P.N. & Lee, H. 2001, "Frizzled signaling and cell-cell interactions in planar polarity", *Current opinion in cell biology*, vol. 13, no. 5, pp. 635-640.

Ahmadi, R. & de Bruijn, J.D. 2008, "Biocompatibility and gelation of chitosan-glycerol phosphate hydrogels", *Journal of biomedical materials research.Part A*, vol. 86, no. 3, pp. 824-832.

Aisen, P. & Leibman, A. 1972, "Lactoferrin and transferrin: a comparative study", *Biochimica et biophysica acta*, vol. 257, no. 2, pp. 314-323.

Alhadlaq, A. & Mao, J.J. 2005, "Tissue-engineered osteochondral constructs in the shape of an articular condyle", *The Journal of bone and joint surgery.American volume*, vol. 87, no. 5, pp. 936-944.

Almeida, M., Han, L., Bellido, T., Manolagas, S.C. & Kousteni, S. 2005, "Wnt proteins prevent apoptosis of both uncommitted osteoblast progenitors and differentiated

osteoblasts by beta-catenin-dependent and -independent signaling cascades involving Src/ERK and phosphatidylinositol 3-kinase/AKT", *The Journal of biological chemistry*, vol. 280, no. 50, pp. 41342-41351.

Alsberg, E., Anderson, K.W., Albeiruti, A., Franceschi, R.T. & Mooney, D.J. 2001, "Cell-interactive alginate hydrogels for bone tissue engineering", *Journal of dental research*, vol. 80, no. 11, pp. 2025-2029.

Alvarez-Perez, M.A., Guarino, V., Cirillo, V. & Ambrosio, L. 2010, "Influence of gelatin cues in PCL electrospun membranes on nerve outgrowth", *Biomacromolecules*, vol. 11, no. 9, pp. 2238-2246.

Amini, A.A. & Nair, L.S. 2011, "Lactoferrin: a biologically active molecule for bone regeneration", *Current medicinal chemistry*, vol. 18, no. 8, pp. 1220-1229.

Amini, A.A. & Nair, L.S. 2011a, *Evaluation of the Osteogenic Activity of Injectable Bovine Lactoferrin Gel*.

Amini, A.A. & Nair, L.S. 2011b, "Injectable Hydrogels for Bone and Cartilage Repair", *Biomedical materials*, vol. 7, no. 2, pp. 024105.

Amini, A.A. & Nair, L.S. 2011c, "Lactoferrin: a biologically active molecule for bone regeneration", *Current medicinal chemistry*, vol. 18, no. 8, pp. 1220-1229.



Amini, A.A. & Nair, L.S. 2012a, *Biological Effects of Cross-linked Recombinant Human lactoferrin Gel on Preosteoblastic Cells in vitro.*

Amini, A.A. & Nair, L.S. 2012b, "Enzymatically Crosslinked Gelatin Gel as Osteoblast Delivery Vehicle", *Journal of Bioactive and Compatible Polymers*, vol. 27, no. 4, pp. 342-355.

Anderson, B.F., Baker, H.M., Dodson, E.J., Norris, G.E., Rumball, S.V., Waters, J.M. & Baker, E.N. 1987, "Structure of human lactoferrin at 3.2-A resolution", vol. 84, pp. 1769-1773.

Anderson, B.F., Baker, H.M., Norris, G.E., Rice, D.W. & Baker, E.N. 1989, "Structure of human lactoferrin: crystallographic structure analysis and refinement at 2.8 Å resolution", *Journal of Molecular Biology*, vol. 209, no. 4, pp. 711-734.

Anderson, B.F., Baker, H.M., Norris, G.E., Rumball, S.V. & Baker, E.N. 1990, "Apolactoferrin structure demonstrates ligand-induced conformational change in transferrins", *Nature*, vol. 344, no. 6268, pp. 784-787.

Annabi, N., Nichol, J.W., Zhong, X., Ji, C., Koshy, S., Khademhosseini, A. & Dehghani, F. 2010, "Controlling the porosity and microarchitecture of hydrogels for tissue engineering", *Tissue engineering.Part B, Reviews*, vol. 16, no. 4, pp. 371-383.

Anseth, K.S., Bowman, C.N. & Brannon-Peppas, L. 1996, "Mechanical properties of hydrogels and their experimental determination", *Biomaterials*, vol. 17, no. 17, pp. 1647-1657.

Aoki, M., Morishita, R., Matsushita, H., Nakano, N., Hayashi, S., Tomita, N., Yamamoto, K., Moriguchi, A., Higaki, J. & Ogihara, T. 1997, "Serum deprivation-induced apoptosis accompanied by up-regulation of p53 and bax in human aortic vascular smooth muscle cells", *Heart and vessels*, vol. Suppl 12, pp. 71-75.

Appelmelk, B.J., An, Y.Q., Geerts, M., Thijs, B.G., de Boer, H.A., MacLaren, D.M., de Graaff, J. & Nuijens, J.H. 1994b, "Lactoferrin is a lipid A-binding protein", *Infection and immunity*, vol. 62, no. 6, pp. 2628-2632.

Arnao, M.B., Acosta, M., del Rio, J.A., Varon, R. & Garcia-Canovas, F. 1990, "A kinetic study on the suicide inactivation of peroxidase by hydrogen peroxide", *Biochimica et biophysica acta*, vol. 1041, no. 1, pp. 43-47.

Arnsdorf, E.J., Tummala, P. & Jacobs, C.R. 2009, "Non-canonical Wnt signaling and N-cadherin related beta-catenin signaling play a role in mechanically induced osteogenic cell fate", *PloS one*, vol. 4, no. 4, pp. e5388.

Aronow, M.A., Gerstenfeld, L.C., Owen, T.A., Tassinari, M.S., Stein, G.S. & Lian,

J.B. 1990a, "Factors that promote progressive development of the osteoblast phenotype in cultured fetal rat calvaria cells", *Journal of cellular physiology*, vol. 143, no. 2, pp. 213-221.

Athanasiou, K.A., Zhu, C., Lanctot, D.R., Agrawal, C.M. & Wang, X. 2000, "Fundamentals of biomechanics in tissue engineering of bone", *Tissue engineering*, vol. 6, no. 4, pp. 361-381.

Atkinson, S.J., Ward, R.V., Reynolds, J.J. & Murphy, G. 1992, "Cell-mediated degradation of type IV collagen and gelatin films is dependent on the activation of matrix metalloproteinases", *The Biochemical journal*, vol. 288 ( Pt 2), no. Pt 2, pp. 605-611.

Babij, P., Zhao, W., Small, C., Kharode, Y., Yaworsky, P.J., Bouxsein, M.L., Reddy, P.S., Bodine, P.V., Robinson, J.A., Bhat, B., Marzolf, J., Moran, R.A. & Bex, F. 2003, "High bone mass in mice expressing a mutant LRP5 gene", *Journal of bone and mineral research: the official journal of the American Society for Bone and Mineral Research*, vol. 18, no. 6, pp. 960-974.

Baker, E.N. & Baker, H.M. 2009, "A structural framework for understanding the multifunctional character of lactoferrin", *Biochimie*, vol. 91, no. 1, pp. 3-10.

Baker, E.N., Anderson, B.F., Baker, H.M., Haridas, M., Jameson, G.B., Norris, G.E., Rumball, S.V. & Smith, C.A. 1991, "Structure, function and flexibility of human

lactoferrin", *International journal of biological macromolecules*, vol. 13, no. 3, pp. 122-129.

Baker, H.M. & Baker, E.N. 2004, "Lactoferrin and iron: structural and dynamic aspects of binding and release", vol. 17, pp. 209-216.

Balakrishnan, B. & Jayakrishnan, A. 2005, "Self-cross-linking biopolymers as injectable in situ forming biodegradable scaffolds", *Biomaterials*, vol. 26, no. 18, pp. 3941-3951.

Baron, R. & Rawadi, G. 2007, "Wnt signaling and the regulation of bone mass", *Current osteoporosis reports*, vol. 5, no. 2, pp. 73-80.

Baumrucker, C.R., Gibson, C.A. & Schanbacher, F.L. 2003, "Bovine lactoferrin binds to insulin-like growth factor-binding protein-3", vol. 24, pp. 287-303.

Baveye, S., Ellass, E., Fernig, D.G., Blanquart, C., Mazurier, J. & Legrand, D. 2000a, "Human lactoferrin interacts with soluble CD14 and inhibits expression of endothelial adhesion molecules, E-selectin and ICAM-1, induced by the CD14-lipopolysaccharide complex", vol. 68, pp. 6519-6525.

Baveye, S., Ellass, E., Mazurier, J. & Legrand, D. 2000b, "Lactoferrin inhibits the binding of lipopolysaccharides to L-selectin and subsequent production of reactive

oxygen species by neutrophils", vol. 469, pp. 5-8.

Baveye, S., Ellass, E., Mazurier, J., Spik, G. & Legrand, D. 1999, "Lactoferrin: a multifunctional glycoprotein involved in the modulation of the inflammatory process", vol. 37, pp. 281-286.

Baylink, D.J., Finkelman, R.D. & Mohan, S. 1993, "Growth factors to stimulate bone formation", *Journal of bone and mineral research : the official journal of the American Society for Bone and Mineral Research*, vol. 8 Suppl 2, pp. S565-72.

Baynton, K.J., Bewtra, J.K., Biswas, N. & Taylor, K.E. 1994, "Inactivation of horseradish peroxidase by phenol and hydrogen peroxide: a kinetic investigation", *Biochimica et biophysica acta*, vol. 1206, no. 2, pp. 272-278.

Bellows, C.G., Heersche, J.N. & Aubin, J.E. 1990, "Determination of the capacity for proliferation and differentiation of osteoprogenitor cells in the presence and absence of dexamethasone", *Developmental biology*, vol. 140, no. 1, pp. 132-138.

Bennett, R.M. & Davis, J. 1981, "Lactoferrin binding to human peripheral blood cells: an interaction with a B-enriched population of lymphocytes and a subpopulation of adherent mononuclear cells", vol. 127, pp. 1211-1216.

Benya, P.D. & Shaffer, J.D. 1982, "Dedifferentiated chondrocytes reexpress the

differentiated collagen phenotype when cultured in agarose gels", *Cell*, vol. 30, no. 1, pp. 215-224.

Betz, M.W., Yeatts, A.B., Richbourg, W.J., Caccamese, J.F., Coletti, D.P., Falco, E.E. & Fisher, J.P. 2010, "Macroporous hydrogels upregulate osteogenic signal expression and promote bone regeneration", *Biomacromolecules*, vol. 11, no. 5, pp. 1160-1168.

Bharadwaj, S., Naidu, A.G., Betageri, G.V., Prasadarao, N.V. & Naidu, A.S. 2009, "Milk ribonuclease-enriched lactoferrin induces positive effects on bone turnover markers in postmenopausal women", vol. 20, pp. 1603-1611.

Birgens, H.S., Hansen, N.E., Karle, H. & Kristensen, L.O. 1983, "Receptor binding of lactoferrin by human monocytes", *British journal of haematology*, vol. 54, no. 3, pp. 383-391.

Blais, A., Malet, A., Mikogami, T., Martin-Rouas, C. & Tome, D. 2009, "Oral bovine lactoferrin improves bone status of ovariectomized mice", *American journal of physiology. Endocrinology and metabolism*, vol. 296, no. 6, pp. E1281-8.

Boanini, E., Rubini, K., Panzavolta, S. & Bigi, A. 2010, "Chemico-physical characterization of gelatin films modified with oxidized alginate", *Acta biomaterialia*, vol. 6, no. 2, pp. 383-388.

Boone, C.W., Mantel, N., Caruso, T.D., Jr, Kazam, E. & Stevenson, R.E. 1971, "Quality control studies on fetal bovine serum used in tissue culture", *In vitro*, vol. 7, no. 3, pp. 174-189.

Bouillon, R. 1991, "Growth hormone and bone", *Hormone research*, vol. 36 Suppl 1, pp. 49-55.

Braun, F., Bertin-Ciftci, J., Gallouet, A.S., Millour, J. & Juin, P. 2011, "Serum-nutrient starvation induces cell death mediated by Bax and Puma that is counteracted by p21 and unmasked by Bcl-x(L) inhibition", *PloS one*, vol. 6, no. 8, pp. e23577.

Breton-Gorius, J., Mason, D.Y., Buriot, D., Vilde, J.L. & Griscelli, C. 1980, "Lactoferrin deficiency as a consequence of a lack of specific granules in neutrophils from a patient with recurrent infections. Detection by immunoperoxidase staining for lactoferrin and cytochemical electron microscopy", *The American journal of pathology*, vol. 99, no. 2, pp. 413-428.

Brines, R.D. & Brock, J.H. 1983, "The effect of trypsin and chymotrypsin on the in vitro antimicrobial and iron-binding properties of lactoferrin in human milk and bovine colostrum. Unusual resistance of human apolactoferrin to proteolytic digestion", vol. 759, pp. 229-235.

Britigan, B.E., Lewis, T.S., Waldschmidt, M., McCormick, M.L. & Krieg, A.M. 2001, "Lactoferrin binds CpG-containing oligonucleotides and inhibits their immunostimulatory effects on human B cells", vol. 167, pp. 2921-2928.

Brock, J. 1995, "Lactoferrin: a multifunctional immunoregulatory protein?", *Immunology today*, vol. 16, no. 9, pp. 417-419.

Brock, J.H. 2002, "The physiology of lactoferrin", vol. 80, pp. 1-6.

Brock, J.H., Arzabe, F., Lampreave, F. & Piñeiro, A. 1976, "The effect of trypsin on bovine transferrin and lactoferrin", vol. 446, pp. 214-225.

Broxmeyer, H.E., Williams, D.E., Hangoc, G., Cooper, S., Gentile, P., Shen, R.N., Ralph, P., Gillis, S. & Bicknell, D.C. 1987, "The opposing actions in vivo on murine myelopoiesis of purified preparations of lactoferrin and the colony stimulating factors", vol. 13, pp. 31-48.

Brunet, A., Bonni, A., Zigmond, M.J., Lin, M.Z., Juo, P., Hu, L.S., Anderson, M.J., Arden, K.C., Blenis, J. & Greenberg, M.E. 1999, "Akt promotes cell survival by phosphorylating and inhibiting a Forkhead transcription factor", *Cell*, vol. 96, no. 6, pp. 857-868.

Bryja, V., Andersson, E.R., Schambony, A., Esner, M., Bryjova, L., Biris, K.K., Hall,



A.C., Kraft, B., Cajanek, L., Yamaguchi, T.P., Buckingham, M. & Arenas, E. 2009, "The extracellular domain of Lrp5/6 inhibits noncanonical Wnt signaling in vivo", *Molecular biology of the cell*, vol. 20, no. 3, pp. 924-936.

Burchardt, H. 1987, "Biology of bone transplantation", *The Orthopedic clinics of North America*, vol. 18, no. 2, pp. 187-196.

Burdick, J.A. & Anseth, K.S. 2002, "Photoencapsulation of osteoblasts in injectable RGD-modified PEG hydrogels for bone tissue engineering", *Biomaterials*, vol. 23, no. 22, pp. 4315-4323.

Burdick, J.A. & Prestwich, G.D. 2011, "Hyaluronic acid hydrogels for biomedical applications", *Advanced materials (Deerfield Beach, Fla.)*, vol. 23, no. 12, pp. H41-56.

Buschmann, M.D., Gluzband, Y.A., Grodzinsky, A.J., Kimura, J.H. & Hunziker, E.B. 1992, "Chondrocytes in agarose culture synthesize a mechanically functional extracellular matrix", *Journal of orthopaedic research : official publication of the Orthopaedic Research Society*, vol. 10, no. 6, pp. 745-758.

Byrd, T.F. & Horwitz, M.A. 1991, "Lactoferrin inhibits or promotes *Legionella pneumophila* intracellular multiplication in nonactivated and interferon gamma-activated human monocytes depending upon its degree of iron saturation. Iron-lactoferrin and nonphysiologic iron chelates reverse monocyte activation against *Legionella*

pneumophila", *The Journal of clinical investigation*, vol. 88, no. 4, pp. 1103-1112.

Cairo, G., Recalcati, S., Pietrangelo, A. & Minotti, G. 2002, "The iron regulatory proteins: targets and modulators of free radical reactions and oxidative damage", *Free radical biology & medicine*, vol. 32, no. 12, pp. 1237-1243.

Campbell, T., Skilton, R.A., Coombes, R.C., Shousha, S., Graham, M.D. & Luqmani, Y.A. 1992, "Isolation of a lactoferrin cDNA clone and its expression in human breast cancer", *British journal of cancer*, vol. 65, no. 1, pp. 19-26.

Caplan, A.I. 2000, "Mesenchymal stem cells and gene therapy", *Clinical orthopaedics and related research*, vol. (379 Suppl), no. 379 Suppl, pp. S67-70.

Cardone, M.H., Roy, N., Stennicke, H.R., Salvesen, G.S., Franke, T.F., Stanbridge, E., Frisch, S. & Reed, J.C. 1998, "Regulation of cell death protease caspase-9 by phosphorylation", *Science (New York, N.Y.)*, vol. 282, no. 5392, pp. 1318-1321.

Carson, J.S. & Bostrom, M.P. 2007, "Synthetic bone scaffolds and fracture repair", *Injury*, vol. 38 Suppl 1, pp. S33-7.

Chan, S.K. & Struhl, G. 2002, "Evidence that Armadillo transduces wingless by mediating nuclear export or cytosolic activation of Pangolin", *Cell*, vol. 111, no. 2, pp. 265-280.

Chaudhary, L.R. & Avioli, L.V. 2000, "Extracellular-signal regulated kinase signaling pathway mediates downregulation of type I procollagen gene expression by FGF-2, PDGF-BB, and okadaic acid in osteoblastic cells", *Journal of cellular biochemistry*, vol. 76, no. 3, pp. 354-359.

Chen, F., Mao, T., Tao, K., Chen, S., Ding, G. & Gu, X. 2003, "Injectable bone", *The British journal of oral & maxillofacial surgery*, vol. 41, no. 4, pp. 240-243.

Chen, L., Jiang, W., Huang, J., He, B.C., Zuo, G.W., Zhang, W., Luo, Q., Shi, Q., Zhang, B.Q., Wagner, E.R., Luo, J., Tang, M., Wietholt, C., Luo, X., Bi, Y., Su, Y., Liu, B., Kim, S.H., He, C.J., Hu, Y., Shen, J., Rastegar, F., Huang, E., Gao, Y., Gao, J.L., Zhou, J.Z., Reid, R.R., Luu, H.H., Haydon, R.C., He, T.C. & Deng, Z.L. 2010, "Insulin-like growth factor 2 (IGF-2) potentiates BMP-9-induced osteogenic differentiation and bone formation", *Journal of bone and mineral research : the official journal of the American Society for Bone and Mineral Research*, vol. 25, no. 11, pp. 2447-2459.

Chen, S. & Singh, J. 2005, "Controlled delivery of testosterone from smart polymer solution based systems: in vitro evaluation", *International journal of pharmaceutics*, vol. 295, no. 1-2, pp. 183-190.

Chen, T., Embree, H.D., Brown, E.M., Taylor, M.M. & Payne, G.F. 2003a, "Enzyme-catalyzed gel formation of gelatin and chitosan: potential for in situ applications",

*Biomaterials*, vol. 24, no. 17, pp. 2831-2841.

Chen, T., Small, D.A., McDermott, M.K., Bentley, W.E. & Payne, G.F. 2003b, "Enzymatic methods for in situ cell entrapment and cell release", *Biomacromolecules*, vol. 4, no. 6, pp. 1558-1563.

Chen, Y. & Alman, B.A. 2009, "Wnt pathway, an essential role in bone regeneration", *Journal of cellular biochemistry*, vol. 106, no. 3, pp. 353-362.

Chen, Y. 2001, "Orthopedic applications of gene therapy", *Journal of orthopaedic science: official journal of the Japanese Orthopaedic Association*, vol. 6, no. 2, pp. 199-207.

Chen, Y., Whetstone, H.C., Lin, A.C., Nadesan, P., Wei, Q., Poon, R. & Alman, B.A. 2007, "Beta-catenin signaling plays a disparate role in different phases of fracture repair: implications for therapy to improve bone healing", *PLoS medicine*, vol. 4, no. 7, pp. e249.

Choi, B.K., Actor, J.K., Rios, S., d'Anjou, M., Stadheim, T.A., Warburton, S., Giaccone, E., Cukan, M., Li, H., Kull, A., Sharkey, N., Gollnick, P., Kocieba, M., Artym, J., Zimecki, M., Kruzel, M.L. & Wildt, S. 2008, "Recombinant human lactoferrin expressed in glycoengineered *Pichia pastoris*: effect of terminal N-acetylneuraminic acid on in vitro secondary humoral immune response", *Glycoconjugate journal*, vol. 25, no. 6,

pp. 581-593.

Choi, J.Y., Lee, B.H., Song, K.B., Park, R.W., Kim, I.S., Sohn, K.Y., Jo, J.S. & Ryoo, H.M. 1996, "Expression patterns of bone-related proteins during osteoblastic differentiation in MC3T3-E1 cells", *Journal of cellular biochemistry*, vol. 61, no. 4, pp. 609-618.

Chueh, B.H., Zheng, Y., Torisawa, Y.S., Hsiao, A.Y., Ge, C., Hsiong, S., Huebsch, N., Franceschi, R., Mooney, D.J. & Takayama, S. 2010, "Patterning alginate hydrogels using light-directed release of caged calcium in a microfluidic device", *Biomedical Microdevices*, vol. 12, no. 1, pp. 145-151.

Clowes, J.A., Riggs, B.L. & Khosla, S. 2005, "The role of the immune system in the pathophysiology of osteoporosis", vol. 208, pp. 207-227.

Cobbett, W.G., Kenchington, A.W. & Ward, A.G. 1962, "The determination of the tyrosine content of gelatins", *The Biochemical journal*, vol. 84, pp. 468-474.

Cohn, D., Lando, G., Sosnik, A., Garty, S. & Levi, A. 2006, "PEO-PPO-PEO-based poly(ether ester urethane)s as degradable reverse thermo-responsive multiblock copolymers", *Biomaterials*, vol. 27, no. 9, pp. 1718-1727.

Collin, P., Nefussi, J.R., Wetterwald, A., Nicolas, V., Boy-Lefevre, M.L., Fleisch, H.

& Forest, N. 1992, "Expression of collagen, osteocalcin, and bone alkaline phosphatase in a mineralizing rat osteoblastic cell culture", *Calcified tissue international*, vol. 50, no. 2, pp. 175-183.

Cornish, J. & Naot, D. 2010, "Lactoferrin as an effector molecule in the skeleton", *Biometals : an international journal on the role of metal ions in biology, biochemistry, and medicine*, vol. 23, no. 3, pp. 425-430.

Cornish, J. 2004, "Lactoferrin promotes bone growth", *Biometals : an international journal on the role of metal ions in biology, biochemistry, and medicine*, vol. 17, no. 3, pp. 331-335.

Cornish, J., Callon, K.E., Naot, D., Palmano, K.P., Banovic, T., Bava, U., Watson, M., Lin, J.M., Tong, P.C., Chen, Q., Chan, V.A., Reid, H.E., Fazzalari, N., Baker, H.M., Baker, E.N., Haggarty, N.W., Grey, A.B. & Reid, I.R. 2004, "Lactoferrin is a potent regulator of bone cell activity and increases bone formation in vivo", *Endocrinology*, vol. 145, no. 9, pp. 4366-4374.

Cornish, J., Palmano, K., Callon, K.E., Watson, M., Lin, J.M., Valenti, P., Naot, D., Grey, A.B. & Reid, I.R. 2006, "Lactoferrin and bone; structure-activity relationships", *Biochemistry and cell biology = Biochimie et biologie cellulaire*, vol. 84, no. 3, pp. 297-302.

Coviello, T., Matricardi, P., Marianecchi, C. & Alhaique, F. 2007, "Polysaccharide

hydrogels for modified release formulations", *Journal of controlled release : official journal of the Controlled Release Society*, vol. 119, no. 1, pp. 5-24.

Cukierman, E., Pankov, R., Stevens, D.R. & Yamada, K.M. 2001, "Taking cell-matrix adhesions to the third dimension", *Science (New York, N.Y.)*, vol. 294, no. 5547, pp. 1708-1712.

Curran, C.S., Demick, K.P. & Mansfield, J.M. 2006, "Lactoferrin activates macrophages via TLR4-dependent and -independent signaling pathways", vol. 242, pp. 23-30.

Currey, J.D. 1970, "The mechanical properties of bone", *Clinical orthopaedics and related research*, vol. 73, pp. 209-231.

Currey, J.D. 1998, "Mechanical properties of vertebrate hard tissues", *Proceedings of the Institution of Mechanical Engineers.Part H, Journal of engineering in medicine*, vol. 212, no. 6, pp. 399-411.

Currey, J.D. 1999, "The design of mineralised hard tissues for their mechanical functions", *The Journal of experimental biology*, vol. 202, no. Pt 23, pp. 3285-3294.

Damiens, E., Mazurier, J., el Yazidi, I., Masson, M., Duthille, I., Spik, G. & Boilly-Marer, Y. 1998, "Effects of human lactoferrin on NK cell cytotoxicity against

haematopoietic and epithelial tumour cells", vol. 1402, pp. 277-287.

Dang, J.M., Sun, D.D., Shin-Ya, Y., Sieber, A.N., Kostuik, J.P. & Leong, K.W. 2006, "Temperature-responsive hydroxybutyl chitosan for the culture of mesenchymal stem cells and intervertebral disk cells", *Biomaterials*, vol. 27, no. 3, pp. 406-418.

Darr, A. & Calabro, A. 2009, "Synthesis and characterization of tyramine-based hyaluronan hydrogels", *Journal of materials science. Materials in medicine*, vol. 20, no. 1, pp. 33-44.

Davies, J.E. & Hosseini, M.M. 2000, "Histodynamics of endosseous wound healing" in *Bone engineering* Toronto, pp. 1-14.

Davis, N.E., Ding, S., Forster, R.E., Pinkas, D.M. & Barron, A.E. 2010a, "Modular enzymatically crosslinked protein polymer hydrogels for in situ gelation", *Biomaterials*, vol. 31, no. 28, pp. 7288-7297.

Davis, N.E., Ding, S., Forster, R.E., Pinkas, D.M. & Barron, A.E. 2010b, "Modular enzymatically crosslinked protein polymer hydrogels for in situ gelation", *Biomaterials*, vol. 31, no. 28, pp. 7288-7297.

de, I.R., Yang, D., Tewary, P., Varadhachary, A. & Oppenheim, J.J. 2008, "Lactoferrin acts as an alarmin to promote the recruitment and activation of APCs and antigen-



specific immune responses", vol. 180, pp. 6868-6876.

Degoricija, L., Bansal, P.N., Sontjens, S.H., Joshi, N.S., Takahashi, M., Snyder, B. & Grinstaff, M.W. 2008, "Hydrogels for osteochondral repair based on photocrosslinkable carbamate dendrimers", *Biomacromolecules*, vol. 9, no. 10, pp. 2863-2872.

Delany, A.M. & Canalis, E. 1998, "Basic fibroblast growth factor destabilizes osteonectin mRNA in osteoblasts", *The American Journal of Physiology*, vol. 274, no. 3 Pt 1, pp. C734-40.

Delloye, C., Cornu, O., Druez, V. & Barbier, O. 2007, "Bone allografts: What they can offer and what they cannot", *The Journal of bone and joint surgery.British volume*, vol. 89, no. 5, pp. 574-579.

Demolliens, A., Boucher, C., Durocher, Y., Jolicoeur, M., Buschmann, M.D. & De Crescenzo, G. 2008, "Tyrosinase-catalyzed synthesis of a universal coil-chitosan bioconjugate for protein immobilization", *Bioconjugate chemistry*, vol. 19, no. 9, pp. 1849-1854.

Devescovi, V., Leonardi, E., Ciapetti, G. & Cenni, E. 2008, "Growth factors in bone repair", *La Chirurgia degli organi di movimento*, vol. 92, no. 3, pp. 161-168.

Dodds, R.A., Merry, K., Littlewood, A. & Gowen, M. 1994, "Expression of mRNA for

IL1 beta, IL6 and TGF beta 1 in developing human bone and cartilage", *The journal of histochemistry and cytochemistry: official journal of the Histochemistry Society*, vol. 42, no. 6, pp. 733-744.

Dreesmann, L., Ahlers, M. & Schlosshauer, B. 2007, "The pro-angiogenic characteristics of a cross-linked gelatin matrix", *Biomaterials*, vol. 28, no. 36, pp. 5536-5543.

Dwek, R.A. 1995, "Glycobiology: "towards understanding the function of sugars"", vol. 23, pp. 1-25.

Eberhard, J., Drosos, Z., Tiemann, M., Jepsen, S. & Schr  der, J.M. 2006, "Immunolocalization of lactoferrin in healthy and inflamed gingival tissues", vol. 77, pp. 472-478.

Ehrbar, M., Rizzi, S.C., Schoenmakers, R.G., Miguel, B.S., Hubbell, J.A., Weber, F.E. & Lutolf, M.P. 2007, "Biomolecular hydrogels formed and degraded via site-specific enzymatic reactions", *Biomacromolecules*, vol. 8, no. 10, pp. 3000-3007.

Elass-Rochard, E., Legrand, D., Salmon, V., Roseanu, A., Trif, M., Tobias, P.S., Mazurier, J. & Spik, G. 1998, "Lactoferrin inhibits the endotoxin interaction with CD14 by competition with the lipopolysaccharide-binding protein", vol. 66, pp. 486-491.

Elass-Rochard, E., Roseanu, A., Legrand, D., Trif, M., Salmon, V., Motas, C., Montreuil, J. & Spik, G. 1995, "Lactoferrin-lipopolysaccharide interaction: involvement of the 28-34 loop region of human lactoferrin in the high-affinity binding to Escherichia coli 055B5 lipopolysaccharide", vol. 312 ( Pt 3), pp. 839-845.

Elisseeff, J., McIntosh, W., Fu, K., Blunk, B.T. & Langer, R. 2001, "Controlled-release of IGF-I and TGF-beta1 in a photopolymerizing hydrogel for cartilage tissue engineering", *Journal of orthopaedic research : official publication of the Orthopaedic Research Society*, vol. 19, no. 6, pp. 1098-1104.

Elrod, K.C., Moore, W.R., Abraham, W.M. & Tanaka, R.D. 1997, "Lactoferrin, a potent tryptase inhibitor, abolishes late-phase airway responses in allergic sheep", vol. 156, pp. 375-381.

Engelmayer, J., Blezinger, P. & Varadhachary, A. 2008, "Talactoferrin stimulates wound healing with modulation of inflammation", vol. 149, pp. 278-286.

Engler, A., Bacakova, L., Newman, C., Hategan, A., Griffin, M. & Discher, D. 2004, "Substrate compliance versus ligand density in cell on gel responses", *Biophysical journal*, vol. 86, no. 1 Pt 1, pp. 617-628.

Engler, A.J., Sen, S., Sweeney, H.L. & Discher, D.E. 2006, "Matrix elasticity directs stem cell lineage specification", *Cell*, vol. 126, no. 4, pp. 677-689.

Eto, A., Muta, T., Yamazaki, S. & Takeshige, K. 2003, "Essential roles for NF-kappa B and a Toll/IL-1 receptor domain-specific signal(s) in the induction of I kappa B-zeta", *Biochemical and biophysical research communications*, vol. 301, no. 2, pp. 495-501.

Eyrich, D., Brandl, F., Appel, B., Wiese, H., Maier, G., Wenzel, M., Staudenmaier, R., Goepferich, A. & Blunk, T. 2007, "Long-term stable fibrin gels for cartilage engineering", *Biomaterials*, vol. 28, no. 1, pp. 55-65.

Fang, X., Yu, S.X., Lu, Y., Bast, R.C., Jr, Woodgett, J.R. & Mills, G.B. 2000, "Phosphorylation and inactivation of glycogen synthase kinase 3 by protein kinase A", *Proceedings of the National Academy of Sciences of the United States of America*, vol. 97, no. 22, pp. 11960-11965.

Fernandez-Tresguerres-Hernandez-Gil, I., Alobera-Gracia, M.A., del-Canto-Pingarron, M. & Blanco-Jerez, L. 2006, "Physiological bases of bone regeneration I. Histology and physiology of bone tissue", *Medicina oral, patologia oral y cirugia bucal*, vol. 11, no. 1, pp. E47-51.

Fisher, J.P., Jo, S., Mikos, A.G. & Reddi, A.H. 2004, "Thermoreversible hydrogel scaffolds for articular cartilage engineering", *Journal of biomedical materials research.Part A*, vol. 71, no. 2, pp. 268-274.

Fox, S.W., Fuller, K. & Chambers, T.J. 2000, "Activation of osteoclasts by interleukin-1: divergent responsiveness in osteoclasts formed in vivo and in vitro", vol. 184, pp. 334-340.

Franceschi, R.T. & Iyer, B.S. 1992, "Relationship between collagen synthesis and expression of the osteoblast phenotype in MC3T3-E1 cells", *Journal of bone and mineral research : the official journal of the American Society for Bone and Mineral Research*, vol. 7, no. 2, pp. 235-246.

Franceschi, R.T. 2005, "Biological approaches to bone regeneration by gene therapy", *Journal of dental research*, vol. 84, no. 12, pp. 1093-1103.

Franceschi, R.T., Iyer, B.S. & Cui, Y. 1994, "Effects of ascorbic acid on collagen matrix formation and osteoblast differentiation in murine MC3T3-E1 cells", *Journal of bone and mineral research : the official journal of the American Society for Bone and Mineral Research*, vol. 9, no. 6, pp. 843-854.

Franceschi, R.T., Xiao, G., Jiang, D., Gopalakrishnan, R., Yang, S. & Reith, E. 2003, "Multiple signaling pathways converge on the Cbfa1/Runx2 transcription factor to regulate osteoblast differentiation", *Connective tissue research*, vol. 44 Suppl 1, pp. 109-116.

Francis, N., Wong, S.H., Hampson, P., Wang, K., Young, S.P., Deigner, H.P., Salmon,

M., Scheel-Toellner, D. & Lord, J.M. 2011, "Lactoferrin inhibits neutrophil apoptosis via blockade of proximal apoptotic signaling events", *Biochimica et biophysica acta*, vol. 1813, no. 10, pp. 1822-1826.

Fujita, T., Azuma, Y., Fukuyama, R., Hattori, Y., Yoshida, C., Koida, M., Ogita, K. & Komori, T. 2004, "Runx2 induces osteoblast and chondrocyte differentiation and enhances their migration by coupling with PI3K-Akt signaling", *The Journal of cell biology*, vol. 166, no. 1, pp. 85-95.

Fujiyama, K., Sakai, Y., Misaki, R., Yanagihara, I., Honda, T., Anzai, H. & Seki, T. 2004, "N-linked glycan structures of human lactoferrin produced by transgenic rice", vol. 68, pp. 2565-2570.

Fukaya, C., Nakayama, Y., Murayama, Y., Omata, S., Ishikawa, A., Hosaka, Y. & Nakagawa, T. 2009, "Improvement of hydrogelation abilities and handling of photocurable gelatin-based crosslinking materials", *Journal of biomedical materials research. Part B, Applied biomaterials*, vol. 91, no. 1, pp. 329-336.

Fuller, K., Murphy, C., Kirstein, B., Fox, S.W. & Chambers, T.J. 2002, "TNF $\alpha$  potently activates osteoclasts, through a direct action independent of and strongly synergistic with RANKL", vol. 143, pp. 1108-1118.

Ge, C., Xiao, G., Jiang, D. & Franceschi, R.T. 2007, "Critical role of the extracellular

signal-regulated kinase-MAPK pathway in osteoblast differentiation and skeletal development", *The Journal of cell biology*, vol. 176, no. 5, pp. 709-718.

Geckil, H., Xu, F., Zhang, X., Moon, S. & Demirci, U. 2010, "Engineering hydrogels as extracellular matrix mimics", *Nanomedicine (London, England)*, vol. 5, no. 3, pp. 469-484.

Ghanaati, S., Barbeck, M., Hilbig, U., Hoffmann, C., Unger, R.E., Sader, R.A., Peters, F. & Kirkpatrick, C.J. 2011, "An injectable bone substitute composed of beta-tricalcium phosphate granules, methylcellulose and hyaluronic acid inhibits connective tissue influx into its implantation bed in vivo", *Acta biomaterialia*.

Ghosh-Choudhury, N., Abboud, S.L., Nishimura, R., Celeste, A., Mahimainathan, L. & Choudhury, G.G. 2002, "Requirement of BMP-2-induced phosphatidylinositol 3-kinase and Akt serine/threonine kinase in osteoblast differentiation and Smad-dependent BMP-2 gene transcription", *The Journal of biological chemistry*, vol. 277, no. 36, pp. 33361-33368.

Gkioni, K., Leeuwenburgh, S.C., Douglas, T.E., Mikos, A.G. & Jansen, J.A. 2010, "Mineralization of hydrogels for bone regeneration", *Tissue engineering.Part B, Reviews*, vol. 16, no. 6, pp. 577-585.

Gong, Y., Slee, R.B., Fukai, N., Rawadi, G., Roman-Roman, S., Reginato, A.M.,

Wang, H., Cundy, T., Glorieux, F.H., Lev, D., Zacharin, M., Oexle, K., Marcelino, J., Suwairi, W., Heeger, S., Sabatakos, G., Apte, S., Adkins, W.N., Allgrove, J., Arslan-Kirchner, M., Batch, J.A., Beighton, P., Black, G.C., Boles, R.G., Boon, L.M., Borrone, C., Brunner, H.G., Carle, G.F., Dallapiccola, B., De Paepe, A., Floege, B., Halfhide, M.L., Hall, B., Hennekam, R.C., Hirose, T., Jans, A., Jäppner, H., Kim, C.A., Keppler-Noreuil, K., Kohlschuetter, A., LaCombe, D., Lambert, M., Lemyre, E., Letteboer, T., Peltonen, L., Ramesar, R.S., Romanengo, M., Somer, H., Steichen-Gersdorf, E., Steinmann, B., Sullivan, B., Superti-Furga, A., Swoboda, W., van, d.B., Van Hul, W., Vikkula, M., Votruba, M., Zabel, B., Garcia, T., Baron, R., Olsen, B.R., Warman, M.L. & Group, O.S.C. 2001, "LDL receptor-related protein 5 (LRP5) affects bone accrual and eye development", vol. 107, pp. 513-523.

Gonzalez-Chavez, S.A., Arevalo-Gallegos, S. & Rascon-Cruz, Q. 2009, "Lactoferrin: structure, function and applications", *International journal of antimicrobial agents*, vol. 33, no. 4, pp. 301.e1-301.e8.

Goodman, R.E. & Schanbacher, F.L. 1991, "Bovine lactoferrin mRNA: sequence, analysis, and expression in the mammary gland", vol. 180, pp. 75-84.

Greenberg, C.S., Birckbichler, P.J. & Rice, R.H. 1991, "Transglutaminases: multifunctional cross-linking enzymes that stabilize tissues", *FASEB journal : official publication of the Federation of American Societies for Experimental Biology*, vol. 5, no. 15, pp. 3071-3077.



Grey, A., Banovic, T., Zhu, Q., Watson, M., Callon, K., Palmano, K., Ross, J., Naot, D., Reid, I.R. & Cornish, J. 2004, "The low-density lipoprotein receptor-related protein 1 is a mitogenic receptor for lactoferrin in osteoblastic cells", *Molecular endocrinology* (Baltimore, Md.), vol. 18, no. 9, pp. 2268-2278.

Grey, A., Chen, Q., Xu, X., Callon, K. & Cornish, J. 2003, "Parallel phosphatidylinositol-3 kinase and p42/44 mitogen-activated protein kinase signaling pathways subserve the mitogenic and antiapoptotic actions of insulin-like growth factor I in osteoblastic cells", vol. 144, pp. 4886-4893.

Grey, A., Zhu, Q., Watson, M., Callon, K. & Cornish, J. 2006, "Lactoferrin potently inhibits osteoblast apoptosis, via an LRP1-independent pathway", *Molecular and cellular endocrinology*, vol. 251, no. 1-2, pp. 96-102.

Griffiths, C.E., Cumberbatch, M., Tucker, S.C., Dearman, R.J., Andrew, S., Headon, D.R. & Kimber, I. 2001, "Exogenous topical lactoferrin inhibits allergen-induced Langerhans cell migration and cutaneous inflammation in humans", vol. 144, pp. 715-725.

Grinnell, F., Ho, C.H., Tamariz, E., Lee, D.J. & Skuta, G. 2003, "Dendritic fibroblasts in three-dimensional collagen matrices", *Molecular biology of the cell*, vol. 14, no. 2, pp. 384-395.

Grossmann, J.G., Neu, M., Pantos, E., Schwab, F.J., Evans, R.W., Townes-Andrews, E., Lindley, P.F., Appel, H., Thies, W.G. & Hasnain, S.S. 1992, "X-ray solution scattering reveals conformational changes upon iron uptake in lactoferrin, serum and ovo-transferrins", *Journal of Molecular Biology*, vol. 225, no. 3, pp. 811-819.

Guillen, C., McInnes, I.B., Vaughan, D.M., Kommajosyula, S., Van Berkel, P.H., Leung, B.P., Aguila, A. & Brock, J.H. 2002, "Enhanced Th1 response to *Staphylococcus aureus* infection in human lactoferrin-transgenic mice", vol. 168, pp. 3950-3957.

Guler, M.O., Hsu, L., Soukasene, S., Harrington, D.A., Hulvat, J.F. & Stupp, S.I. 2006, "Presentation of RGDS epitopes on self-assembled nanofibers of branched peptide amphiphiles", *Biomacromolecules*, vol. 7, no. 6, pp. 1855-1863.

Hajduch, E., Litherland, G.J. & Hundal, H.S. 2001, "Protein kinase B (PKB/Akt)--a key regulator of glucose transport?", *FEBS letters*, vol. 492, no. 3, pp. 199-203.

Hall, H., Baechi, T. & Hubbell, J.A. 2001, "Molecular properties of fibrin-based matrices for promotion of angiogenesis in vitro", *Microvascular research*, vol. 62, no. 3, pp. 315-326.

Hara, K., Ueda, S., Ohno, Y., Tanaka, T., Yagi, H., Okazaki, S., Kawahara, R., Masayuki, T., Enomoto, T., Hashimoto, Y., Masuko, K. & Masuko, T. 2012, "NIH3T3

cells overexpressing CD98 heavy chain resist early G1 arrest and apoptosis induced by serum starvation", *Cancer science*.

Haridas, M., Anderson, B.F. & Baker, E.N. 1995, "Structure of human diferric lactoferrin refined at 2.2 Å resolution", *Acta crystallographica. Section D, Biological crystallography*, vol. 51, no. Pt 5, pp. 629-646.

Harrington, D.A., Cheng, E.Y., Guler, M.O., Lee, L.K., Donovan, J.L., Claussen, R.C. & Stupp, S.I. 2006, "Branched peptide-amphiphiles as self-assembling coatings for tissue engineering scaffolds", *Journal of biomedical materials research. Part A*, vol. 78, no. 1, pp. 157-167.

Harrington, J.P. 1992, "Spectroscopic analysis of the unfolding of transition metal-ion complexes of human lactoferrin and transferrin", vol. 24, pp. 275-280.

Hartgerink, J.D. 2004, "Covalent capture: a natural complement to self-assembly", *Current opinion in chemical biology*, vol. 8, no. 6, pp. 604-609.

Haversen, L., Ohlsson, B.G., Hahn-Zoric, M., Hanson, L.A. & Mattsby-Baltzer, I. 2002, "Lactoferrin down-regulates the LPS-induced cytokine production in monocytic cells via NF-kappa B", vol. 220, pp. 83-95.

Hawkins, B.J. 2010, "Biologics in foot and ankle surgery", *Foot and ankle clinics*, vol.

15, no. 4, pp. 577-596.

Hayes, T.G., Falchook, G.F., Varadhachary, G.R., Smith, D.P., Davis, L.D., Dhingra, H.M., Hayes, B.P. & Varadhachary, A. 2006, "Phase I trial of oral talactoferrin alfa in refractory solid tumors", vol. 24, pp. 233-240.

Hennink, W.E. & van Nostrum, C.F. 2002, "Novel crosslinking methods to design hydrogels", *Advanced Drug Delivery Reviews*, vol. 54, no. 1, pp. 13-36.

Hern, D.L. & Hubbell, J.A. 1998, "Incorporation of adhesion peptides into nonadhesive hydrogels useful for tissue resurfacing", *Journal of Biomedical Materials Research*, vol. 39, no. 2, pp. 266-276.

Herz, J., Gotthardt, M. & Willnow, T.E. 2000, "Cellular signalling by lipoprotein receptors", vol. 11, pp. 161-166.

Hesse, E., Hefferan, T.E., Tarara, J.E., Haasper, C., Meller, R., Krettek, C., Lu, L. & Yaszemski, M.J. 2010, "Collagen type I hydrogel allows migration, proliferation, and osteogenic differentiation of rat bone marrow stromal cells", *Journal of biomedical materials research.Part A*, vol. 94, no. 2, pp. 442-449.

Hidaka, K., Kanematsu, T., Takeuchi, H., Nakata, M., Kikkawa, U. & Hirata, M. 2001, "Involvement of the phosphoinositide 3-kinase/protein kinase B signaling pathway in

insulin/IGF-I-induced chondrogenesis of the mouse embryonal carcinoma-derived cell line ATDC5", *The international journal of biochemistry & cell biology*, vol. 33, no. 11, pp. 1094-1103.

Hoshikawa, A., Nakayama, Y., Matsuda, T., Oda, H., Nakamura, K. & Mabuchi, K. 2006, "Encapsulation of chondrocytes in photopolymerizable styrenated gelatin for cartilage tissue engineering", *Tissue engineering*, vol. 12, no. 8, pp. 2333-2341.

Hosseinkhani, H., Hosseinkhani, M., Khademhosseini, A., Kobayashi, H. & Tabata, Y. 2006a, "Enhanced angiogenesis through controlled release of basic fibroblast growth factor from peptide amphiphile for tissue regeneration", *Biomaterials*, vol. 27, no. 34, pp. 5836-5844.

Hosseinkhani, H., Hosseinkhani, M., Tian, F., Kobayashi, H. & Tabata, Y. 2006b, "Ectopic bone formation in collagen sponge self-assembled peptide-amphiphile nanofibers hybrid scaffold in a perfusion culture bioreactor", *Biomaterials*, vol. 27, no. 29, pp. 5089-5098.

Howell, B.W. & Herz, J. 2001, "The LDL receptor gene family: signaling functions during development", vol. 11, pp. 74-81.

Hu, B.H. & Messersmith, P.B. 2003, "Rational design of transglutaminase substrate peptides for rapid enzymatic formation of hydrogels", *Journal of the American Chemical*

*Society*, vol. 125, no. 47, pp. 14298-14299.

Hu, B.H. & Messersmith, P.B. 2005, "Enzymatically cross-linked hydrogels and their adhesive strength to biosurfaces", *Orthodontics & craniofacial research*, vol. 8, no. 3, pp. 145-149.

Hu, K., Radhakrishnan, P., Patel, R.V. & Mao, J.J. 2001, "Regional structural and viscoelastic properties of fibrocartilage upon dynamic nanoindentation of the articular condyle", *Journal of structural biology*, vol. 136, no. 1, pp. 46-52.

Hu, M., Kurisawa, M., Deng, R., Teo, C.M., Schumacher, A., Thong, Y.X., Wang, L., Schumacher, K.M. & Ying, J.Y. 2009, "Cell immobilization in gelatin-hydroxyphenylpropionic acid hydrogel fibers", *Biomaterials*, vol. 30, no. 21, pp. 3523-3531.

Hu, M., Kurisawa, M., Deng, R., Teo, C.M., Schumacher, A., Thong, Y.X., Wang, L., Schumacher, K.M. & Ying, J.Y. 2009, "Cell immobilization in gelatin-hydroxyphenylpropionic acid hydrogel fibers", *Biomaterials*, vol. 30, no. 21, pp. 3523-3531.

Hu, W.L., Mazurier, J., Sawatzki, G., Montreuil, J. & Spik, G. 1988, "Lactotransferrin receptor of mouse small-intestinal brush border. Binding characteristics of membrane-bound and triton X-100-solubilized forms", *The Biochemical journal*, vol. 249, no. 2, pp.

435-441.

Huang, G.Y., Zhou, L.H., Zhang, Q.C., Chen, Y.M., Sun, W., Xu, F. & Lu, T.J. 2011, "Microfluidic hydrogels for tissue engineering", *Biofabrication*, vol. 3, no. 1, pp. 012001.

Huang, N., Bethell, D., Card, C., Cornish, J., Marchbank, T., Wyatt, D., Mabery, K. & Playford, R. 2008, "Bioactive recombinant human lactoferrin, derived from rice, stimulates mammalian cell growth", *In vitro cellular & developmental biology. Animal*, vol. 44, no. 10, pp. 464-471.

Hughes-Fulford, M. & Li, C.F. 2011, "The role of FGF-2 and BMP-2 in regulation of gene induction, cell proliferation and mineralization", *Journal of orthopaedic surgery and research*, vol. 6, no. 1, pp. 8.

Hunziker, E.B., Quinn, T.M. & Hauselmann, H.J. 2002, "Quantitative structural organization of normal adult human articular cartilage", *Osteoarthritis and cartilage / OARS, Osteoarthritis Research Society*, vol. 10, no. 7, pp. 564-572.

Hurley, M.M. & Marie, P.J. 2002, "Fibroblast growth factor (FGF) and FGF receptor families in bone." in *Principles of bone biology*, 2nd edition edn, Academic Press, pp. 825-851.

Hurley, W.L., Grieve, R.C., Magura, C.E., Hegarty, H.M. & Zou, S. 1993,

"Electrophoretic comparisons of lactoferrin from bovine mammary secretions, milk neutrophils, and human milk", vol. 76, pp. 377-387.

Hutchens, T.W., Magnuson, J.S. & Yip, T.T. 1989, "Interaction of human lactoferrin with DNA: one-step purification by affinity chromatography on single-stranded DNA-agarose", vol. 26, pp. 618-622.

Hutmacher, D.W. 2000, "Scaffolds in tissue engineering bone and cartilage", *Biomaterials*, vol. 21, no. 24, pp. 2529-2543.

Huynh, D.P., Im, G.J., Chae, S.Y., Lee, K.C. & Lee, D.S. 2009, "Controlled release of insulin from pH/temperature-sensitive injectable pentablock copolymer hydrogel", *Journal of controlled release: official journal of the Controlled Release Society*, vol. 137, no. 1, pp. 20-24.

Hwang, C.M., Sant, S., Masaeli, M., Kachouie, N.N., Zamanian, B., Lee, S.H. & Khademhosseini, A. 2010, "Fabrication of three-dimensional porous cell-laden hydrogel for tissue engineering", *Biofabrication*, vol. 2, no. 3, pp. 035003.

Ieni, A., Barresi, V., Grosso, M., Rosa, M.A. & Tuccari, G. 2009, "Lactoferrin immuno-expression in human normal and neoplastic bone tissue", vol. 27, pp. 364-371.

Ishitani, T., Kishida, S., Hyodo-Miura, J., Ueno, N., Yasuda, J., Waterman, M.,



Shibuya, H., Moon, R.T., Ninomiya-Tsuji, J. & Matsumoto, K. 2003, "The TAK1-NLK mitogen-activated protein kinase cascade functions in the Wnt-5a/Ca(2+) pathway to antagonize Wnt/beta-catenin signaling", *Molecular and cellular biology*, vol. 23, no. 1, pp. 131-139.

Isner, J.M. & Asahara, T. 1999, "Angiogenesis and vasculogenesis as therapeutic strategies for postnatal neovascularization", vol. 103, pp. 1231-1236.

James, E., Xiao, L., Hurley, M.M. & Nair, L.S. 2011, Lactoferrin is a Regulator of FGF Expression in Osteoblast-like MC3T3 cells.

Jeong, B., Bae, Y.H. & Kim, S.W. 2000, "In situ gelation of PEG-PLGA-PEG triblock copolymer aqueous solutions and degradation thereof", *Journal of Biomedical Materials Research*, vol. 50, no. 2, pp. 171-177.

Ji, Z.S. & Mahley, R.W. 1994, "Lactoferrin binding to heparan sulfate proteoglycans and the LDL receptor-related protein. Further evidence supporting the importance of direct binding of remnant lipoproteins to HSPG", vol. 14, pp. 2025-2031.

Jiang, R. & Lonnerdal, B. 2012, "Apo- and holo-lactoferrin stimulate proliferation of mouse crypt cells but through different cellular signaling pathways", *The international journal of biochemistry & cell biology*, vol. 44, no. 1, pp. 91-100.

Jiang, R., Lopez, V., Kelleher, S.L. & Lonnerdal, B. 2011, "Apo- and holo-lactoferrin are both internalized by lactoferrin receptor via clathrin-mediated endocytosis but differentially affect ERK-signaling and cell proliferation in Caco-2 cells", *Journal of cellular physiology*, vol. 226, no. 11, pp. 3022-3031.

Jiang, T., Kumbar, S.G., Nair, L.S. & Laurencin, C.T. 2008, "Biologically active chitosan systems for tissue engineering and regenerative medicine", *Current topics in medicinal chemistry*, vol. 8, no. 4, pp. 354-364.

Jin, R., Hiemstra, C., Zhong, Z. & Feijen, J. 2007, "Enzyme-mediated fast in situ formation of hydrogels from dextran-tyramine conjugates", *Biomaterials*, vol. 28, no. 18, pp. 2791-2800.

Jin, R., Moreira Teixeira, L.S., Dijkstra, P.J., Karperien, M., van Blitterswijk, C.A., Zhong, Z.Y. & Feijen, J. 2009, "Injectable chitosan-based hydrogels for cartilage tissue engineering", *Biomaterials*, vol. 30, no. 13, pp. 2544-2551.

Jin, R., Moreira Teixeira, L.S., Dijkstra, P.J., van Blitterswijk, C.A., Karperien, M. & Feijen, J. 2011, "Chondrogenesis in injectable enzymatically crosslinked heparin/dextran hydrogels", *Journal of controlled release: official journal of the Controlled Release Society*, vol. 152, no. 1, pp. 186-195.

Jin, R., Moreira Teixeira, L.S., Dijkstra, P.J., Zhong, Z., van Blitterswijk, C.A.,

Karperien, M. & Feijen, J. 2010a, "Enzymatically crosslinked dextran-tyramine hydrogels as injectable scaffolds for cartilage tissue engineering", *Tissue engineering. Part A*, vol. 16, no. 8, pp. 2429-2440.

Jin, R., Teixeira, L.S., Dijkstra, P.J., van Blitterswijk, C.A., Karperien, M. & Feijen, J. 2010b, "Enzymatically-crosslinked injectable hydrogels based on biomimetic dextran-hyaluronic acid conjugates for cartilage tissue engineering", *Biomaterials*, vol. 31, no. 11, pp. 3103-3113.

Jin, T., George Fantus, I. & Sun, J. 2008, "Wnt and beyond Wnt: multiple mechanisms control the transcriptional property of beta-catenin", *Cellular signalling*, vol. 20, no. 10, pp. 1697-1704.

Joa, S., Engelb, A.G. & Mikos, A.G. 2000, "Synthesis of poly(ethylene glycol)-tethered poly(propylene fumarate) and its modification with GRGD peptide", *Polymer*, vol. 41, no. 21, pp. 7595-7604.

Jonasch, E., Stadler, W.M., Bukowski, R.M., Hayes, T.G., Varadhachary, A., Malik, R., Figlin, R.A. & Srinivas, S. 2008, "Phase 2 trial of talactoferrin in previously treated patients with metastatic renal cell carcinoma", vol. 113, pp. 72-77.

Jung, H.H., Park, K. & Han, D.K. 2010, "Preparation of TGF-beta1-conjugated biodegradable pluronic F127 hydrogel and its application with adipose-derived stem

cells", *Journal of controlled release : official journal of the Controlled Release Society*, vol. 147, no. 1, pp. 84-91.

Jung, Y., Wang, J., Schneider, A., Sun, Y.X., Koh-Paige, A.J., Osman, N.I., McCauley, L.K. & Taichman, R.S. 2006, "Regulation of SDF-1 (CXCL12) production by osteoblasts; a possible mechanism for stem cell homing", *Bone*, vol. 38, no. 4, pp. 497-508.

Kaliman, P., Vinals, F., Testar, X., Palacin, M. & Zorzano, A. 1996, "Phosphatidylinositol 3-kinase inhibitors block differentiation of skeletal muscle cells", *The Journal of biological chemistry*, vol. 271, no. 32, pp. 19146-19151.

Kanczler, J.M., Ginty, P.J., White, L., Clarke, N.M., Howdle, S.M., Shakesheff, K.M. & Oreffo, R.O. 2010, "The effect of the delivery of vascular endothelial growth factor and bone morphogenic protein-2 to osteoprogenitor cell populations on bone formation", *Biomaterials*, vol. 31, no. 6, pp. 1242-1250.

Kanczler, J.M., Ginty, P.J., White, L., Clarke, N.M., Howdle, S.M., Shakesheff, K.M. & Oreffo, R.O. 2010, "The effect of the delivery of vascular endothelial growth factor and bone morphogenic protein-2 to osteoprogenitor cell populations on bone formation", *Biomaterials*, vol. 31, no. 6, pp. 1242-1250.

Kasper, F.K., Tanahashi, K., Fisher, J.P. & Mikos, A.G. 2009, "Synthesis of

poly(propylene fumarate)", *Nature protocols*, vol. 4, no. 4, pp. 518-525.

Kawaguchi, H., Pilbeam, C.C., Gronowicz, G., Abreu, C., Fletcher, B.S., Herschman, H.R., Raisz, L.G. & Hurley, M.M. 1995, "Transcriptional induction of prostaglandin G/H synthase-2 by basic fibroblast growth factor", *The Journal of clinical investigation*, vol. 96, no. 2, pp. 923-930.

Kawasaki, A., Torii, K., Yamashita, Y., Nishizawa, K., Kanekura, K., Katada, M., Ito, M., Nishimoto, I., Terashita, K., Aiso, S. & Matsuoka, M. 2007, "Wnt5a promotes adhesion of human dermal fibroblasts by triggering a phosphatidylinositol-3 kinase/Akt signal", *Cellular signalling*, vol. 19, no. 12, pp. 2498-2506.

Kelly, O.G., Pinson, K.I. & Skarnes, W.C. 2004, "The Wnt co-receptors Lrp5 and Lrp6 are essential for gastrulation in mice", *Development (Cambridge, England)*, vol. 131, no. 12, pp. 2803-2815.

Kempen, D.H., Lu, L., Heijink, A., Hefferan, T.E., Creemers, L.B., Maran, A., Yaszemski, M.J. & Dhert, W.J. 2009, "Effect of local sequential VEGF and BMP-2 delivery on ectopic and orthotopic bone regeneration", *Biomaterials*, vol. 30, no. 14, pp. 2816-2825.

Keskin, D.S., Tezcaner, A., Korkusuz, P., Korkusuz, F. & Hasirci, V. 2005, "Collagen-chondroitin sulfate-based PLLA-SAIB-coated rhBMP-2 delivery system for bone repair",

*Biomaterials*, vol. 26, no. 18, pp. 4023-4034.

Khatiwala, C.B., Peyton, S.R. & Putnam, A.J. 2006, "Intrinsic mechanical properties of the extracellular matrix affect the behavior of pre-osteoblastic MC3T3-E1 cells", *American journal of physiology. Cell physiology*, vol. 290, no. 6, pp. C1640-50.

Kim, C.W., Son, K.N., Choi, S.Y. & Kim, J. 2006, "Human lactoferrin upregulates expression of KDR/Flk-1 and stimulates VEGF-A-mediated endothelial cell proliferation and migration", *FEBS letters*, vol. 580, no. 18, pp. 4332-4336.

Kim, K., Yeatts, A., Dean, D. & Fisher, J.P. 2010, "Stereolithographic bone scaffold design parameters: osteogenic differentiation and signal expression", *Tissue engineering. Part B, Reviews*, vol. 16, no. 5, pp. 523-539.

Kim, K.S., Park, S.J., Yang, J.A., Jeon, J.H., Bhang, S.H., Kim, B.S. & Hahn, S.K. 2011, "Injectable hyaluronic acid-tyramine hydrogels for the treatment of rheumatoid arthritis", *Acta biomaterialia*, vol. 7, no. 2, pp. 666-674.

Kim, T.K., Sharma, B., Williams, C.G., Ruffner, M.A., Malik, A., McFarland, E.G. & Elisseeff, J.H. 2003, "Experimental model for cartilage tissue engineering to regenerate the zonal organization of articular cartilage", *Osteoarthritis and cartilage / OARS, Osteoarthritis Research Society*, vol. 11, no. 9, pp. 653-664.

Kimber, I., Cumberbatch, M., Dearman, R.J., Headon, D.R., Bhushan, M. & Griffiths, C.E. 2002, "Lactoferrin: influences on Langerhans cells, epidermal cytokines, and cutaneous inflammation", vol. 80, pp. 103-107.

Kloxin, A.M., Kloxin, C.J., Bowman, C.N. & Anseth, K.S. 2010, "Mechanical properties of cellularly responsive hydrogels and their experimental determination", *Advanced materials (Deerfield Beach, Fla.)*, vol. 22, no. 31, pp. 3484-3494.

Kobayashi, S., Uyama, H. & Kimura, S. 2001, "Enzymatic polymerization", *Chemical reviews*, vol. 101, no. 12, pp. 3793-3818.

Komori, T. 2002, "Runx2, a multifunctional transcription factor in skeletal development", *Journal of cellular biochemistry*, vol. 87, no. 1, pp. 1-8.

Kopecek, J. & Yang, J. 2009, "Peptide-directed self-assembly of hydrogels", *Acta biomaterialia*, vol. 5, no. 3, pp. 805-816.

Kruzel, M.L. 2003, "Role of lactoferrin in development of inflammation.", vol. 57, pp. 377-404.

Kruzel, M.L., Harari, Y., Mailman, D., Actor, J.K. & Zimecki, M. 2002, "Differential effects of prophylactic, concurrent and therapeutic lactoferrin treatment on LPS-induced inflammatory responses in mice", vol. 130, pp. 25-31.

Kudo, O., Fujikawa, Y., Itonaga, I., Sabokbar, A., Torisu, T. & Athanasou, N.A. 2002, "Proinflammatory cytokine (TNF $\alpha$ /IL-1 $\alpha$ ) induction of human osteoclast formation", vol. 198, pp. 220-227.

Kuhl, M., Sheldahl, L.C., Park, M., Miller, J.R. & Moon, R.T. 2000, "The Wnt/Ca<sup>2+</sup> pathway: a new vertebrate Wnt signaling pathway takes shape", *Trends in genetics: TIG*, vol. 16, no. 7, pp. 279-283.

Kurisawa, M., Chung, J.E., Yang, Y.Y., Gao, S.J. & Uyama, H. 2005, "Injectable biodegradable hydrogels composed of hyaluronic acid-tyramine conjugates for drug delivery and tissue engineering", *Chemical communications (Cambridge, England)*, vol. (34), no. 34, pp. 4312-4314.

Kuroda, R., Usas, A., Kubo, S., Corsi, K., Peng, H., Rose, T., Cummins, J., Fu, F.H. & Huard, J. 2006, "Cartilage repair using bone morphogenetic protein 4 and muscle-derived stem cells", *Arthritis and Rheumatism*, vol. 54, no. 2, pp. 433-442.

Kuwahara, K., Yang, Z., Slack, G.C., Nimni, M.E. & Han, B. 2010, "Cell delivery using an injectable and adhesive transglutaminase-gelatin gel", *Tissue engineering. Part C, Methods*, vol. 16, no. 4, pp. 609-618.

Kwon, Y.J. & Peng, C.A. 2002, "Calcium-alginate gel bead cross-linked with gelatin



as microcarrier for anchorage-dependent cell culture", *BioTechniques*, vol. 33, no. 1, pp. 212-4, 216, 218.

Lai, C.F. & Cheng, S.L. 2002, "Signal transductions induced by bone morphogenetic protein-2 and transforming growth factor-beta in normal human osteoblastic cells", *The Journal of biological chemistry*, vol. 277, no. 18, pp. 15514-15522.

Lai, J.Y. & Li, Y.T. 2010, "Functional assessment of cross-linked porous gelatin hydrogels for bioengineered cell sheet carriers", *Biomacromolecules*, vol. 11, no. 5, pp. 1387-1397.

Lambert, L.A. 2012, "Molecular evolution of the transferrin family and associated receptors", *Biochimica et biophysica acta*, vol. 1820, no. 3, pp. 244-255.

Landers, R., Hubner, U., Schmelzeisen, R. & Mulhaupt, R. 2002, "Rapid prototyping of scaffolds derived from thermoreversible hydrogels and tailored for applications in tissue engineering", *Biomaterials*, vol. 23, no. 23, pp. 4437-4447.

Laurencin, C.T., Ambrosio, A.M., Borden, M.D. & Cooper, J.A., Jr 1999, "Tissue engineering: orthopedic applications", *Annual Review of Biomedical Engineering*, vol. 1, pp. 19-46.

Laurencin, C.T., Attawia, M.A., Lu, L.Q., Borden, M.D., Lu, H.H., Gorum, W.J. &

Lieberman, J.R. 2001, "Poly(lactide-co-glycolide)/hydroxyapatite delivery of BMP-2-producing cells: a regional gene therapy approach to bone regeneration", *Biomaterials*, vol. 22, no. 11, pp. 1271-1277.

Lauw, F.N., Pajkrt, D., Hack, C.E., Kurimoto, M., van Deventer, S.J. & van, d.P. 2000, "Proinflammatory effects of IL-10 during human endotoxemia", vol. 165, pp. 2783-2789.

Lee, F., Chung, J.E. & Kurisawa, M. 2009, "An injectable hyaluronic acid-tyramine hydrogel system for protein delivery", *Journal of controlled release: official journal of the Controlled Release Society*, vol. 134, no. 3, pp. 186-193.

Lee, F., Chung, J.E. & Kurisawa, M. 2009, "An injectable hyaluronic acid-tyramine hydrogel system for protein delivery", *Journal of controlled release : official journal of the Controlled Release Society*, vol. 134, no. 3, pp. 186-193.

Lee, J.S., Wagoner Johnson, A.J. & Murphy, W.L. 2010, "A modular, hydroxyapatite-binding version of vascular endothelial growth factor", *Advanced materials (Deerfield Beach, Fla.)*, vol. 22, no. 48, pp. 5494-5498.

Lee, P.Y., Cobain, E., Huard, J. & Huang, L. 2007, "Thermosensitive hydrogel PEG-PLGA-PEG enhances engraftment of muscle-derived stem cells and promotes healing in diabetic wound", *Molecular therapy : the journal of the American Society of Gene Therapy*, vol. 15, no. 6, pp. 1189-1194.

Lee, S.H., Pyo, C.W., Hahm, D.H., Kim, J. & Choi, S.Y. 2009, "Iron-saturated lactoferrin stimulates cell cycle progression through PI3K/Akt pathway", *Molecules and cells*, vol. 28, no. 1, pp. 37-42.

Lee, W.J., Farmer, J.L., Hilty, M. & Kim, Y.B. 1998, "The protective effects of lactoferrin feeding against endotoxin lethal shock in germfree piglets", vol. 66, pp. 1421-1426.

Lee, Y., Bhattarai, G., Aryal, S., Lee, N., Lee, M., Kim, T., Jhee, E., Kim, H. & Yi, H. 2010, vol. 256, no. 20, pp. 5887.

Legrand, D., Ellass, E., Carpentier, M. & Mazurier, J. 2005, "Lactoferrin: a modulator of immune and inflammatory responses", *Cellular and molecular life sciences : CMLS*, vol. 62, no. 22, pp. 2549-2559.

Levay, P.F. & Viljoen, M. 1995b, "Lactoferrin: a general review", *Haematologica*, vol. 80, no. 3, pp. 252-267.

Li, X., Gao, Y., Kuang, Y. & Xu, B. 2010, "Enzymatic formation of a photoresponsive supramolecular hydrogel", *Chemical communications (Cambridge, England)*, vol. 46, no. 29, pp. 5364-5366.

Li, X., Qin, L., Bergenstock, M., Bevelock, L.M., Novack, D.V. & Partridge, N.C. 2007, "Parathyroid hormone stimulates osteoblastic expression of MCP-1 to recruit and increase the fusion of pre/osteoclasts", *The Journal of biological chemistry*, vol. 282, no. 45, pp. 33098-33106.

Li, Y., Cam, J. & Bu, G. 2001, "Low-density lipoprotein receptor family: endocytosis and signal transduction", vol. 23, pp. 53-67.

Liao, H., Zhang, H. & Chen, W. 2009, "Differential physical, rheological, and biological properties of rapid in situ gelable hydrogels composed of oxidized alginate and gelatin derived from marine or porcine sources", *Journal of materials science. Materials in medicine*, vol. 20, no. 6, pp. 1263-1271.

Liao, H.T., Chen, C.T. & Chen, J.P. 2011, "Osteogenic Differentiation and Ectopic Bone Formation of Canine Bone Marrow-Derived Mesenchymal Stem Cells in Injectable Thermo-Responsive Polymer Hydrogel", *Tissue engineering. Part C, Methods*, .

Linkhart, T.A., Mohan, S. & Baylink, D.J. 1996, "Growth factors for bone growth and repair: IGF, TGF beta and BMP", *Bone*, vol. 19, no. 1 Suppl, pp. 1S-12S.

Liu, X., Das, A.M., Seideman, J., Griswold, D., Afuh, C.N., Kobayashi, T., Abe, S., Fang, Q., Hashimoto, M., Kim, H., Wang, X., Shen, L., Kawasaki, S. & Rennard, S.I. 2007, "The CC chemokine ligand 2 (CCL2) mediates fibroblast survival through IL-6",

American journal of respiratory cell and molecular biology, vol. 37, no. 1, pp. 121-128.

Liu, X., Smith, L.A., Hu, J. & Ma, P.X. 2009, "Biomimetic nanofibrous gelatin/apatite composite scaffolds for bone tissue engineering", *Biomaterials*, vol. 30, no. 12, pp. 2252-2258.

Liu, Y., Lu, W.L., Wang, J.C., Zhang, X., Zhang, H., Wang, X.Q., Zhou, T.Y. & Zhang, Q. 2007, "Controlled delivery of recombinant hirudin based on thermo-sensitive Pluronic F127 hydrogel for subcutaneous administration: In vitro and in vivo characterization", *Journal of controlled release : official journal of the Controlled Release Society*, vol. 117, no. 3, pp. 387-395.

Lo, C.M., Wang, H.B., Dembo, M. & Wang, Y.L. 2000, "Cell movement is guided by the rigidity of the substrate", *Biophysical journal*, vol. 79, no. 1, pp. 144-152.

Logan, C.Y. & Nusse, R. 2004, "The Wnt signaling pathway in development and disease", *Annual Review of Cell and Developmental Biology*, vol. 20, pp. 781-810.

Lorget, F., Clough, J., Oliveira, M., Daury, M.C., Sabokbar, A. & Offord, E. 2002, "Lactoferrin reduces in vitro osteoclast differentiation and resorbing activity", *Biochemical and biophysical research communications*, vol. 296, no. 2, pp. 261-266.

Lu, L., Stamatas, G.N. & Mikos, A.G. 2000, "Controlled release of transforming growth factor beta1 from biodegradable polymer microparticles", *Journal of Biomedical*

*Materials Research*, vol. 50, no. 3, pp. 440-451.

Lu, L., Yaszemski, M.J. & Mikos, A.G. 2001, "TGF-beta1 release from biodegradable polymer microparticles: its effects on marrow stromal osteoblast function", *The Journal of bone and joint surgery.American volume*, vol. 83-A Suppl 1, no. Pt 2, pp. S82-91.

Luca, L., Rougemont, A.L., Walpoth, B.H., Boure, L., Tami, A., Anderson, J.M., Jordan, O. & Gurny, R. 2011, "Injectable rhBMP-2-loaded chitosan hydrogel composite: osteoinduction at ectopic site and in segmental long bone defect", *Journal of biomedical materials research. Part A*, vol. 96, no. 1, pp. 66-74.

Lutolf, M.P. & Hubbell, J.A. 2003, "Synthesis and physicochemical characterization of end-linked poly(ethylene glycol)-co-peptide hydrogels formed by Michael-type addition", *Biomacromolecules*, vol. 4, no. 3, pp. 713-722.

Ma, L. & Wang, H.Y. 2006, "Suppression of cyclic GMP-dependent protein kinase is essential to the Wnt/cGMP/Ca<sup>2+</sup> pathway", *The Journal of biological chemistry*, vol. 281, no. 41, pp. 30990-31001.

Ma, P.X. & Elisseeff, J. 2005, *Scaffolding In Tissue Engineering*, CRC Press.

Machnicki, M., Zimecki, M. & Zagulski, T. 1993, "Lactoferrin regulates the release of tumour necrosis factor alpha and interleukin 6 in vivo", vol. 74, pp. 433-439.

Mader, J.S., Smyth, D., Marshall, J. & Hoskin, D.W. 2006, "Bovine lactoferricin inhibits basic fibroblast growth factor- and vascular endothelial growth factor165-induced angiogenesis by competing for heparin-like binding sites on endothelial cells", vol. 169, pp. 1753-1766.

Maes, C., Goossens, S., Bartunkova, S., Drogat, B., Coenegrachts, L., Stockmans, I., Moermans, K., Nyabi, O., Haigh, K., Naessens, M., Haenebalcke, L., Tuckermann, J.P., Tjwa, M., Carmeliet, P., Mandic, V., David, J.P., Behrens, A., Nagy, A., Carmeliet, G. & Haigh, J.J. 2010, "Increased skeletal VEGF enhances beta-catenin activity and results in excessively ossified bones", *The EMBO journal*, vol. 29, no. 2, pp. 424-441.

Mäkelä, M., Salo, T., Uitto, V.J. & Larjava, H. 1994, "Matrix metalloproteinases (MMP-2 and MMP-9) of the oral cavity: cellular origin and relationship to periodontal status", vol. 73, pp. 1397-1406.

Malet, A., Bournaud, E., Lan, A., Mikogami, T., Tome, D. & Blais, A. 2011, "Bovine lactoferrin improves bone status of ovariectomized mice via immune function modulation", *Bone*, vol. 48, no. 5, pp. 1028-1035.

Manassero, M., Viateau, V., Retorillo, J., Deschepper, M., Bensidhoum, M., Logeart-Avramoglou, D. & Petite, H. 2012, "In vivo Evaluation of Human Mesenchymal Stem Cells Survival in a Large Segmental Bone Defect in Mice.", *Orthopaedic Research*

Society, pp. Poster 0406.

Mann, B.K., Schmedlen, R.H. & West, J.L. 2001, "Tethered-TGF-beta increases extracellular matrix production of vascular smooth muscle cells", *Biomaterials*, vol. 22, no. 5, pp. 439-444.

Mann, B.K., Tsai, A.T., Scott-Burden, T. & West, J.L. 1999, "Modification of surfaces with cell adhesion peptides alters extracellular matrix deposition", *Biomaterials*, vol. 20, no. 23-24, pp. 2281-2286.

Mann, D.M., Romm, E. & Migliorini, M. 1994, "Delineation of the glycosaminoglycan-binding site in the human inflammatory response protein lactoferrin", vol. 269, pp. 23661-23667.

Manolagas, S.C. 2000, "Birth and death of bone cells: basic regulatory mechanisms and implications for the pathogenesis and treatment of osteoporosis", vol. 21, pp. 115-137.

Matsuo, K. & Irie, N. 2008, "Osteoclast-osteoblast communication", *Archives of Biochemistry and Biophysics*, vol. 473, no. 2, pp. 201-209.

Mbalaviele, G., Sheikh, S., Stains, J.P., Salazar, V.S., Cheng, S.L., Chen, D. & Civitelli, R. 2005, "Beta-catenin and BMP-2 synergize to promote osteoblast



differentiation and new bone formation", *Journal of cellular biochemistry*, vol. 94, no. 2, pp. 403-418.

McHale, M.K., Setton, L.A. & Chilkoti, A. 2005, "Synthesis and in vitro evaluation of enzymatically cross-linked elastin-like polypeptide gels for cartilaginous tissue repair", *Tissue engineering*, vol. 11, no. 11-12, pp. 1768-1779.

Meijer, G.J., de Bruijn, J.D., Koole, R. & van Blitterswijk, C.A. 2008, "Cell based bone tissue engineering in jaw defects", *Biomaterials*, vol. 29, no. 21, pp. 3053-3061.

Meilinger, M., Haumer, M., Szakmary, K.A., SteinbÄck, F., Scheiber, B., Goldenberg, H. & Huettinger, M. 1995, "Removal of lactoferrin from plasma is mediated by binding to low density lipoprotein receptor-related protein/alpha 2-macroglobulin receptor and transport to endosomes", vol. 360, pp. 70-74.

Menger, F.M. & Caran, K.L. 2000, "Anatomy of a Gel. Amino Acid Derivatives That Rigidify Water at Submillimolar Concentrations", *Journal of the American Chemical Society*, vol. 122, no. 47, pp. 11679-11691.

Miljkovic, N.D., Lin, Y.C., Cherubino, M., Minter, D. & Marra, K.G. 2009, "A novel injectable hydrogel in combination with a surgical sealant in a rat knee osteochondral defect model", *Knee surgery, sports traumatology, arthroscopy : official journal of the ESSKA*, vol. 17, no. 11, pp. 1326-1331.

Miller, J.R. 2002, "The Wnts", *Genome biology*, vol. 3, no. 1, pp. REVIEWS3001.

Mimura, T., Imai, S., Okumura, N., Li, L., Nishizawa, K., Araki, S., Ueba, H., Kubo, M., Mori, K. & Matsusue, Y. 2011, "Spatiotemporal control of proliferation and differentiation of bone marrow-derived mesenchymal stem cells recruited using collagen hydrogel for repair of articular cartilage defects", *Journal of biomedical materials research.Part B, Applied biomaterials*, vol. 98B, no. 2, pp. 360-368.

Miyauchi, H., Hashimoto, S., Nakajima, M., Shinoda, I., Fukuwatari, Y. & Hayasawa, H. 1998, "Bovine lactoferrin stimulates the phagocytic activity of human neutrophils: identification of its active domain", vol. 187, pp. 34-37.

Miyazawa, K., Mantel, C., Lu, L., Morrison, D.C. & Broxmeyer, H.E. 1991, "Lactoferrin-lipopolysaccharide interactions. Effect on lactoferrin binding to monocyte/macrophage-differentiated HL-60 cells", vol. 146, pp. 723-729.

Moon, R.T., Bowerman, B., Boutros, M. & Perrimon, N. 2002, "The promise and perils of Wnt signaling through beta-catenin", *Science (New York, N.Y.)*, vol. 296, no. 5573, pp. 1644-1646.

Morita, Y., Matsuyama, H., Serizawa, A., Takeya, T. & Kawakami, H. 2008, "Identification of angiogenin as the osteoclastic bone resorption-inhibitory factor in

bovine milk", vol. 42, pp. 380-387.

Mosiewicz, K.A., Johnsson, K. & Lutolf, M.P. 2010, "Phosphopantetheinyl transferase-catalyzed formation of bioactive hydrogels for tissue engineering", *Journal of the American Chemical Society*, vol. 132, no. 17, pp. 5972-5974.

Mountziaris, P.M. & Mikos, A.G. 2008, "Modulation of the inflammatory response for enhanced bone tissue regeneration", *Tissue engineering.Part B, Reviews*, vol. 14, no. 2, pp. 179-186.

Mukozawa, A., Ueki, K., Marukawa, K., Okabe, K., Moroi, A. & Nakagawa, K. 2011, "Bone healing of critical-sized nasal defects in rabbits by statins in two different carriers", *Clinical oral implants research*, vol. 22, no. 11, pp. 1327-1335.

Mundlos, S. 1994, "Expression patterns of matrix genes during human skeletal development", *Progress in histochemistry and cytochemistry*, vol. 28, no. 3, pp. 1-47.

Nair, L.S. & Laurencin, C.T. 2006, "Polymers as biomaterials for tissue engineering and controlled drug delivery", *Advances in Biochemical Engineering/Biotechnology*, vol. 102, pp. 47-90.

Nair, L.S. Lactoferrin-based biomaterials for Tissue Regeneration and Drug Delivery.

Nair, L.S., Starnes, T., Ko, J.W. & Laurencin, C.T. 2007, "Development of injectable thermogelling chitosan-inorganic phosphate solutions for biomedical applications", *Biomacromolecules*, vol. 8, no. 12, pp. 3779-3785.

Nakajima, K.I., Kanno, Y., Nakamura, M., Gao, X.D., Kawamura, A., Itoh, F. & Ishisaki, A. 2011, "Bovine milk lactoferrin induces synthesis of the angiogenic factors VEGF and FGF2 in osteoblasts via the p44/p42 MAP kinase pathway", *Biometals : an international journal on the role of metal ions in biology, biochemistry, and medicine*, .

Nakano, Y., Addison, W.N. & Kaartinen, M.T. 2007, "ATP-mediated mineralization of MC3T3-E1 osteoblast cultures", *Bone*, vol. 41, no. 4, pp. 549-561.

Nakayama, K., Otsuki, K., Yakuwa, K., Hasegawa, A., Sawada, M., Mitsukawa, K., Chiba, H., Nagatsuka, M. & Okai, T. 2008, "Recombinant human lactoferrin inhibits matrix metalloproteinase (MMP-2, MMP-3, and MMP-9) activity in a rabbit preterm delivery model", vol. 34, pp. 931-934.

Nandi, S., Yalda, D., Lu, S., Nikolov, Z., Misaki, R., Fujiyama, K. & Huang, N. 2005, "Process development and economic evaluation of recombinant human lactoferrin expressed in rice grain", vol. 14, pp. 237-249.

Naot, D., Chhana, A., Matthews, B.G., Callon, K.E., Tong, P.C., Lin, J.M., Costa, J.L., Watson, M., Grey, A.B. & Cornish, J. 2011, "Molecular mechanisms involved in the

mitogenic effect of lactoferrin in osteoblasts", *Bone*, vol. 49, no. 2, pp. 217-224.

Naot, D., Grey, A., Reid, I.R. & Cornish, J. 2005, "Lactoferrin--a novel bone growth factor", vol. 3, pp. 93-101.

Nave, B.T., Ouwens, M., Withers, D.J., Alessi, D.R. & Shepherd, P.R. 1999, "Mammalian target of rapamycin is a direct target for protein kinase B: identification of a convergence point for opposing effects of insulin and amino-acid deficiency on protein translation", *The Biochemical journal*, vol. 344 Pt 2, pp. 427-431.

Neels, J.G., van Den Berg, B.M., Lookene, A., Olivecrona, G., Pannekoek, H. & van Zonneveld, A.J. 1999, "The second and fourth cluster of class A cysteine-rich repeats of the low density lipoprotein receptor-related protein share ligand-binding properties", *The Journal of biological chemistry*, vol. 274, no. 44, pp. 31305-31311.

Nefussi, J.R., Brami, G., Modrowski, D., Oboeuf, M. & Forest, N. 1997, "Sequential expression of bone matrix proteins during rat calvaria osteoblast differentiation and bone nodule formation in vitro", *The journal of histochemistry and cytochemistry : official journal of the Histochemistry Society*, vol. 45, no. 4, pp. 493-503.

Nemoto, E., Ebe, Y., Kanaya, S., Tsuchiya, M., Nakamura, T., Tamura, M. & Shimauchi, H. 2012, "Wnt5a signaling is a substantial constituent in bone morphogenetic protein-2-mediated osteoblastogenesis", *Biochemical and biophysical research*

communications, .

Nguyen, M.K. & Lee, D.S. 2010, "Injectable biodegradable hydrogels", *Macromolecular bioscience*, vol. 10, no. 6, pp. 563-579.

Nguyen, T.P. & Lee, B.T. 2011, "Fabrication of oxidized alginate-gelatin-BCP hydrogels and evaluation of the microstructure, material properties and biocompatibility for bone tissue regeneration", *Journal of Biomaterials Applications*, .

Nicholson, G.C., Malakellis, M., Collier, F.M., Cameron, P.U., Holloway, W.R., Gough, T.J., Gregorio-King, C., Kirkland, M.A. & Myers, D.E. 2000, "Induction of osteoclasts from CD14-positive human peripheral blood mononuclear cells by receptor activator of nuclear factor kappaB ligand (RANKL)", vol. 99, pp. 133-140.

Nicodemus, G.D. & Bryant, S.J. 2008, "Cell encapsulation in biodegradable hydrogels for tissue engineering applications", *Tissue engineering.Part B, Reviews*, vol. 14, no. 2, pp. 149-165.

Nie, T., Baldwin, A., Yamaguchi, N. & Kiick, K.L. 2007, "Production of heparin-functionalized hydrogels for the development of responsive and controlled growth factor delivery systems", *Journal of controlled release : official journal of the Controlled Release Society*, vol. 122, no. 3, pp. 287-296.

Niemeier, A., Kassem, M., Toedter, K., Wendt, D., Ruether, W., Beisiegel, U. & Heeren, J. 2005, "Expression of LRP1 by human osteoblasts: a mechanism for the delivery of lipoproteins and vitamin K1 to bone", vol. 20, pp. 283-293.

Nishida, T., Kubota, S., Kojima, S., Kuboki, T., Nakao, K., Kushibiki, T., Tabata, Y. & Takigawa, M. 2004, "Regeneration of defects in articular cartilage in rat knee joints by CCN2 (connective tissue growth factor)", *Journal of bone and mineral research : the official journal of the American Society for Bone and Mineral Research*, vol. 19, no. 8, pp. 1308-1319.

Norrby, K. 2004, "Human apo-lactoferrin enhances angiogenesis mediated by vascular endothelial growth factor A in vivo", vol. 41, pp. 293-304.

Norrby, K., Mattsby-Baltzer, I., Innocenti, M. & Tuneberg, S. 2001, "Orally administered bovine lactoferrin systemically inhibits VEGF(165)-mediated angiogenesis in the rat", vol. 91, pp. 236-240.

Novak, A. & Dedhar, S. 1999, "Signaling through beta-catenin and Lef/Tcf", *Cellular and molecular life sciences : CMLS*, vol. 56, no. 5-6, pp. 523-537.

O'Dell, S.D. & Day, I.N. 1998, "Insulin-like growth factor II (IGF-II)", *The international journal of biochemistry & cell biology*, vol. 30, no. 7, pp. 767-771.

Ogushi, Y., Sakai, S. & Kawakami, K. 2007, "Synthesis of enzymatically-gellable carboxymethylcellulose for biomedical applications", *Journal of bioscience and bioengineering*, vol. 104, no. 1, pp. 30-33.

Okino, H., Nakayama, Y., Tanaka, M. & Matsuda, T. 2002, "In situ hydrogelation of photocurable gelatin and drug release", *Journal of Biomedical Materials Research*, vol. 59, no. 2, pp. 233-245.

Olivares-Navarrete, R., Hyzy, S.L., Park, J.H., Dunn, G.R., Haithcock, D.A., Wasilewski, C.E., Boyan, B.D. & Schwartz, Z. 2011, "Mediation of osteogenic differentiation of human mesenchymal stem cells on titanium surfaces by a Wnt-integrin feedback loop", *Biomaterials*, vol. 32, no. 27, pp. 6399-6411.

Olson, D.J. & Gibo, D.M. 1998, "Antisense wnt-5a mimics wnt-1-mediated C57MG mammary epithelial cell transformation", *Experimental cell research*, vol. 241, no. 1, pp. 134-141.

Orr, A.W., Pedraza, C.E., Pallero, M.A., Elzie, C.A., Goicoechea, S., Strickland, D.K. & Murphy-Ullrich, J.E. 2003, "Low density lipoprotein receptor-related protein is a calreticulin coreceptor that signals focal adhesion disassembly", *The Journal of cell biology*, vol. 161, no. 6, pp. 1179-1189.

Owen, T.A., Aronow, M.S., Barone, L.M., Bettencourt, B., Stein, G.S. & Lian, J.B.



1991, "Pleiotropic effects of vitamin D on osteoblast gene expression are related to the proliferative and differentiated state of the bone cell phenotype: dependency upon basal levels of gene expression, duration of exposure, and bone matrix competency in normal rat osteoblast cultures", *Endocrinology*, vol. 128, no. 3, pp. 1496-1504.

Papadopoulos, A., Bichara, D.A., Zhao, X., Ibusuki, S., Randolph, M.A., Anseth, K.S. & Yaremchuk, M.J. 2011, "Injectable and photopolymerizable tissue-engineered auricular cartilage using poly(ethylene glycol) dimethacrylate copolymer hydrogels", *Tissue engineering.Part A*, vol. 17, no. 1-2, pp. 161-169.

Paramonov, S.E., Jun, H.W. & Hartgerink, J.D. 2006, "Self-assembly of peptide-amphiphile nanofibers: the roles of hydrogen bonding and amphiphilic packing", *Journal of the American Chemical Society*, vol. 128, no. 22, pp. 7291-7298.

Parfitt, A.M. 1976, "The actions of parathyroid hormone on bone: relation to bone remodeling and turnover, calcium homeostasis, and metabolic bone disease. Part IV of IV parts: The state of the bones in uremic hyperparathyroidism--the mechanisms of skeletal resistance to PTH in renal failure and pseudohypoparathyroidism and the role of PTH in osteoporosis, osteopetrosis, and osteofluorosis", *Metabolism: clinical and experimental*, vol. 25, no. 10, pp. 1157-1188.

Park, K.M., Ko, K.S., Joung, Y.K., Shin, H. & Park, K.D. 2011, "In situ cross-linkable gelatin-poly(ethylene glycol)-tyramine hydrogel via enzyme-mediated reaction for tissue

regenerative medicine", *Journal of Materials Chemistry*, vol. 21, no. 35, pp. 13180-13187.

Park, K.M., Lee, S.Y., Joung, Y.K., Na, J.S., Lee, M.C. & Park, K.D. 2009, "Thermosensitive chitosan-Pluronic hydrogel as an injectable cell delivery carrier for cartilage regeneration", *Acta biomaterialia*, vol. 5, no. 6, pp. 1956-1965.

Patel, Z.S., Young, S., Tabata, Y., Jansen, J.A., Wong, M.E. & Mikos, A.G. 2008, "Dual delivery of an angiogenic and an osteogenic growth factor for bone regeneration in a critical size defect model", *Bone*, vol. 43, no. 5, pp. 931-940.

Payne, R.G., Yaszemski, M.J., Yasko, A.W. & Mikos, A.G. 2002, "Development of an injectable, in situ crosslinkable, degradable polymeric carrier for osteogenic cell populations. Part 1. Encapsulation of marrow stromal osteoblasts in surface crosslinked gelatin microparticles", *Biomaterials*, vol. 23, no. 22, pp. 4359-4371.

Peifer, M. & Polakis, P. 2000, "Wnt signaling in oncogenesis and embryogenesis--a look outside the nucleus", *Science (New York, N.Y.)*, vol. 287, no. 5458, pp. 1606-1609.

Pelham, R.J., Jr & Wang, Y. 1997, "Cell locomotion and focal adhesions are regulated by substrate flexibility", *Proceedings of the National Academy of Sciences of the United States of America*, vol. 94, no. 25, pp. 13661-13665.

Peng, S., Hua, J., Cao, X. & Wang, H. 2010, "Gelatin Induces Trophectoderm Differentiation of Mouse Embryonic Stem Cells.", *Cell Biology International*, .

Peppas, N.A. & Sahlin, J.J. 1996, "Hydrogels as mucoadhesive and bioadhesive materials: a review", *Biomaterials*, vol. 17, no. 16, pp. 1553-1561.

Peter, S.J., Lu, L., Kim, D.J., Stamatias, G.N., Miller, M.J., Yaszemski, M.J. & Mikos, A.G. 2000, "Effects of transforming growth factor beta1 released from biodegradable polymer microparticles on marrow stromal osteoblasts cultured on poly(propylene fumarate) substrates", *Journal of Biomedical Materials Research*, vol. 50, no. 3, pp. 452-462.

Peter, S.J., Yaszemski, M.J., Suggs, L.J., Payne, R.G., Langer, R., Hayes, W.C., Unroe, M.R., Alemany, L.B., Engel, P.S. & Mikos, A.G. 1997, "Characterization of partially saturated poly(propylene fumarate) for orthopaedic application", *Journal of biomaterials science.Polymer edition*, vol. 8, no. 11, pp. 893-904.

Place, E.S., Rojo, L., Gentleman, E., Sardinha, J.P. & Stevens, M.M. 2011, "Strontium- and Zinc-Alginate Hydrogels for Bone Tissue Engineering", *Tissue engineering.Part A*, .

Pockwinse, S.M., Stein, J.L., Lian, J.B. & Stein, G.S. 1995, "Developmental stage-specific cellular responses to vitamin D and glucocorticoids during differentiation of the

osteoblast phenotype: interrelationship of morphology and gene expression by in situ hybridization", *Experimental cell research*, vol. 216, no. 1, pp. 244-260.

Ponticiello, M.S., Schinagl, R.M., Kadiyala, S. & Barry, F.P. 2000, "Gelatin-based resorbable sponge as a carrier matrix for human mesenchymal stem cells in cartilage regeneration therapy", *Journal of Biomedical Materials Research*, vol. 52, no. 2, pp. 246-255.

Porter, B.D., Oldham, J.B., He, S.L., Zobitz, M.E., Payne, R.G., An, K.N., Currier, B.L., Mikos, A.G. & Yaszemski, M.J. 2000, "Mechanical properties of a biodegradable bone regeneration scaffold", *Journal of Biomechanical Engineering*, vol. 122, no. 3, pp. 286-288.

Pratap, J., Javed, A., Languino, L.R., van Wijnen, A.J., Stein, J.L., Stein, G.S. & Lian, J.B. 2005, "The Runx2 osteogenic transcription factor regulates matrix metalloproteinase 9 in bone metastatic cancer cells and controls cell invasion", *Molecular and cellular biology*, vol. 25, no. 19, pp. 8581-8591.

Puckett, S., Pareta, R. & Webster, T.J. 2008, "Nano rough micron patterned titanium for directing osteoblast morphology and adhesion", *International journal of nanomedicine*, vol. 3, no. 2, pp. 229-241.

Puddu, P., Valenti, P. & Gessani, S. 2009, "Immunomodulatory effects of lactoferrin

on antigen presenting cells", vol. 91, pp. 11-18.

Quaglia, F. 2008, "Bioinspired tissue engineering: the great promise of protein delivery technologies", *International journal of pharmaceuticals*, vol. 364, no. 2, pp. 281-297.

Quarles, L.D., Yohay, D.A., Lever, L.W., Caton, R. & Wenstrup, R.J. 1992, "Distinct proliferative and differentiated stages of murine MC3T3-E1 cells in culture: an in vitro model of osteoblast development", *Journal of bone and mineral research : the official journal of the American Society for Bone and Mineral Research*, vol. 7, no. 6, pp. 683-692.

Randhawa, R. & Cohen, P. 2005, "The role of the insulin-like growth factor system in prenatal growth", *Molecular genetics and metabolism*, vol. 86, no. 1-2, pp. 84-90.

Rath, S.N., Prymachuk, G., Bleiziffer, O.A., Lam, C.X., Arkudas, A., Ho, S.T., Beier, J.P., Horch, R.E., Hutmacher, D.W. & Kneser, U. 2011, "Hyaluronan-based heparin-incorporated hydrogels for generation of axially vascularized bioartificial bone tissues: in vitro and in vivo evaluation in a PLDLLA-TCP-PCL-composite system", *Journal of materials science. Materials in medicine*, vol. 22, no. 5, pp. 1279-1291.

Rea, S.M., Best, S.M. & Bonfield, W. 2004, "Bioactivity of ceramic-polymer composites with varied composition and surface topography", *Journal of materials*

*science.Materials in medicine*, vol. 15, no. 9, pp. 997-1005.

Roiron, D., Amouric, M., Marvaldi, J. & Figarella, C. 1989, "Lactoferrin-binding sites at the surface of HT29-D4 cells. Comparison with transferrin", *European journal of biochemistry / FEBS*, vol. 186, no. 1-2, pp. 367-373.

Rose, F.R. & Oreffo, R.O. 2002, "Bone tissue engineering: hope vs hype", *Biochemical and biophysical research communications*, vol. 292, no. 1, pp. 1-7.

Rowley, J.A. & Mooney, D.J. 2002, "Alginate type and RGD density control myoblast phenotype", *Journal of Biomedical Materials Research*, vol. 60, no. 2, pp. 217-223.

Rowley, J.A., Madlambayan, G. & Mooney, D.J. 1999, "Alginate hydrogels as synthetic extracellular matrix materials", *Biomaterials*, vol. 20, no. 1, pp. 45-53.

Ruel-Gariepy, E. & Leroux, J.C. 2004, "In situ-forming hydrogels--review of temperature-sensitive systems", *European journal of pharmaceutics and biopharmaceutics : official journal of Arbeitsgemeinschaft fur Pharmazeutische Verfahrenstechnik e.V*, vol. 58, no. 2, pp. 409-426.

Rydholm, A.E., Bowman, C.N. & Anseth, K.S. 2005, "Degradable thiol-acrylate photopolymers: polymerization and degradation behavior of an in situ forming biomaterial", *Biomaterials*, vol. 26, no. 22, pp. 4495-4506.

Sakai, S., Yamada, Y., Zenke, T. & Kawakami, K. 2009, "Novel chitosan derivative soluble at neutral pH and *in-situ* gellable via peroxidase-catalyzed enzymatic reaction", *Journal of Material Chemistry*, vol. 19, pp. 230-235.

Sakanaka, C., Weiss, J.B. & Williams, L.T. 1998, "Bridging of beta-catenin and glycogen synthase kinase-3beta by axin and inhibition of beta-catenin-mediated transcription", *Proceedings of the National Academy of Sciences of the United States of America*, vol. 95, no. 6, pp. 3020-3023.

Sakaue, H., Ogawa, W., Matsumoto, M., Kuroda, S., Takata, M., Sugimoto, T., Spiegelman, B.M. & Kasuga, M. 1998, "Posttranscriptional control of adipocyte differentiation through activation of phosphoinositide 3-kinase", *The Journal of biological chemistry*, vol. 273, no. 44, pp. 28945-28952.

Sala, A., Ehrbar, M., Trentin, D., Schoenmakers, R.G., Voros, J. & Weber, F.E. 2010, "Enzyme mediated site-specific surface modification", *Langmuir : the ACS journal of surfaces and colloids*, vol. 26, no. 13, pp. 11127-11134.

Salinas, C.N. & Anseth, K.S. 2009, "Mesenchymal stem cells for craniofacial tissue regeneration: designing hydrogel delivery vehicles", *Journal of dental research*, vol. 88, no. 8, pp. 681-692.

Samyn-Petit, B., Gruber, V., Flahaut, C., Wajda-Dubos, J.P., Farrer, S., Pons, A., Desmaizieres, G., Slomianny, M.C., Theisen, M. & Delannoy, P. 2001, "N-glycosylation potential of maize: the human lactoferrin used as a model", *Glycoconjugate journal*, vol. 18, no. 7, pp. 519-527.

Samyn-Petit, B., Wajda Dubos, J.P., Chirat, F., Coddeville, B., Demaizieres, G., Farrer, S., Slomianny, M.C., Theisen, M. & Delannoy, P. 2003, "Comparative analysis of the site-specific N-glycosylation of human lactoferrin produced in maize and tobacco plants", vol. 270, pp. 3235-3242.

Sands, R.W. & Mooney, D.J. 2007, "Polymers to direct cell fate by controlling the microenvironment", *Current opinion in biotechnology*, vol. 18, no. 5, pp. 448-453.

Sawatzki, G. & Rich, I.N. 1989, "Lactoferrin stimulates colony stimulating factor production in vitro and in vivo", vol. 15, pp. 371-385.

Schanbacher, F.L., Goodman, R.E. & Talhouk, R.S. 1993, "Bovine mammary lactoferrin: implications from messenger ribonucleic acid (mRNA) sequence and regulation contrary to other milk proteins", vol. 76, pp. 3812-3831.

Schaper, W. & Ito, W.D. 1996, "Molecular mechanisms of coronary collateral vessel growth", *Circulation research*, vol. 79, no. 5, pp. 911-919.



Selmi, T.A., Verdonk, P., Chambat, P., Dubrana, F., Potel, J.F., Barnouin, L. & Neyret, P. 2008, "Autologous chondrocyte implantation in a novel alginate-agarose hydrogel: outcome at two years", *The Journal of bone and joint surgery.British volume*, vol. 90, no. 5, pp. 597-604.

Sheldahl, L.C., Park, M., Malbon, C.C. & Moon, R.T. 1999, "Protein kinase C is differentially stimulated by Wnt and Frizzled homologs in a G-protein-dependent manner", *Current biology : CB*, vol. 9, no. 13, pp. 695-698.

Shim, W.S., Kim, J.H., Park, H., Kim, K., Chan Kwon, I. & Lee, D.S. 2006, "Biodegradability and biocompatibility of a pH- and thermo-sensitive hydrogel formed from a sulfonamide-modified poly(epsilon-caprolactone-co-lactide)-poly(ethylene glycol)-poly(epsilon-caprolactone-co-lactide) block copolymer", *Biomaterials*, vol. 27, no. 30, pp. 5178-5185.

Shimamura, M., Yamamoto, Y., Ashino, H., Oikawa, T., Hazato, T., Tsuda, H. & Iigo, M. 2004, "Bovine lactoferrin inhibits tumor-induced angiogenesis", vol. 111, pp. 111-116.

Shimazaki, K., Tazume, T., Uji, K., Tanaka, M., Kumura, H., Mikawa, K. & Shimo-Oka, T. 1998, "Properties of a heparin-binding peptide derived from bovine lactoferrin", *Journal of dairy science*, vol. 81, no. 11, pp. 2841-2849.

Shimizu, K., Matsuzawa, H., Okada, K., Tazume, S., Dosako, S., Kawasaki, Y., Hashimoto, K. & Koga, Y. 1996, "Lactoferrin-mediated protection of the host from murine cytomegalovirus infection by a T-cell-dependent augmentation of natural killer cell activity", vol. 141, pp. 1875-1889.

Sibai, T., Morgan, E.F. & Einhorn, T.A. 2011, "Anabolic agents and bone quality", *Clinical orthopaedics and related research*, vol. 469, no. 8, pp. 2215-2224.

Siggelkow, H., Rebenstorff, K., Kurre, W., Niedhart, C., Engel, I., Schulz, H., Atkinson, M.J. & Hufner, M. 1999, "Development of the osteoblast phenotype in primary human osteoblasts in culture: comparison with rat calvarial cells in osteoblast differentiation", *Journal of cellular biochemistry*, vol. 75, no. 1, pp. 22-35.

Silkstone, D., Hong, H. & Alman, B.A. 2008, "Beta-catenin in the race to fracture repair: in it to Wnt", *Nature clinical practice.Rheumatology*, vol. 4, no. 8, pp. 413-419.

Silva, G.A., Czeisler, C., Niece, K.L., Beniash, E., Harrington, D.A., Kessler, J.A. & Stupp, S.I. 2004, "Selective differentiation of neural progenitor cells by high-epitope density nanofibers", *Science (New York, N.Y.)*, vol. 303, no. 5662, pp. 1352-1355.

Sims, C.D., Butler, P.E., Casanova, R., Lee, B.T., Randolph, M.A., Lee, W.P., Vacanti, C.A. & Yaremchuk, M.J. 1996, "Injectable cartilage using polyethylene oxide polymer substrates", *Plastic and Reconstructive Surgery*, vol. 98, no. 5, pp. 843-850.

Singh, D., Tripathi, A., Nayak, V. & Kumar, A. 2010, "Proliferation of Chondrocytes on a 3-D Modelled Macroporous Poly(Hydroxyethyl Methacrylate)-Gelatin Cryogel", *Journal of biomaterials science. Polymer edition*.

Slaughter, B.V., Khurshid, S.S., Fisher, O.Z., Khademhosseini, A. & Peppas, N.A. 2009, "Hydrogels in regenerative medicine", *Advanced materials* (Deerfield Beach, Fla.), vol. 21, no. 32-33, pp. 3307-3329.

Slusarski, D.C., Corces, V.G. & Moon, R.T. 1997, "Interaction of Wnt and a Frizzled homologue triggers G-protein-linked phosphatidylinositol signalling", *Nature*, vol. 390, no. 6658, pp. 410-413.

Smetana, K., Jr 1993, "Cell biology of hydrogels", *Biomaterials*, vol. 14, no. 14, pp. 1046-1050.

Sorimachi, K., Akimoto, K., Hattori, Y., Ieiri, T. & Niwa, A. 1997, "Activation of macrophages by lactoferrin: secretion of TNF- $\alpha$ , IL-8 and NO", *Biochemistry and molecular biology international*, vol. 43, no. 1, pp. 79-87.

Spadaro, M., Caorsi, C., Ceruti, P., Varadhachary, A., Forni, G., Pericle, F. & Giovarelli, M. 2008, "Lactoferrin, a major defense protein of innate immunity, is a novel maturation factor for human dendritic cells", *FASEB journal : official publication of the*

*Federation of American Societies for Experimental Biology*, vol. 22, no. 8, pp. 2747-2757.

Spadaro, M., Caorsi, C., Ceruti, P., Varadhachary, A., Forni, G., Pericle, F. & Giovarelli, M. 2008, "Lactoferrin, a major defense protein of innate immunity, is a novel maturation factor for human dendritic cells", *FASEB journal : official publication of the Federation of American Societies for Experimental Biology*, vol. 22, no. 8, pp. 2747-2757.

Spik, G., Strecker, G., Fournet, B., Bouquelet, S., Montreuil, J., Dorland, L., van Halbeek, H. & Vliegenthart, J.F. 1982, "Primary structure of the glycans from human lactotransferrin", *European journal of biochemistry / FEBS*, vol. 121, no. 2, pp. 413-419.

Spotnitz, W.D. & Burks, S. 2008, "Hemostats, sealants, and adhesives: components of the surgical toolbox", *Transfusion*, vol. 48, no. 7, pp. 1502-1516.

Steffens, G.C., Yao, C., Prevel, P., Markowicz, M., Schenck, P., Noah, E.M. & Pallua, N. 2004, "Modulation of angiogenic potential of collagen matrices by covalent incorporation of heparin and loading with vascular endothelial growth factor", *Tissue engineering*, vol. 10, no. 9-10, pp. 1502-1509.

Stenzel, K.H., Miyata, T. & Rubin, A.L. 1974, "Collagen as a biomaterial", *Annual Review of Biophysics and Bioengineering*, vol. 3, no. 0, pp. 231-253.

Stern, P.H. 2006, "The calcineurin-NFAT pathway and bone: intriguing new findings", vol. 6, pp. 193-196.

Strickland, D.K., Gonias, S.L. & Argraves, W.S. 2002, "Diverse roles for the LDL receptor family", vol. 13, pp. 66-74.

Sudo, H., Kodama, H.A., Amagai, Y., Yamamoto, S. & Kasai, S. 1983, "In vitro differentiation and calcification in a new clonal osteogenic cell line derived from newborn mouse calvaria", *The Journal of cell biology*, vol. 96, no. 1, pp. 191-198.

Suh, J.K. & Matthew, H.W. 2000, "Application of chitosan-based polysaccharide biomaterials in cartilage tissue engineering: a review", *Biomaterials*, vol. 21, no. 24, pp. 2589-2598.

Sun, H., Qu, Z., Guo, Y., Zang, G. & Yang, B. 2007, "In vitro and in vivo effects of rat kidney vascular endothelial cells on osteogenesis of rat bone marrow mesenchymal stem cells growing on polylactide-glycolic acid (PLGA) scaffolds", *Biomedical engineering online*, vol. 6, pp. 41.

Szuster-Ciesielska, A., Kamińska, T. & Kandefer-Szerszeń, M. 1995, "Phagocytosis-enhancing effect of lactoferrin on bovine peripheral blood monocytes in vitro and in vivo", vol. 35, pp. 63-71.

Tahinci, E., Thorne, C.A., Franklin, J.L., Salic, A., Christian, K.M., Lee, L.A., Coffey,

R.J. & Lee, E. 2007, "Lrp6 is required for convergent extension during *Xenopus* gastrulation", *Development* (Cambridge, England), vol. 134, no. 22, pp. 4095-4106.

Takaoka, R., Hikasa, Y., Hayashi, K. & Tabata, Y. 2011, "Bone regeneration by lactoferrin released from a gelatin hydrogel", *Journal of biomaterials science.Polymer edition*, vol. 22, no. 12, pp. 1581-1589.

Takayama, Y. & Mizumachi, K. 2008, "Effect of bovine lactoferrin on extracellular matrix calcification by human osteoblast-like cells", vol. 72, pp. 226-230.

Takayama, Y. & Mizumachi, K. 2009, "Effect of lactoferrin-embedded collagen membrane on osteogenic differentiation of human osteoblast-like cells", *Journal of bioscience and bioengineering*, vol. 107, no. 2, pp. 191-195.

Takayama, Y., Mizumachi, K. & Takezawa, T. 2002, "The bovine lactoferrin region responsible for promoting the collagen gel contractile activity of human fibroblasts", *Biochemical and biophysical research communications*, vol. 299, no. 5, pp. 813-817.

Takayanagi, H. 2005, "Mechanistic insight into osteoclast differentiation in osteoimmunology", vol. 83, pp. 170-179.

Tamai, K., Semenov, M., Kato, Y., Spokony, R., Liu, C., Katsuyama, Y., Hess, F., Saint-Jeannet, J. & He, X. 2000, "LDL-receptor-related proteins in Wnt signal

transduction", vol. 407, pp. 530-535.

Tang, L., Cui, T., Wu, J.J., Liu-Mares, W., Huang, N. & Li, J. 2010, "A rice-derived recombinant human lactoferrin stimulates fibroblast proliferation, migration, and sustains cell survival", *Wound repair and regeneration : official publication of the Wound Healing Society [and] the European Tissue Repair Society*, vol. 18, no. 1, pp. 123-131.

Tanigo, T., Takaoka, R. & Tabata, Y. 2010, "Sustained release of water-insoluble simvastatin from biodegradable hydrogel augments bone regeneration", *Journal of controlled release : official journal of the Controlled Release Society*, vol. 143, no. 2, pp. 201-206.

Teixeira, L.S., Feijen, J., van Blitterswijk, C.A., Dijkstra, P.J. & Karperien, M. 2012, "Enzyme-catalyzed crosslinkable hydrogels: emerging strategies for tissue engineering", *Biomaterials*, vol. 33, no. 5, pp. 1281-1290.

Terao, K., Nagasawa, N., Nishida, H., Furusawa, K., Mori, Y., Yoshii, F. & Dobashi, T. 2003, "Reagent-free crosslinking of aqueous gelatin: manufacture and characteristics of gelatin gels irradiated with gamma-ray and electron beam", *Journal of biomaterials science. Polymer edition*, vol. 14, no. 11, pp. 1197-1208.

Toba, Y., Takada, Y., Yamamura, J., Tanaka, M., Matsuoka, Y., Kawakami, H., Itabashi, A., Aoe, S. & Kumegawa, M. 2000, "Milk basic protein: a novel protective

function of milk against osteoporosis", vol. 27, pp. 403-408.

Tobimatsu, T., Kaji, H., Sowa, H., Naito, J., Canaff, L., Hendy, G.N., Sugimoto, T. & Chihara, K. 2006, "Parathyroid hormone increases beta-catenin levels through Smad3 in mouse osteoblastic cells", *Endocrinology*, vol. 147, no. 5, pp. 2583-2590.

Togawa, J., Nagase, H., Tanaka, K., Inamori, M., Nakajima, A., Ueno, N., Saito, T. & Sekihara, H. 2002, "Oral administration of lactoferrin reduces colitis in rats via modulation of the immune system and correction of cytokine imbalance", vol. 17, pp. 1291-1298.

Toh, W.S., Lee, E.H., Guo, X.M., Chan, J.K., Yeow, C.H., Choo, A.B. & Cao, T. 2010, "Cartilage repair using hyaluronan hydrogel-encapsulated human embryonic stem cell-derived chondrogenic cells", *Biomaterials*, vol. 31, no. 27, pp. 6968-6980.

Topol, L., Jiang, X., Choi, H., Garrett-Beal, L., Carolan, P.J. & Yang, Y. 2003, "Wnt-5a inhibits the canonical Wnt pathway by promoting GSK-3-independent beta-catenin degradation", *The Journal of cell biology*, vol. 162, no. 5, pp. 899-908.

Torii, K., Nishizawa, K., Kawasaki, A., Yamashita, Y., Katada, M., Ito, M., Nishimoto, I., Terashita, K., Aiso, S. & Matsuoka, M. 2008, "Anti-apoptotic action of Wnt5a in dermal fibroblasts is mediated by the PKA signaling pathways", *Cellular signalling*, vol. 20, no. 7, pp. 1256-1266.



Torres, M.A., Yang-Snyder, J.A., Purcell, S.M., DeMarais, A.A., McGrew, L.L. & Moon, R.T. 1996, "Activities of the Wnt-1 class of secreted signaling factors are antagonized by the Wnt-5A class and by a dominant negative cadherin in early *Xenopus* development", *The Journal of cell biology*, vol. 133, no. 5, pp. 1123-1137.

Tran, N.Q., Joung, Y.K., Lih, E., Park, K.M. & Park, K.D. 2010, "Supramolecular hydrogels exhibiting fast in situ gel forming and adjustable degradation properties", *Biomacromolecules*, vol. 11, no. 3, pp. 617-625.

Tse, J.R. & Engler, A.J. 2010, "Preparation of hydrogel substrates with tunable mechanical properties", *Current protocols in cell biology* / editorial board, Juan S.Bonifacino ...[et al.], vol. Chapter 10, pp. Unit 10.16.

Tsuji, M., Kawano, S., Tsuji, S., Sawaoka, H., Hori, M. & DuBois, R.N. 1998, "Cyclooxygenase regulates angiogenesis induced by colon cancer cells", vol. 93, pp. 705-716.

Vaccaro, A.R. 2002, "The role of the osteoconductive scaffold in synthetic bone graft", *Orthopedics*, vol. 25, no. 5 Suppl, pp. s571-8.

van Berkel, P.H., van Veen, H.A., Geerts, M.E. & Nuijens, J.H. 2002, "Characterization of monoclonal antibodies against human lactoferrin", *Journal of*

immunological methods, vol. 267, no. 2, pp. 139-150.

van Berkel, P.H., Welling, M.M., Geerts, M., van Veen, H.A., Ravensbergen, B., Salaheddine, M., Pauwels, E.K., Pieper, F., Nuijens, J.H. & Nibbering, P.H. 2002a, "Large scale production of recombinant human lactoferrin in the milk of transgenic cows", vol. 20, pp. 484-487.

van Hooijdonk, A.C., Kussendrager, K.D. & Steijns, J.M. 2000, "In vivo antimicrobial and antiviral activity of components in bovine milk and colostrum involved in non-specific defence", vol. 84 Suppl 1, pp. S127-34.

van, d.S., Beljaars, L., Molema, G., Harmsen, M.C. & Meijer, D.K. 2001, "Antiviral activities of lactoferrin", vol. 52, pp. 225-239.

Varadhachary, A., Wolf, J.S., Petrak, K., O'Malley, B.W., Spadaro, M., Curcio, C., Forni, G. & Pericle, F. 2004, "Oral lactoferrin inhibits growth of established tumors and potentiates conventional chemotherapy", vol. 111, pp. 398-403.

Vary, C.P., Li, V., Raouf, A., Kitching, R., Kola, I., Franceschi, C., Venanzoni, M. & Seth, A. 2000, "Involvement of Ets transcription factors and targets in osteoblast differentiation and matrix mineralization", *Experimental cell research*, vol. 257, no. 1, pp. 213-222.

Vash, B., Phung, N., Zein, S. & DeCamp, D. 1998, "Three complement-type repeats of the low-density lipoprotein receptor-related protein define a common binding site for RAP, PAI-1, and lactoferrin", vol. 92, pp. 3277-3285.

Veeman, M.T., Axelrod, J.D. & Moon, R.T. 2003, "A second canon. Functions and mechanisms of beta-catenin-independent Wnt signaling", *Developmental cell*, vol. 5, no. 3, pp. 367-377.

Vernon, B., Tirelli, N., Bachi, T., Haldimann, D. & Hubbell, J.A. 2003, "Water-borne, in situ crosslinked biomaterials from phase-segregated precursors", *Journal of biomedical materials research.Part A*, vol. 64, no. 3, pp. 447-456.

Vogel, H.J. 2012, "Lactoferrin, a bird's eye view", *Biochemistry and cell biology = Biochimie et biologie cellulaire*, .

Wakabayashi, H., Takakura, N., Teraguchi, S. & Tamura, Y. 2003, "Lactoferrin feeding augments peritoneal macrophage activities in mice intraperitoneally injected with inactivated *Candida albicans*", vol. 47, pp. 37-43.

Walsh, G. & Jefferis, R. 2006, "Post-translational modifications in the context of therapeutic proteins", vol. 24, pp. 1241-1252.

Wan, L.Q., Jiang, J., Arnold, D.E., Guo, X.E., Lu, H.H. & Mow, V.C. 2008, "Calcium

Concentration Effects on the Mechanical and Biochemical Properties of Chondrocyte-Alginate Constructs", *Cellular and molecular bioengineering*, vol. 1, no. 1, pp. 93-102.

Wan, M., Yang, C., Li, J., Wu, X., Yuan, H., Ma, H., He, X., Nie, S., Chang, C. & Cao, X. 2008, "Parathyroid hormone signaling through low-density lipoprotein-related protein 6", *Genes & development*, vol. 22, no. 21, pp. 2968-2979.

Wang, C., Varshney, R.R. & Wang, D.A. 2010, "Therapeutic cell delivery and fate control in hydrogels and hydrogel hybrids", *Advanced Drug Delivery Reviews*, vol. 62, no. 7-8, pp. 699-710.

Wang, D., Christensen, K., Chawla, K., Xiao, G., Krebsbach, P.H. & Franceschi, R.T. 1999, "Isolation and characterization of MC3T3-E1 preosteoblast subclones with distinct in vitro and in vivo differentiation/mineralization potential", *Journal of bone and mineral research : the official journal of the American Society for Bone and Mineral Research*, vol. 14, no. 6, pp. 893-903.

Wang, L. & Stegemann, J.P. 2010, "Thermogelling chitosan and collagen composite hydrogels initiated with beta-glycerophosphate for bone tissue engineering", *Biomaterials*, vol. 31, no. 14, pp. 3976-3985.

Wang, L. & Stegemann, J.P. 2011, "Glyoxal crosslinking of cell-seeded chitosan/collagen hydrogels for bone regeneration", *Acta biomaterialia*, vol. 7, no. 6, pp.

2410-2417.

Wang, L.S., Chung, J.E., Chan, P.P. & Kurisawa, M. 2010, "Injectable biodegradable hydrogels with tunable mechanical properties for the stimulation of neurogenesis differentiation of human mesenchymal stem cells in 3D culture", *Biomaterials*, vol. 31, no. 6, pp. 1148-1157.

Wang, W.M., Lee, S., Steiglitz, B.M., Scott, I.C., Lebares, C.C., Allen, M.L., Brenner, M.C., Takahara, K. & Greenspan, D.S. 2003, "Transforming growth factor-beta induces secretion of activated ADAMTS-2. A procollagen III N-proteinase", *The Journal of biological chemistry*, vol. 278, no. 21, pp. 19549-19557.

Ward, P.P., Paz, E. & Conneely, O.M. 2005, "Multifunctional roles of lactoferrin: a critical overview", *Cellular and molecular life sciences : CMLS*, vol. 62, no. 22, pp. 2540-2548.

Ward, P.P., Uribe-Luna, S. & Conneely, O.M. 2002, "Lactoferrin and host defense", vol. 80, pp. 95-102.

Wee, S. & Gombotz, W.R. 1998, "Protein release from alginate matrices", *Advanced Drug Delivery Reviews*, vol. 31, no. 3, pp. 267-285.

Wegman, F., Bijenhof, A., Schuijff, L., Oner, F.C., Dhert, W.J. & Alblas, J. 2011,

"Osteogenic differentiation as a result of BMP-2 plasmid DNA based gene therapy in vitro and in vivo", *European cells & materials*, vol. 21, pp. 230-42; discussion 242.

Weinberg, E.D. 2006, "Iron loading: a risk factor for osteoporosis", *Biometals : an international journal on the role of metal ions in biology, biochemistry, and medicine*, vol. 19, no. 6, pp. 633-635.

Weinstein, R.S., Jilka, R.L., Parfitt, A.M. & Manolagas, S.C. 1998, "Inhibition of osteoblastogenesis and promotion of apoptosis of osteoblasts and osteocytes by glucocorticoids. Potential mechanisms of their deleterious effects on bone", *The Journal of clinical investigation*, vol. 102, no. 2, pp. 274-282.

Weitzmann, M.N. & Pacifici, R. 2007, "T cells: unexpected players in the bone loss induced by estrogen deficiency and in basal bone homeostasis", *Annals of the New York Academy of Sciences*, vol. 1116, pp. 360-375.

Weng, Y., Cao, Y., Silva, C.A., Vacanti, M.P. & Vacanti, C.A. 2001, "Tissue-engineered composites of bone and cartilage for mandible condylar reconstruction", *Journal of oral and maxillofacial surgery : official journal of the American Association of Oral and Maxillofacial Surgeons*, vol. 59, no. 2, pp. 185-190.

Williams, C.G., Kim, T.K., Taboas, A., Malik, A., Manson, P. & Elisseeff, J. 2003, "In vitro chondrogenesis of bone marrow-derived mesenchymal stem cells in a

photopolymerizing hydrogel", *Tissue engineering*, vol. 9, no. 4, pp. 679-688.

Willnow, T.E., Goldstein, J.L., Orth, K., Brown, M.S. & Herz, J. 1992, "Low density lipoprotein receptor-related protein and gp330 bind similar ligands, including plasminogen activator-inhibitor complexes and lactoferrin, an inhibitor of chylomicron remnant clearance", vol. 267, pp. 26172-26180.

Winslow, M.M., Pan, M., Starbuck, M., Gallo, E.M., Deng, L., Karsenty, G. & Crabtree, G.R. 2006, "Calcineurin/NFAT signaling in osteoblasts regulates bone mass", vol. 10, pp. 771-782.

Wissink, M.J., Beernink, R., Poot, A.A., Engbers, G.H., Beugeling, T., van Aken, W.G. & Feijen, J. 2000, "Improved endothelialization of vascular grafts by local release of growth factor from heparinized collagen matrices", *Journal of controlled release : official journal of the Controlled Release Society*, vol. 64, no. 1-3, pp. 103-114.

Wodarz, A. & Nusse, R. 1998, "Mechanisms of Wnt signaling in development", *Annual Review of Cell and Developmental Biology*, vol. 14, pp. 59-88.

Wolf, J.S., Li, G., Varadhachary, A., Petrak, K., Schneyer, M., Li, D., Ongkasuwan, J., Zhang, X., Taylor, R.J., Strome, S.E. & O'Malley, B.W., Jr 2007, "Oral lactoferrin results in T cell-dependent tumor inhibition of head and neck squamous cell carcinoma in vivo", *Clinical cancer research : an official journal of the American Association for Cancer*

*Research*, vol. 13, no. 5, pp. 1601-1610.

Wong, R.W. & Rabie, A.B. 2006, "Statin-induced osteogenesis uses in orthodontics: a scientific review", *World journal of orthodontics*, vol. 7, no. 1, pp. 35-40.

Wozney, J.M., Rosen, V., Celeste, A.J., Mitsock, L.M., Whitters, M.J., Kriz, R.W., Hewick, R.M. & Wang, E.A. 1988, "Novel regulators of bone formation: molecular clones and activities", *Science (New York, N.Y.)*, vol. 242, no. 4885, pp. 1528-1534.

Wu, L.Q., Bentley, W.E. & Payne, G.F. 2011, "Biofabrication with biopolymers and enzymes: potential for constructing scaffolds from soft matter", *The International journal of artificial organs*, vol. 34, no. 2, pp. 215-224.

Xiao, C., Zhou, H., Liu, G., Zhang, P., Fu, Y., Gu, P., Hou, H., Tang, T. & Fan, X. 2011, "Bone marrow stromal cells with a combined expression of BMP-2 and VEGF-165 enhanced bone regeneration", *Biomedical materials (Bristol, England)*, vol. 6, no. 1, pp. 015013.

Xiao, G., Jiang, D., Thomas, P., Benson, M.D., Guan, K., Karsenty, G. & Franceschi, R.T. 2000, "MAPK pathways activate and phosphorylate the osteoblast-specific transcription factor, Cbfa1", *The Journal of biological chemistry*, vol. 275, no. 6, pp. 4453-4459.



Xu, X.L., Lou, J., Tang, T., Ng, K.W., Zhang, J., Yu, C. & Dai, K. 2005, "Evaluation of different scaffolds for BMP-2 genetic orthopedic tissue engineering", *Journal of biomedical materials research.Part B, Applied biomaterials*, vol. 75, no. 2, pp. 289-303.

Yagi, M., Suzuki, N., Takayama, T., Arisue, M., Kodama, T., Yoda, Y., Otsuka, K. & Ito, K. 2009, "Effects of lactoferrin on the differentiation of pluripotent mesenchymal cells", *Cell biology international*, vol. 33, no. 3, pp. 283-289.

Yamamoto, M., Takahashi, Y. & Tabata, Y. 2006, "Enhanced bone regeneration at a segmental bone defect by controlled release of bone morphogenetic protein-2 from a biodegradable hydrogel", *Tissue engineering*, vol. 12, no. 5, pp. 1305-1311.

Yamamoto, M., Yamazaki, S., Uematsu, S., Sato, S., Hemmi, H., Hoshino, K., Kaisho, T., Kuwata, H., Takeuchi, O., Takeshige, K., Saitoh, T., Yamaoka, S., Yamamoto, N., Yamamoto, S., Muta, T., Takeda, K. & Akira, S. 2004, "Regulation of Toll/IL-1-receptor-mediated gene expression by the inducible nuclear protein IkappaBzeta", *Nature*, vol. 430, no. 6996, pp. 218-222.

Yamano, E., Miyauchi, M., Furusyo, H., Kawazoe, A., Ishikado, A., Makino, T., Tanne, K., Tanaka, E. & Takata, T. 2010, "Inhibitory effects of orally administrated liposomal bovine lactoferrin on the LPS-induced osteoclastogenesis", vol. 90, pp. 1236-1246.

Yamauchi, K., Wakabayashi, H., Hashimoto, S., Teraguchi, S., Hayasawa, H. &

Tomita, M. 1998, "Effects of orally administered bovine lactoferrin on the immune system of healthy volunteers", vol. 443, pp. 261-265.

Yang, X.B., Bhatnagar, R.S., Li, S. & Oreffo, R.O. 2004, "Biomimetic collagen scaffolds for human bone cell growth and differentiation", *Tissue engineering*, vol. 10, no. 7-8, pp. 1148-1159.

Yaszemski, M.J., Payne, R.G., Hayes, W.C., Langer, R. & Mikos, A.G. 1996, "Evolution of bone transplantation: molecular, cellular and tissue strategies to engineer human bone", *Biomaterials*, vol. 17, no. 2, pp. 175-185.

Ying, X., Cheng, S., Wang, W., Lin, Z., Chen, Q., Zhang, W., Kou, D., Shen, Y., Cheng, X., Peng, L., Zi Xu, H. & Zhu Lu, C. 2012, "Effect of lactoferrin on osteogenic differentiation of human adipose stem cells", *International orthopaedics*, vol. 36, no. 3, pp. 647-653.

Yoon, J.J., Chung, H.J., Lee, H.J. & Park, T.G. 2006, "Heparin-immobilized biodegradable scaffolds for local and sustained release of angiogenic growth factor", *Journal of biomedical materials research.Part A*, vol. 79, no. 4, pp. 934-942.

Yoshida, H., Hayashi, S., Kunisada, T., Ogawa, M., Nishikawa, S., Okamura, H., Sudo, T., Shultz, L.D. & Nishikawa, S. 1990, "The murine mutation osteopetrosis is in the coding region of the macrophage colony stimulating factor gene", *Nature*, vol. 345,

no. 6274, pp. 442-444.

Young, S., Patel, Z.S., Kretlow, J.D., Murphy, M.B., Mountziaris, P.M., Baggett, L.S., Ueda, H., Tabata, Y., Jansen, J.A., Wong, M. & Mikos, A.G. 2009, "Dose effect of dual delivery of vascular endothelial growth factor and bone morphogenetic protein-2 on bone regeneration in a rat critical-size defect model", *Tissue engineering.Part A*, vol. 15, no. 9, pp. 2347-2362.

Young, S., Wong, M., Tabata, Y. & Mikos, A.G. 2005, "Gelatin as a delivery vehicle for the controlled release of bioactive molecules", *Journal of controlled release : official journal of the Controlled Release Society*, vol. 109, no. 1-3, pp. 256-274.

Yu, L., Chang, G.T., Zhang, H. & Ding, J.D. 2008, "Injectable block copolymer hydrogels for sustained release of a PEGylated drug", *International journal of pharmaceutics*, vol. 348, no. 1-2, pp. 95-106.

Yu, T., Guo, C., Wang, J., Hao, P., Sui, S., Chen, X., Zhang, R., Wang, P., Yu, G., Zhang, L., Dai, Y. & Li, N. 2010, "Comprehensive Characterization of the Site-Specific N-Glycosylation of Wild-Type and Recombinant Human Lactoferrin Expressed in Milk of Transgenic Cloned Cattle", .

Yung, C.W., Bentley, W.E. & Barbari, T.A. 2010, "Diffusion of interleukin-2 from cells overlaid with cytocompatible enzyme-crosslinked gelatin hydrogels", *Journal of*

*biomedical materials research.Part A*, vol. 95, no. 1, pp. 25-32.

Yung, C.W., Wu, L.Q., Tullman, J.A., Payne, G.F., Bentley, W.E. & Barbari, T.A. 2007, "Transglutaminase crosslinked gelatin as a tissue engineering scaffold", *Journal of biomedical materials research.Part A*, vol. 83, no. 4, pp. 1039-1046.

Zagulski, T., Lipinski, P., Zagulska, A., Broniek, S. & Jarzabek, Z. 1989, "Lactoferrin can protect mice against a lethal dose of *Escherichia coli* in experimental infection in vivo", *British journal of experimental pathology*, vol. 70, no. 6, pp. 697-704.

Zhang, S. 2002, "Emerging biological materials through molecular self-assembly", *Biotechnology Advances*, vol. 20, no. 5-6, pp. 321-339.

Zhang, S. 2003, "Fabrication of novel biomaterials through molecular self-assembly", *Nature biotechnology*, vol. 21, no. 10, pp. 1171-1178.

Zhao, Q., Wang, X., Liu, Y., He, A. & Jia, R. 2010, "NFATc1: functions in osteoclasts", vol. 42, pp. 576-579.

Zhao, X., Kim, J., Cezar, C.A., Huebsch, N., Lee, K., Bouhadir, K. & Mooney, D.J. 2011, "Active scaffolds for on-demand drug and cell delivery", *Proceedings of the National Academy of Sciences of the United States of America*, vol. 108, no. 1, pp. 67-72.

Zilberberg, A., Yaniv, A. & Gazit, A. 2004, "The low density lipoprotein receptor-1, LRP1, interacts with the human frizzled-1 (HFz1) and down-regulates the canonical Wnt signaling pathway", vol. 279, pp. 17535-17542.

Zimecki, M. & Machnicki, M. 1994, "Lactoferrin inhibits the effector phase of the delayed type hypersensitivity to sheep erythrocytes and inflammatory reactions to *M. bovis* (BCG)", vol. 42, pp. 171-177.

Zimecki, M., Kocieba, M. & Kruzel, M. 2002, "Immunoregulatory activities of lactoferrin in the delayed type hypersensitivity in mice are mediated by a receptor with affinity to mannose", *Immunobiology*, vol. 205, no. 1, pp. 120-131.

Zimmermann, S. & Moelling, K. 1999, "Phosphorylation and regulation of Raf by Akt (protein kinase B)", *Science* (New York, N.Y.), vol. 286, no. 5445, pp. 1741-1744.

Zweiman, B., Kucich, U., Shalit, M., Von Allmen, C., Moskovitz, A., Weinbaum, G. & Atkins, P.C. 1990, "Release of lactoferrin and elastase in human allergic skin reactions", vol. 144, pp. 3953-3960.